Emission and dynamics of halocarbons from seagrass meadows traced by stable carbon isotopes

Dissertation

zur Erlangung des Doktorgrades der Naturwissenschaften im
Fachbereich Geowissenschaften der Universität Hamburg

vorgelegt von

Ingo Weinberg

aus Bremen

Hamburg

2013

Als Dissertation angenommen vom Fachbereich Geowissenschaften der Universität Hamburg auf Grund der Gutachten von Dr. Richard Seifert und Prof. Dr. Jens Hartmann.

Hamburg, den 28.01.2014

Prof. Dr. Christian Betzler

(Leiter des Fachbereichs Geowissenschaften)

Abstract

Despite their low atmospheric mixing ratios, halocarbons strongly influence a variety of chemical key processes in the atmosphere. This includes their function as significant carriers of reactive halogens to the stratosphere which in turn contribute to ozone depletion. The current scientific endeavours focus on the identification and quantification of sources and sinks as well as on the elucidation of the driving parameters determining the environmental fate of these substances. To date, many uncertainties are connected to the atmospheric budgets represented by still unknown and/or rather crude quantified sources. In this context, coastal zones have been found to inhabit important source ecosystems for halocarbons such as macroalgae, salt marshes, and mangroves. Seagrass meadows, one of the key ecosystems in the worlds' coastlines, have to date been neglected as an additional source for halocarbons.

The overall objective of this thesis was to elucidate the emission and dynamics of halocarbons from seagrass meadows and to get insights into the underlying biogeochemical processes using stable carbon isotope distribution. Sampling and analytical methodologies suitable for field measurements were developed in order to determine the concentration and stable carbon isotopes of these low-concentrated compounds in the environment. Fluxes from seagrass ecosystems were obtained using dynamic flux chambers. In total, three sampling campaigns were conducted in intertidal seagrass meadows in Sylt, Germany and in the lagoon Ria Formosa, Portugal. These field measurements were complemented by laboratory incubation experiments with seagrass.

During all field campaigns seagrass meadows were a net source for chloromethane (CH_3Cl), bromomethane (CH_3Br), iodomethane (CH_3I), and bromoform ($CHBr_3$). The observed high variability in fluxes was attributed to multiple sources and sinks interacting simultaneously in such systems. Furthermore, solar irradiance was one of the drivers stimulating the emission of halocarbons from seagrass meadows during air exposure. In periods of low radiation, the emission fluxes decreased or even turned into deposition fluxes. This is in accordance with the results of the incubation experiments. Supported by continuous CO_2 and methane measurements as well as discrete sampling for other trace gases, it was demonstrated that halocarbon emissions were furthermore substantially regulated by the tidal regime. Maximum emission fluxes up to 100 nmol CH_3Cl m^{-2} h^{-1}, 130 nmol CH_3Br m^{-2} h^{-1}, 8 nmol CH_3I m^{-2} h^{-1}, and 11 nmol $CHBr_3$ m^{-2} h^{-1} were observed during tidal changes from inundation to air exposure and conversely. Moreover, detailed considerations of halocarbons and other trace gases along the tidal regime revealed increased emissions during tidal inundation if compared to air exposure which contradicts previous findings.

The stable carbon isotope data of the low-concentrated compounds CH_3Br, CH_3I, and $CHBr_3$ presented in this thesis are among the first reported for the atmosphere and water phase. By construing dynamic flux chamber data using a coupled mass and isotope balance it was demonstrated that source-related isotope data can be significantly improved when internal sinks are accounted for. The average

isotopic source signatures of constituents emitted by seagrass meadows were -50‰ for CH_3Cl, -52‰ for CH_3Br, -63‰ for CH_3I, and -14‰ for $CHBr_3$. The isotopic source signatures and rates from seagrass meadow emissions along with isotope and concentration measurements from the atmosphere and water phase were used to identify the sources and sinks in the Ria Formosa. The results suggest seagrass meadows and sediments to belong to the most prominent halocarbon sources in this system, rather than phytoplankton and macroalgae which are generally considered as key sources for halocarbons in coastal waters.

Overall, the emission rates of halocarbons from seagrass meadows fall in the same range as those of other coastal habitats, namely temperate salt marshes and mangroves. Though a tentative estimate revealed that seagrass meadows are a rather minor source for halocarbons on a global scale, these ecosystems will certainly have a strong impact on the atmosphere on local and regional scales due to their high abundance in coastal zones.

Zusammenfassung

Halogenierte Kohlenwasserstoffe haben, trotz ihres vergleichsweise niedrigen Mischungsverhältnisses, einen erheblichen Einfluss auf eine Vielzahl chemischer Prozesse in der Atmosphäre. Unter anderem gehören sie zu den bedeutenden Vorläufern für reaktive Halogenverbindungen, welche zum stratosphärischen Ozonabbau beitragen. Die Identifizierung und Quantifizierung der Quellen und Senken halogenierter Kohlenwasserstoffe sowie der Einflussfaktoren, die ihr Verhalten in der Umwelt bestimmen, sind daher Gegenstand aktueller Forschung. Die atmosphärischen Budgets der halogenierten Kohlenwasserstoffe sind derzeit mit großen Unsicherheiten verbunden; zum Einen sind die bereits bekannten Quellen nicht ausreichend quantifiziert, zum Anderen existieren vermutlich noch nicht identifizierte Quellen. In diesem Zusammenhang wurden in den letzten Jahren insbesondere Küstenbereiche als potentiell bedeutende Quellregionen für halogenierte Kohlenwasserstoffe intensiv untersucht. Diese Arbeiten betrafen Mangrovenwälder und besonders Makroalgen und Salzmarschen; inwiefern Seegraswiesen, die weltweit zu den Schlüsselökosystemen in Küstenzonen zählen, ein zusätzliches Quellengebiet für halogenierte Kohlenwasserstoffe darstellen, ist jedoch bis heute weitgehend unbekannt.

Das Hauptziel dieser Dissertation ist daher die Quantifizierung der Emissionen und die Beschreibung der Flussdynamik von halogenierten Kohlenwasserstoffen aus Seegraswiesen. Darüber hinaus werden anhand der Kohlenstoffisotopenverhältnisse dieser Verbindungen Einblicke in die zugrunde liegenden biogeochemischen Prozesse abgeleitet. Dazu wurden zunächst geeignete Probenahme- und Analysemethoden entwickelt, die die Bestimmung von Konzentrationen und Isotopenverhältnissen der niedrig konzentrierten halogenierten Kohlenwasserstoffe in Umweltproben ermöglichen. Die Flussraten aus Seegraswiesen wurden dabei mittels dynamischer Flusskammern bestimmt. Diese Methoden wurden auf insgesamt drei Feldkampagnen in intertidalen Seegraswiesen auf Sylt sowie in der Lagune Ria Formosa (Portugal) eingesetzt und durch Inkubationsversuche im Labor ergänzt.

Während aller Feldkampagnen waren Seegraswiesen eine Nettoquelle für Chlormethan (CH_3Cl), Brommethan (CH_3Br), Iodmethan (CH_3I) und Bromoform ($CHBr_3$). Die dabei festgestellte hohe Variabilität der Flussraten wurde einerseits auf die heterogenen internen Quellen und Senken in derartigen Systemen zurückgeführt. Zudem konnte gezeigt werden, dass eine erhöhte Strahlungsintensität zu erhöhten Emissionen führt. In Phasen geringer Sonneneinstrahlung verminderten sich die Flussraten bis hin zu Depositionsflüssen. Diese Beobachtung wurde in den Inkubationsexperimenten bestätigt. Durch begleitende kontinuierliche CO_2- und Methanmessungen sowie Messungen weiterer Spurengase konnte gezeigt werden, dass die Flussraten zusätzlich stark von der Tide beeinflusst werden. Die höchsten Emissionsraten wurden dabei beim Tidenwechsel aufgezeichnet. Diese betrugen 100 nmol CH_3Cl m^{-2} h^{-1}, 130 nmol CH_3Br m^{-2} h^{-1}, 8 nmol CH_3I m^{-2} h^{-1} und 11 nmol $CHBr_3$ m^{-2} h^{-1}. Zudem wurden, im Vergleich zu den Messungen bei Ebbe, erhöhte

Emissionsraten unter Wasserbedeckung gemessen; ein Befund, der den gängigen Annahmen zu Spurengasemissionen aus Küstenzonen widerspricht.

Die im Laufe dieser Dissertation ermittelten Isotopendaten gehören, insbesondere für CH_3Br, CH_3I und $CHBr_3$, zu den Ersten, die für die Atmosphäre und Wasserphase bestimmt wurden. Durch eine gekoppelte Massen- und Isotopenbilanz für ein dynamisches Flusskammersystem wurde gezeigt, dass die Quellensignaturen der halogenierten Kohlenwasserstoffe deutlich besser erfasst werden können, wenn interne Abbauprozesse berücksichtigt werden. Die mittleren δ^{13}C-Quellsignaturen der halogenierten Kohlenwasserstoffe aus Seegraswiesen betrugen -50‰ für CH_3Cl, -52‰ für CH_3Br, -63‰ für CH_3I und -14‰ für $CHBr_3$.

Diese Quellensignaturen und Emissionsraten aus Seegraswiesen wurden zusammen mit den Isotopen- und Konzentrationsdaten aus der Atmosphäre und Wasserphase verwendet, um die Quellen und Senken in der Ria Formosa zu identifizieren. Die Ergebnisse zeigen einen starken Einfluss von Seegraswiesen und Sedimenten auf die Gesamtemissionen halogenierter Kohlenwasserstoffe, der deutlich über dem von Phytoplankton- und Makroalgengemeinschaften liegt, die in der Regel als Hauptquellen in Küstengewässern in Betracht gezogen werden.

Die Emissionsraten halogenierter Kohlenwasserstoffe aus Seegraswiesen liegen insgesamt in der gleichen Größenordnung, wie die aus Salzmarschen gemäßigter Breiten und Mangrovenwäldern. Obwohl eine erste Hochrechnung ergab, dass Emissionen aus Seegraswiesen global eine eher geringe Quelle darstellen, besitzen sie jedoch, angesichts ihrer weiten Verbreitung in Küstenzonen, das Potential, die atmosphärischen Budgets auf lokaler und regionaler Ebene maßgeblich zu beeinflussen.

Table of contents

List of figures

List of tables

Abbreviations

A	bottom surface area of the flux chamber
CAS	Chemical Abstracts Service
$CBrF_3$	bromotrifluoromethane
CCMAR	Centre of Marine Sciences
CFC	chlorofluorocarbon
CFC-12	dichlorodifluoromethane
$CHBr_3$	bromoform
$CHCl_3$	chloroform
CH_3Br	bromomethane
CH_3Cl	chloromethane
CH_3I	iodomethane
CH_4	methane
C_a	air concentration
$C_{chamber}$	air mixing ratio within the flux chamber
C_{in}	air mixing ratios at the inlet of the flux chamber
C_{out}	air mixing ratios at the outlet of the flux chamber
CO_2	carbon dioxide
COS	cyrbonyl sulphide
CR	community respiration
CSIRMS	compound specific isotope ratio mass spectrometry
CS_2	carbondisulfide
C_w	water concentration
$\delta^{13}C$	isotope ratio of R = $^{13}C/^{12}C$
$\delta^{13}C_{em}$	isotope ratio of emissions
$\delta^{13}C_{in}$	isotope ratio at the inlet of the flux chamber
$\delta^{13}C_{out}$	isotope ratio at the outlet of the flux chamber
$\delta^{13}C_{seawater}$	isotope ratio from seawater
$\delta^{13}C_{seagrass}$	isotope ratio from seagrass
DIC	dissolved inorganic carbon
DME	dimethylether
DMS	dimethyl sulphide
DOM	dissolved organic matter
DW	dry weight
Eq.	equation
e.g.	for example

F_{de}	sinks within the flux chamber
F_{in}	mass flows at the inlet of the flux chamber
F_{em}	sum of internal sources in the flux chamber
F_{out}	mass flows at the outlet of the flux chamber
$F_{seagrass}$	flux from seagrass
$F_{seawater}$	flux from seawater
FW	fresh weight
GCP	gross community production
GC-IRMS	gas chromatograph mass spectrometer isotope ratio mass spectrometer
GC-MS	gas chromatography mass spectrometry
GDAS	Global Data Assimilation System
GWP	global warming potential
HFC-142b	1-Chloro-1,1,difluoroethane
HCFC	hydrochlorofluorocarbon
H_2O_2	hydrogen peroxide
H_2S	hydrogen sulfide
IRMS	isotope ratio mass spectrometer
i.d.	inner diameter
k_{de}	deposition velocity
KIE	kinetic isotope effect
KIE_{de}	kinetic isotope effect of deposition
MS	mass spectrometer
m/z	mass to charge ratio
NCP	net community production
NEP	net ecosystem production
NMVOC	non methane volatile organic compound
N_2	nitrogen
n.a.	not available
n.d.	not detected
ODP	ozone depletion potential
OH	hydroxyl radical
O_2	oxygen
PFA	perfluoralkoxy-polymere
ppm	parts per million
ppt	parts per trillion
pptv	parts per trillion by volume
Q_N	flushing flowrate through the chamber

XII

RT	retention time
SAM	S-adenosyl-L-methionine
SD	standard deviation
SOLAS	Surface Ocean and Lower Atmospheric Studies
SOPRAN	Surface Ocean Processes in the Anthropocene
UV	ultraviolet
V_N	air volume at norm conditions (1013.25 mbar and 298.15 K)
VOC	volatile organic compound
VPDB	Vienna Pee Dee Belemnite
WMO	World meteorological organization

1. Introduction

To date, almost 5000 naturally occurring organohalogen compounds from various sources have been identified (Gribble, 2009). The appearance of these chlorine, bromine, iodine, and fluorine containing substances range from quite simple molecules such as C1 compounds to complex macromolecules (Gribble, 2003). In the atmosphere, the most studied halogenated trace gases predominantly are comprised of one to two carbon atoms and various degrees of halogenation. For these compounds the well-established collective term "halocarbons" (**halo**genated hydro**carbons**) is used throughout this thesis.

The first evidence that halogenated gases occur naturally was presented by Duce et al. (1965). Within their study, they found high amounts of iodine and bromine in atmospheric samples whose origin could not be specified. Thus, they stated: *"There is definitely some gaseous component of I and Br present, and this is the first instance of this in supposedly non-polluted areas".* After the invention of analytical techniques such as the electron capture detector (ECD), Lovelock and Maggs (1973) presented the first measurements of naturally occurring halocarbons in air and seawater. This was rather a coincidence as they basically investigated the distribution of the exclusively man-made trichloromonofluoromethane (CCl_3F, CFC-11) as an inert tracer for transport regimes in the atmosphere and the ocean. The authors found iodomethane (CH_3I) supersaturated in oceanic waters suggesting natural sources in this medium for the first time. Since then, numerous studies detected a variety of other halocarbons in the environment and investigated sources which are able to produce these compounds. This scientific interest was stimulated by findings that halogens including those from organohalogens strongly affect the atmospheric chemistry (e.g. oxidation capacity, climate) and contribute to the destruction of ozone. After first considerations regarding the latter point (Zafiriou, 1974), this topic became more and more important later on. Accordingly, terms as "ozone hole" and "ozone destruction" attracted the political and public attention. Long-lived anthropogenic chlorofluorocarbons (CFCs) used as propellants were particularly identified destroying the stratospheric ozone layer. Nevertheless, other halocarbons of natural and man-made origin also have the same capability. These findings led to the constitution of the Montreal protocol (United Nations Environmental Programme, UNEP) issued to control, reduce, and monitor the anthropogenic emissions for various halocarbons in order to protect the stratospheric ozone layer (UNEP, 1987). In fact, due to the phase-out of anthropogenic CFC production, the atmospheric mixing ratios of CFCs and related compounds are declining (WMO, 2011).

Coming from this rather historical perspective, several scientific communities comprising atmospheric chemistry, biogeochemistry, marine chemistry, physics, and biology are to date involved to elucidate the dynamics of naturally produced halocarbons in the environment. The major objectives are to identify and quantify sources and sinks as well as transportation and transformation processes in and between the biosphere, lithosphere (soil), hydrosphere, and atmosphere. In the light of climate change,

the current endeavours, overall, contribute to a better understanding of the environmental processes and pave the way to assess possible future conditions.

This thesis was prepared in the framework of SOPRAN (**S**urface **O**cean **Pr**ocesses in the **An**tropocene) which is the German contribution of the international research initiative SOLAS (**S**urface **O**cean – **L**ower **A**tmosphere **S**tudy). SOPRAN research endeavours focus on the present oceanic cycles and ocean-atmosphere interactions and their response on the global atmospheric change.

1.1 Halocarbons in the atmosphere

Although there are a huge number of naturally produced halocarbons, this thesis focuses primarily on the three monohalomethanes chloromethane (CH_3Cl), bromomethane (CH_3Br), CH_3I, and the trihalomethane bromoform ($CHBr_3$). The chemical structures and some physico-chemical properties are displayed in figure 1.
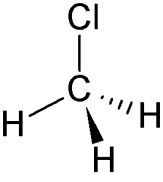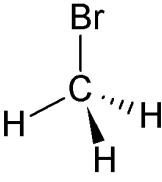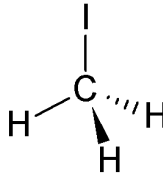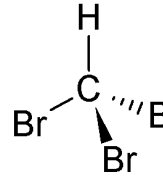
CH₃Cl	**CH₃Br**	**CH₃I**	**CHBr₃**	
50.49	94.94	141.94	252.75	molecular weight (g mol^{-1})
575 [a]	257 [a]	53 [a]	0.7 [a]	Vapor pressure (kPa; 25°C)
5.3 [b]	15.2 [b]	13.8 [b]	3.1 [b]	Water solubility (g L^{-1}; 25°C)
951 [c]	596 [d]	541 [e]	62 [c]	Henry const. (Pa m^3 mol^{-1}; 25°C)

Figure 1: Target compounds of this thesis and their physico-chemical properties. [a] **Mackay et al. (2006)** [b] **Horvath (1982)** [c] **Mackay and Shiu (1981)** [d] **King and Saltzman (1997)** [e] **Glew and Moelwyn-Hughes (1953)**

The atmospheric lifetimes of the four halocarbons are rather short in comparison to those of man-made CFCs (up to several hundred years). Nevertheless, with atmospheric lifetimes of 1.0 years and 0.8 years CH_3Cl and CH_3Br belong to the long-lived substances (WMO, 2011). In contrast, CH_3I and $CHBr_3$ are generally categorized into the "very short-lived substances" with lifetimes of 7 days and 24 days, respectively (WMO, 2011). Like other trace gases such as CO_2 and methane, halocarbons are radiative active compounds and contribute to global warming by absorption of radiation in the infrared region. Quantitatively, this effect can be measured by the global warming potential (GWP). This is a relative measure which compares the radiative forcing to that of CO_2 (GWP=1) on a mass basis. The GWPs for CH_3Cl and CH_3Br on a 20 years time horizon are 45 and 19 (WMO, 2011). Due to the short atmospheric residence time the concept of GWP is not contrivable for CH_3I and $CHBr_3$ (WMO, 2011).

Beside their relevance on the global climate, halocarbons participate in heterogenic processes in the troposphere and stratosphere.

Naturally-produced halocarbons are important precursors of reactive halogen species in the atmosphere by chemical and photochemical reactions. Halogens in turn are, after transport to the stratosphere, responsible for the catalytic destruction of ozone (Read et al., 2008). The efficiency of parent compounds to deliver free halogens depends on their mixing ratios, atmospheric life times, and amount of halogen molecules. For example, CH_3Cl contributes to about 16% to the tropospheric organic chlorine. Even 50% to the organic bromine comes from CH_3Br (WMO, 2003). Moreover, various studies revealed that also very short-lived source gases such as $CHBr_3$ are also significant contributors to ozone destruction in the stratosphere (e.g. Dvortsov et al., 1999; Pfeilsticker et al., 2000). Once reaching the stratosphere, bromine is 45 times more efficient in destroying ozone than chlorine on atom basis reflecting certain higher ozone depletion potential (ODP) (Daniel et al., 1999). In the light of the decline of anthropogenic halocarbons such as CFCs in the atmosphere, the relative contribution of naturally produced CH_3Cl and CH_3Br to the total atmospheric burden increases (WMO, 2007). For CH_3I, there is evidence that this compound also contributes to the stratospheric ozone depletion (Solomon et al., 1994). However, due to the short live time and thus the requirement of rapid upward lifts of air masses, the magnitude is currently under further investigations (Tegtmeier et al., 2013).

Whereas ozone in the stratosphere protects the earth from UV radiation, it is harmful to the living environment in the troposphere. Furthermore, ozone is an important precursor of hydroxyl radicals which are very reactive components controlling the oxidation capacity of the atmosphere (von Glasow, 2008). Halogen oxides (IO, BrO, ClO), derived from either, organic halogenated compounds or oxidation of sea salt aerosols (Platt and Hönninger, 2003), contribute significantly to the destruction of tropospheric ozone by various reaction pathways. Furthermore, especially chlorine is an oxidation partner and can for example oxidize hydrocarbons (Sander et al., 1997).

Among other organic iodinated trace gases, CH_3I contributes indirectly to the formation of aerosols. After photooxidation of these compounds, the soluble iodine fraction binds to atmospheric aerosols forming cloud condensation nuclei (O'Dowd et al., 2002). This production of atmospheric particles on the one hand, affects the radiation budget of the earth. On the other hand, it depicts an important transport route for iodine into terrestrial environments which are generally scarce in this essential nutrient (Carpenter, 2003). Beside these processes, iodine species also influence various atmospheric reactions such as the dimethyl sulphide (DMS) and nitrogen oxide cycles (Carpenter, 2003).

More details on the complex atmospheric chemistry of halogens in the troposphere can be found in von Glasow and Crutzen (2003) and Saiz-Lopez and von Glasow (2012).

1.2 Sources

1.2.1 Anthropogenic sources

Human activity results in the environmentally significant emissions of halocarbons to the atmosphere. In particular, this holds true for CH_3Br, CH_3I, and $CHBr_3$. Due to the harmful properties, CH_3Br has been widely used as fumigant of soils and various kinds of commodities as especially containers for shipping (Chitwood and Deshusses, 2001). Since the legal efforts of the Montreal protocol reducing the anthropogenic emissions of CH_3Br, CH_3I is considered as replacement (WMO, 2007). Furthermore, $CHBr_3$ is used as disinfection reagent for drinking water (Quack and Wallace, 2003). Waste incineration (McCulloch et al., 1999) and biomass burning (Mead et al., 2008b) are significant emission sources for compounds such as CH_3Cl and CH_3Br. Since this thesis primarily focuses on halocarbons from natural sources, the anthropogenic sources are not further discussed in detail. Moreover, for the halocarbons studied in this work, natural sources dominate over anthropogenic ones.

1.2.2 Natural sources

Up to now, numerous investigations on the identification of natural halocarbons sources have been performed in various marine and terrestrial environments. One of the main focuses were on plant-based ecosystems which depict significant portions of the worlds' area and/or are most prolific emitters. In general, the main identified biological sources can be grouped into the following categories: i) Higher plants ii) Macroalgae iii) Phytoplankton iv) Fungi, and v) Marine bacteria.

i) Higher plants. The first evidence that higher plants can produce halocarbons was reported by Varns (1982) for CH_3Cl from harvested potato tubers. Ongoing research further revealed that plants of different regions and genera are able to produce CH_3I (Saini et al., 1995). Meanwhile, it is clear that especially monohalomethanes (among others) are likely emitted by plants. Inspired by these results several investigators elucidated the role of higher plants to the global halocarbon budgets. Therefore, salt marshes (Rhew et al., 2000; Cox et al., 2004; Manley et al., 2006; Valtanen et al., 2009; Blei et al., 2010b) mangroves (Manley et al., 2007), subtropical-and tropical rainforests (Yokouchi et al., 2002; Gebhardt et al., 2008; Blei et al., 2010a), coastal wetlands (Varner et al., 1999), temperate forests (Drewer et al., 2008), and rice plantations (Redeker et al., 2000, 2004; Redeker and Cicerone, 2004; Khan et al., 2011) were extensively studied on several spatial and temporal scales.

ii) Macroalgae. Since the fundamental discovery of Lovelock (1975) presenting the first evidence for elevated concentrations of CH_3I in kelp beds of Northern Ireland, numerous studies investigated various species of macroalgae (e.g. Gschwend et al., 1985; Manley and Dastoor, 1987; Nightingale et al., 1995; Giese et al., 1999; Carpenter et al., 2000; Laturnus et al., 2000, 2004). It turned out that they are one of the most efficient halocarbon producers in the marine realm. However, there seems to be a huge discrepancy of production potential between individual species (Carpenter et al., 2000). The compounds emitted by these species are manifold. For example, the red seaweed *Asparagopsis taxiformis* alone emits more than 120 halocarbons with less than six carbon atoms (Paul and Pohnert,

2011 and references therein). Recent investigations revealed that macroalgae produce exceptional high amounts of $CHBr_3$ (Carpenter and Liss, 2000; Carpenter et al., 2000). This is less pronounced for the monohalomethanes where emissions from these coastal macrophytes seem to be distinctively lower (Itoh et al., 1997; Baker et al., 2001).

iii) Phytoplankton. Given that about two thirds of earths surface are covered by water, it appears to be of importance to investigate phytoplankton regarding their ability of producing halocarbons. Accordingly, the report of Tait and Moore (1995) revealed that a variety of diatoms are able to produce monohalomethanes. Further investigations extended their measurements concerning other classes of phytoplankton such as microalgae and dinoflagellates (e.g. Scarrat and Moore, 1996, 1998; Saemundsdottir and Matrai, 1998). Moreover, incubation experiments as well as measurements from coastal and oceanic waters revealed considerable $CHBr_3$ production from phytoplankton communities (Quack and Wallace, 2003).

iv) Fungi. Fungi, using wood as substrate, belong to the most important biological sources for atmospheric CH_3Cl (Watling and Harper, 1998). In particular, these organisms tend to form the halides in the dying wood material utilizing cellulose as substrate (Harper and Hamilton, 2003). For example, fungi are able to convert up to 90% of chlorine in the tissue into CH_3Cl. Although further emissions of CH_3Br and CH_3I were detected from these organisms, it was assumed that this process is most likely only atmospherically relevant for CH_3Cl (Harper and Hamilton, 2003).

v) Marine bacteria. Several investigators suspected marine bacteria being involved in the generation of CH_3I. First evidence was presented by Manley and Dastoor (1988) from uncharacterized microbial communities from dried kelp macroalgae tissues. Later on, further investigations revealed the production of CH_3I by various terrestrial and marine bacteria under naturally occurring iodine concentrations (Amachi et al., 2001, 2003). Most recent studies revealed widely abundant marine cyanobacteria as emitters of CH_3Cl, CH_3I, CH_3Br, (Smythe-Wright et al., 2006; Brownell et al., 2010; Smythe-Wright et al., 2010), and $CHBr_3$ (Hughes et al., 2013). Although the reported emissions cover roughly five orders of magnitude between the individual studies (Hughes et al., 2011), the cyanobacteria *Prochlorococcus* alone may be responsible for a large fraction of the global oceanic CH_3I flux (Smythe-Wright et al., 2006).

1.2.3 Biogenic production mechanisms

Considering the enormous number of different natural sources it is worthwhile to give some information on the underlying production mechanisms. The in-vivo production of halocarbons proceeds via heterogenic processes, but most importantly are catalyzed by two distinct biochemical/chemical reactions which utilize enzymes. Thereby, the biosynthesis of monohalomethanes proceeds by methyltransferases while di- and polyhalomethanes are formed by haloperoxidases.

The methyltransferases deliver the halide ions to the respective substrate which acts as methyl donor (Wuosmaa and Hager, 1990). Mostly, these substrates contain sulphur activated methyl groups

reflecting a reactive site supporting the cleavage of the methyl group. Figure 2 presents the most prominent reaction pathway of biosynthetic CH_3Cl production utilizing the methyl donor S-adenosyl-L-methionine (SAM).
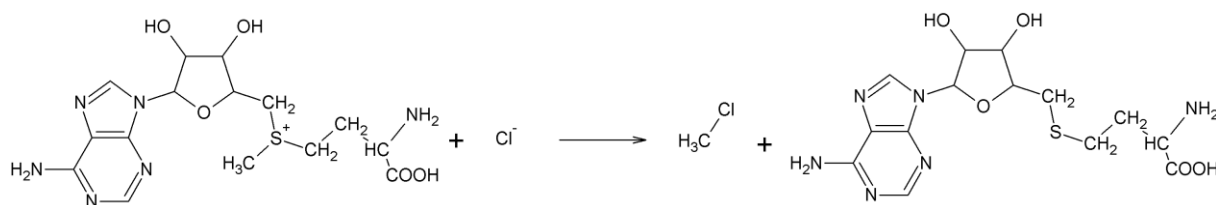
Figure 2: Chemical reaction of SAM with chloride forming CH₃Cl (after Manley (2002))

Based on the halide nucleophilicy the order of preference for this reaction is basically iodine > bromine > chlorine (Wuosmaa and Hager, 1990). However, in the environment this is likely a matter of ambient concentration of these halides than of reactivity. So far, various organisms have been reported to use this SAM pathway such as plants (Attieh et al., 1995), fungi (Saxena et al., 1998), and algae (Wuosmaa and Hager, 1990).

The biosynthesis of polyhalomethanes proceeds indirectly by haloperoxidases activity (Chloro-, bromo-, and iodoperoxidases). One possible reaction pathway leading to the generation of $CHBr_3$ is displayed in figure 3. The substrates for these reactions are halides, hydrogen peroxide (H_2O_2), and various organic compounds with an activated carbon in the alpha position.
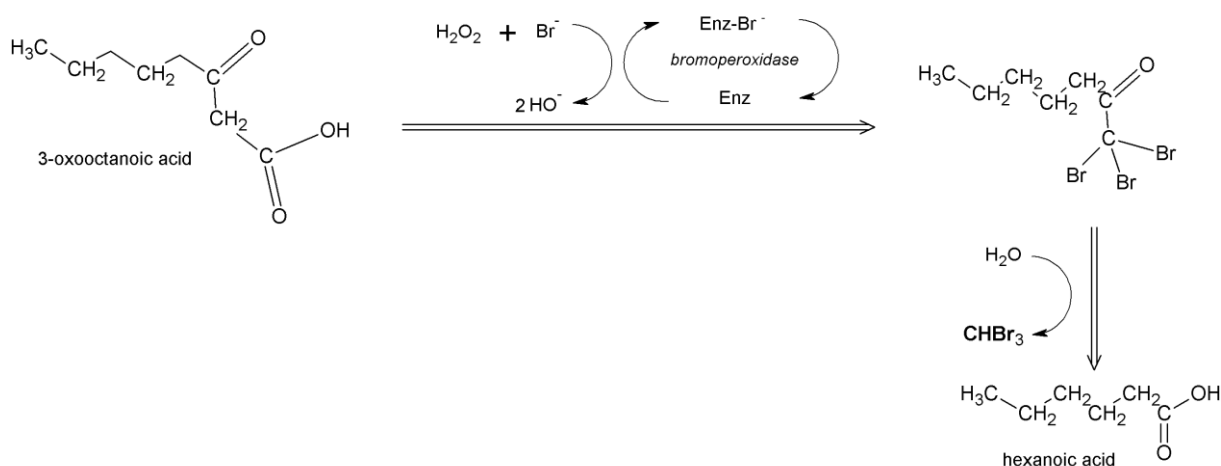
Figure 3: Biogenic formation of CHBr₃ (after Theiler et al. (1978) and Manley (2002))

Principally this reaction reassembles two different steps: Firstly, the peroxidase forms reactive electrophilic halogen species using H_2O_2 as oxidant. Secondly, the resulting halide molecule cleaves an H atom from the organic compound. This process is stepwise and the so-called "haloform reaction"

finally leads to a polybrominated ketone. Afterwards, the non-enzymatic hydrolysis results in the release of $CHBr_3$.

Giving the variety of source organisms producing halocarbons, it is likely that there is a common function to do this. However, an inevitable explanation is not available, yet. For example, some authors suggest the halocarbon production of salt tolerant plants, is a regulative function in order to excrete halide ions from their tissues (Ni and Hager, 1999). Others relate the activity of methyltransferase in plants rather to the sulphur metabolism than to those of halides (Attieh et al., 1995). This would mean that the production of monohalomethanes is rather a side effect of other metabolic processes. Although H_2O_2 is a by-product of primary metabolisms in the cells, it is nevertheless harmful for living organisms. Haloperoxidase activity is able to scavenge the H_2O_2 by using halide ions as shown above. This finally leads to the generation of halocarbons more indirectly than directly and thus, it could be "metabolic accident" (Manley, 2002). Some halocarbons have antimicrobial and antiherbivory properties which in turn can be eventually regarded as part of a chemical defence of the source organisms (Manley, 2002).

1.2.4 Abiotic production mechanisms

Abiotic routes to monohalomethanes in the environment are nucleophilic substitution reactions in soils, sediments, and organic rich waters (Keppler et al., 2000) as well as radical substitutions occurring for instance during biomass burning (Manö and Andreae, 1994). During the oxidation of organic matter and an appropriate electron acceptor (e.g. Fe^{3+}), halide ions are methylated forming monohalomethanes via nucleophlic substitutions (figure 4).
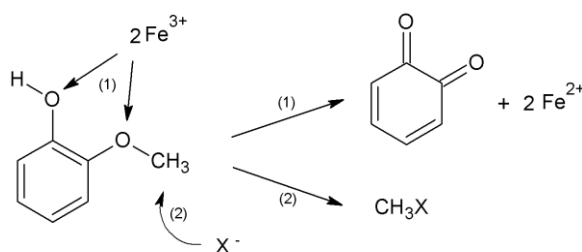
Figure 4: Abiotic formation of monohalomethanes by nucleophilic substitution (after Keppler et al. (2000))

This kind of reaction is inhibited when either halides or ferrihydrite were absent underlining that both reaction partners are essential (Keppler et al., 2000). Somehow in analogy to this reaction, Hamilton et al. (2003) proposed abiotic production of CH_3Cl from dying plant material. CH_3Cl is formed directly within the senescent leaf material using pectin as methyl donor.

Abiotic formation reactions are furthermore reported to occur in seawater. Aqueous CH_3Br and CH_3I are substituted by seawater chlorine. This results in the degradation of both compounds and production of CH_3Cl; the so-called transhalogenation (Zafiriou, 1975). Another mechanism proposed by Moore

and Zafiriou (1994) involves photochemical reactions with seawater. Thereby dissolved organic matter (DOM) and seawater iodine are destructed into radicals followed by readily recombination forming CH_3I. Due to the high reaction rate, this process tends to be significant in oceanic environments (Moore and Zafiriou, 1994). Moreover, it was shown that photochemical mechanisms can also lead to the production of CH_3Cl (Moore, 2008; Dallin et al., 2009).

1.3 Sinks

In the atmosphere the predominant removal pathway of CH_3Cl and CH_3Br is the reaction with the hydroxyl radical (OH radical) (WMO, 2003). Due to the high amounts of chloride emitted by the oceans, CH_3Cl is furthermore significantly degraded by chlorine radicals in the marine boundary layer (WMO, 2003). In the troposphere, CH_3Cl and CH_3Br are quite stable against photolysis which is reflected by the quite high lifetimes in this medium (section 1.1). This is in contrast to the very short-lived CH_3I and $CHBr_3$ whose main destruction mechanism is photodissociation (WMO, 2007). Nevertheless, OH and Cl radicals could be responsible for about 10-20% of the CH_3I removal (Cotter et al., 2001).

In the ocean, monohalomethanes are degraded by various chemically and biologically-mediated processes. Regarding the long-lived compounds CH_3Cl and CH_3Br, the ocean can therefore act as both, a source (as shown chapter 1.2) and a sink. Several processes are significant in terms of the oceanic sink. Chemical degradation pathways of CH_3Br comprise hydrolysis and transhalogenation as the most relevant ones (Elliott and Rowland, 1993, 1995). Both reactions are highly temperature dependent with higher decomposition rates at higher temperatures (Tokarczyk and Saltzman, 2001). The chemical degradation of CH_3Cl is in turn rather slow (Elliott and Rowland, 1995; Tokarczyk et al., 2003).

CH_3I in seawater is subject to transhalogenation and thus degradation results in the production of CH_3Cl (section 1.2.4). Other processes such as photolysis and hydrolysis are to date not well quantified but are assumed being negligible (Carpenter, 2003). Abiotic destruction of $CHBr_3$ in seawater by processes such as hydrolysis, halogen substitution and photolysis are rather slow with half-lives of up to 74 years (Quack and Wallace, 2003).

Microbial degradation of monohalomethanes has been widely reported from seawater and marine bacterial cultures (King and Saltzman, 1997; Schäfer et al., 2007 and references therein). For example, while some bacteria contain a methyltransferase pathway for the oxidation of CH_3Br and CH_3Cl (Schäfer et al., 2005), other strains are capable to use CH_3Br as sole carbon and energy source (Hoeft et al., 2000). Though there is some evidence that microbial degradation (e.g. by ammonia oxidizer) for $CHBr_3$ is substantial (Wahman, et al., 2005, 2006), it is still the question whether this could be environmentally significant (Hughes et al., 2013). Soils and sediments have been reported to degrade monohalomethanes by microbial activity (Oremland et al., 1994; Shorter et al., 1995; Hines et al., 1998; Miller et al., 2004). Thus, soils depict one of the prominent sinks for CH_3Cl and CH_3Br.

1.4 Halocarbon budgets

Due to the high relevance of halocarbons to a variety of processes in the atmosphere, the understanding of their sources and sinks is mandatory. Therefore, enormous efforts have been made since about three decades to quantify their budgets. The results are regularly summarized by the reports of World Meteorological Organisation (WMO), especially for long-lived CH_3Cl and CH_3Br. Table 1 presents the current state budgets for both compounds derived from these reports and, for the very short-lived compounds CH_3I and $CHBr_3$, from recent literature. Overall, the ranges mirror the current understanding of the contribution of respective sources and sinks and give an indication how good they are quantified, yet.

As derived from earlier estimates, it was believed that the dominant source for CH_3Cl is biomass burning (WMO, 1999). Afterwards, the highly-regarded report of Butler (2000) presented an imbalance in global CH_3Cl budgets with sinks dominating the sources. The author argued that the missing sources are most certainly not oceanic since the ocean is not sufficiently supersaturated with this compound. Concomitantly, numerous studies reported considerable emissions from coastal and tropical terrestrial sources such as salt marshes (Rhew et al., 2000), mangroves (Manley et al., 2007), tropical plants (Yokouchi et al., 2002), and abiotic production in soils and from leaf litter (Keppler et al., 2000; Blei et al., 2010a; Blei and Heal, 2011). To date, it is generally assumed that these sources are able to balance the atmospheric budgets of CH_3Cl, but large uncertainties remain as given by the wide range of reported emissions (table 1).

Despite the obvious uncertainties also existing for CH_3Br, it is generally assumed that the known sinks are likely larger than the identified sources. Due to the restrictions on the anthropogenic use of CH_3Br, the atmospheric burden of CH_3Br decreased during the last decade (WMO, 2011). Moreover, an elevated contribution of the oceans, salt marshes, fresh water wetlands, were recently revised downward (WMO, 2011). This supports the assumption that there is indeed a source or multiple sources missing to fill the gap in the budget. Likewise, recent model calculations accounting for the decline of anthropogenic CH_3Br imply a missing source of about 20% relative to the known and quite well quantified sinks (Yvon-Lewis et al., 2009; WMO 2011).

Regarding the short-lived CH_3I and $CHBr_3$, it should be noted that sink strengths calculated by Bell et al. (2002) and Quack and Wallace (2003 and references therein) (table 1) rely on the respective source strengths used in their estimates. Due to the short lifetimes of these compounds in the atmosphere, it can be generally assumed that the atmospheric budgets for both compounds are likely balanced.

The ocean is the predominant source for CH_3I and $CHBr_3$. To date, there is a high uncertainty regarding the magnitude of fluxes for these compounds. Obviously, there is a strong mismatch between oceanic emission estimates and those which were conducted with a direct source-relationship on a species basis. Macroalgae and phytoplankton have been identified as most prominent emitters so far. However, by no means the estimates of these two sources are sufficient to reach those of the ocean (table 1).

Table 1: Atmospheric budgets of CH₃Cl, CH₃Br as well as sources and sinks of CH₃I, and CHBr₃

Source	Source strength (Gg yr⁻¹)			Sink	Sink strength (Gg yr⁻¹)		
	Mean	min	max		Mean	min	max
CH₃Cl [1]							
(Sub)tropical plants	-	820	8200	OH reaction	-	3800	4100
Senescent plants	-	30	2500	Cl reaction	-	180	550
Biomass burning	-	325	1125	Loss to stratosphere	-	100	300
Oceans	-	380	500	oceans	-	93	145
Fossil fuel	-	5	205	Soils	-	100	1600
Waste incineration	-	15	75				
Wetlands	48	-	-				
Industrial processes	10	-	-				
Salt marshes	-	6 [15]	440				
Mangroves [3]	12	11	12				
Rice plantations	-	2.4	4.9				
Fungi	-	43	470				
Total	**-**	**1637**	**13532**	**Total**	**-**	**4273**	**6695**
CH₃Br [2]							
Ocean	42	34	49	OH / photolysis	63.6	-	-
Fumigation	14.3	11.7	17.1	Oceans	49	45	52
Biomass burning	29	10	40	Soils	32	19	44
Leaded gasoline	5.7	-	-				
Salt marshes	7	0.6	14				
Mangroves [3]	1.3	1.2	1.3				
Rapeseeds	5.1	4	6.1				
Fungi	1.7	0.5	5.2				
Peat lands	0.6	-0.1	1.3				
Shrub lands	0.2	0	1				
Rice plantations	0.7	0.1	1.7				
Total	**107.6**	**-**	**-**	**Total**	**144.6**	**-**	**-**
CH₃I							
Ocean [4]	610	-	-	Photolysis [16]	304	-	-
Macroalgae [5,6]	-	<0.1	0.6				
Phytoplankton [7,8]	-	1	614				
Vegetation and soils [9]	33	-	-				
Ride plantations [10]	-	16	29				
Mangroves [3]	11	-	-				
Biomass burning [11]	<10	-	-				
Peat- and wetlands [12]	8.7	-	-				
Salt marshes [13]	3.0	-	-				
CHBr₃ [14]							
Ocean	842	253	1853	OH / photolysis	-	202	986
Macroalgae	135	34	227		-	-	-
Phytoplankton	-	88	91		-	-	-
Anthropogenic	29	21	117		-	-	-

[1] WMO (2007); [2] WMO (2011); [3] Manley et al. (2007); [4] Butler et al. (2007); [5] Giese et al. (1999); [6] Manley et al. (1992); [7] Smythe-Wright et al. (2006); [8] Manley and de la Cuesta (1997); [9] Sive et al. (2007); [10] Lee-Taylor and Redeker (2005); [11] Andreae et al. (1996); [12] Dimmer et al. (2001); [13] Manley et al. (2006); [14] Quack and Wallace (2003 and references therein); [15] Blei et al. (2010b); [16] Bell et al. (2002)

This strongly suggests not yet identified sources for these trace gases or that known sources are insufficiently quantified (e.g. marine bacteria). Accordingly, coastal oceans are often reported as "hot spots" for very short-lived compounds which contribute largely to the global budgets (Quack and Wallace, 2003; Butler et al., 2007).

Overall, current budgets suggest for all compounds studied either the existence of unknown sources or that already indentified sources are subject to high uncertainties. This reflects a strong need to further investigate the origin of halocarbons in the environment. Important source regions are coastal zones as represented by elevated global contribution from oceanic waters, phytoplankton, and coastal macrophytic systems such as mangroves and salt marshes. Since all these systems are complex in their biogeochemistry, the magnitude of fluxes is highly variable in space and time. It is therefore strongly recommended to elucidate their potential drivers leading to emission and decomposition. This can in turn contribute to a better understanding for the halocarbon budgets.

A further possibility to elucidate the dynamics of halocarbons in the environment is to use their stable carbon isotopes as tracer for the biogeochemical cycles and underlying processes.

1.5 Stable carbon isotopes of halocarbons

Carbon has two stable isotopes (^{12}C and ^{13}C). The relative natural abundance is higher for the lighter (^{12}C: 98.890%) than for the heavier isotope (^{13}C: 1.110%). According to an international convention the isotope compositions of carbon are generally expressed in delta notation ($\delta^{13}C$) which denotes the ratio of the heavy to light isotope. $\delta^{13}C$ values are reported in per mill (‰) relative to the international accepted Vienna Pee Dee Belemnite (VPDB) scale using the following equation (McKinney et al., 1950):

$$\delta^{13}C = \left[\frac{\left(^{13}C/^{12}C_{sample} - ^{13}C/^{12}C_{standard} \right)}{^{13}C/^{12}C_{standard}} \right] \times 1000$$

Since the heavier isotope is mostly less reactive, this leads to a relative enrichment of the lighter isotope in the product and an enrichment of the heavier isotope in the remaining educt in non-equilibrium reactions. This isotopic fractionation results in the $\delta^{13}C$ values of carbon by the carbon source itself as well by the metabolism and biosynthesis and can be used to trace carbon cycling (Craig, 1953; Hayes, 1983; 2001). The isotopic fractionation of a substrate to a product is generally denoted as the kinetic isotope effect (KIE) or as fractionation factor which are often used analogically.

1.5.1 What determines the $\delta^{13}C$ values of halocarbons?

In general, halocarbons are formed by abiotic and enzyme-catalyzed reaction pathways utilizing various precursor compounds in the respective tissues or environmental settings as substrate (figure 5).These precursor compounds (e.g. SAM) itself have a certain $\delta^{13}C$ value which is most cases unknown, but generally the bulk biomass is taken as representative. If halocarbons are produced from this substrate, the isotopic signal/isotopic fractionation depends on the pathway of formation.

Methyltransferase-catalyzed reactions and the abiotic formation (see section 1.2.3) are S_N2 reactions which are known to have strong isotopic fractionation of -42 to -66‰ (e.g. Morasch and Hunkeler, 2009). Due to the more reactive ^{12}C compound, this isotope is preferentially incorporated in the produced halocarbon fraction. Accordingly, large fractionation for the production of monohalomethanes have been reported for CH_3Cl produced by several plant species by Harper et al. (2001; 2003) and Saito and Yokouchi (2008) equivalent to a ^{13}C-depletion of about 35-50‰ relative to the respective biomass.
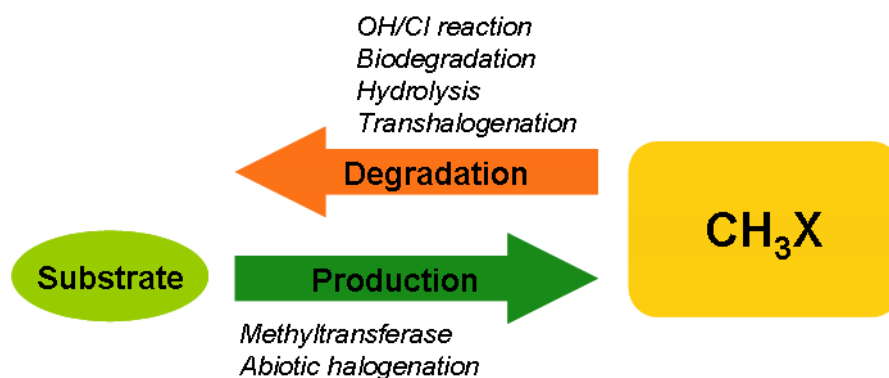
Figure 5: General halocarbon cycling and the factors influencing the $\delta^{13}C$ values

As already mentioned in section 1.2.3, $CHBr_3$ is likely generated by a different type of (bio) chemical reaction (haloperoxidase-catalyzed pathway). The underlying haloform reaction involves repeated electrophilic halogenation reactions of an activated carbon atom followed by carbon bond cleavage. Although electrophilic halogenation reactions are assigned with a fairly small isotopic fractionation (Kokil and Fry, 1986), it is not clear whether this applies also to the haloform reaction with multiple halogenation and subsequent hydrolysis forming $CHBr_3$. In general, this different reaction pathway likely result in less depleted $CHBr_3$ than those for S_N2 reactions such as the methyltransferase pathway. This consideration is in line with emission data from an incubation study with the macroalgae *Fucus serratus* and the phytoplanktonic algae *Dunaliella tertiolecta* revealing $\delta^{13}C$ values for $CHBr_3$ of -14 and -22‰, respectively (Auer et al., 2006) which are near to those of the respective biomass (-14‰ to -18‰ *F. serratus* (Brenchley et al., 1997) and -14 to -24‰ *D. tertiolecta* (Sachs et al., 1999).

Once, halocarbons are generated and released in the environment they are subject to various degradation mechanisms (see section 1.3). During destruction of halocarbons the remaining halocarbon fraction becomes enriched in ^{13}C. Therefore, knowledge on the fractionation factors is essential to evaluate the biogeochemical behaviour of the respective halocarbon. Microbial destructions of halocarbons in soils (and sediments) are assigned with substantial fractionation. For example, mean fractionation factors for CH_3Cl and CH3Br were reported being 46‰ and 65‰, respectively (Miller et al., 2001). In the atmosphere, destructions initiated by OH and Cl radicals result

in substantial fractionation factors of on average 59‰ and 70‰ (Gola et al., 2005). CH₃Br in seawater is rapidly degraded chemically accompanied by a considerable isotopic fractionation of 69‰ (King and Saltzman, 1997).

Overall, heterogenic processes lead to the production and decomposition of halocarbons in the environment. These processes are not uniform and often occur simultaneously. Therefore, stable carbon isotope analysis provides essential additional information on the biogeochemistry in various environmental settings which cannot be solely derived from concentration data.

1.5.2 Source signatures and budget estimations

While the determination of halocarbon concentrations continues since about four decades, the determination of $\delta^{13}C$ values is still quite "juvenile". The first report on isotopic CH₃Cl was published by Rudolph et al. (1997). Since then, the isotopic behaviour of this compound has been studied in a variety of environmental settings. Meanwhile, the stable carbon isotope approach has been used to improve knowledge on the atmospheric budget for CH₃Cl (Keppler et al., 2005; Saito and Yokouchi, 2008). Thereby, these approaches take advantage of the distinctly different isotopic fingerprints of the inherent sources and sinks (figure 6).
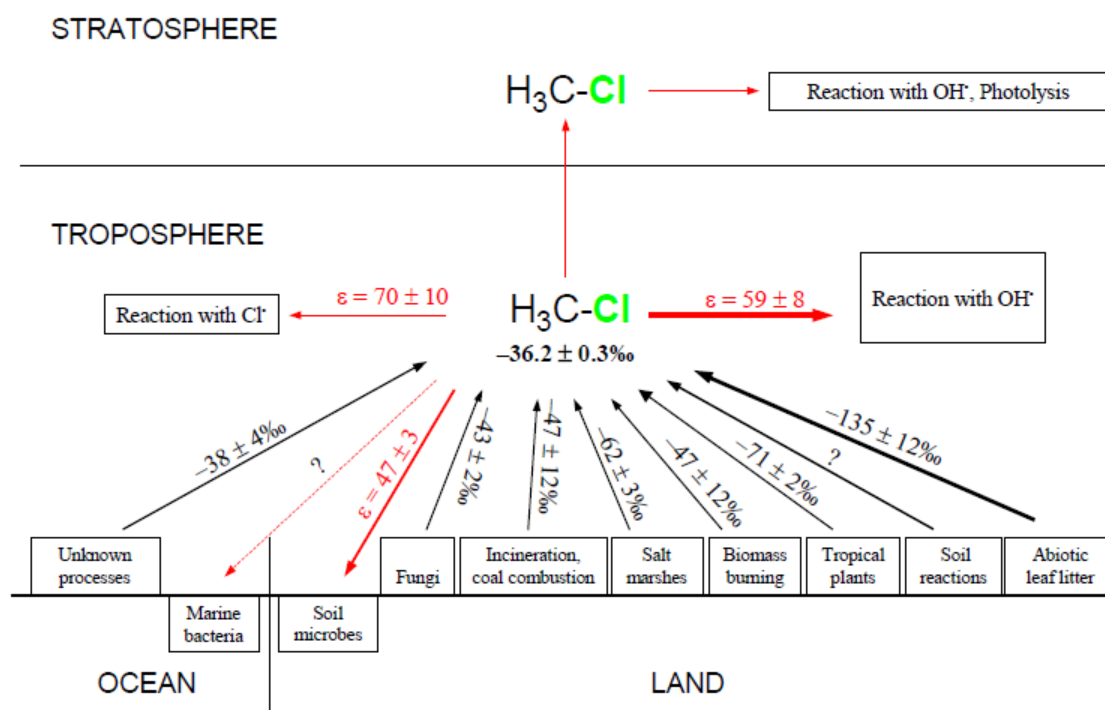
Figure 6: Scheme of sources (black arrows) and sinks (red arrows) and the corresponding source signatures and fractionation factors for CH₃Cl (compiled by Keppler et al. (2005))

This generally proceeds by integration of emission data with the particular source signatures of pertinent sources and the fractionation factors of investigated sinks (isotope and mass balance). The major outcome of this kind of approach by Keppler et al. (2005) was that the missing source in the

CH_3Cl budget likely comes from senescent leaf litter, in particular by abiotic formation (see section 1.2.4). However, Saito and Yokouchi (2008) recently revised this estimation by a detailed study on source signatures of tropical plants which turned out to produce isotopically lighter CH_3Cl (-83‰) than used in the previous calculations by Keppler et al. (2005) (-71‰, figure 6). This finally would lead to a lower contribution of CH_3Cl emission from abiotic processes (Saito and Yokouchi, 2008). However, field observations are currently lacking which could prove the environmental significance of this abiotic formation mechanism.

While a lot of progress has been made to better quantify the budgets of CH_3Cl by this isotopic approach, less is known for CH_3Br, CH_3I, and $CHBr_3$. Since these compounds are at least 10 to 100 times lower concentrated in the troposphere as CH_3Cl, the sampling and analysis is very challenging. Only four studies reported $\delta^{13}C$ values of CH_3Br, which include data from the atmosphere (Bill et al., 2004) as well as source signatures from manufacture (McCauley et al., 1999), soil fumigation (Bill et al., 2002a), and salt marshes (Bill et al., 2002b). Using a newly developed purge and trap system, Auer (2005) and Auer et al. (2006) were able to present first source signatures for CH_3I and $CHBr_3$ from macroalgae and phytoplankton production.

Thus, there is currently a strong need to extend this isotopic approach to the lower concentrated halocarbons in order to gain further insights into their biogeochemistry. On the other hand, the $\delta^{13}C$ values of dissolved halocarbons could further provide insights in the biogeochemical behaviour in coastal and oceanic waters. However, except three studies which report isotopic values for CH_3I and $CHBr_3$ (Auer, 2005; Auer et al., 2006) as well as for CH_3Cl (Komatsu et al., 2004) almost none is known, yet.

1.6 Seagrass meadows: a potentially neglected source

1.6.1 General overview of seagrass ecosystems

Seagrasses evolved approximately 100 million years ago from land plants which returned into the sea. Thus, they possess roots, stems, leafs, and flowers as characteristics for higher plants (figure 7). Seagrasses are able to conduct photosynthesis and carbon uptake from the water column by the leaves. The rhizomes are for the clonal reproduction, though seagrasses are able to reproduce sexually, and for the translocation of nutrients.
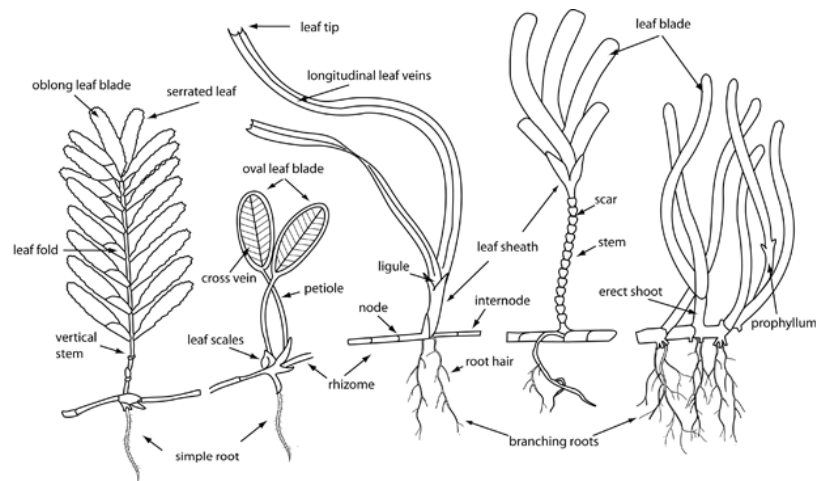
Figure 7: Example for different morphologies of seagrasses (McKenzie, 2008)

To date, roughly 60 different species have been described (Green and Short, 2003) forming a rather ecological group than a taxonomic group (den Hartog and Kuo, 2006). Most seagrasses are perennial and thus remain green throughout the year. However, in temperate regions above-ground biomass ceases in autumn and recovers in spring. Although species-specific, seagrasses are able to survive in both the intertidal and subtidal of the coastal oceans forming dense meadows. Their abundance is in particular driven by the availability of light and thus, they are able to extent in water depths of up to 90 meters (Duarte, 1991). Due to their unique physiological adaptations seagrass meadows cover a greater latitudinal range than other coastal habitats such as coral reefs, salt marshes, and macroalgae (Orth et al., 2006).

Seagrass meadows are of great ecological importance worldwide. They belong to the most productive ecosystems with a net primary production of 1211 g C m^{-2} yr^{-1} which is in the same range as other macrophytic systems such as salt marshes (1585 g C m^{-2} yr^{-1}) and macroalgae (1587 g C m^{-2} yr^{-1}) (Duarte et al., 2005). Fourqurean et al. (2012) estimated the carbon storage in seagrasses and underlying sediments with at least 10% of the global organic carbon burial in the oceans. Due to the most anoxic sediments in seagrass meadows these carbon storages of up to several meters thickness could persist for millennia (Mateo et al., 2006). Furthermore, seagrass meadows are important storages for nutrients and act as filter of particles from the water phase enhancing water clearance (Duarte, 2002). Moreover, they comprise important nursery habitats for juvenile fishes and invertebrates as well as serve as important food resource for grazers such as fish, turtles, and dugongs (Gillanders, 2006; Valentine and Duffy, 2006). Seagrass meadows offer protection of coastlines such as wave/current braking and sediment stabilization (Duarte, 2002).

Despite these important services and ecosystem functions, seagrass meadows are threatened due to direct or indirect anthropogenic influences such as eutrophication, changes in land use, and climate change (Waycott et al., 2009). While this is somehow in accordance to other marine systems such as coral reefs and mangroves, seagrass meadows have unfortunately hardly reached the public and political attention of the others (Orth et al., 2006).

1.6.1 Trace gas production by seagrass meadows?

Due to their emerging role in the carbon cycle, seagrass meadows were extensively studied in terms of CO_2 dynamics on various temporal and spatial scales (e.g. Mateo et al., 2006 and references therein). However, other source gases were less studied. Among those, are sulphur compounds such as DMS (Jonkers et al., 2000; Lopez and Duarte, 2004) and methane (Oremland, 1975). Until now, almost none is known about halocarbon emissions from seagrass meadows. The only evidence for the capability of seagrasses to produce halocarbons was presented from an incubation study of the seagrass *Zostera marina* (Urhahn, 2003). During the experiments he identified more than 30 different halogenated compounds, among those CH_3Br and CH_3I. The work was rather qualitatively than quantitatively. Thus, there is currently no attempt available which further presents evidence for the halocarbon production in these coastal systems. This is quite surprising since seagrass meadows belong to the large-scale ecosystems of the worlds' coastlines. As given in table 2, they cover similar areas as mangroves, and salt marshes which in turn have been already studied (see sections 1.2.2 and 1.4).

Table 2: Global abundance and net ecosystem production (NEP) of coastal macropyhtic ecosystems

Coastal habitat	Areal coverage 10^6 km^2	NEP g C m^{-2} yr^{-1}	Reference
Seagrass meadows	0.3-0.6	1211	Duarte et al. (2005); Charpy-Robaud and Sournia (1990)
Salt marshes	0.4	1585	Duarte et al. (2005)
Mangroves	0.2	221	Duarte et al. (2005)
Macroalgae	1.4	1587	Duarte et al. (2005)

Thus, solely on the basis of areal coverage and productivity, seagrass meadows could be an additional source for halocarbons with global relevance. Moreover, seagrass meadows are complex systems with a suit of potential source organisms beside the seagrass itself. Among those are epiphytes such microalgae/diatoms and the underlying sediments including microphytobenthos and bacteria communities. Furthermore, seagrass possess aerenchymatic tissues which are used for the delivery of oxygen to the roots in order to counteract the mostly anoxic conditions in the sediments (Smith et al., 1984). These parts of the plants are in turn potentially capable to promote the release of sedimentary trace gases as reported for other plant species (Laanbroek, 2010).

2. Objectives and outline of this thesis

Given the consideration from the introductive sections, the halocarbon budgets are not fully balanced and/or are assigned with large uncertainties. Moreover, very short-lived CH_3I and $CHBr_3$ fluxes are hardly quantified, yet. Accordingly, this opens the possibility that additional sources exist which have not identified, yet. Coastal zones have been emerged as particular source regions for halocarbons as represented by already studied macrophytic systems (salt marshes, mangroves, and macroalgae communities). Though, there is some evidence that wide abundant seagrass meadows could be one of the missing source ecosystems, actually emission data of halocarbons is astonishingly not available. The emission decomposition pattern from these systems are quite complex and thus it is obligatory to elucidate the driving factors. Likewise, in the light of the complex biogeochemistry of halocarbons, stable carbon isotopes emerged as promising tool to study the behaviour of these compounds and to improve the atmospheric budgets. However, the analysis is challenging and up to now there are only a limited number of analytical methods and datasets for halocarbons available. This in particular holds true for low concentrated ones such as CH_3Br, CH_3I, and $CHBr_3$.

Therefore, the objectives of this thesis were:

- To develop a sampling and analytical method capable to determine the stable carbon isotopes of halocarbons (and other trace gases)
- To generate first source-related isotope data from seagrass meadows
- To gain insights into the environmental controls of halocarbons dynamics by using concentration and isotopic data
- To determine the significance of seagrass meadows as source for halocarbons to the atmosphere

This thesis comprise in total 9 chapters. After the introduction (chapter 1) and the objectives (chapter 2), chapter 3 describes the sampling and analytical method to determine the concentration and stable carbon isotopes of halocarbons from atmospheric samples. This method was used for the determination of fluxes and isotope composition of halocarbons during a first study from a temperate seagrass meadow in Northern Germany (chapter 4). The chapters 5 and 6 mainly focus on the environmental controls and magnitude of emissions of halocarbons (and other trace gases) from a subtropical seagrass site in the lagoon Ria Formosa, Portugal. In chapter 7, an estimate of annual halocarbon production from seagrass meadows in comparison to other abundant sources in the lagoon was conducted. Simplifying the complex nature of the seagrass ecosystem, chapter 8 presents emission and isotopic data of solely seagrass from laboratory incubations. Finally, chapter 9 closes with the general conclusions and outlook.

The chapters 3, 4, 5, and 6 are based on already published manuscripts or manuscripts to submission for peer-reviewed scientific journals.

Chapter 3:

Bahlmann, E., Weinberg, I., Seifert, R., Tubbesing, C., and Michaelis, W.: A high volume sampling system for isotope determination of volatile halocarbons and hydrocarbons, *Atmospheric Measurement Techniques*, 4, 2073-2086, 2011.

My contribution to chapter 3: Air sampling, measurements, recovery experiments, co-work in manuscript preparation and discussion

Chapter 4:

Weinberg, I., Bahlmann, E., Michaelis, W., and Seifert, R.: Determination of fluxes and isotopic composition of halocarbons from seagrass meadows using a dynamic flux chamber, *Atmospheric Environment*, 73, 34-40, 2013.

Chapter 5:

Weinberg, I., Bahlmann, E., Eckhardt, T., Michaelis, W., and Seifert, R.:
A halocarbon survey from a seagrass dominated subtropical lagoon, Ria Formosa (Portugal): Flux pattern and isotopic composition, *in preparation.*

Chapter 6:

Bahlmann, E., Weinberg, I., Santos, R., Eckhardt, T., Lavric, J.V., Michaelis, W., and Seifert, R.: Tidal controls on trace gas dynamics in a subtropical seagrass meadow of Ria Formosa lagoon (southern Portugal), *in preparation.*

My contribution to chapter 6: Sampling, measurements, co-work in manuscript preparation and discussion

3. A high volume sampling system for isotope determination of volatile halocarbons and hydrocarbons

Enno Bahlmann, Ingo Weinberg, Richard Seifert, Christoph Tubbesing, and Walter Michaelis
Published in *Atmospheric Measurement Techniques*, 4, 2073-2086, 2011.

Abstract

The isotopic composition of volatile organic compounds (VOCs) can provide valuable information on their sources and fate not deducible from mixing ratios alone. In particular the reported carbon stable isotope ratios of chloromethane and bromomethane from different sources cover a δ^{13}C-range of almost 100‰ making isotope ratios a very promising tool for studying the biogeochemistry of these compounds. So far, the determination of the isotopic composition of C_1 and C_2 halocarbons other than chloromethane is hampered by their low mixing ratios.

In order to determine the carbon isotopic composition of C_1 and C_2 halocarbons with mixing ratios as low as 1 pptv i) a field suitable cryogenic high volume sampling system and ii) a chromatographic set up for processing these samples have been developed and validated. The sampling system was tested at two different sampling sites, an urban and a coastal location in Northern Germany. The average δ^{13}C values for bromomethane at the urban site were -42.9±1.1‰ and agreed well with previously published results. But at the coastal site bromomethane was substantially enriched in ^{13}C by almost 10‰. Less pronounced differences were observed for chlorodifluoromethane, 1,1,1-trichloroethane and chloromethane. We suggest that these differences are related to the turnover of these compounds in ocean surface waters. Furthermore we report first carbon isotope ratios for iodomethane (-40.4‰ to -79.8‰), bromoform (-13.8‰ to 22.9‰), and other halocarbons.

3.1 Introduction

Compound specific isotope ratio mass spectrometry (CSIRMS) of non methane volatile organic compounds (NMVOCs) emerged as a powerful tool to distinguish different sources and to provide information on sinks (Rudolph et al., 1997; Tsunogai et al., 1999; Rudolph and Czuba, 2000; Thompson et al., 2002; Goldstein and Shaw, 2003 and references therein; Archbold et al., 2005; Redeker et al., 2007; Mead et al., 2008a).

In particular, stable carbon isotope ratios have been proposed for constraining the origin and fate of atmospheric chloromethane (Harper et al., 2003; Keppler et al., 2005) and bromomethane (McCauley et al., 1999); as the reported carbon isotope ratios of the known sources cover a broad range of δ^{13}C values from -40‰ for anthropogenic and marine sources to -147‰ for chloromethane synthesized from pectin (c.f. Keppler et al., 2005). Tremendous progress has recently been made for the carbon isotopic analysis of dissolved halocarbons (Auer et al., 2006), which now allows to extend this

approach to short lived halocarbons such as iodomethane (CH_3I), dibromomethane (CH_2Br_2) and bromoform ($CHBr_3$). Accompanying determination of the carbon isotope ratios of these compounds could provide valuable additional information that can not be derived from the determination of mixing ratios.

For determining carbon isotope ratio of atmospheric VOCs both, air sampling canisters (Rudolph et al., 1997; Tsunogai et al., 1999; Thompson et al., 2002; Archbold et al., 2005, Redeker et al., 2007) and adsorbent tubes (Mead et al., 2008a) have successfully been used. Given a minimum carbon amount between 0.25 ng and 1 ng required for carbon isotope analysis, these sampling methods are sufficient for measurements of chloromethane (Rudolph et al. 1997; Tsunogai et al., 1999; Thompson et al., 2002; Archbold et al., 2005; Redeker et al., 2007; Mead et al., 2008a) and several chlorofluorocarbons and hydrofluorocarbons (Thompson et al., 2002; Redeker et al., 2007; Mead et al., 2008a) but not for bromomethane and other halocarbons such as bromoform and iodomethane with typical mixing ratios between 0.5 and 10 pptv.

To the best of our knowledge, there is only one study reporting carbon isotope ratios for atmospheric bromomethane (Bill et al., 2004) in which a cryogenic sampling system was used.

The main objective of this study was to develop a simple and robust sampling system appropriate for field work enabling the isotope ratio determination of atmospheric halocarbons in the low pptv range, notably bromomethane, bromoform and iodomethane. Here, we describe the configuration and validation of the developed sampling system and report first results from its application within a survey on air samples from an urban (Hamburg, Germany) and a coastal site (Sylt, Germany).

3.2 Methods

3.2.1 Overview

Briefly, up to 500 L of air were drawn through a cryotrap. The trap was then heated to 125°C and the analytes were transferred to an adsorption tube for storage and analysis. A direct analysis of the isotopic composition of the target compounds is not possible due to multiple interferences from other compounds. Therefore, the samples were first pre-separated on a GasPro column and the target compounds were recollected on two cryotraps. For carbon isotope determination each fraction was then separated on a PorabondQ column and analysed on a GC-C-IRMS/MS system.

3.2.2 Standards and samples

A Scott EPA TO 15/17 standard containing 65 compounds (1 ppm each in nitrogen) was used as a working standard. For further tests single component standards of chloromethane, bromomethane, iodomethane and dichlorodifluoromethane (each 100 ppm in nitrogen) were used.

Three ambient air samples were taken at the institute building in the center of Hamburg, Northern Germany (53.56'86''N, 9.97'36''W) from 19th to 24th September 2010. The sampling system inlet was placed at 30 m above the ground. The sampling duration was 2 h and the start time varied between

10:00 a.m. and 02:00 p.m. local time. Possible local sources include traffic exhaust, emissions from the harbor area and volatiles from laboratory activities in the vicinity.

In addition, three marine influenced air samples were taken at the AWI Wadden Sea Station in List/Sylt, Northern Germany (55.02'26''N. 8.43'96''W) between 29th August and 5th September 2010. The sampling system was placed directly at the coastline 200 m away from the Wadden Sea Station. As for the urban location the sampling duration was 2 h and the start time varied between 10:00 a.m. and 02:00 p.m. local time. Potential local sources for halocarbons include emissions from salt marshes, tidal flats and, to a minor degree, harbor activities in List.

72 h back trajectories were calculated by Hysplit 4.8 for an arriving height of 30 m (Hamburg samples) and 2 m (Sylt samples) using NCEP's Global Data Assimilation System (GDAS) data (Draxler and Rolph, 2011). The backward trajectories indicate a prevailing marine and coastal influence for the samples taken at Sylt and a prevailing continental influence for the samples taken at Hamburg.

3.2.3 Sampling system

The sampling system (figure 8) was designed with respect to field suitability and integrity of the isotopic composition of the target compounds. To avoid contamination, all system parts were made of stainless steel or silanized glass.
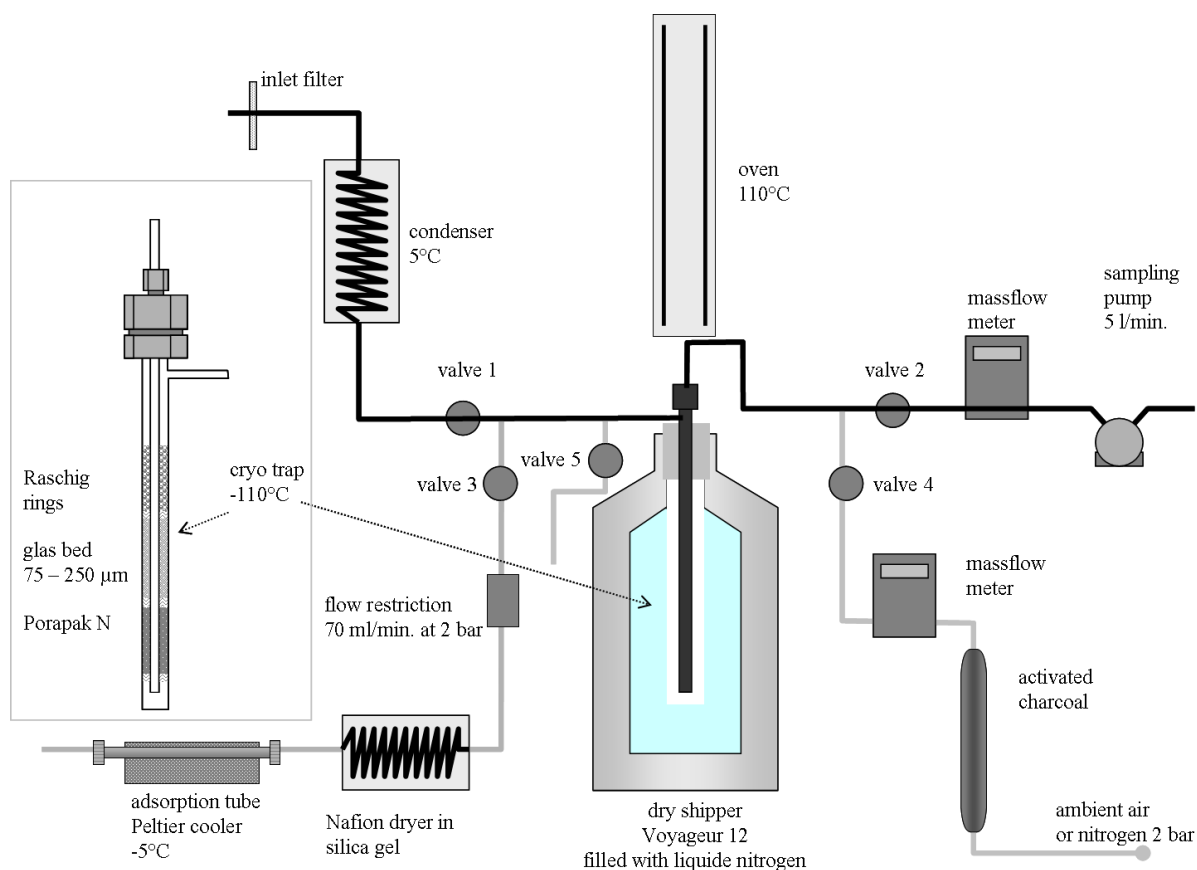
Figure 8: Scheme of the sampling system

The sampling consists of three consecutive steps: 1) the cryogenic adsorption of the target compounds from ambient air, 2) the transfer of the analytes from the cryotrap to an adsorption tube and 3) the conditioning of the cryotrap.

1) During sampling the valves 1 and 2 were open. 300 to 500 L of ambient air were drawn with a membrane pump (KNF Neuberger N86 KNDC, Freiburg, Germany) through the sampling system with a flowrate between 3 and 5 L min^{-1}. The flowrate and the sampling volume were monitored with a mass flowmeter (Omega FMA-1608A, Deckenpfronn, Germany). The air first passed a particle filter (Sartorius, Teflon membrane filter, diameter: 45 mm, pore size: 0.2 µm) and was then directed through a condenser kept at approximately 5 °C reducing the water vapour of the air. It has previously been shown that a condenser does not affect the recovery of high boiling compounds such as $CHBr_3$ (Christof et al., 2002). Finally, the target compounds were enriched in the cryotrap at a temperature of ≤ -110 °C provided by a dry shipper.

2) After sampling, valve 1 and 2 were closed and valve 3 to the adsorption tube was opened. The cryotrap was carefully removed from the dry shipper. Co-trapped argon and traces of O_2 and N_2 were rapidly released into the gas phase. To prevent analyte losses during sample transfer (usually observed at a flowrate >100 mL min^{-1}), a restriction capillary (restriction flow 70 mL min^{-1} at 2 bar) was placed behind valve 3. Without this restriction we observed losses of highly volatile analytes such as chloromethane and dichlorodifluoromethane. After 20 min, valve 4 was opened for 40 min, the cryotrap was heated to 125 °C and flushed with either nitrogen (50 mL min^{-1}) or pre cleaned ambient air. Before entering the adsorption tube, water vapour was removed from the gas stream by a Nafion dryer (Perma Pure Inc. NJ, USA) placed in silica gel. During sample transfer the adsorption tube was cooled to –5 °C using a Peltier cooler to prevent breakthrough of the analytes. Under these conditions non-polar compounds with a boiling point as high as 150 °C were completely transferred from the cryotrap to the adsorption tube, while polar water soluble compounds, such as alcohols and aldehydes, were fractionated between the water remaining in the cryotrap and the adsorption tube. After the transfer of samples the adsorption tube was closed and stored at ≤ -80 °C until analysis.

3) After sample transfer, valve 3 was closed and valve 5 was opened for conditioning the cryotrap with a stream of nitrogen (1000 mL min^{-1}) for 30 min at a temperature of 125 °C.

3.2.3.1 Cryofocussing and design of the cryotrap

Classical cryogenic sampling systems use either liquid nitrogen or liquid argon for the extraction of the target compounds from air (Bill et al., 2004; Pupek et al., 2005; Zuiderweg et al., 2011). More recently, a cryostat has been applied in cryogenic sampling systems (Miller et al., 2008). However, both approaches require a well established technical infrastructure limiting the use of such sampling systems in field campaigns, especially for field work in remote areas. In order to overcome the limitations of classical cryogenic sampling systems we employed a dry shipper (Voyageur 12, Air Liquide, Düsseldorf, Germany) as a cooling source. A dry shipper is a dewar that contains an adsorbent taking up liquid nitrogen. The Voyageur 12 can adsorb up to 14 L of liquid nitrogen and

provides a temperature of -176 °C for 28 days in the gas phase above the adsorbed liquid nitrogen. It has an approval for air transport allowing cryogenic sampling in remote places where no liquid nitrogen is available. For the sampling system the stopcock of the dry shipper was shortened to 10 cm and a hole of 20 mm diameter was drilled into the stopcock to insert the cryotrap. The effective temperature inside the cryotrap depended on the flushing flow rate and was below -110 °C for flowrates up to 5 L min^{-1}.

The cryotrap consists of an outer stainless steel tube (¾ inch, 50 cm length) with an air inlet at the side 4 cm below the top and an inner ¼ inch stainless steel tube that is connected to the sampling pump (figure 8).

To achieve complete trapping at -110 °C the space between both tubes is filled with adsorbents separated by plugs of precleaned silanized glass wool. From the top to the bottom the package of the trap was as follows: 0 – 20 cm: empty; 20 – 25cm silanized raschig rings; 25 – 35 cm silanized glass beads 60 – 250 µm; 35 – 41 cm Tenax TA; 41 – 47 cm Porapak N; 47 – 50 cm: empty. The empty space at the top and the silanized glass rings were mainly designated for trapping water vapour and CO_2.

3.2.3.2 Adsorption tubes

The adsorption tubes were made of stainless steel (¼ inch outer diameter, 7 inch length) and filled with 77 mg Carboxen 1016®, 215 mg Carbopack X 569®, 80 mg Carboxen® 1003 and 9 mg Tenax® TA in order of the sampling flow direction. The filling was fixed with stainless steel plugs. Silanized glass wool was used for separating the adsorbents. Before use, the packed tubes were conditioned for 24 h in a tube conditioner (TC ½, Gerstel, Mühlheim, Germany) at 320 °C and a flow of 100 mL min^{-1} of nitrogen.

3.2.3.3 Removal of CO_2 and water

Before analysis water and CO_2 must be removed. Chemical traps frequently used in trace gas analysis to remove excessive CO_2, such as Ascarite or Soda lime (Rudolph et al., 1997; Redeker et al., 2007) reduce the recovery of polyhalogenated methyl halides especially of polybrominated compounds and thus have been ruled out. The adsorbents used in the adsorption tubes have a low affinity for CO_2 and most of the CO_2 from the cryotrap passes the adsorbent tubes during sample transfer. Prior to analysis, the adsorbent tubes were flushed with helium at room temperature (2 min, 20 mL min^{-1}) further reducing the CO_2 content of the samples. The remaining CO_2 was removed during the GC pre-separation by an initial flushing step.

Chemical traps such as magnesium perchlorate or phosphorus pentoxide are not suitable for water removal in high-volume sampling systems due to the large amount of water (up to 30 mL m^{-3}) present in ambient air. Water was removed from the sample at three stages during sampling and analysis. First, the water vapour pressure in the sampled air was reduced by means of a condenser kept at 5°C. We found this suitable to prevent clogging of the cryotrap for air samples up to 500 L. The remaining

air moisture was frozen out in the cryotrap. During the sample transfer only a small fraction of the water was mobilized from the cryotrap. This water was removed by a Nafion dryer placed in silica gel. Remaining traces of water were finally removed by means of a second Nafion dryer during analysis.

Nafion dryers have the potential for artefact formation. So far, transformation of carbonyl compounds to alcohols and reactions of compounds containing double or triple bonds have been reported (Miller et al., 2008).

During first tests, we attached the Nafion dryer in front of the cryotrap to reduce the water offload to the cryotrap. With this setup we observed elevated levels of bromomethane. Parallel runs with and without the Nafion dryer indicated an artificial formation of bromomethane on the Nafion membrane of up to 10 pptv. Further tests revealed that the sulfonic acid groups of the Nafion membrane can catalyze the nucleophilic substitution of methanol to bromomethane in the presence of bromide. Nevertheless, with the Nafion dryer behind the cryotrap we did not observe any artificial formation of bromomethane.

3.2.4 Carbon isotope ratio determination

A direct analysis of the isotopic composition of the target compounds was not possible due to multiple interferences from other compounds. Therefore, the sample was first pre-separated on a Gas-Pro column and the target compounds were recollected on two cryotraps. For carbon isotope determination each fraction was then separated on a PorabondQ column and analysed on a GC-C-IRMS/MS system. A scheme of the analytical set up is shown in figure 9.

Two exemplary chromatograms showing the mass 44 trace and the mz 45/44 ratio from a coastal sample as well as the mass spectra of selected halocarbons are presented in the Appendix.
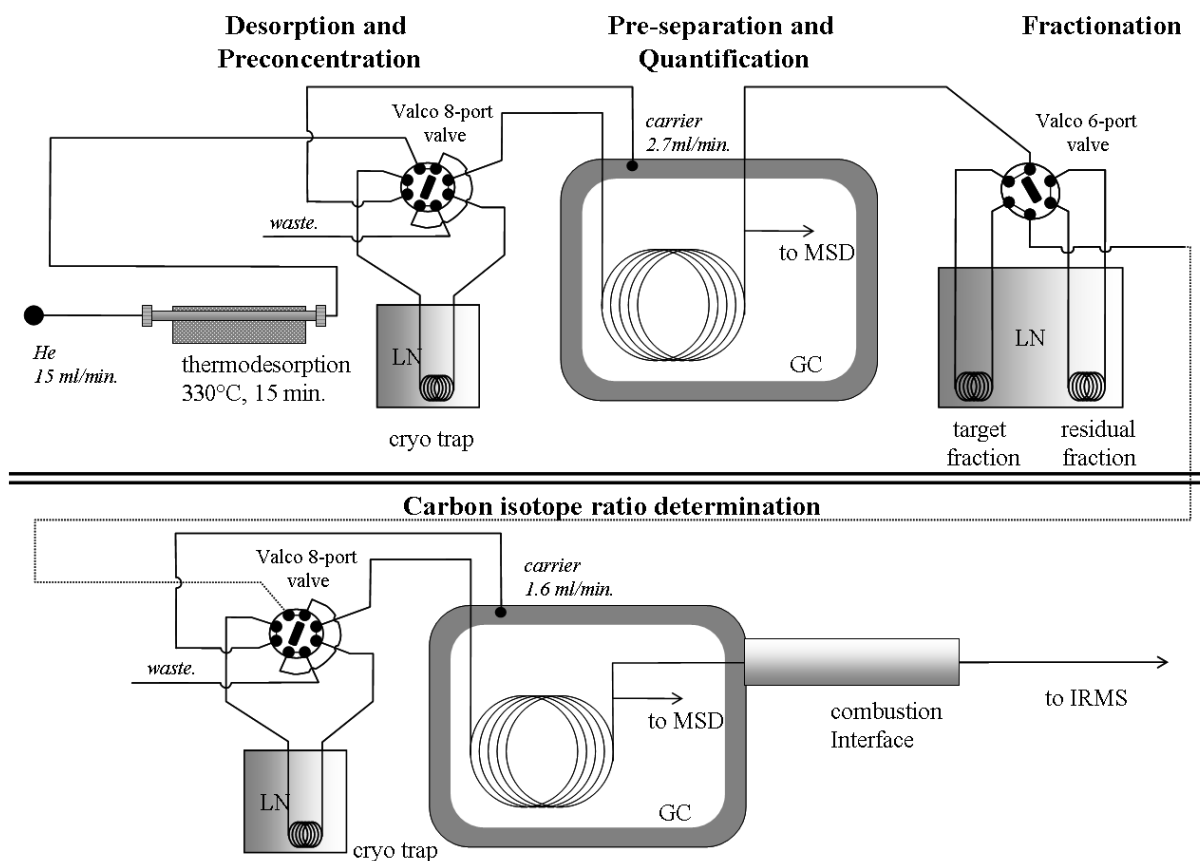
Figure 9: Scheme of the analytical system

3.2.4.1 Pre-separation

The pre-separation was performed on a 6890N/5975B GC-MS (Agilent, Waldbronn, Germany). The analytes were desorbed from the adsorbent tube into a helium gas carrier at 330 °C (15 min, 25 mL min^{-1}), directed through a Nafion dryer and refocused on a quartz capillary (0.32 i.d., 60 cm length) immersed in liquid nitrogen. Afterwards the analytes were desorbed at 25 °C and separated on a GasPro column (Agilent, 30 m, 0.32 µm i.d.) with helium as a carrier. The flowrate was set to 5 mL for 4 min to remove the CO_2 and then ramped to 2.7 mL min^{-1}. The oven temperature program was as follows: 40 °C, hold for 5 min; 6° C min^{-1} to 240°C, hold for 10 min.

About 20% of the sample were directed into the MS via a split for monitoring the fractionation. The remaining 80% of the sample were directed to a Valco six port valve (Vici, Schenkon, Switzerland) and recollected on two cryotraps (Silica steel 1/16#, 0.32 id., 25 cm length), one containing the target compounds and the other containing the remaining components.

3.2.4.2 Isotope ratio determination

For the isotope ratio determination each fraction was analysed on a Thermo Finnigan GC-C-IRMS/MS system (Trace GC II; combustion Interface III; DeltaV IRMS and DSQ II) using a CP-PorabondQ column (Varian, 25 m, 250 µm i.d.) for final separation of the analytes. Again, 20 % of the sample

were directed to a Quadrupole mass spectrometer (Thermo Finnigan DSQ II) for monitoring the peak purity. The remaining 80 % were directed to a commercial combustion interface (GC-combustion interface III; Thermo Finnigan) converting the analytes to CO_2. Water was further removed by a Nafion dryer and about 0.5 mL min^{-1} of the flow were transferred to an DeltaV isotope ratio mass spectrometer via an open split.

Prior to sample analysis, the performance of the IRMS was evaluated by repeated injections of a certified CO_2 reference gas (Air Liquide, Germany, -26.8± 0.2‰) via an open split. The Scott TOC EPA 15/17 standard was used as a daily working standard to monitor the repeatability. Results are only reported for peaks that met the following quality criteria: i) peak purity better than 90% ii) peak separation better than 90% valley.

All isotope values are reported relative to the Vienna Pee Dee Belemnite (VPDB) scale and within the lab uncertainties, unless otherwise stated, are reported on the 1σ level.

3.2.4.3 Identification, quantification, and purity control of VOCs

The analytes were identified by comparison of their retention time and mass spectra with known standards. Further compounds were identified by comparison of the obtained mass spectra with the Nist mass spectral database version 2.0. Primary quantification was done on the Agilent system used for pre-separation against the Scotty TOC EPA 15/17 standard. Compounds not quantified against a standard were quantified on the IRMS via the CO_2 intensities against chloromethane and bromomethane as internal standards. The uncertainty of this procedure is estimated to ±15% on the 1σ level. This estimate is based on tests with known standards at different concentration levels. It is further justified from the variability of the mixing ratios determined for long lived compounds such as chlorodifluoromethane at the coastal sites as the variation of the mixing ratios for these compounds is typically less than a few percent in rural and background air masses.

3.3 Results and discussion

3.3.1 Trapping and desorption efficiency of the sampling system

The trapping and desorption efficiency was tested for the entire sampling procedure on a 0.2 nmole level by injecting 5 mL of the Scott TOC EPA 15/17 and 50 µL of the iodomethane standard into a stream of nitrogen and pre-concentrating the analytes on the cryotrap at a flow of 5 L min^{-1} for 100 min (total volume 500 L). Extraction was done as described above and the recovery rates were calculated against direct injections of the standard mixture onto the Agilent GC-MS system used for pre-separation and quantification.

The results of these tests are given in table 3. The recovery rates for the entire sampling procedure averaged 97.8% (range from 87% to 110%) and the reproducibility ranged from 1% to 7%. Our data indicate a slight decrease of the recovery rates with increasing boiling points for compounds with boiling points above 80°C. However, there are no statistically significant differences between the

recovery rates for direct injection on the adsorption tubes and those for the entire sampling process. Therefore, we conclude that no significant losses of the target analytes occur during sampling.

Table 3: Comparison of the carbon isotope ratios obtained with and without pre-separation for the Scott Speciality Gases TOC 15/17 standard and recovery rates for a sampling volume of 500 L. Results are only given for compounds that were free of interferences from other compounds.

	compound	CAS =	RT =	after pre-separation			direct injection	
				Recovery	$\delta^{13}C$		$\delta^{13}C$	
				mean ±σ	mean ±σ	n	mean ±σ	n
			(s)	(%)	(‰)		(‰)	
1	Propene	115-07-1	743	93±5	-27.9±0.5	6	-	-
2	Chloromethane	74-87-3	744	109±3	-61.3±1.9	6	-	-
3	Methanol	67-56-1	790	-	-39.6±1.8	6	-	-
4	Dichlorodifluoromethane	75-71-8	908	101±2	-31.0±1.9	6	-	-
5	Vinylchloride	75-01-04	1026	107±2	-30.2±1.0	6	-	-
6	Bromomethane	74-83-9	1096	92±7	-61.7±1.8	6	-63.6±0.8	6
7	Chloroethane	75-00-3	1196	102±3	-30.9±0.9	6	-	-
8	1,2-dichloro-1,1,2,2-tetrafluoroethane	76-14-2	1243	-	-27.0±0.8	6	-	-
30	Iodomethane	74-88-4	1548	106±6	-66.8±1.4	6	-	-
9	Trichlorofluoromethane	75-69-4	1608	98±5	-17.0±1.4	6	-	-
11	1,2 Dichloroethene trans	156-60-5	1763	100±4	-21.2±0.9	6	-21.2±1.0	6
12	1,2 Dichloroethene cis	156-59-2	1884	101±4	-20.9±1.1	6	-	-
10	1,1 Dichloroethene	75-35-4	1628	98±4	-29.1±6.6	6	-	-
13	1,1 Dichloroethane	75-34-3	1901	99±5	-22.3±0.6	6	-24.0±0.4	6
14	1,1,2 trichloro- 1,2,2 trifluoroethane	76-13-1	1963	100±3	-24.1±1.3	6	-	-
19	Chloroform	67-66-3	1986	100±5	-44.3±1.6	6	-45.1±1.1	6
15	1,2 Dichloroethane	107-06-2	2094	97±4	-26.8±0.7	6	-	-
20	Benzene	71-73-2	2216	97±2	-26.8±0.5	6	-	-
23	Carbontetrachloride	56-23-5	2225	96±1	-41.1±1.1	6	-	-
29	Hexane	110-54-3	2249	-	-29.9±0.9	6	-	-
	Trichloroethene	79-01-06	2252	96±2	-39.6±0.8	6	-	-
27	Bromodichloromethane	75-27-4	2295	98±2	-50.1±0.8	6	-48.6±0.5	6
21	Cyclohexane	110-82-7	2297	93±3	-27.3±0.6	6	-	-
17	1,1,2 Trichloroethene	79-00-5	2536	95±2	-29.2±1.1	6	-	-
22	Dibromochloromethane	124-48-1	2584	90±2	-44.3±1.4	6	-	-
18	1,2 Dibromoethane	106-93-4	2613	92±2	-21.2±2.5	6	-	-
24	Heptane	142-82-5	2623	98±2	-26.5±1.4	6	-	-
25	Chlorobenzene	108-90-7	2777	93±2	-26.4±1.1	6	-	-
26	Bromoform	75-25-2	2856	87±4	-33.8±2.8	6	-38.6±3.1	6
28	Ethylbenzene	100-41-4	3001	85±3	-27.7±0.8	6	-	-

3.3.2 Reproducibility of the carbon isotope determination

3.3.2.1 Reproducibility versus concentration

Due to the low mixing ratios of some target compounds such as CH_3Br, CH_3I and, $CHBr_3$ (usually <10 pptv), we determined the linearity and reproducibility of the carbon isotope ratios for low levels of carbon in the sub-nmole range. This was performed by repeated injections of chloromethane and bromomethane into the GC-IRMS. The injected carbon amounts ranged from 0.02 to 20 nmol (n ≥ 6

for each concentration level) corresponding to mixing ratios between 1 and 1000 pptv for a 500 L sample. The results of the reproducibility tests are depicted in figure 10.
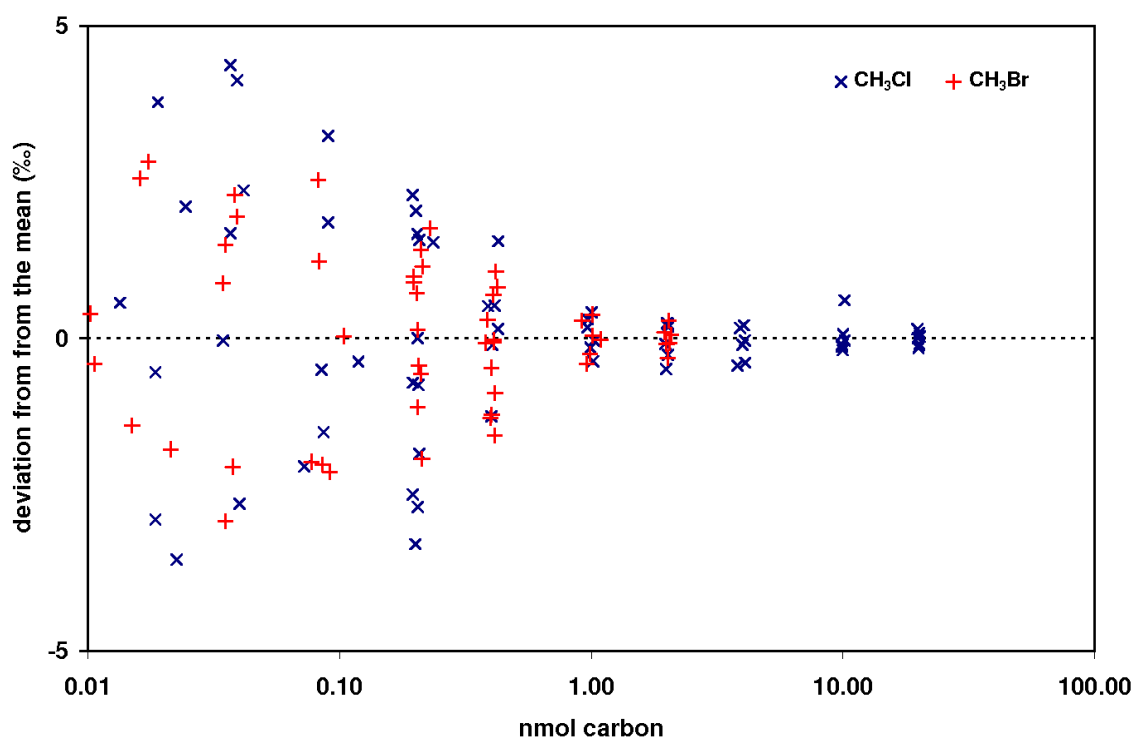
Figure 10: Reproducibility of the δ^{13}C measurements versus the carbon amount for CH$_3$Cl and CH$_3$Br. Results are given as deviation from the mean. The respective means were calculated from all measurements with carbon amounts from 1.0 to 20 nmol. The mean δ^{13}C values of the single component standards were -32.5‰ and -40.7‰ for CH$_3$Cl and CH$_3$Br, respectively.

The carbon isotope ratio determination was free of a systematic bias for carbon amounts down to 0.02 nmole. The overall standard deviation for carbon amounts between 20 and 1 nmole were 0.25‰ for chloromethane (n=30) and bromomethane (n=12), respectively. The standard deviation for each concentration level (n=6) varied between 0.12‰ and 0.30‰. However, below 1 nmole the standard deviation for both compounds increased and was 2.6‰ for chloromethane and 1.8‰ for bromomethane at carbon levels below 0.04 nmole. This corroborates the study of Rudolph et al. (1997) and Redeker et al. (2007) who observed similar deviations for comparable amounts of carbon.

3.3.2.2 Reproducibility of the analytical system

Since the sampling procedure showed an excellent recovery of 98±5%, it is expected to be free of analytical artefacts. Blanks were checked on a routine base at regular intervals and the blanks contributed less than 0.5% to the overall signal. Thus, we can rule out blank contribution as a significant source of bias. Adsorptive losses or incomplete desorption of the target compounds remain as the most important source of bias during sampling. The kinetic isotope effects for such physical processes are generally small. For instance, adsorption of various aromatic hydrocarbons does not appear to cause significant carbon isotope fractionations (Goldstein and Shaw, 2003 and references

therein). Even adsorptive losses of 10% that are associated with a hypothetical kinetic isotope effect of 5‰ would lead to a bias of less than 0.6‰. Thus, the reproducibility of the carbon isotope ratio determination was only tested for the analytical system. The effect of the pre-separation was tested on the 0.2 nmole level with the Scott TOC EPA 15/17 standard. 5 mL of the standard were injected into the GC-MS system, pre-separated and analysed for stable carbon isotope ratios as described in sections 3.2.4.1 and 3.3.4.2. Results were compared to the isotope ratios obtained without pre-separation. Without pre-seperation the isotopic composition could only be determined for 7 compounds because of coelutions and peak overlaps. After pre-separation, isotope ratios for 31 compounds could be determined. The results for these compounds are displayed in table 3.

Standard deviations (n=6) ranged from 0.5‰ for propene and benzene to 2.8‰ for bromoform and generally decreased with increasing numbers of carbon atoms. The average standard deviation for C_1-compounds, C_2-compounds and C_3-compounds were 1.5‰, 1.1‰, and 0.9‰, respectively. A Mann-Whitney-U-test ($p < 0.05$) revealed usually no significant influence of the pre-separation on the carbon isotope ratios. However, a significant difference between both procedures has been observed for bromoform (direct: -38.6±3.1‰; n=6; pre-separation: -33.8±2.8, n=6; p=0.025) and for 1,1-dichloroethane (direct: -24.0±0.4‰; pre-separation: -22.3±0.6, n=6; p=0.004).

3.3.3 Ambient air samples

The carbon isotope ratios and mixing ratios of the ambient air samples as well as results from previous studies are presented in table 4. The range of the carbon isotope ratios of selected halocarbons is depicted in figure 11. Data are only presented for compounds which could be clearly identified either by comparison with standards or by their mass spectra and which met the quality criteria outlined above. In total, we could determine carbon isotope ratios of 37 compounds with mixing ratios between 0.3 pptv for chlorobenzene and up to 1600 pptv for propane. The high amounts of hydrocarbons in urban air samples caused strongly tailing peaks in the IRMS and thus prevented the carbon isotope determination of several organohalogens. This applied for chloroethane, iodomethane, chloroform, and bromoform in all and for carbon tetrachloride and 1,1,2-trichloro-1,2,2-triflouorethane in some of the urban air samples.

Table 4: Averaged concentrations and isotopic values for all compounds reported in this paper from the coastal and the urban sampling site.

Compound	CAS =	RT = (s)	Coastal site mixing ratio mean ±σ (pptv)	δ^{13}C mean ±σ (‰)	n	Urban site mixing ratio mean ±σ (pptv)	δ^{13}C mean ±σ (‰)	n	other studies mean ± σ (‰)
1.1.1 Trifluoroethane *	420-46-2	546	12±0.3	-29.0±1.3	2	13.1±0.4	-35.7±5.3	3	-
Bromotrifluoromethane*	75-63-8	610	3.7±0.2	-39.1±10.3	2	-	-		-
Hexafluoropropene*	116-15-4	687	1.2±0.1	-57.1±1.9	2	-	-		-
Chlorodifluoromethane	75-45-6	703	231±26	-44.2±3.3	3	222.0±25	-53.2±4.6	3	-42.9 ± 5.6 [b]; -33.9 ± 1.0 [c]
Propene	115-07-1	743	61±33	-26.3±1.0	3	73±21	-24.3±2.1	3	25.0 ± 2.5 [b]; -21.6 ± 4.0 [e]
Chloromethane	74-87-3	744	620±30	-36.2±0.7	3	524±36	-39.9±1.9	3	-36.2 ± 0.3 [a]; -39.0 ± 2.3 [b]; -29 to -45 [c]; -37.4 [h]
Propane*	74-98-6	819	193±75	-28.1±0.8	3	1615±413	-29.4±1.3	3	-29.8 ± 1.3 [b]; -27.1 ± 1.5 [e]
Propadiene*	463-49-0	831	-	-	-	10.6±4.1	-18.1±0.3	2	-
Cyclopropane*	75-19-4	834	16±3	-24.9±0.2	2	-	-		-
Dimethylether*	115-10-6	893	10.0±8	-36.5±1.9	3	87±36	-34.1±0.8	3	-
Dichlorodifluoromethane	75-78-1	908	554±88	-41.2±0.2	3	614±60	-37.9±1.1	3	-37.2 ± 3.9 [b]; -33.5 ± 0.8 [c]
Vinylchloride	75-01-4	1026	-	-	-	5.3±3.5	-0.5±2.1	2	-
Bromomethane	74-83-9	1096	7.0±1	-31.0±0.3	3	10.0±3.0	-41.5±3.3	3	-43.0 ± 1.7 [f]
1-Chloro-1.1-difluoroethane*	75-68-3	1112	25±2	-24.6±0.1	3	27.3±1.3	-23.5±3.2	3	-
Isobutane*	75-28-5	1171	15±8	-29.4±1.8	3	503±167	-28.2±1.1	3	-29.0 ± 1.2 [b]
Chloroethane	75-00-3	1196	2.0±0.7	-36.5±1.7	3	-	-		-
Butane*	106-97-8	1243	52±23	-28.3±0.9	3	304±109	-28.0±1.8	3	-28.5 ± 1.1 [b]; -28.5 ± 1.7 [e]
Propenal*	107-02-8	1319	96±140	-24.6±1.5	3	6.1±2.7	-17.2±2.3	3	-
Propene-methyl*	115-11-7	1336	186±99	-25.5±2.1	3	-	-	-	21.4 ± 3.7 [b]
Furane*	110-009	1350	2.1±0.4	-29.3±1.8	3	-	-	-	-
Propanal*	123-38-6	1358	242±86	-24.3±1.8	3	-	-	-	-26.2 ± 2.4 [g]
Iodomethane	74-88-4	1377	2.6±2.1	-53.6±22.6	3	-	-	-	-
2-Butene cis	519-18-1	1570	138±31	-25.5±2.1	3	-	-	-	-25.9 ± 4.9 [b]; -24.5 ± 6.5 [e]
Trichlorfluoromethane	75-69-4	1608	277±14	-31.5±2.6	3	283.0±26	-29.5±5.3	3	-27.3 ± 4.4 [b]
1.1-Dichloro-1-flouorethane*	1717-00-6	1646	22±5	-25.7±3.8	3	8.0±0.9	-15.7±2.9	3	-
Isopentane*	78-78-4	1694	32±22	-29.5±1.6		680±210	-31.7±1.2	3	-28.0 ± 1.9 [b]
2-Butyne*	503-17-3	1736	-	-	-	0.4±0.2	-13.6±8.2	2	-21.7 ± 4.2 [b]
Pentane*	109-66-0	1737	20±10	-31.0±1.2	3	530±100	-28.3±1.4	3	-27.4 ± 2.2 [b]; -27.7 ± 1.3 [e]
1.1.2-Trichloro-1.2.2-Triflouroethane	76-13-1	1963	69±37	-25.4±1.1	3	72±21	-29.3±4.7	2	-23.3 ± 9.6 [a]; -28.1 ± 4.6 [b]
Chloroform	67-66-3	1968	10.0±2.1	-37.2±6.5	3	22±11			-37.4 ± 6.4 [b]; -22.5 ± 1.7 [c]
Carbontetrachloride	56-23-5	2225	104±0	-28.9±1.9	3	92±25	-36.5±5.3	2	-27.1±1.2 [c]
1.2-Dichloropropane	78-87-5	2396	1.1	-29.5	1	-	-	-	-
Trichloroethene	79-01-06	2536	-	-	-	44	-34.4	1	-18.1± 9.1 [c]
Toluene	108-88-3	2660	34±16	-26.8±0.6	3	-	-	-	-33.7 ± 2.0 [g]
Chlorobenzene	108-90-7	2777	0.3±0.1	-26.9±6.8	2	-	-	-	-
Bromoform	75-25-2	2856	2.4±0.5	-18.3±4.6	3	-	-	-	-

* Mixing ratios have been calculated from the CO_2 intensities on the IRMS against chloromethane and bromomethane as internal standards. [a] Thompson et al. (2002); [b] Redeker et al. (2007), [c] Mead et al. (2008a), [d] Tsunogai et al. (1999), [e] Rudolph et al. (2000), [f] Bill et al. (2004), [g] Giebel et al. (2010), [h] Rudolph et al. (1997)

3.3.3.1 Hydrocarbons and oxygenated VOCs

The carbon isotope ratios obtained for the hydrocarbons agree with the results of previous studies (Rudolph et al., 1997; Tsunogai et al., 1999; Redeker et al., 2007). $\delta^{13}C$ values of the alkanes propane, butane, isobutane, pentane and isopentane ranged from -31.8‰ to -25.0‰ with individual standard deviations between 0.8‰ to 2.2‰. Except for butane that co-eluted with 1,2-dichloro-1,1,2,2-tetrafluoroethane, the compounds were well separated. The portion of 1.2-dichloro-1.1.2.2-tetrafluoroethane to the butane carbon was less than 2% in urban samples and there-with negligible. In samples from the coastal site this portion amounted to 5 to 20% and thus may have affected the carbon isotope ratio determination of butane. However, the carbon isotope ratios from both sites showed no significant differences. Even though the average mixing ratios between both sites differed by roughly one order of magnitude (urban site: 304-1620 pptv; coastal site: 11-193 pptv), we observed no significant differences in $\delta^{13}C$ values neither between the alkanes nor between the two sites. This is in line with the small fractionation factors (1.41-3.44‰) reported for the reaction of alkanes with OH-radicals (Rudolph et al., 2000). Furthermore, the alkanes most likely stem from local traffic related sources at both sites and therefore obtain similar isotopic signatures.

On average the alkenes, propene and 2-butene were enriched in ^{13}C by 3.0‰ relative to the alkanes, which is conform to previous studies (Redeker et al., 2007). Propadiene and 2-butyne were even more enriched with $\delta^{13}C$ values of -18.1±0.3‰ and -13.6±8.2‰, respectively. Propene, the only unsaturated hydrocarbon that could be determined at both sites, showed no site specific differences in the $\delta^{13}C$ values. As the atmospheric degradation of propene by OH-radicals is assigned with a considerable fractionation factor of 11.7‰ (Rudolph et al., 2000), the lack of a site specific difference in $\delta^{13}C$ thus points towards local sources rather than towards propene transported over a long distance from urban to coastal areas.

We also could determine carbon isotope ratios of several oxygenated compounds including dimethylether (DME), furane, propanal, and propenal which were identified based on their mass-spectra. The carbon isotope ratios of the aldehydes (-25.4±1.6‰) were mainly in the same range as those of the alkenes with the exception of propenal that was strongly enriched in the urban air samples (-17.2± 2.3‰). Furane showed $\delta^{13}C$ values of -29.0±1.3‰. DME was depleted relative to the saturated hydrocarbons showing a mean $\delta^{13}C$ value of -34.1±0.8‰ in the urban samples and of -37.2‰ at the coastal site.

3.3.3.2 Organohalogens

The mixing ratios of the long-lived CFCs and chloromethane generally fell within ±30% of the atmospheric background levels. The average carbon isotope ratios of the organohalogens covered a broad range of $\delta^{13}C$ values. Vinylchloride was strongly enriched in ^{13}C with an average $\delta^{13}C$ value of 0.5‰. In contrast, hexafluoropropene was strongly depleted in ^{13}C with average $\delta^{13}C$ value of -57.1‰.

Dichlorodifluoromethane (CFC-12): The average mixing ratios of dichlorodifluoromethane (614±60 pptv for the urban site and 554±87 pptv for the coastal site) showed no significant difference between the two sites. The average $\delta^{13}C$ value was -39.6‰ with slightly enriched $\delta^{13}C$ values at the urban site (coastal site: -41.2±0.2‰; urban site: -37.9±1.1‰). Our data are in the range reported by Redeker et al. (2007), who gave an average $\delta^{13}C$ value of -37.1±3.9‰ from a coastal and an urban area in Ireland, but are depleted in comparison to those reported by Mead et al. (2008a) from Bristol, UK (-33.5± 0.8‰).

Chloromethane: Chloromethane mixing ratios were 524±36 pptv for the urban and 620±30 pptv for the coastal site. The $\delta^{13}C$ value average over both sites was -38.0±4.1‰ (n=7) with a slight difference between the urban (-39.9± 1.9‰) and the coastal site (-36.2± 0.7‰). The values mirror previously

Figure 11: Variability of the $\delta^{13}C$ values of selected halocarbons in urban and coastal air samples. Urban air samples are marked with red diamonds and coastal samples are marked with blue dots.

published results. Tsunogai and co-workers (1999) reported an average $\delta^{13}C$ of -36‰ for the marine background in the subtropical Pacific. Thompson et al. (2002) determined an average $\delta^{13}C$ value of -36.4±1.6‰ from a remote site in the arctic (Alert, Canada). Slightly more depleted values of -39± 2.3‰ were reported by Redeker et al. (2007) from Belfast, Ireland.

Bromomethane: The $\delta^{13}C$ values of bromomethane in the urban samples were -41.5±3.3‰ (n=4) being in excellent agreement with the only previous reported values of -43.0±1.7‰ from a suburban site in Berkeley, USA (Bill et al., 2004). At the coastal site the $\delta^{13}C$ values averaged -31.0±0.3‰. This isotopic enrichment by 10‰ is accompanied by a decrease of the average mixing ratios from 10±3 pptv at the urban site to 7±1 pptv at the coastal site. However, this difference in the mixing ratios is mainly driven by one urban sample showing an elevated mixing ratio and thus we cannot state a systematic relation between the carbon isotope ratios and the mixing ratios.

Iodomethane: Iodomethane coeluted with carbon disulfide, dichloromethane, and propenal. Although the mixing ratios in all samples were generally sufficient for the carbon isotope ratio determination we were only able to determine carbon isotope ratios of iodomethane in the coastal samples after a careful adjustment of the time intervals for the fractionation of the samples. Iodomethane belongs to the few compounds revealing a strong within site variation of the carbon isotope ratios. For the three coastal samples determined, $\delta^{13}C$ values were -79.8‰, -40.4‰, and -40.8‰. Given the respective mixing ratios of 1.9, 1.0 and 4.9 pptv no clear relation between variations of the $\delta^{13}C$ values and of mixing ratios becomes evident. Iodomethane has a relative short atmospheric lifetime of only a few days (Harper and Hamilton, 2003). Therefore both, the mixing ratios and the carbon isotope values, more likely provide a snapshot than an integrated signal, which may explain the lack of any correlation. There are no literature data on carbon isotope ratios of atmospheric iodomethane available to compare with. But our own unpublished data from incubation experiments and greenhouse experiments revealed $\delta^{13}C$ values of -47±11‰ for iodomethane emitted from different halophytes which correspond with the more enriched atmospheric values in our study. The strongly depleted $\delta^{13}C$ value was determined in air masses coming from the open North Sea while the more enriched $\delta^{13}C$ values were determined in more coastal influenced air masses. A potential important source in open oceans currently under discussion is the photolytic formation of iodomethane in the sea surface layer (Moore and Zafirou, 1994). Nevertheless, we can currently not substantiate the reasons for the observed large within site variation of the carbon isotope ratios.

Bromoform: A reliable determination of bromoform $\delta^{13}C$ values was only possible in the coastal samples. In the urban air samples the determination was hampered by co-eluting C_8 hydrocarbons. The average $\delta^{13}C$ values of bromoform in the coastal samples was -18.3±4.6‰ (-22.9‰, -13.8‰, and -18.2‰). The isotope ratios reported here were corrected for the isotopic shift observed for the standard (see section 3.3.2.2). Due to this correction we estimated the overall reproducibility for the $\delta^{13}C$ determination of bromoform to ±4.1‰ on the 1σ level. This is close to the natural variability in these samples and it thus remains unresolved weather the variability of the $\delta^{13}C$ values for bromoform reflects the natural variability or simply the analytical uncertainty. As for iodomethane, there are no literature data available on the isotopic composition of atmospheric bromoform. However, similar isotope ratios were reported for bromoform produced in incubation experiments by the brown algae *Fucus serratus* ($\delta^{13}C$ of -15‰) and the planktonic algae *Dunaliella tertiolecta* ($\delta^{13}C$ of -24‰) (Auer et al., 2006). In the same study the $\delta^{13}C$ value of dissolved bromoform in a sea water sample from the Baltic Sea was determined to -28‰.

Chloroethane: $\delta^{13}C$ values of chloroethane could only be determined in the samples from the coastal site. In the urban air samples the tailing of the butane peak impeded a reliable carbon isotope ratio determination of this compound. Average mixing ratios were 2.0±0.7 pptv and the $\delta^{13}C$ values (-36.5 ±1.7‰) were comparable to those of chloromethane.

V*inyl chloride:* Vinyl chloride was only detectable in the urban air samples with mixing ratios of 5.3±3.5 pptv. With an average δ^{13}C-alue of -0.5 ± 2.1‰ it was strongly enriched in ^{13}C as compared to the other chlorinated compounds. To the best of our knowledge, no isotopic data for atmospheric vinylchloride are so far published. Based on our reference standard one might assume a δ^{13}C value of –30.1‰ for industrially produced vinyl chloride. In the atmosphere, vinylchloride is rapidly degraded mainly by OH-radicals. The fractionation factor (ε) of this reaction has not been determined yet. As the OH-radical attacks the double bound it may be in the same order as the ε of 11.4‰ reported for the atmospheric degradation of propene by OH-radicals (Rudolph et al., 2000). In addition, incubation experiments with different soils indicate a large ε of 21.5 to 26.0‰ for the microbial degradation of vinylchloride in soils (Bloom et al., 2000). Thus, this extraordinary high δ^{13}C value of vinylchloride may result from its rapid atmospheric degradation and/or evasion of isotopically enriched vinylchloride from sources such as landfills.

Chloroform: Chloroform stable isotope ratios could only be determined in the coastal samples due to strong chromatographic interferences from 2-methyl-1-butene in the urban samples. δ^{13}C values analysed were -33.8‰, -33.1‰, and -44.8‰. The relative enriched isotope ratios were observed in air masses from the North and North East respectively while the depleted ^{13}C value of -44.8‰ was observed in westerly air masses that passed along the Dutch and the German coast. It is noteworthy that this depletion in ^{13}C for chloroform occurred not in the same sample as the depletion in ^{13}C for iodomethane. This depletion in ^{13}C is surprising as it was not accompanied by significant differences in the mixing ratios (10.0±2.1 pptv, n=3). Anyhow the mixing ratios found here for chloroform were by almost two orders of magnitude lower than those reported by Redeker et al. (2007) but the carbon isotope ratios found here fell into the range of -37.4±6.4‰ given for chloroform in that study. In contrast, the carbon isotope ratios reported for chloroform by Mead et al. (2008a) were on average more than 10‰ enriched in ^{13}C.

Carbontetrachloride: The average found δ^{13}C value of carbontetrachloride was -28.9±1.9‰ (n=3) and average mixing ratios were 104±8 pptv for the coastal site. This agrees well with the results of Mead et al. (2008a) who reported an average δ^{13}C value of -27.1±1.2‰. The average mixing ratio of carbontetrachloride in the urban samples was 92±25 pptv with a mean δ^{13}C value of -36.5±5.3‰. The isotopic signal in the urban air samples might be influenced by incomplete recovery of carbontetrachloride in the target fraction (85 and 90%) and thus has to be taken with great care.

Chlorodifluoromethane: In contrast to dichlorodifluoromethane, chlorodifluoromethane was significantly depleted in ^{13}C at the urban site (δ^{13}C of -53.2±4.6‰) as compared to the coastal site (-44.2±3.3‰). Our values from the coastal site resemble those reported in the study of Redeker et al. (2007) who provided an average δ^{13}C value of -42.9±5.6‰ for Belfast (Ireland). More enriched δ^{13}C values of –33.9±1.0‰, have been reported from Bristol, UK (Mead et al., 2008a). Interestingly, Redeker et al. (2007) observed a slight although statistically not significant enrichment of ^{13}C for

chlorodifluoromethane in northerly air masses as compared to westerly air masses and air masses from Europe.

Trichlorofluoromethane: The isotope ratios of trichlorodifluoromethane were -29.5±5.3‰ for the urban site and -31.5±2.6‰ for the coastal site. As for dichlorodifluoromethane, no significant differences in $\delta^{13}C$ between the sites were observed. Our values corroborate the results of Redeker et al. (2007) who gave an average $\delta^{13}C$ value of -27.3±4.4‰.

1-Chloro-1,1,difluoroethane (HFC-142b): The average $\delta^{13}C$ value for 1-chloro-1,1,difluoroethane was -24.6±2.8.‰ without any significant difference between both sites.

Pentafluoroethane, norflurane and bromotrifluoromethane: Unusually ^{13}C enriched carbon isotope ratios were observed for pentafluoroethane (16.5±5.3‰) and norflurane (4.3±3.3‰). A thorough reanalysis of these data revealed interferences on the m/z 45 and m/z 46 signals. As both compounds elute shortly after carbonylsulfide in an interval where the m/z 46/44 ratio is still affected by sulphur, we presume these interferences to result from the formation of fluoro-sulfur-compounds in the combustion interface or in the ion source. This is further supported by the carbon isotope ratio measurements of bromotrifluoromethane ($CBrF_3$). Interestingly, we observed the opposite effect for bromotrifluoromethane, eluting 15.3 s after carbonylsulfide. In the urban air samples it was recollected in the same fraction as carbonylsulfide and yielded an average $\delta^{13}C$ value of -86.0±0.4‰ Again a reanalysis of our data revealed substantial interferences on the m/z 45 and m/z 46 signal For the coastal samples, where $CBrF_3$ and carbonylsulfide were recollected in different fractions, we obtained an average $\delta^{13}C$ value of -39.1±10.0‰ and found no indication for interferences. As $CBrF_3$ has an average atmospheric lifetime of 65 years and the mixing ratios for both sites were comparable (3.7±0.2 pptv) this huge discrepancy is rather due to the analytical interferences than to atmospheric degradation or source-related processes.

3.3.3.3 Variability of the carbon isotope ratios

Our data reveal considerable isotopic differences between the urban and the coastal sampling site for several compounds. A pronounced enrichment in ^{13}C was observed for 1,1-dichloro-1-fluoroethane (10.0‰) and propenal (7.6‰) in urban samples. The mixing ratios of both compounds were significantly elevated at the coastal site as compared to the urban site (22.6 pptv versus 8.0 pptv and 96 pptv versus 6 pptv) pointing towards a strong coastal or marine source. In contrast, a pronounced enrichment in ^{13}C was observed for bromomethane (10.5‰), chlorodifluoromethane (9.0‰), and 1,1,1-triflouroethane (6.7‰) in coastal samples. Concurrently, chloromethane and 1,1,2-trichloro-1,2,2-trifluoroethane were less enriched (3.6‰ and 4.0‰, respectively).

For chloromethane and bromomethane these differences between both sites are in line with our current understanding of the atmospheric cycling of these compounds. But they are surprising for the long lived CFC's and HCFC's with atmospheric lifetime of several decades along with the lack of any significant actual sources implies a natural variability close to the experimental uncertainty. With exception of the dichlorodifluoromethane measurements at the coastal site, both the within site

variability and the in between site variability exceed what one might expect for such inert tropospheric trace gases. If we compare our data with those of Redeker et al. (2007) and Mead et al. (2008a), it becomes obvious that the repeatability (reproducibility within a lab) reported in all three studies is comparable. But the average $\delta^{13}C$ values reported for several (H)CFC's show substantially larger variations pointing towards a poor reproducibility. For instance the average $\delta^{13}C$ values for dichlorodifluoromethane vary from -33.5 ‰ to -41.2 ‰ and those for chlorodifluoromethane vary from -33.9 ‰ to -53.2 ‰. If the assumption that these trace gases are inert in the troposphere is valid we can currently state only a poor reproducibility for these compounds.

On other hand we can currently not rule out that CFC's and other long-lived organohalogens are degraded in ocean surface waters (Yvon and Butler, 1996; Yvon-Lewis and Butler, 2002). For carbon tetrachloride the oceanic lifetime driven by hydrolysis has been estimated to 2599 days and might be reduced to 94 days due to (micro)biological activity as suggested by Butler et al. (1997). The estimates of oceanic lifetimes of chlorofluorocarbons that showed an isotopic enrichment in our study range from 1100 days to more than 120000 days without considering an additional biological sink in the oceans. As already pointed out by Yvon-Lewis and Butler (2002), there is substantial evidence for a microbial degradation of chlorofluorocarbons from different environmental settings. If such degradation processes also occur in the surface ocean and are assigned with a substantial large fractionation factor, they may imprint the isotopic composition of these trace gases in the atmosphere. Nevertheless, any justification of the isotopic variability of the long lived CFC's and HCFC's require a careful evaluation of potential sources of errors and bias for each compound.

The enrichments in ^{13}C of chloromethane and bromomethane at the coastal site were not accompanied by a significant decrease of the mixing ratios which would point towards an enhanced degradation in the marine boundary layer e.g. due to reactions with chlorine radicals. Therefore, we suppose atmospheric degradation processes not to be the decisive factor for these differences. We assume these isotopic differences are caused by the air sea exchange of these compounds in concert with partial degradation in surface oceans altering the isotopic signatures. Bromomethane from both, intrinsic sources and from the atmosphere, is known to be rapidly degraded in marine surface waters by biotic and abiotic processes with overall degradation rates of up to 20% per day (King and Saltzman, 1997 and references therein). The abiotic degradation due to hydrolysis and transhalogenation is assigned with a large ε of 69±8‰ (King and Saltzman, 1997) and the degradation of bromomethane by methylotrophic bacteria is assigned with an ε of 45±10‰ (Miller et al., 2001). Simultaneously, bromomethane is produced in the surface water. Although the isotopic composition of the intrinsic bromomethane is unknown, it appears reasonable to presume the bromomethane emitted back into the atmosphere to be isotopically enriched considering its rapid degradation and the exceptional strong isotopic fractionation of this process.

3.4 Conclusions

In this study a simple and field suitable cryogenic sampling system for subsequent determination of carbon isotope ratios of a wide range of VOCs was developed. The dry shipper has shown to be a suitable and easy-to-use cooling source that can replace conventional dewars or cryostats in various applications. Up to 30 samples can be taken over a period of two weeks without the need of any technical infrastructure allowing for sampling campaigns in remote areas. Recovery rates for the entire sampling procedure ranged from 92 to 105% with low standard deviations. The analytical repeatability (1σ) for carbon isotope determination on the 0.2 nmole level ranged from 0.5‰ to 2.8‰. With a sampling volume of 500 L, carbon isotope ratios of compounds with typical mixing ratios between 1 and 10 pptv can be determined with a precision better than 2‰. Nevertheless, the determination of these compounds in urban air masses is often hampered by high loads of hydrocarbons.

We reported isotope ratios for a broad range of VOCs in urban and marine air in Northern Germany. Several compounds have not yet been analyzed for their isotopic composition. For the organohalogens having been measured in previous studies the carbon isotope ratios found here are consistent with those previously reported.

The $\delta^{13}C$ values for bromomethane from the urban site of -41.5±3.3‰ are in excellent agreement with those reported by Bill et al. (2004). In contrast, bromomethane $\delta^{13}C$ values were enriched in ^{13}C by about 10‰ in the coastal samples. A similar but less pronounced trend was observed chloromethane. We hypothesize that these differences are related to atmosphere-ocean exchange with fractionating biotic and abiotic degradation processes in the surface ocean and suggest carbon isotope ratio determination as a promising tool for better constraining the role of the ocean in the global cycle of these compounds.

Additional remarks (not part of the publication)

During the course of the PhD work the analytical system was further improved. Thereby, both GC systems described in section 3.2.4 were coupled by a cryogenic interface resulting in a 2D GC. For the purpose of optimal chromatography both GC-oven temperatures and column flow rates were carefully adjusted to each other. As already described, the compounds were thermally desorbed from the sampling tubes, cryofocused, and sent to the GC-MS (Agilent, Gaspro column) for monitoring the sample fractionation. The remainder of about 90% is then directed to an 8 port valco valve equipped with two cryotraps (quartz capillaries). The individual fractions of the samples are then collected on these traps using liquid nitrogen and released directly to the GC-MS-IRMS System (PorabondQ column) (split ratio: ~10% MS, ~90% IRMS). Afterwards the cryotraps can be repeatedly used to scavenge the next fraction with subsequent delivery of compounds to the IRMS. This fractionation process can be manually adjusted ranging from a compound specific trapping to trapping of entire groups of compounds minimizing peak overlaps. Moreover, this improvement allows reacting on certain different matrices such as clean background air or trace gas enriched urban air.

4. Determination of fluxes and isotopic composition of halocarbons from seagrass meadows using a dynamic flux chamber

Ingo Weinberg, Enno Bahlmann, Walter Michaelis, and Richard Seifert

Abstract

Halocarbons are important vectors of reactive halogens to the atmosphere, where the latter participate in several chemical key processes. Many efforts have been made to quantify their sources and sinks. However, those are still designated to large uncertainties. In contrast to other coastal habitats such as salt marshes and kelp communities, seagrass meadows have so far not been investigated with regard to trace gases. In order to study seagrass meadows as a potential source for halocarbons to the atmosphere, we conducted dynamic flux chamber measurements at a coastal site in List/Sylt, Northern Germany. Emissions of halocarbons from seagrass meadows into the atmosphere were found for chloromethane (CH_3Cl), bromomethane (CH_3Br), iodomethane (CH_3I), and bromoform ($CHBr_3$) being the main compounds, while the sediment seems to be a net sink for CH_3Cl and CH_3Br. Stable carbon isotopes of halocarbons were determined using a newly developed comprehensive coupled isotope and mass balance for dynamic flux chambers. Mean stable carbon isotope compositions of the emitted halocarbons were -50‰ (CH_3Cl), -52‰ (CH_3Br), -63‰ (CH_3I) and -14‰ ($CHBr_3$).

4.1 Introduction

Halocarbons, such as chloromethane (CH_3Cl), bromomethane (CH_3Br), and bromoform ($CHBr_3$) are precursors of reactive halogens, which contribute to the destruction of stratospheric ozone (Wofsy et al., 1975; Crutzen and Gidel, 1983; Solomon et al., 1994; Sturges et al., 2000), and, in the case of iodomethane (CH_3I), also to the formation of aerosols in the marine boundary layer (Carpenter, 2003). Known natural sources of halocarbons include salt marshes (Rhew et al., 2000; Manley et al., 2006), oceans (Butler et al., 2007; Quack et al., 2007), algae (Gschwend et al., 1985), fungi (Watling and Harper, 1998), and terrestrial plants (Saini et al., 1995; Saito and Yokouchi, 2006). However, there are still large uncertainties concerning their atmospheric budgets. This particularly holds true for CH_3Br, whose known sinks exceed the known sources by more than 20% (Yvon-Lewis et al., 2009). Though recent modelling and field studies suggest that the atmospheric budget of CH_3Cl can be nominally closed by large emissions from tropical forests (Gebhardt et al., 2008; Saito and Yokouchi, 2008; Xiao et al., 2010), the strength of its known distinct sources are assigned with large uncertainties (Keppler et al., 2005; WMO, 2011). Furthermore, the role of coastal zones as sources for short-lived CH_3I and $CHBr_3$ remain scarcely resolved (Butler et al., 2007).

Incubation experiments have shown the ability of seagrasses to form a variety of halocarbons (Urhahn, 2003), and thus indicate that seagrass meadows might be a source of these compounds. Moreover, seagrass meadows cover a significant portion of global coastal zones with estimates of about 300,000 km^2 (Duarte et al., 2005).

Stable carbon isotopes of halocarbons have been applied to elucidate their sources and sinks (Miller et al., 2001; Bill et al., 2002b; Harper et al., 2003; Bill et al., 2004; Keppler et al., 2004; Bahlmann et al., 2011). This holds especially true for CH_3Cl which has a typical tropospheric background concentration of about 550 ppt (WMO, 2011). The reported $\delta^{13}C$ values of CH_3Cl from different sources cover a broad range of about 100‰ making them a useful tool to infer the sources and sinks of this compound (Keppler et al., 2005). Integrating isotopic data on source signatures and isotopic fractionations associated with degradation processes, atmospheric isotope and mass balances of CH_3Cl and CH_3Br were proposed (McCauley et al., 1999; Keppler et al., 2005; Saito and Yokouchi, 2008). However, still limited isotopic field data are available for CH_3Br (Bill et al., 2002b, 2004) as well as CH_3I and $CHBr_3$, yet (Auer et al., 2006; Bahlmann et al., 2011). This is particularly due to their low atmospheric mixing ratios with tropospheric background concentrations usually in the lower ppt range making the determination of the stable isotope ratios of these halocarbons a challenging task. Most recently, Bahlmann et al. (2011) developed a sampling method which allows determining the stable carbon isotopes of such low-concentrated compounds.

The objectives of this study were i) to provide first flux measurements of halocarbons from a temperate seagrass meadow ii) to improve the isotopic datasets for CH_3Cl and CH_3Br as well as to generate first source-related isotope field data of low concentrated CH_3I and $CHBr_3$ and iii) to develop a comprehensive coupled isotope and mass balance for a dynamic flux chamber system which includes source and sink terms.

4.2 Experimental

4.2.1 Sampling

Sampling was conducted in an intertidal seagrass meadow at List/Sylt (55°1'N, 8°25'E), Northern Germany, from 26th August to 4th September 2010 which is rather end of the growing season (late summer/ autumn). Ambient temperatures averaged 16°C with partly strong cloud cover (181-617 W m^{-2}). The sampled seagrass species were *Zostera marina L.* (n=5) and *Zostera noltii Hornem.* (n=4) which are the dominant species in the study region. The sampled seagrass patches were free of visible epiphytes, and residuals of macroalgae material were removed from the patches to avoid interferences. However, it should be noted that the flux measurements were carried out on the community and not on the species level. The canopy coverage of the two seagrass species were estimated to >80% (*Z. marina*) and 50-60% (*Z. noltii*). The leave biomass above ground enclosed by the chamber was about 16 g (fresh weight) for *Z. marina* and 11 g (fresh weight) for *Z. noltii*. Mixed beds of both species were avoided. Additional flux measurements were carried out above adjacent bare sediment patches

(n=2). The measurements were made during low tide by placing a semicylindrical flux chamber made of quartz glass (0.3 cm wall thickness) directly on the seagrass and bare sediment patches, respectively. Quartz was chosen as an appropriate material for the flux chamber because of its high transparency in the UV band and chemical inertness. The chamber had a headspace volume of 7 L and a bottom surface area of 0.1 m^2. Prior to sampling, it was sealed by surrounding muddy sands. For the simultaneous sampling of the chamber (outlet) and ambient air (inlet), two sampling systems were operated. During the experiments we observed a slight temperature increase between chamber and ambient air ($\leq 5°C$). The sampling was performed as described by Bahlmann et al. (2011). Briefly, air was drawn through the sampling system using membrane pumps (KNF Neuberger N86 KNDC, Freiburg, Germany) at a flow of 1 L min^{-1}. The sampling durations were between 60-90 min resulting in an average air volume of 70 L per sample. Sampling times depended on the tidal conditions and were between 10 a.m. to 6 p.m. local time. The target compounds were enriched in cryotraps, submerged in a dry shipper filled with liquid nitrogen as cooling source. After sampling, the compounds were transferred to adsorption tubes, sealed and stored at -80°C until analysis.

4.2.2 Measurements and quantification

The determination of the mixing ratios and the isotope composition of halocarbons from air samples is described in detail elsewhere (Bahlmann et al., 2011). Briefly, the compounds were thermally desorbed from the adsorption tubes, cryofocused and directed to a GC-MS (6890N/5975B, Agilent, Germany). After chromatographic pre-separation on a Gaspro column (Agilent, 30 m, 0.32 μm i.d.), about 20% of sample is directed to the MS for quantification of the target analytes. The remaining portion is externally fractionated into a target and a residual fraction. This fractionation procedure is to isolate the target compounds from the bulk of co-trapped compounds and hence to avoid peak overlapping during isotope ratio determination. Both fractions are then injected to a GC-MS-IRMS system (DSQ II, DeltaV IRMS, Thermo Finnigan, Germany) equipped with a CP-PorabondQ column (Varian, 25 m, 250 μm i.d.) in order to determine the stable carbon isotopes of the target compounds. The coupled MS was simultaneously operated to monitor the purity of the analytes. Quantification of CH_3Cl, CH_3Br, CH_3I and $CHBr_3$ was performed on the Agilent system used for pre-separation against a working standard (Scott EPA TO 15/17 Sigma-Aldrich, Germany). The analytical precision of the stable carbon isotope determination was $\pm 0.25‰$ for CH_3Cl, $\pm 1.8‰$ for CH_3Br, $\pm 2.2‰$ for CH_3I, and $\pm 2.7‰$ for $CHBr_3$ (Bahlmann et al., 2011).

4.3 Calculations

Halocarbon fluxes have often been determined using static chamber systems (Rhew et al., 2000; Manley et al., 2006; Blei et al., 2010b; Redeker and Kalin, 2012). Here, we employed a dynamic flux chamber as dynamic chambers allow for larger sampling volumes and longer sampling times, which is a prerequisite for determining the carbon isotope ratios of the emitted halocarbons and/or the apparent kinetic isotope effects (KIEs) of the deposition fluxes. Dynamic flux chambers have been widely used

in trace gas studies (Kim and Lindberg, 1995; Gao et al., 1997; Zhang et al., 2002), whereas net fluxes are commonly calculated according to

$$F_{Net} = \frac{Q_N \times (C_{out} - C_{in})}{A \times V_N \times 1000} \times 60 \tag{1}$$

where F_{Net} is the net flux (nmol m^{-2} h^{-1}), Q_N is the flushing flow rate through the chamber (L min^{-1}, at 1013.25 mbar and 298.15 K), C_{out} and C_{in} are the air mixing ratios of target compounds (ppt) at the outlet and the inlet of the flux chamber, respectively, A is bottom surface area of the flux chamber (m^2), and V_N (L) is the molar volume at 1013.25 mbar and 298.15 K. The number 60 results from the conversion from min^{-1} to h^{-1}.

Moyes et al. (2010) and Powers et al. (2010) used a dynamic flux chamber to determine the fluxes and isotope ratios of CO_2 effluxes from soils. The authors proposed a mass weighted isotope balance to calculate the isotope ratios of the emitted CO_2 from the mixing and isotope ratios measured at the inlet and outlet, respectively. However, their approach does not account for simultaneous occurring emission and deposition fluxes between the plant soil system and the chamber air. For practical reasons a differentiation between different sources is often not feasible. Moreover, for inferring the atmospheric budgets of trace gases it is in most cases sufficient to obtain source-related isotope signatures and/or apparent KIEs on the community level. Nevertheless, it is necessary to differentiate between the sources and sinks as both may be affected by the flux chamber system, which may in turn lead to biases in the determination of the source related carbon isotope ratios. It is well known that flux chambers may alter trace gas fluxes across interfaces i) by altering the aerodynamic resistance at the interface (Zhang et al., 2002) and ii) by altering the concentration gradient across the interface (Gao et al., 1997). While modifications of the aerodynamic resistance will affect emission and deposition fluxes equally, changes of the concentration gradient will have opposite effects on the emission fluxes and the deposition fluxes (e.g. an increase of the headspace concentration inside the chamber is prone to suppress emission fluxes but increase deposition fluxes). Therefore, we developed a more comprehensive model covering both processes (figure 12).
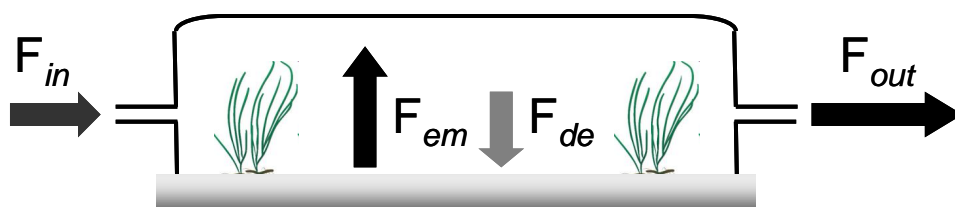
Figure 12: Scheme of the dynamic flux chamber. Respective mass flows of halocarbons are given in nmol h^{-1}. F_{in}= mass flow at the inlet; F_{out}= mass flow at the outlet; F_{em}: emission flux at the outlet; F_{de}= deposition flux inside the chamber

Due to the high inertness of the chamber material and atmospheric lifetime of halocarbons that by far exceeds the turnover rate of the chamber we assumed blanks and losses due to reactions in the

chamber air being negligible. Hence for steady state conditions the mass balance of the chamber is given by:

$$F_{in} + F_{em} + F_{out} + F_{de} = 0 \tag{2}$$

Here, F_{in} and F_{out} are the mass flows (nmol h^{-1}) at the inlet and the outlet, respectively. F_{em} denotes the sum of the internal sources (nmol h^{-1}) and F_{de} (nmol h^{-1}) the sinks inside the chamber. By definition F_{de} and F_{out} are negative while F_{in} and F_{em} are positive. Here the net flux (F_N) is not normalised to the bottom surface area and is defined as:

$$F_N = F_{em} - F_{de} = -(F_{out} + F_{in}) \tag{3}$$

The stable carbon isotope ratios are expressed in the δ-notation (in ‰) relative to the Vienna Pee Dee Belemnite (V-PDB) standard:

$$\delta^{13}C = \left[\frac{\left({}^{13}C/{}^{12}C_{sample} - {}^{13}C/{}^{12}C_{standard} \right)}{{}^{13}C/{}^{12}C_{standard}} \right] \times 1000 \tag{4}$$

The mass weighted isotope balance for the dynamic flux chamber system is derived from McCauley et al. (1999), who proposed a mass weighted isotope balance for constraining the atmospheric budget of CH$_3$Br. In the δ-notation the mass weighted isotope balance for the dynamic flux chamber can be written as:

$$\delta^{13}C_{chamber} = \frac{\left(\delta^{13}C_{in} \times F_{in} + \overline{\delta^{13}C_{em}} \times F_{em} \right)}{\left(F_{in} + F_{em} \right)} + \frac{\left(\overline{KIE_{de}} \times F_{de} + KIE_{out} \times F_{out} \right)}{\left(F_{de} + F_{out} \right)} \tag{5}$$

where $\delta^{13}C$ denotes the carbon isotope ratio of a compound and the KIE denotes the apparent kinetic isotope effect (‰) assigned to a sink for this compound. The indices are the same as used for the fluxes in equation 2 and 3.

As a consequence of the steady state conditions we can assume that $\delta^{13}C_{chamber}$ is equal to $\delta^{13}C_{out}$ and consequently the KIE_{out} is 0. Thus, equation 5 simplifies to:

$$\delta^{13}C_{out} = \frac{\left(\delta^{13}C_{in} \times F_{in} + \overline{\delta^{13}C_{em}} \times F_{em} \right)}{\left(F_{in} + F_{em} \right)} + \frac{\left(\overline{KIE_{de}} \times F_{de} \right)}{\left(F_{de} + F_{out} \right)} \tag{6}$$

With $F_{in} + F_{em} = -(F_{de} + F_{out})$ (eq. 2) rearrangement of eq. 6 leads to:

$$\delta^{13}C_{em} = \frac{\left(-\delta^{13}C_{out} \times (F_{out} + F_{de}) + \overline{KIE_{de}} \times F_{de} - \delta^{13}C_{in} \times F_{in} \right)}{F_{em}} \tag{7}$$

Similarly for a net sink the apparent fractionation factor can be calculated according to:

$$\overline{KIE_{de}} = \frac{\left(\delta^{13}C_{in} \times F_{in} + \overline{\delta^{13}C_{em}} \times F_{em} + \delta^{13}C_{out} \times (F_{out} + F_{de}) \right)}{F_{de}} \tag{8}$$

With $\overline{\delta^{13}C_{em}} \times F_{em} = \sum_{i=l}^{n} \delta^{13}C_{em_i} \times F_{em_i}$ and $\overline{KIE_{de}} \times F_{de} = \sum_{l=l}^{n} KIE_{de_i} \times F_{de_i}$ the model can be extended to cover multiple sources and sinks.

4.4 Results and Discussion

4.4.1 Fluxes

Average fluxes of CH_3Cl, CH_3Br, CH_3I and $CHBr_3$ for seagrass covered areas and sediments are given in table 5 and individual fluxes in table A1 (Appendix).

Table 5: Average net fluxes (nmol m^{-2} h^{-1}) of halocarbons from the two seagrass species *Z. marina* and *Z. noltii* covered areas from five sampling days during low tide. The sampling times were between 10 a.m. and 6 p.m., local time. Values in parentheses refer to the range of fluxes. Fluxes for sediment incubations are given as single values. n.d.: not detected.

	Z. marina (n=5)	*Z. noltii* (n=4)	Sediment (n=2)
CH$_3$Cl	4.7 (1.23-9.70)	7.8 (2.29-10.11)	-2.16, -3.66
CH$_3$Br	0.1 (-0.01-0.21)	0.3 (0.16-0.36)	-0.04, -0.08
CH$_3$I	0.8 (0.13-2.29)	0.9 (0.52-1.37)	0.02, 0.19
CHBr$_3$	0.3 (0.02-0.70)	0.4 (0.08-0.50)	n.d.

The seagrass meadows were a net source for all investigated halocarbons although slight deposition fluxes of CH_3Br were occasionally detected above *Z. marina*. The fluxes of all monohalomethanes emitted from seagrass meadows were correlated to each other ($r^2 \geq 0.61$, $p<0.05$, n=9). In contrast, the emitted $CHBr_3$ from both seagrass species showed no correlation to the monohalomethanes. This may suggest an either different source or a different production mechanism. The experiments over bare sediment revealed a net consumption of CH_3Cl and CH_3Br. In contrast, CH_3I was emitted from the sediments in considerable amounts. Thus, the sediments seem to play a significant role regarding the dynamics of monohalomethanes within the seagrass ecosystem. The net consumption of CH_3Cl and CH_3Br confirms various studies reporting degradation processes of both compounds in soils and sediments (Oremland et al., 1994; Shorter et al., 1995; Hines et al., 1998; Rhew et al., 2003; Miller et al., 2004; Redeker and Kalin, 2012). Emissions of CH_3I are reported from marine algae (Nightingale et al., 1995) and phytoplankton (Manley and de la Cuesta, 1997). A possible microbial source for CH_3I associated to decaying seaweed material was pointed out by Manley and Dastoor (1988). Amachi et al. (2001, 2003) revealed the ability of various microbial strains to produce enzymatically CH_3I in soils and sediments.

The halocarbon fluxes were characterized by a high variability. These variations of halocarbon fluxes were previously reported from other coastal systems and attributed to biomass (Rhew et al., 2002), diurnal cycles (Blei et al., 2010b), and tidal cycles (Carpenter et al., 1999). Due to the limited dataset our study cannot account for such effects and depicts rather a baseline study for future research. However, maximum CH_3Cl fluxes from the seagrass meadows found here are in the same order of magnitude as mean fluxes reported from salt marshes in temperate regions (Valtanen et al., 2009; Blei et al., 2010b), but at least one order of magnitude lower than fluxes from subtropical salt marshes in California, USA (Rhew et al., 2000; Manley et al., 2006). Fluxes of CH_3Br from seagrass meadows

were distinctly lower than those from salt marsh vegetation (Rhew et al., 2000; Manley et al., 2006; Blei et al., 2010b). In contrast, fluxes of CH_3I observed from seagrass incubations are in good agreement with fluxes from most of Californian salt marsh plants (Manley et al., 2006). The emissions of CH_3I and $CHBr_3$ from seagrass meadows were clearly below those obtained from incubation experiments of macroalgae (Carpenter et al., 2000).

4.4.2 Isotopic composition

In order to calculate the apparent KIEs for the sedimentary sink of CH_3Cl and CH_3Br, we assumed negligible contributions from an additional sedimentary source. Thus, eq. 8 simplifies to

$$\overline{KIE}_{de} = \frac{F_{in} \times \left(\delta^{13}C_{in} - \delta^{13}C_{out}\right)}{-(F_{out} + F_{in})} \tag{9}$$

With this assumption the sedimentary sink of CH_3Cl was accompanied with an apparent KIE of 9 and 6‰. This rather low fractionation is in contrast to KIEs found for bacterial and enzymatic degradation processes of CH_3Cl ranging from 21 to 50‰ (Miller et al., 2001, 2004). The observed relatively low KIEs may either be attributed to an unidentified sedimentary source or may indicate that the bacterial degradation is not the rate limiting step. We found apparent KIEs of 22 and 59‰ for the sedimentary sink of CH_3Br. The KIE of 22‰ is similar to those determined under field conditions by Miller et al. (2001) (17‰) and Bill et al. (2002a) (11.6‰). The higher fractionation factor of 59‰ corresponds to the values ranging between 57 and 72‰ obtained by Miller et al. (2001, 2004) from incubation experiments. Thus, the severely different KIEs observed for the sedimentary sink of CH_3Br and CH_3Cl may result from variations between the relevance of distinct degradation processes and possible additional sedimentary sources. From the experiments above the bare sediments we calculated the deposition velocity (k_{de}, (mol h^{-1}x 0.001)) for both compounds according to:

$$F_{de} = c_{chamber} \times k_{de} = c_{out} \times k_{de} \tag{10}$$

Under the assumption of comparable deposition velocities above the bare sediment patches and the seagrass spots, the isotopic composition of the CH_3Cl and CH_3Br emitted from the seagrass was finally calculated according to:

$$\overline{\delta^{13}C}_{em} = \frac{\left(-\delta^{13}C_{out} \times (F_{out} + F_{de}) + \overline{KIE}_{de} \times c_{out} \times k_{de} - \delta^{13}C_{in} \times F_{in}\right)}{F_{em}} \tag{11}$$

The calculated carbon isotope ratios for CH_3Cl and CH_3Br with and without sink correction are presented in table 6.

Table 6: Calculated average $\delta^{13}C$ values (‰) and absolute standard deviations of CH_3Cl and CH_3Br without sink correction and with sink correction. KIEs and degradation rates are derived from two incubation experiments above bare sediment (see text and table A2, Appendix).

	$\delta^{13}C$ without sink correction	$\delta^{13}C$ with sink correction	
CH_3Cl		Scenario A	Scenario B
average	-53.7 ± 18.0	-49.9 ± 8.6	-50.2 ± 5.5
n	9	9	9
CH_3Br		Scenario A	Scenario B
average	-32.9 ± 5.2	-47.2 ± 8.5	-57.1 ± 4.2
n	7	9	8

The mean outliers were eliminated by a Grubbs test (p<0.05). Due to the variable apparent KIE and/or deposition rates obtained in particular for the sedimentary sink of CH_3Br the $\delta^{13}C$ values were calculated separately in two scenarios (A and B) using the results from the two sediment experiments (details can be found in table A2, Appendix). Without sink correction the isotopic composition of the CH_3Cl emitted from the seagrass meadows is calculated to -53.7± 18.0‰. After sink correction using the two data sets from the sediment incubations we obtain -49.9± 8.6‰ (scenario A) and-50.2 ± 5.5‰ (scenario B). For CH_3Br, the calculated $\delta^{13}C$ value was -32.9± 5.2‰ without sink correction. Here, the low variability of the isotopic signal results from the removal of two extreme values (-5.8‰ and -225.8‰). In contrast, integration of the sink function yields values of -47.2± 8.5‰ (scenario A) and -57.1± 4.2 (scenario B). These variations are on the one hand due to the different KIEs and deposition rates derived from the sediment incubations. On the other hand, the differences between both scenarios were increased when the difference between the mixing ratios at the inlet and the outlet were rather small resulting in enhanced uncertainties regarding the determination of the mixing ratios. Thus, using the average of the sink corrected values from both scenarios the best estimate for the isotopic CH_3Br is -51.8± 8.3‰.

While the uncorrected results indicate large differences in the isotopic composition of CH_3Cl and CH_3Br, the sink corrected $\delta^{13}C$ values for both compounds are comparable. This is in line with a common source as indicated by the correlation of the fluxes of both compounds. Previous studies revealed strong fractionations of 20-50‰ relative to the respective bulk biomass during the enzymatic generation of CH_3Cl in e.g. higher plants and fungi via the methyl donor S-adenosyl-L-methionine (SAM) (Harper at al., 2001, 2003, Saito and Yokouchi, 2008). Assuming the same metabolic production mechanism, the CH_3Cl and CH_3Br emitted produced within the seagrass meadows should possess isotopic values as reflected by the sink corrected values rather than by those without sink correction.

Since the isotopic values for CH_3I and $CHBr_3$ measured in the inlet were below the detection limit, an isotope and mass balance was not contrivable for these compounds. However, due to the high enrichment of these compounds in the chamber air, the isotopic composition at the inlet should bear a

rather small influence on the isotopic composition at the outlet. Furthermore, we did not detect any deposition fluxes of both compounds during our sediment incubations which may have an effect on the isotopic signals. Accordingly, using the mean isotopic data of CH_3I (-53.6‰) and $CHBr_3$ (-18.3‰) reported by Bahlmann et al. (2011) from ambient air samples of a nearby site as inlet values, the resulting effect on the $\delta^{13}C$ of the emissions were ≤4‰ for CH_3I and ≤2‰ for $CHBr_3$.

The calculated isotopic compositions of halocarbons emitted by the seagrass meadows are given in table 7 in comparison to those previously reported for other natural sources.

Table 7: Average $\delta^{13}C$ values (‰) of halocarbons and absolute standard deviations emitted from the two seagrass species _Z. marina_ and _Z. noltii_ covered areas in comparison to reported natural sources.

Source	CH_3Cl	CH_3Br	CH_3I	$CHBr_3$
Salt marshes [a]	-62 ± 3	-43 ± 2	-	-
Tropical plants [b]	-83 ± 15	-	-	-
Fungi [c]	-43 ± 2	-	-	-
Macroalgae [d]	-	-	-	-15
Phytoplankton [d]	-	-	-	-23
Senescent and leaf litter [e]	-135 ± 12	-	-	-
Oceans [f]	-38 ± 4	-	-	-
Seagrass meadow [g]	-50 ± 7	-52 ± 8	-63 ± 11	-14 ± 5

[a] emission weighted daily means from Bill et al. (2002b)
[b] mean values from Saito and Youkouchi (2008)
[c] mean values from Harper et al. (2001)
[d] Auer et al. (2006)
[e] mean of heating experiments at 40°C from Keppler et al. (2004)
[f] Komatsu et al. (2004)
[g] this study, values of CH_3Cl and CH_3Br account for their respective sink terms obtained from two sediment incubations based on their respective scenario calculations (see text and Table A2, Appendix).

For CH_3Cl and CH_3Br, the mean calculated isotope values from the both scenarios from seagrass meadows were -50± 7‰ and -52±8 ‰, respectively. The values for CH_3Cl are about 10‰ ^{13}C-enriched and about 10‰ depleted for CH_3Br compared to those of Bill et al. (2002b) who reported emission weighted mean $\delta^{13}C$ values of -63± 3‰ (CH_3Cl) and -43± 2 ‰ (CH_3Br) from a coastal salt marsh in California. However, the authors observed a strong diurnal shift in $\delta^{13}C$ values ranging from -45‰ to -71‰ for CH_3Cl and -2‰ to -65‰ for CH_3Br with more ^{13}C-enriched values and lower fluxes at night for both compounds. The authors provided two hypotheses to explain this diurnal variability; i) changing ratios in the production and degradation with the latter having a more pronounced effect during low emission events (nighttime) and ii) a diurnal variation in the isotopic composition of the precursor of the monohalomethanes, in this case presumably SAM. Although our measurements did not cover the whole diurnal cycle, our results rather support the first hypothesis and underline the need to account for intrinsic sinks when determining isotopic source signatures of atmospheric trace gases.

An alternative production mechanism utilizing pectin as methyl donor during senescence of plant material has been suggested for CH_3Cl (Hamilton et al., 2003; Keppler et al., 2004). The resulting $\delta^{13}C$ values of CH_3Cl by this abiotic formation are extremely depleted in comparison to those from the seagrass meadow (table 7). The production rates of CH_3Cl increase drastically with decreasing water

content. Since living seagrass material contains a lot of water, it is uncertain to which degree the abiotic mechanism can take place. Thus, we assume that this production pathway is negligible for the CH_3Cl emissions from seagrass meadows.

With regard to CH_3I emissions, the stable carbon isotopes differed between both seagrass species. We observed isotopic values of -53‰ for *Z. marina* being in the same range as those detected for CH_3Cl and CH_3Br. In contrast, the values from *Z. noltii* were more depleted in ^{13}C (-72 ± 6‰). Presumably, CH_3I emissions from the sediments may have altered the isotopic source signal of the seagrass emission. Unfortunately our isotopic data for the sedimentary emission are not sufficient to account for this second source. Amachi et al. (2001, 2003) reported bacteria-mediated production of CH_3I from soils and sediments. As for higher plants, the methylation of iodine proceeds with SAM as the substrate (Wuosmaa and Hager, 1990). Thus, the formation of CH_3I by this additional source would presumably also lead to rather depleted isotopic values. However, at this stage of our investigations, the origin of the differing isotope values between the two seagrass species remains unclear. To the best of our knowledge, isotopic data for CH_3I were only reported by Bahlmann et al. (2011), so far. They found $\delta^{13}C$ values between -41‰ and -80‰ in air samples of a coastal site adjacent to the seagrass meadow in Northern Germany. Although the available data for CH_3I are quite limited, there is some evidence that CH_3I has rather depleted $\delta^{13}C$ values compared to other monohalomethanes but is subject to varying fractionation processes which should be investigated in the future.

As for CH_3I, we observed isotope ratio differences of $CHBr_3$ between the emissions of the two seagrass species. The values for $CHBr_3$ were -17± 2‰ for *Z. marina* and -10± 2‰ for *Z. noltii*, respectively. This ^{13}C-enrichment of $CHBr_3$ is substantial compared to the other halocarbons. The production mechanism of $CHBr_3$ may have a significant effect on the $\delta^{13}C$ values for this compound. In contrast to monohalomethanes, polyhalomethanes are presumably formed via a haloperoxidase catalyzed reaction and a haloform reaction with repeated electrophilic halogenation of the substrate (Manley, 2002). To the best of our knowledge no fractionation factors for this particular reaction are available. However, electrophilic halogenations are assigned with a fairly low fractionation (Kokil and Fry, 1986), which presumably explains the generally enriched $\delta^{13}C$ values of $CHBr_3$. These strongly enriched isotope ratios of $CHBr_3$ are in accordance with data from incubation experiments of macroalgae and phytoplankton (-15 to -23‰) (Auer et al., 2006) as well as from ambient air samples in Northern Germany (-13.5± 4.6‰) (Bahlmann et al., 2011).

4.5 Conclusions

Seagrass meadows are a source for the halocarbons CH_3Cl, CH_3I, CH_3Br, and $CHBr_3$ to the atmosphere. For CH_3Cl and CH_3I the emission rates are close to those observed for salt marshes in temperate regions. However, any quantitative measurements of halocarbon emissions from seagrass meadows require more detailed studies. They should examine seagrass ecosystems of different regions in order to extrapolate to global scales. These investigations must include diurnal and seasonal cycles as well as the determination of halocarbon fluxes during tidal inundation.

The use of stable carbon isotope ratios to infer the atmospheric budgets of trace gases requires precise measurements of source-related isotopic data and information on isotopic fractionation factors. In order to gain source-related isotopic data from seagrass meadows we applied a coupled mass and isotope balance which integrates source and sink terms for trace gases. It was demonstrated that it is necessary to account for production and degradation processes in order to decrease uncertainties in isotopic data. Accordingly, the $\delta^{13}C$ values of CH_3Cl with sink correction reduced the variability in comparison to the uncorrected values. Moreover, the integration of the sink function for CH_3Br increases the number of valid isotopic data accompanied with more depleted values by almost 20‰. The isotopic values of CH_3Cl are distinguishable from other natural sources such as salt marshes and tropical plants, and fungi (table 7). Isotopic data of CH_3Br resembles those of CH_3Cl suggesting a common source (mechanism) which was also observed in correlation analysis of fluxes. First isotopic field data of CH_3I indicate rather depleted values as for other monohalomethanes studied. However, there are still some unresolved findings regarding the fractionation processes of CH_3I and the contribution of the sediments. As previously reported, the isotopic values of $CHBr_3$ were strikingly enriched in ^{13}C in comparison to those of monohalomethanes.

5. A halocarbon survey from a seagrass dominated subtropical lagoon, Ria Formosa (Portugal): Flux pattern and isotopic composition

Ingo Weinberg, Enno Bahlmann, Tim Eckhardt, Walter Michaelis, and Richard Seifert

Manuscript

Abstract

Here we report fluxes of chloromethane (CH_3Cl), bromomethane (CH_3Br), iodomethane (CH_3I), and bromoform ($CHBr_3$) from two sampling campaigns (summer and spring) in the seagrass dominated subtropical lagoon Ria Formosa, Portugal. Dynamic flux chamber measurements were performed when seagrass patches were air-exposed and submerged. Overall, we observed highly variable fluxes from the seagrass meadows and attributed them to diurnal cycles, tidal effects, and the variety of possible sources and sinks in the seagrass meadows. Highest emissions with up to 130 nmol m^{-2} h^{-1} for CH_3Br were observed during tidal changes from air exposure to submergence and conversely. Furthermore, at least during the spring campaign, the emissions of halocarbons were significantly elevated during tidal inundation as compared to air exposure.

Accompanying water sampling during both campaigns revealed elevated concentrations of CH_3Cl and CH_3Br indicating productive sources within the lagoon. Stable carbon isotopes of halocarbons from the air and water phase along with source signatures were used to allocate the distinctive sources and sinks in the lagoon. Results suggest CH_3Cl rather originating from seagrass meadows and water column than from salt marshes. Aqueous and atmospheric CH_3Br was substantially enriched in ^{13}C in comparison to source signatures for seagrass meadows and salt marshes. This suggests a significant contribution of the water column to the atmospheric CH_3Br in the lagoon.

A rough global upscaling yields annual productions from seagrass meadows of 2.3-4.5 Gg yr^{-1}, 0.5-1.0 Gg yr^{-1}, 0.6-1.2 Gg yr^{-1}, and 1.9-3.7 Gg yr^{-1} for CH_3Cl, CH_3Br, CH_3I, and $CHBr_3$ respectively. This suggests a minor contribution from seagrass meadows to the global production of these halocarbons with about 0.1 % for CH_3Cl and about 0.7 % for CH_3Br.

5.1 Introduction

The halocarbons chloromethane (CH_3Cl), bromomethane (CH_3Br), iodomethane (CH_3I), and bromoform ($CHBr_3$) are prominent precursors of reactive halogens which affect the oxidative capacity of the atmosphere and initiate stratospheric ozone destruction (Saiz-Lopez and von Glasow, 2012 and references therein). Furthermore, CH_3I may further contribute to the formation of aerosols in the marine boundary layer (Carpenter, 2003). Therefore, during the last decades, the sources and sinks of these trace gases were intensively studied.

For CH_3Cl, recent atmospheric budget calculations suggest that the known sinks can be balanced by large emissions from tropical terrestrial sources (Saito and Yokouchi, 2008; Xiao et al., 2010). Nevertheless, these calculations still incorporate large uncertainties. The atmospheric budget of CH_3Br remains still out-weighted with the known sinks exceeding known sources by about 30% (Yvon-Lewis et al., 2009). The current emission estimates for CH_3I and $CHBr_3$ are assigned with even larger uncertainties (Bell et al., 2002 and reference therein; Quack and Wallace, 2003 and references therein).

Stable carbon isotopes of halocarbons have been applied to further elucidate their sources and sinks by using individual source signatures (Keppler et al., 2005 and references therein). While this was primarily done for CH_3Cl, first isotopic source signatures of naturally-produced CH_3Br were recently reported (Bill et al., 2002; Weinberg et al., 2013). Moreover, the biogeochemical cycling of halocarbons underlies various transformation processes which can be studied by the stable carbon isotope approach in addition to flux and/or concentration measurements.

Coastal zones are reported being vital source regions of halocarbons. In these salt water affected systems halocarbon producers comprise phytoplankton (Scarratt and Moore, 1996, 1998), macroalgae (Gschwend et al., 1985), salt marshes (Rhew et al., 2000), and mangroves (Manley et al., 2007).

Seagrass meadows are one of the most productive ecosystems with a similar global abundance as mangroves and salt marshes (Duarte et al., 2005). They cover huge areas of the intertidal and subtidal as well in temperate as in subtropical/tropical regions. Thus, they may represent an additional source for halocarbons to the atmosphere which is not sufficiently studied, yet. Seagrass meadows are highly diverse ecosystems with respect to potential halocarbon producers. Along with the seagrass itself, they comprise epiphytes such as microalgae and diatoms, and sediment reassembling microphytobenthos and bacteria communities. All these constituents of the benthic community have been generally reported to produce halocarbons (Tokarczyk and Moore, 1994; Moore et al., 1996; Amachi et al., 2001; Rhew et al., 2002; Urhahn, 2003; Manley et al., 2006; Blei et al., 2010a). While first evidence for the release of halocarbons from seagrass was obtained by incubation experiments (Urhahn, 2003), we could recently confirm this production potential in a field study of a temperate seagrass meadow in Northern Germany (Weinberg et al., 2013).

In order to refine these results we conducted two field campaigns in the subtropical lagoon Ria Formosa, Portugal in 2011 and 2012. Here we report the results of these campaigns comprising dynamic flux chamber measurements for halocarbons over seagrass meadows during air exposure and tidal inundation. Using the flux and isotopic data, we present first insights in the environmental controls of halocarbon dynamics within this ecosystem. To complement the chamber-based measurements, the results of a series of air and water samples for dissolved halocarbons and their isotopic composition from both campaigns are discussed. Finally, we compare seagrass meadows emission rates of halocarbons with those of other coastal sources and give a first rough estimation of the seagrass source strength on a global scale.

5.2 Materials and methods

5.2.1 Sampling site

The Ria Formosa, covering a surface area of 84 km^2, is a mesotidal lagoon at the South-eastern coast of the Algarve, Portugal (figure 13). It is separated from the Atlantic Ocean by a series of barrier islands and two peninsulas. About 80% of the lagoon is intertidal with a semi-diurnal tidal regime and tidal ranges between 1.3 m during neap tides and 3.5 m during spring tides (Cabaço et al., 2012). Due to negligible inflow of fresh water and high exchange of water with the open Atlantic during each tidal cycle, the salinity within the lagoon is 35 to 36 year round, except for periods of heavy rainfalls. About one-fourth of the intertidal (13.04 km²) is covered by dense stands of *Zostera noltii Hornem* (Guimarães et al., 2012; Rui Santos, pers. comm.) Further but much less abundant seagrass species in the lagoon are *Zostera marina L.* and *Cymodocea nodosa (Ucria) Ascherson* which are mainly located in shallow parts of the subtidal (Santos et al., 2004). About 30% of the lagoon's area is covered with salt marsh communities (Rui Santos, pers. comm.).
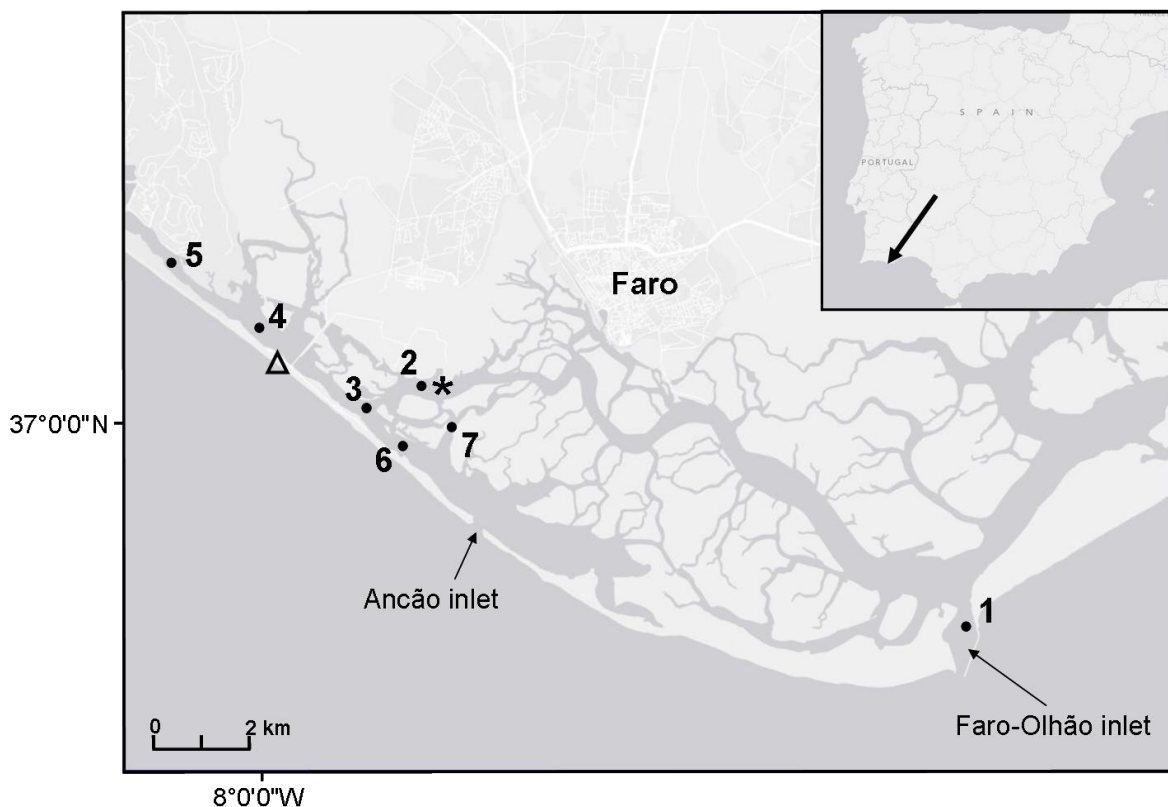
Figure 13: Map of the lagoon Ria Formosa, Portugal. Asterisk: site of seagrass meadow studies; triangle: sampling site on the Praia de Faro (upwind position). Dots with numbers represent sampling points during the transect cruise.

5.2.2 Sampling

We conducted two sampling campaigns in the western part of the lagoon at the Ramalhete research station (Centre of marine Sciences (CCMAR), Universidade do Algarve) in the vicinity of Faro

(37.0°N, 7.6 W) (figure 13). The sampling was carried out from July 23rd – August 7th 2011 and April 17th – April 28th 2012 coinciding with the beginning (2012 campaign) and peak (2011 campaign) of the seagrass reproductive season. Ambient air temperatures were distinctively different between both campaigns ranging from 21 to 27°C (mean 24°C) with almost entirely clear weather in summer and 13 to 23°C (mean 17°C) in spring with frequent strong cloud cover. Mean water temperatures were 25.9°C (summer) and 17.5°C (spring). The prevailing wind direction during both campaigns was West to South-West to with rather low average wind speeds of 4 m s^{-1} during summer and 5 m s^{-1} during spring.

During the two campaigns we used different dynamic flux chamber systems. Firstly, during the 2011 campaign, we measured the halocarbon fluxes during air exposure using a quartz-glass chamber as described in Weinberg et al. (2013) with some adjustments. For this study a permanent backup flow (3± 0.2 L min^{-1}) through the flux chamber during sampling and the change of cryotraps was applied to ensure sufficient mixing. Further, to overcome analytical problems with the high humidity in the sampled air, the water content was reduced using a condenser (-15°C). Briefly, the quartz-glass flux chamber was placed on the seagrass patch and sealed with surrounding sediment. Two sampling systems were operated simultaneously measuring inlet and outlet air of the flux chamber (flow rate 1± 0.2 L min^{-1}). Prior to sampling, the flux chamber was flushed for about 10 min ensuring sufficient equilibration of compounds in the chamber air.

During the 2012 campaign, we used a dynamic flux chamber system suitable for flux measurements during both, periods of air exposure and tidal immersion. The properties and setup of this dynamic chamber system is in detail described elsewhere (Bahlmann et al., in prep., chapter 6). Since this system acts as an ordinary purge and trap system, the extraction efficiencies was simulated using halocarbon equilibrated artificial seawater. While the results from these tests revealed that monohalomethanes were almost completely extracted (≥90%), the purge efficiencies for CHBr$_3$ were only 33%. Thus, the fluxes for CHBr$_3$ from seagrass meadows under submerged conditions reported here represent rather a lower limit.

Based on the sampling system for the determination of stable carbon isotopes of halocarbons Bahlmann et al. (2011), we modified the cryogenic trapping system for the measurements of halocarbon mixing ratios, in order to establish a better temporal resolution by reducing the analysis time. This results in a final air volume 28± 5 L of air at the inlet and the outlet of the chambers, respectively. The specifications along with the results from test surveys are given in the supplementary.

The seagrass species sampled was exclusively *Z. noltii*. The seagrass patches sampled had an area coverage of >95% and were free of visible epiphytes such as macroalgae. In this low to medium intertidal the epiphytes of *Z .noltii* are almost exclusively diatoms whose contribution ranges from 0.5 to 4% of the total seagrass biomass (Cabaço et al., 2009). We further determined the fluxes from an adjacent bare sediment spot during the 2011 campaign. On 2nd August 2011, these chamber-based

measurements were complemented by atmospheric sampling at a nearby beach (Praia de Faro) about 3 km distant from the lagoon during the summer campaign 2011 (figure 13). At this time the wind direction was south-westerly reflecting background air from the coastal ocean.

Discrete water samples for the determination of dissolved halocarbons concentration and isotopic composition at high tide were taken during both campaigns. The samples were taken directly above the studied seagrass meadow using Duran glass bottles (1-2 L volume). Air and sediment intrusions during water sampling were avoided. The water depth was between 0.3 m and 1 m. On April 24th 2012, a transect cruise through the middle and western part of the lagoon was conducted during rising waters (figure 13). The water samples were taken from a water depth of 1 m. Dissolved halocarbons were extracted from seawater using a purge and trap system. Seawater was purged with helium 5.0 (purge flow 1L min^{-1}) for 30 minutes. After water vapour reduction of the purge gas, the compounds were enriched on cryotraps (submerged in a dry shipper). The shape of the cryotraps used here was the same as those for flux chamber and atmospheric samples. The water samples were usually processed within 30 minutes after sampling. Samples from the transect cruise were stored in the dark at 4°C and analyzed within eight hours. Purge efficiencies of monohalomethanes from lagoon water were ≥95% (1 L and 2 L samples). However, the less volatile $CHBr_3$ was only extracted with 50% (1 L samples) and 30% (2 L samples). Therefore, the results of water concentration were corrected for the respective purge efficiency for this compound.

5.2.3 Measurement and quantification

The measurement procedure is described in detail in the Appendix. Briefly, compounds enriched on the cryotraps, were thermally desorbed and transferred to peltier-cooled adsorption tubes. The analytes were further desorbed from the adsorption tubes and refocused cryogenically before injection to the GC-MS system. Air and water samples were measured onsite at Ramalhete research station using a GC-MS system (6890N/5975B, Agilent, Germany) equipped with a CP-PorabondQ column (25 m, 0.25 µm i.d., Varian, Germany). The GC-MS was operated in the electron impact mode. Identification of compounds was executed by retention times and respective mass spectra. Aliquots of gas standards containing CH_3Cl, CH_3Br, and $CHBr_3$ (1 ppm each) among others were applied to quantify the target compounds. During onsite measurements, CH_3I was quantified using the response factor against CH_3Br. The accuracy of the entire sampling method (sampling, sample treatment, measurement) was derived from test samples in triplicates. The deviation between the individual samples for CH_3Cl, CH_3Br, CH_3I, and $CHBr_3$ was 5.4%, 6.3%, 15.4% and 6.7%, respectively. A series of procedural blanks (cryotraps and adsorption tubes) were taken during the sampling campaigns. We observed only occasional blanks for CH_3Cl and CH_3Br with contributions of not more than 3% to the individual samples. Therefore, the halocarbon fluxes were not blank corrected.

Air and water samples for determining the isotopic composition of halocarbons were transferred to adsorption tubes and stored at -80°C until measurements. The analysis was conducted using the GC-

MS-IRMS system at our home laboratory (Bahlmann et al., 2011). Additional transport and storage blanks were processed which revealed no contamination for all halocarbons studied.

5.2.4 Calculations

The fluxes were determined with dynamic flux chambers. The principle is as follows: The chamber is positioned on the desired sampling spot and flushed continuously with ambient air. The mixing ratios of compounds at the inlet and outlet air are then measured. The obtained difference along with the flushing rate and the bottom surface area are used for the flux calculation. The net fluxes (F_{Net}, nmol m^{-2} h^{-1}) of the compounds are commonly calculated by

$$F_{Net} = \frac{Q \times (C_{out} - C_{in})}{A \times V \times 1000} \tag{1}$$

Here, Q is the flushing rate of air through the chamber (L h^{-1}), C_{out} and C_{in} are the mixing ratios of target compounds (picomoles mol^{-1}, ppt) at the outlet and the inlet of the flux chamber. A is the enclosed surface area of the flux chamber (m^2) and V is the molar volume (L) at 1013.25 mbar and 298.15 K.

For calculation the sea-air fluxes from the lagoon water, the inlet samples of the flux chamber were used which reflect the air mixing ratios. Where no corresponding inlet sample was available, the campaign means were applied. After conversion of the air mixing ratios to pmol L^{-1}, the sea-air fluxes (F, nmol m^{-2} h^{-1}) of halocarbons were calculated by the common equation:

$$F = k_w \times (C_w - C_a \times H^{-1}) \tag{2}$$

where k_w is the gas exchange velocity (cm h^{-1}), C_w and C_a the water concentration and air concentration (pmol L^{-1}), respectively, and H the dimensionless and temperature dependent Henry's law constant taken from Moore (2000) for CH$_3$Cl, Elliott and Rowland (1993) for CH$_3$Br and CH$_3$I, and Moore et al. (1995a) for CHBr$_3$. Several approximations emerged to estimate the relationship between the gas exchange velocity k and the wind speed u for open and coastal oceans (e.g. Wanninkhof, 1992; Nightingale et al., 2000). These estimations rely on assumptions that trace gas exchange is based on wind-driven turbulence. This is not applicable in shallow estuarine and riverine systems were the sea-air gas exchange is further driven by wind-independent currents and the bottom turbulence and thus, water depth and current velocities further play a major role (Raymond and Cole, 2001). Studying the sea-air exchange in the Ria Formosa, these additional factors have to be considered in addition to wind driven outgassing. Therefore, we used the parameterization of k_w with the assumption that wind speed and water current driven turbulence are additive (Borges et al., 2004):

$$k_w = 1.0 + 1.719 \times w^{0.5} \times h^{-0.5} + 2.58 \times u \tag{3}$$

where w is the water current (cm s^{-1}), h the water depth (m) and u the wind speed (m s^{-1}). For the calculations of the sea-air flux in the lagoon a mean water depth of 1.5m (Tett et al., 2003) and a mean water current of 24 cm s^{-1} (Durham, 2000) was used. The Schmidt number (Sc) expresses the ratio of transfer coefficients of the kinematic viscosity of water and gas diffusivity of interest. The gas

exchange velocity k_w for each gas was then normalized to a Schmidt number of 660, assuming a proportionality to $Sc^{-0.5}$ (Borges et al., 2004). The individual Schmidt numbers were obtained from Tait (1995) for CH_3Cl, De Bruyn and Saltzman (1997) for CH_3Br and CH_3I, and Quack and Wallace (2003) for $CHBr_3$.

5.3 Results

5.3.1 Halocarbons in the atmosphere and lagoon water

The air mixing ratios in the lagoon were adopted from the inlets of the flux chambers at 1 m above ground during both campaigns. The results of these measurements and those of the upwind site outside the lagoon (Praia de Faro) are presented in table 8. In summer, the mean air mixing ratios were 828 ppt for CH_3Cl, 22 ppt for CH_3Br, 3 ppt for CH_3I, and 15 ppt for $CHBr_3$. Elevated air mixing ratios of the monohalomethanes were observed during periods of easterly winds when air masses at the sampling site had presumably passed over major parts of the lagoon. These mixing ratios reached up to 1490 ppt for CH_3Cl, 61 ppt for CH_3Br, and 11 ppt for CH_3I reflecting a potent source in this system. The mixing ratios at the upwind site (Praia de Faro) were distinctively lower with mean values of 613 ppt (CH_3Cl), 13 ppt (CH_3Br), 1 ppt (CH_3I), and 8 ppt ($CHBr_3$) further indicating a source inside the lagoon. In spring 2012, the mean air mixing ratios in the lagoon were significantly lower than during summer with 654 ppt for CH_3Cl, 12 ppt for CH_3Br, 1 ppt for CH_3I, and 2 ppt for $CHBr_3$.

Table 8: General overview of air mixing ratios and water concentrations of halocarbons in the Ria Formosa and at the background site (Praia de Faro) for the sampling campaigns in summer 2011 and spring 2012. Samples from the Ria Formosa are data from the inlet of the flux chambers with a sampling height of 1 m above ground (summer: n=36; Praia de Faro: n=5; spring n=47). Given water concentrations refer to n=8 (summer) and n=10 (spring).

	Air mixing ratio Ria Formosa (ppt)		Air mixing ratio Praia de Faro (ppt)	Water concentration Ria Formosa (pmol L^{-1})
	mean	median	mean	
summer 2011				
CH$_3$Cl	828	753	613	220 (123-301)
CH$_3$Br	22	14	13	8 (5-11)
CH$_3$I	3	3	1	12 (4-18)
CHBr$_3$	15	13	8	102 (66 -194)
spring 2012				
CH$_3$Cl	654	646	-	166 (101-267)
CH$_3$Br	12	11	-	10 (6-28)
CH$_3$I	1	1	-	7 (2-16)
CHBr$_3$	2	1	-	62 (39 - 133)

Punctual water samples were taken above the studied seagrass meadow during tidal inundation (summer n=9; spring n=10). The results are presented in table 8. In summer, concentrations ranged from 158 to 301 pmol L^{-1} (CH_3Cl), 5 to 11 pmol L^{-1} (CH_3Br), 4 to 11 pmol L^{-1} (CH_3I), and 67 to 194 pmol L^{-1} ($CHBr_3$). CH_3Cl and CH_3Br were significantly correlated to each other (R^2 0.71, $p<0.05$) as well as CH_3Br and CH_3I (R^2 0.69, $p<0.05$). However, the relationship between CH_3I and CH_3Cl was

rather weak (R^2 0.20). $CHBr_3$ was generally not correlated to one of the other halocarbons studied. During the spring campaign, the water concentrations were 102 to 267 pmol L^{-1} for CH_3Cl, 6 to 28 pmol L^{-1} for CH_3Br, 2 to 16 pmol L^{-1} for CH_3I, and 39 to 133 pmol L^{-1} for $CHBr_3$. Correlation analysis revealed only weak correlation between the compounds ($R^2 \leq 0.48$).

The results obtained from samples of the transect cruise covered in 2012 (figure 13) are given in table 9.

Table 9: Water concentration (pmol L^{-1}) and stable carbon isotope ratios of halocarbons (‰) obtained from a two-hours transect cruise on 24th April 2012 (see figure 13 for sampling positions).

Sample	Time (local)	CH_3Cl pmol L^{-1}	‰	CH_3Br pmol L^{-1}	‰	CH_3I pmol L^{-1}	‰	$CHBr_3$ pmol L^{-1}	‰
1	15:09	121	-40.9	5	-25.6	5	-20.0	26	-25.8
2	15:50	241	-42.3	7	-21.2	5	-31.1	55	-18.3
3	15:58	96	-	9	-	2	-	21	-
4	16:10	106	-	11	-	5	-	31	-
5	16:21	180	-44.3	19	-35.9	14	-44.5	95	-18.9
6	16:46	72	-	5	-	3	-	18	-
7	16:50	82	-	4	-	5	-	14	-

We observed an about two-fold increase of concentration for CH_3Cl (from 121 to 241 pmol L^{-1}) and $CHBr_3$ (from 26 to 55 pmol L^{-1}) between position 1 (Faro-Olhão inlet) and position 2 (near to the seagrass meadows studied). The increase was less pronounced for CH_3Br (5 to 7 pmol L^{-1}) and not notable for CH_3I. The seawater at positions 6 and 7, the nearest to the Ancão inlet, revealed rather low concentrations for all compounds. We further observed rising concentrations for all halocarbons along positions 3, 4, and 5 with increasing distance to the Ancão inlet. They increased from 96 to 180 pmol L^{-1} for CH_3Cl, from 9 to 19 pmol L^{-1} for CH_3Br, 2 to 14 pmol L^{-1} for CH_3I, and 21 to 95 pmol L^{-1} for $CHBr_3$. The difference in concentration along the transect was accompanied by variations in the carbon isotopic composition of all compounds. The most ^{13}C depleted values of CH_3Cl, CH_3Br, and CH_3I were detected at the position furthest from the inlet. Interestingly, $CHBr_3$ showed the opposite trend with more ^{13}C enriched values in the lagoon (-25.8‰ vs. ~ -18‰).

5.3.2 Fluxes from seagrass meadows, sediment, and sea-air exchange

The mean fluxes and ranges of CH_3Cl, CH_3Br, CH_3I, and $CHBr_3$ from seagrass meadows, sediment, and from sea-air exchange calculations obtained from the two sampling campaigns are given in table 10. During the summer campaign (air exposure), we observed highly variable emission and deposition fluxes ranging from -49.3 to 74.0 nmol m^{-2} h^{-1} and -5.7 to 129.8 nmol m^{-2} h^{-1} for CH_3Cl and CH_3Br, respectively. The variability was less pronounced for CH_3I (0.5 to 2.8 nmol m^{-2} h^{-1}) and $CHBr_3$ (-0.6 to 5.7 nmol m^{-2} h^{-1}) where predominantly emissions were measured. Strongly elevated fluxes up to 129.8 nmol m^{-2} h^{-1} for CH_3Br were recorded in conjunction with tidal change from air exposure to inundation and conversely. These high fluxes were substantiated by a concurrent enhanced atmospheric mixing ratios ranging from 23 ppt to 118 ppt (campaign median 14 ppt). Omitting these

compound-specific tidal phenomena, the fluxes of CH_3Cl and CH_3Br were positively correlated to each other (R^2 0.55, p< 0.05). However, CH_3I and $CHBr_3$ fluxes correlated neither with each other nor with any of the other investigated halocarbons. Due to the inherent high variability of the fluxes, a direct comparison of halocarbon fluxes with solar radiation revealed a rather low correlation ($R^2 \leq$ 0.20).

Table 10: Mean net fluxes (bold) and ranges of halocarbons from flux chamber experiments seagrass meadows and sediments as well as those from sea-air exchange calculations. Data were obtained during the summer 2011 and spring 2012 campaigns in the Ria Formosa.

	n	CH_3Cl nmol m^{-2} h^{-1}	CH_3Br nmol m^{-2} h^{-1}	CH_3I nmol m^{-2} h^{-1}	$CHBr_3$ nmol m^{-2} h^{-1}
Summer 2011					
air exposure	28	**15.6** (-49.3 - 74.0)	**6.5** (-5.7 - 129.8)	**1.2** (0.5 - 2.8)	**1.8** (-0.6 - 5.7)
air exposure (sediment)	5	**3.6** (-1.9 - 8.1)	**0.6** (-0.2 - 1.1)	**0.2** (0.1 - 0.6)	**0.8** (-0.3 - 1.9)
Sea-air exchange	8	**29.8** (12.8 - 44.7)	**1.3** (0.6 - 1.7)	**2.2** (0.5 - 3.2)	**4.7** (1.0 - 8.0)
Spring 2012					
air exposure	17	**1.0** (-29.6 - 69.0)	**0.4** (-0.8 - 3.9)	**0.6** (-0.6 - 2.6)	**0.4** (-0.5 - 1.3)
tidal inundation	18	**16.6** (-58.3 - 99.7)	**1.8** (-1.6 - 8.3)	**1.9** (0.1 - 8.0)	**3.0** (-0.4 - 10.6)
tidal change	5	**40.1** (-14.2 - 99.7)	**2.7** (0.1 - 8.3)	**3.3** (0.1 - 8.0)	**2.9** (0.2 - 10.6)
incoming tide	6	**11.4** (-14.7 - 36.6)	**1.8** (0.2 - 3.3)	**1.6** (0.1 - 2.9)	**2.8** (0.2 - 5.1)
tidal maximum	2	-18.1, -58.3	-0.5, -1.6	0.1, 0.1	0.5, -0.1
ebb flow	5	**21.3** (-13.5 - 46.2)	**2.1** (0.1 - 4.4)	**1.5** (0.2 - 3.0)	**4.5** (-0.4 - 8.6)
Sea-air exchange	10	**15.2** (3.5 - 32.2)	**1.4** (0.5 - 4.1)	**1.3** (0.3 - 3.7)	**8.3** (3.8 - 23.8)

The flux chamber measurements over the sediment during air exposure revealed predominantly emissions of all four halocarbons (n=5). These fluxes were 3.6±4.3 nmol m^{-2} h^{-1} (CH_3Cl), 0.6±0.5 nmol m^{-2} h^{-1} (CH_3Br), 0.2±0.2 nmol m^{-2} h^{-1} (CH_3I), and 0.8±1.0 nmol m^{-2} h^{-1} ($CHBr_3$). Hence, the bare sediment may contribute to the overall emissions above the seagrass by about 10 to 20% for the monohalomethanes and 45% for $CHBr_3$.

During the 2012 spring campaign the halocarbon fluxes from seagrass meadows were determined during both, periods of air exposure and periods of tidal immersion. Furthermore, the measurements were complemented by other trace gases including hydrocarbons and sulphur containing compounds. High-time resolution CO_2 and methane flux measurements were further conducted to gain insights in the biogeochemistry and tidal controls in this system. These measurements along with other trace gases are reported in more detail in Bahlmann et al. (in prep., chapter 6). As in the summer campaign, the seagrass meadows were a net source for all halocarbons studied, but on a lower level. The individual ranges of air exposure measurements were -29.6 to 69.0 nmol m^{-2} h^{-1} (CH_3Cl), -0.8 to 3.9 nmol m^{-2} h^{-1} (CH_3Br), -0.6 to 2.6 nmol m^{-2} h^{-1} (CH_3I), and -0.5 to 1.3 nmol m^{-2} h^{-1} ($CHBr_3$). On average, the seagrass meadows were a net source also under submerged conditions ranging from -58.3 to 99.7 nmol m^{-2} h^{-1} for CH_3Cl, -1.6 to 8.3 nmol m^{-2} h^{-1} for CH_3Br, 0.1 to 8.0 nmol m^{-2} h^{-1} for CH_3I, and -0.4 to 10.6 nmol m^{-2} h^{-1} for $CHBr_3$. Despite this high variability in production/decomposition during air exposure and inundation, the monohalomethanes were significantly correlated to each other ($R^2 \geq 0.53$). These correlations were enhanced compared to those found when the seagrass meadows

were air-exposed. In this case, only CH_3I and CH_3Br were significantly correlated (R^2 0.51, p<0.05). $CHBr_3$ was only slightly correlated to CH_3I (R^2 0.42) as well as to CH_3Cl and CH_3Br ($R^2 \leq 0.34$).

While deposition fluxes of CH_3Cl and CH_3Br of air-exposed seagrass meadows occurred predominantly during periods of low irradiance in summer, no obvious relation to the time of day and/or solar radiation was observed during spring when deposition fluxes were frequently detected. For CH_3I and $CHBr_3$, uptake was only occasional observed and situations of emission clearly dominated.

As in summer campaign, we observed some remarkable tidal effects on halocarbon fluxes during the spring campaign. Firstly, the highest fluxes of all halocarbons were measured when the lagoon water was just reaching the sampling site. Occasionally this was also observed from air exposure to tidal inundation, although less pronounced. However, these short-timed effects were not as strong as during the summer campaign. Secondly, we observed deposition fluxes for CH_3Cl and CH_3Br at tidal maximum. Though uptake was not always observed for CH_3I and $CHBr_3$, their emissions turned out to decline in any case. Before and after this period emission fluxes during incoming tide and ebb flow dominated.

The lagoon water was a net source for all investigated halocarbons to the atmosphere during both campaigns. In summer, the flux ranges were 12.8-44.7 nmol m^{-2} h^{-1} (CH_3Cl), 0.6-1.7 nmol m^{-2} h^{-1} (CH_3Br), 0.5-3.2 nmol m^{-2} h^{-1} (CH_3I), and 1.0-8.0 nmol m^{-2} h^{-1} ($CHBr_3$). The respective fluxes in spring were 3.5-32.2 (CH_3Cl), 0.5-4.1 (CH_3Br), 0.3-3.7 (CH_3I), 3.8-23.8 ($CHBr_3$).

5.3.3 Stable carbon isotopes of halocarbons

Stable carbon isotope ratios of halocarbons were determined for selected samples of both campaigns (table 11). Isotopic source signatures from seagrass meadows for CH_3Cl and CH_3Br were calculated using a coupled isotope and mass balance without integration of a possible sink function (Weinberg et al., 2013).

Table 11: Compilation of stable carbon isotope values of halocarbons from the two sampling campaigns.

	Atmosphere Ria Formosa (‰)	n	Atmosphere Praia de Faro (‰)	n	lagoon water (‰)	n	source signature seagrass meadow (‰)	n
summer 2011								
CH₃Cl	-42 ± 2	7	-39 ± 0.4	5	-43 ± 3	7	-51 ± 6	5
CH₃Br	-29 ± 5	7	-38 ± 3	5	-23 ± 3	7	-42 ± 17	4
CH₃I	-	-	-	-	-39 ± 9	7	-	-
CHBr₃	-	-	-	-	-13 ± 1	7	-	-
spring 2012								
CH₃Cl	-38 ± 1	3	-	-	-42 ± 1	5	-56 ± 2	3
CH₃Br	-23 ± 10	3	-	-	-33 ± 8	5	-26; -33	2
CH₃I	-	-	-	-	-37 ± 7	5	-	-
CHBr₃	-	-	-	-	-18 ± 1	5	-	-

In 2011, the difference in atmospheric mixing ratios of CH_3Cl and CH_3Br between within the lagoon and the upwind position (Praia de Faro) was accompanied by a shift of $\delta^{13}C$ values. More ^{13}C depleted values were found for CH_3Cl in the lagoon (-42±2‰) compared to the upwind position (-39±0.4‰). In contrast, the $\delta^{13}C$ values of CH_3Br were significantly enriched in ^{13}C by about 10‰ inside the lagoon (-29±5‰) as compared to the upwind site (-38±3). These $\delta^{13}C$ values found in air samples in the lagoon roughly correspond to the $\delta^{13}C$ values of CH_3Cl (-43±3‰) and CH_3Br (-23±3‰) found in samples of lagoon waters.

Atmospheric CH_3Cl and CH_3Br were on average more enriched in ^{13}C in spring than in summer by 4 and 6‰, respectively. While the $\delta^{13}C$ values of CH_3Cl in the lagoon water were quite similar between both periods of the year, those of CH_3Br were on average more depleted in ^{13}C during spring suggesting certain changes in production/decomposition processes. The isotopic composition of CH_3I in lagoon water was quite similar between summer (-39± 9‰) and spring (mean -37±7‰). As for CH_3Br, the $\delta^{13}C$ values of $CHBr_3$ were more enriched in ^{13}C in summer if compared with those of the spring campaign.

Using the fluxes and $\delta^{13}C$ values from the inlet and outlet of the flux chamber we were able to calculate the source signatures of seagrass covered areas. The resulting source signatures of CH_3Cl from seagrass meadows were with -51±6 and -56±2 similar between both campaigns and independent from the strength of emission. For CH_3Br, we observed most depleted $\delta^{13}C$ values of -53‰ and -58‰ at increased emission fluxes in summer, but values of -26‰ and -29‰ during periods of low emission. This corroborates the findings of isotopically heavy CH_3Br produced within the seagrass meadows (-29‰) in spring 2012 when all samples analysed for the isotopic composition were taken at situations of low emission.

5.4 Discussion

5.4.1 Dissolved halocarbons

Despite the short residence time of the lagoon water masses of which 50-75% is exchanged during one tidal cycle (Brito et al., 2010), the transect cruise along the main channels revealed a successive enrichment of halocarbon concentration in the water with increasing distance from the main inlets (figure 13 and table 9). Therefore, the halocarbon net production in the lagoon appears to clearly exceed that outside the lagoon. This is supported by the distinctively increased air mixing ratios of halocarbons in the lagoon as compared to the upwind site (table 8).

A comparison to other measurements of coastal Atlantic waters found in the literature is displayed in table 12. The lagoon waters appeared to be highly enhanced in CH_3Cl. Except one early study of Tait et al. (1994), our measurements gave the most elevated concentrations for this compound. Enhanced concentrations in the lagoon waters were also found for CH_3Br. Given the mean concentrations from other coastal Atlantic studies (Baker et al., 1999; Carpenter et al., 2000; Hu et al., 2010), we recorded higher concentration by a factor of 2 to 3 at our sampling site. The average water concentrations in the

lagoon of CH_3I were in the same range as reported from other parts of the Atlantic (Moore and Groszko, 1999; Zhou et al., 2005). However, especially those regions where macroalgae are the dominating source organisms possess higher maximum values (Bravo-Lineares and Mudge, 2009; Jones et al., 2009). This is even more pronounced for $CHBr_3$, for which the seawater concentration within or in the vicinity of macroalgae beds are strongly elevated (Carpenter et al., 2000; Bravo-Lineares and Mudge, 2009; Jones et al., 2009). Accordingly, the area occupied by the prevalent macroalgae species *Enteromorpha spp.* and *Ulva spp.* in the Ria Formosa is estimated to 2.5 km^2 (Duarte et al., 2008), considerably below that of other abundant sources such as seagrass meadows. We cannot exclude that phytoplankton contributes significantly to the water concentration of halocarbons, but the predominantly low chlorophyll a concentrations (3.06 μg L^{-1} from long-term measurements, Brito et al., 2012) and low water volumes seem to limit the impact from this source. Overall, the lagoon seems to comprise highly potent halocarbon sources into the water column for CH_3Cl and CH_3Br rather than for CH_3I and $CHBr_3$.

Table 12: Mean concentrations and ranges of dissolved halocarbons (pmol L^{-1}) from the subtropical lagoon Ria Formosa in summer 2011 (n=9) and spring 2012 (n=10) in comparison to published data from coastal Atlantic waters.

location	CH$_3$Cl	CH$_3$Br	CH$_3$I	CHBr$_3$
Faro, Portugal (summer) [1]	**220** (123 - 301)	**8** (5-12)	**12** (4 - 18)	**102** (66 -194)
Faro, Portugal (spring) [1]	**166** (102 - 267)	**10** (6 - 28)	**7** (2 - 16)	**62** (39 - 133)
East Atlantic [2,#]	-	-	-	**68.3** (36.6 - 102.0)
Roscoff, France [3,#]	-	-	**12.9** (9.0 - 31.8)	**217.4** (124.8 - 519.4)
Greenland, NW Atlantic [4]	104 - 260	-	0.2 - 16.1	-
Norfolk, UK [5]	-	**3.2** (1.7 - 8.7)	-	-
Menai Strait, UK [6,#]	-	-	**6.7** (0.0 - 80.0)	**214.2** (3.0 - 3588.4)
Mace Head, Ireland [7,#]	-	**3.7** (1.7 - 5.7)	**15.3** (10.9 - 19.2)	**388.0** (221.8 - 554.3)
West Atlantic [8]	**88.4** (61.5 - 179.0)	**1.9** (0.8-5)	-	-
North West Atlantic [9]	**71.0** (55.0 - 106.0)	-	-	-
Nova Scotia, Canada [10]	-	-	4 - 6	-
Gulf of Maine, UK [11,#]	-	-	8 -18	40 - 1240

[1] this study; [2] Carpenter et al. (2009); [3] Jones et al. (2009); [4] Tait et al. (1994); [5] Baker et al. (1999); [6] Bravo-Linares and Mudge (2009); [7] Carpenter et al. (2000); [8] Hu et al. (2010); [9] MacDonald and Moore (2007); [10] Moore and Groszko (1999); [11] Zhou et al. (2005); [#] macroalgae dominated

5.4.2 Flux pattern from seagrass meadows

The halocarbon fluxes from seagrass meadows were characterized by a high variability with deposition and emission fluxes occurring at all sampling spots. The like was observed within other studies investigating halocarbon fluxes in coastal environments (e.g. Rhew et al., 2000; Manley et al., 2006; Blei et al., 2010a). Halocarbon dynamics in coastal systems were multiple sources and sinks interact are apparently quite complex. It should be noted that the fluxes discussed here refer to the entire benthic community constituting the seagrass meadows. Thus, some variability may relate to the activity of distinct source organisms which may be stimulated by different environmental factors. To

gain insights into the common environmental controls for this ecosystem we discuss the following factors i) diurnal variations ii) tidal effects and iii) seasonal dependence.

i) Diurnal variations. The correlation analysis with solar radiation resulted in only a weak influence on the magnitude of fluxes. However, after grouping by daytime, our data provide some indication for a diurnal pattern (figure 14). For CH_3Cl, there was the most obvious relationship between time of day and actual emissions. Highest emissions were observed during day periods with increased sunlight (midday and afternoon). In contrast, deposition fluxes were exclusively recorded during periods of low radiation and nighttimes. The same was also observed for CH_3Br. However, highest mean emissions of this compound seemed to be shifted towards the afternoon. CH_3I was constantly emitted from the seagrass covered spot revealing a weak diurnal dependence. The emissions did not cease during periods of low irradiance and darkness. Nevertheless, elevated mean emissions were observed in the afternoon. Except one occasion, $CHBr_3$ was emitted throughout the sampling periods. Mean emissions were higher around midday and afternoon as during night.
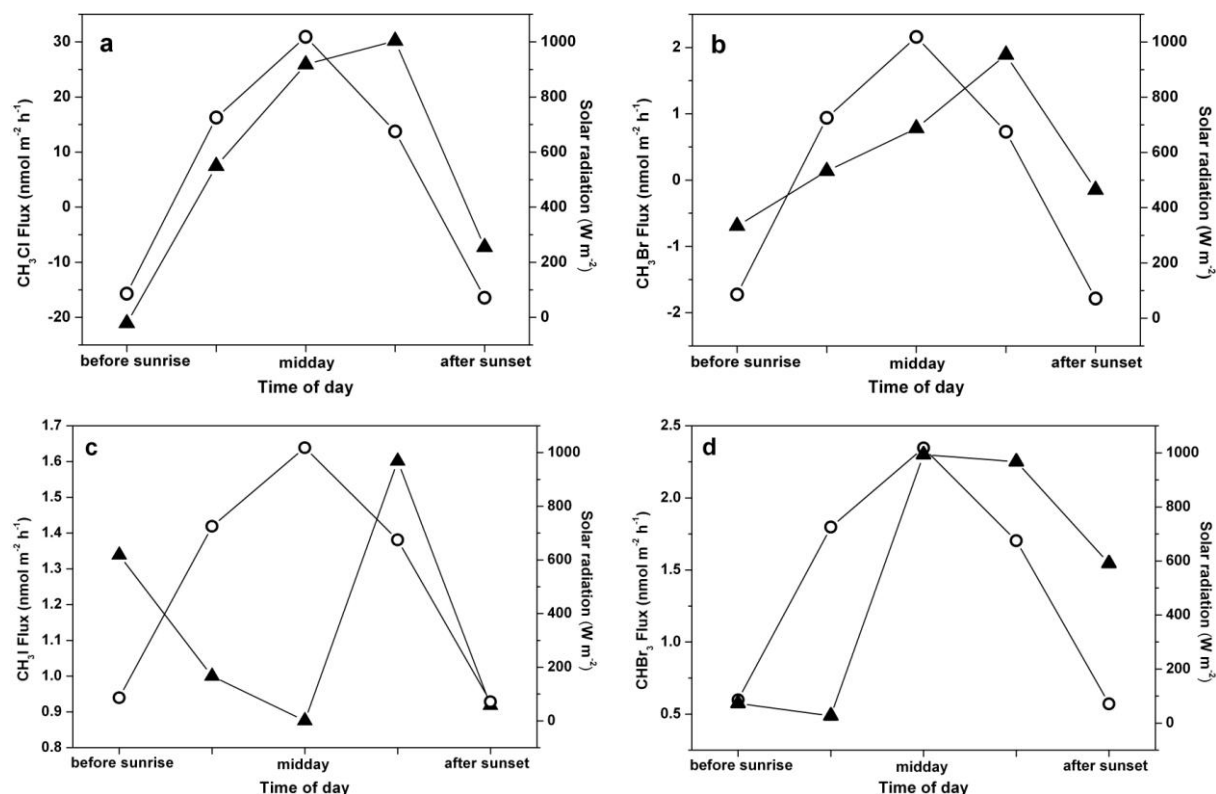
Figure 14 a-d: Diurnal variation of mean halocarbon fluxes (triangles) from seagrass meadows during periods of air exposure in summer 2011 (a: CH_3Cl, b: CH_3Br, c: CH_3I, d: $CHBr_3$). Circles are solar radiation values. Note that the scales on y-axis are different for each compound.

Several studies especially from salt marshes reported a diurnal trend of halocarbon emissions initiated by irradiance (Rhew et al., 2000; Dimmer et al., 2001; Rhew et al., 2002; Drewer et al., 2006). The flux data of halocarbons from the summer campaign with elevated fluxes during midday and afternoon suggest a similar pattern also in seagrass meadows. However, this was more obvious for CH_3Cl and

CH_3Br than for CH_3I and $CHBr_3$. The lower production of CH_3I during the time of highest light intensity cannot fully be explained. Possibly, the emissions might derive from sources within the benthic community different from those of other halocarbons. This is also supported by the rather low correlations to CH_3Br and CH_3Cl. For example, Amachi et al. (2001) reported microbial production of CH_3I which may not relate to solar irradiance. $CHBr_3$ emission which peaked during midday and afternoon did not instantly cease when radiation becomes low. This could be an effect of the low volatility of the compound resulting in a time-delayed release from the system.

Blei et al. (2010a) reported that the main environmental control in salt marshes is rather ambient temperature than light. However, during the summer campaign, temperature variations (day/night) were too low to explain the observed emission/deposition pattern of CH_3Cl and CH_3Br.

It is known that coastal sediments can act as sink for CH_3Cl and CH_3Br mainly due to microbial degradation (Oremland et al., 1994; Miller et al., 2004). This would support our findings of the deposition fluxes during night times where production above the sediment is presumably lower than during daytime (summer campaign). While in general the deposition fluxes of CH_3Cl and CH_3Br occurred more frequently during spring, they did not exhibit a certain day-night-relationship. Moreover, the dependence of light intensity on the magnitude of emission fluxes of halocarbons seemed to have a minor effect during this period of the year.

ii) Tidal effects. During the spring campaign, mean fluxes derived from submerged seagrass meadows were remarkably elevated by factors of 17 (CH_3Cl), 5 (CH_3Br), 3 (CH_3I), and 8 ($CHBr_3$) when compared to the average fluxes during air exposure. This clearly higher production of halocarbons under submerged conditions was quite unexpected. In general it is believed that the production of trace gases during low tide exceeds that during inundation. For halocarbons this was suggested for example by Carpenter et al. (1999) and Jones et al. (2009) from atmospheric measurements over intertidal macroalgae beds in Mace Head, Ireland. Nevertheless, in accordance with our results from halocarbon measurements we also observed higher primary productivity by increased CO_2 uptake during submerged conditions (Bahlmann et al. in prep., chapter 6). Furthermore, the correlation analysis revealed a different behaviour of halocarbons between the two tidal states with stronger correlations between monohalomethanes during tidal inundation than air exposure. Obviously, the change in environmental conditions was accompanied with a shift in the halocarbon production-decomposition pattern of the benthic community and/or different source organisms were stimulated.

An interesting outcome of both campaigns is the observation of strongly elevated halocarbon fluxes during tidal change from air exposure to submergence and reversely (table 10). Continuous high-time resolution CO_2 and methane flux measurements performed in spring 2012 (Bahlmann et al. in prep., chapter 6) principally support this observation. At the particular moment when the water reached the sampling site, we observed a distinct peak flux of methane and CO_2. This may be an evidence for processes in the sediments attributable to changes in hydrodynamic pressures resulting in the release of trace gases trapped in sedimentary pore spaces (Bahlmann et al. in prep., chapter 6). On the other

hand, these most likely sedimentary driven emission processes can hardly explain our observation of enhanced emissions also when the water was leaving the sampling site. Perhaps these emission increases relate to physiological stress reaction of the benthic community to the short-timed changing environmental conditions at the transition from inundation to air-exposure.

The remarkable deposition flux of CH_3Cl and CH_3Br during the maximum water level (table 10) was accompanied by highest emissions of other trace gases such as methanethiol and hydrogen sulfide as discussed by Bahlmann et al. (in prep., chapter 6). These compounds are effective nucleophiles which could have contributed to the degradation of halocarbons. This suggests a significantly different biogeochemistry during this period as during incoming tide and ebb flow. Although we actually have no inevitable prove for an existence of light dependence under these submerged conditions, it is however possible that production of photoautotrophic sources is reduced during this high tide state where solar irradiance is presumably the lowest.

Overall, while there is evidence for a tidal control on halocarbon production and decomposition, additional research is needed to further elucidate these phenomena.

iii) Seasonal dependence. There are considerable differences between the results from spring and summer. We observed strongly elevated mixing ratios for all halocarbons in ambient air as well as higher water concentrations for CH_3Cl, CH_3I, and $CHBr_3$ compounds in summer (table 8). For the water phase, this went along with higher correlations between the compounds in summer as compared to the spring period. This observed signal of general increased halocarbon production in the lagoon during summer might even be attenuated by assumedly enhanced degradation in the water phase and sediments at higher temperatures. Nevertheless, given the calculated sea-air flux there is only little evidence for a pronounced seasoning of halocarbon volatilisation to the atmosphere from the lagoon water. While the fluxes of CH_3Cl appeared to be enhanced in summer, those of CH_3Br and CH_3I seemed to be quite similar between spring and summer. $CHBr_3$ emissions were actually higher in spring than in summer due to higher water concentrations.

Comparing the data obtained from air-exposed sites during the two campaigns, the fluxes in summer were strongly enhanced by factors of 16 (CH_3Cl and CH_3Br), 2 (CH_3I), and 5 ($CHBr_3$) indicating that halocarbon fluxes increase from beginning of the growing season (spring) to the period where seagrass reproductive status is the highest (summer). This corresponds to the results from salt marshes where elevated fluxes for monohalomethanes where observed during the short flowering period (Manley et al., 2006). The differences of ambient conditions between the campaigns with lower air temperatures and cloudy sky in spring may have contributed to the differences in the emission patterns of halocarbons. That temperature is one of the emission controlling factors was reported from temperate salt marshes (Blei et al., 2010a). Moreover, the halocarbon fluxes showed a distinct diurnal cycle during summer but not during spring. This suggests either a less productive benthic community or much stronger degradation processes during spring. The latter point is rather unlikely since the temperatures were distinctively lower and thus, degradation processes are tentatively slower.

Overall, these differences observed in periods of air exposure between spring and summer suggest a strong seasonality in seagrass meadows. However, further studies covering the entire seasoning are necessary to unravel the annual halocarbon emissions from seagrass meadows.

5.4.3 Halocarbons sources in the lagoon: an isotopic perspective

The results from the atmospheric sampling of Praia de Faro air (upwind) and lagoon air revealed certain difference regarding the mixing ratios and isotopic composition of CH_3Cl and CH_3Br (tables 8 and 11). We observed elevated concentrations in the lagoon for both compounds, whereby the higher concentrations were accompanied with shifts towards isotopically light CH_3Cl but heavy CH_3Br. Beside the studied seagrass meadows other sources, in particular wide-abundant salt marshes, may have substantially contributed to the elevated mixing ratios. Assuming atmospheric stable conditions with negligible sinks in the atmosphere, the difference of air mixing ratios and $\delta^{13}C$ values between upwind air and lagoon air should reflect the isotopic source signature within the lagoon. Therefore, as a first approach, an isotope mass balance was used by integrating mean data from both sampling sites (tables 8 and 11). The resulting source signatures within the lagoon are -49‰ for CH_3Cl and -16‰ for CH_3Br.

Isotopic source signatures of CH_3Cl from seagrass meadows during incubations (air exposure) in the Ria Formosa were -51±6‰ (summer) and -56±2‰ (spring). During the summer campaign, CH_3Cl emissions from the salt marsh plant *Spartina maritima* were determined with $\delta^{13}C$ values of -66 and -72‰. These values are in good agreement with those of Bill et al. (2002) from a Californian salt marsh (-69 to -71‰, daytime values). Unfortunately, we do not have isotopic data for the inundated periods from seagrass meadows, but the $\delta^{13}C$ values of CH_3Cl in the water phase (-42±2‰) come close to those measured in the atmosphere. An abiotic production mechanism has been reported for CH_3Cl from senescent plant material (Hamilton et al., 2003). While we cannot generally exclude additional CH_3Cl generation via this pathway, the isotopic data obtained in the Ria Formosa do not mirror strongly ^{13}C depleted values ($\delta^{13}C$ of -135±12‰, Keppler et al., 2004) as expected for compounds built by this production mechanism. Overall, this rather indicates a stronger imprint of the seagrass meadows and/or water column on the atmospheric CH_3Cl than from salt marshes or abiotic processes.

With $\delta^{13}C$ values of -42±17‰ the source signature of CH_3Br from seagrass meadows are tend to be more depleted in ^{13}C as the calculated source signature from the atmospheric samples. It should be noted that the $\delta^{13}C$ values for this compound were more depleted in ^{13}C during periods of increased emission (-55‰) than during low emissions (-28‰). This shift can most likely be explained by degradation processes which occurred simultaneously. This corroborates our observations from Northern Germany with subsequent recalculation of a sedimentary sink function from accompanied sediment measurements (Weinberg et al., 2013). Reported source signatures of CH_3Br from salt marshes range from -59 to -65‰ (day time values, Bill et al., 2002). Our own measurements in the Ria Formosa indicate similar $\delta^{13}C$ values (-65‰) or even more depleted ones (unpublished data). In any case, neither source signatures from seagrass meadows nor salt marshes seem to match the overall

source signature estimated from the atmospheric samples. Therefore, it is most likely that the atmospheric CH_3Br is strongly influenced by emissions from the water column reassembling $\delta^{13}C$ values of -23±3‰ (summer). Even during periods of low tide the water remains in the deep channels which may be sufficient to have an impact on the local atmosphere. Thus, despite the sources in the lagoon presumably producing isotopically light CH_3Br, $\delta^{13}C$ values in the atmosphere strongly reflect decomposed CH_3Br whose residual fraction is actually enriched in ^{13}C. Accordingly, aqueous CH_3Br appears to become rapidly degraded by biotic/abiotic processes such as hydrolysis, transhalogenation, and microbial degradation with strong isotopic fractionation (King and Saltzman, 1997). These decomposition mechanisms are temperature dependent with increasing destruction with increasing seawater temperature. This is most likely the reason why the $\delta^{13}C$ values in the lagoon waters in summer are more enriched in ^{13}C as those from the spring campaign.

As shown by the water samples from the transect cruise, the sources in the lagoon may produce isotopic light CH_3I. Given this, CH_3I seems to some extent follow the $\delta^{13}C$ values of CH_3Cl. These sources may be biotic by e.g. phytoplankton, seagrass meadows, or bacteria. On the other hand, Moore and Zafirou (1994) reported a photochemical source for CH_3I by radical recombination of iodine with seawater dissolved organic matter. Due to the lack of isotopic source signatures and fractionation factors for production (and consumption), it is demanding to draw conclusions from the data yet.

The $\delta^{13}C$ values of $CHBr_3$ were more depleted in ^{13}C from the lagoon inlet towards the parts deeper inside. This suggests a different combination of sources in water masses coming from the Atlantic. Moreover, this potential variation of source contribution can be further assumed by the certain change between summer and spring where e.g. macroalgae are more abundant in the latter period (Anibal et al., 2007). Already reported source signatures of phytoplankton, macroalgae, and seagrass meadows cover the range of -10‰ to -23‰ (Auer et al., 2006; Weinberg et al., 2013), thus demonstrating certain differences in their isotopic fingerprint. Actually we cannot exclude that degradation might also have an effect on the $\delta^{13}C$ values determined in lagoon waters. As for CH_3I there is still need for further research on the $CHBr_3$ cycling utilizing stable carbon isotopes.

5.4.4 Magnitude of fluxes and comparison to other coastal measurements and first estimate of global source strength

The areal based fluxes of CH_3Cl, CH_3Br, and CH_3I from seagrass meadows in comparison to emission data of other coastal sources are presented in figure 15. In comparison to the emissions from temperate seagrass meadow in Northern Germany (Weinberg et al., 2013), fluxes were elevated in the subtropical lagoon in summer during air exposure. This was more pronounced for CH_3Br (factor 33) than for CH_3Cl (factor 2), CH_3I (factor 2), and $CHBr_3$ (factor 5). In contrast, fluxes from air-exposed seagrass meadows recorded during spring are comparable to those determined in Northern Germany. Thus, the difference between fluxes from temperate and subtropical regions is less pronounced as reported for salt marshes with emissions from subtropical regions exceeding those from temperate regions by up to two orders of magnitude for CH_3Cl and CH_3Br (Rhew et al., 2000; Dimmer et al.,

2001; Cox et al., 2004; Drewer et al., 2006; Manley et al., 2006; Valtanen et al., 2009; Blei et al. 2010a; Rhew and Mazéas, 2010). Beside this regional (climatic) difference several authors attributed this to a highly species-dependent emission potential.

Average emissions of CH_3Cl from the air-exposed seagrass meadows in summer are in the same range as those determined in temperate salt marshes (Dimmer et al., 2001; Cox et al., 2004; Drewer et al., 2006; Valtanen et al., 2009; Blei et al., 2010a). In contrast, subtropical counterparts of these macrophytes are distinctively stronger emitters of this compound by at least one order of magnitude (Rhew et al., 2000; Manley et al., 2006; Rhew and Mazéas, 2010). Greenhouse grown mangroves produce significantly more CH_3Cl than seagrass meadows revealing a higher emission potential for these plants species on per area basis (Manley et al., 2007).

Fluxes of CH_3Br from subtropical seagrass meadows during air exposure exceed those of temperate macroalgae from Mace Head, Ireland (Carpenter et al., 2000) and temperate salt marshes (Dimmer et al., 2001; Cox et al., 2004; Drewer et al., 2006; Valtanen et al., 2009; Blei et al., 2010a). However, the CH_3Br fluxes from seagrass meadows are distinctively lower than those of subtropical salt marsh plants (Rhew et al., 2000; Manley et al., 2006; Rhew and Mazéas, 2010). Mangroves seem to have a similar emission potential as seagrass meadows (Manley et al., 2007).

For CH_3I, seagrass meadows are a minor source in comparison to the high release of macroalgae in subtropical areas (Leedham et al., 2013). Except for salt marshes from Tasmania (Cox et al., 2004), plant-related communities such as mangroves (Manley et al., 2007) and salt marshes (Dimmer et al., 2001) are more pronounced emission sources of this compound. The same holds true for $CHBr_3$, where macroalgae communities from temperate and subtropical/tropical regions dominate the emissions of polyhalomethanes on a per area basis (e.g. Gschwend et al., 1985; Carpenter et al., 2000; Leedham et al., 2013).
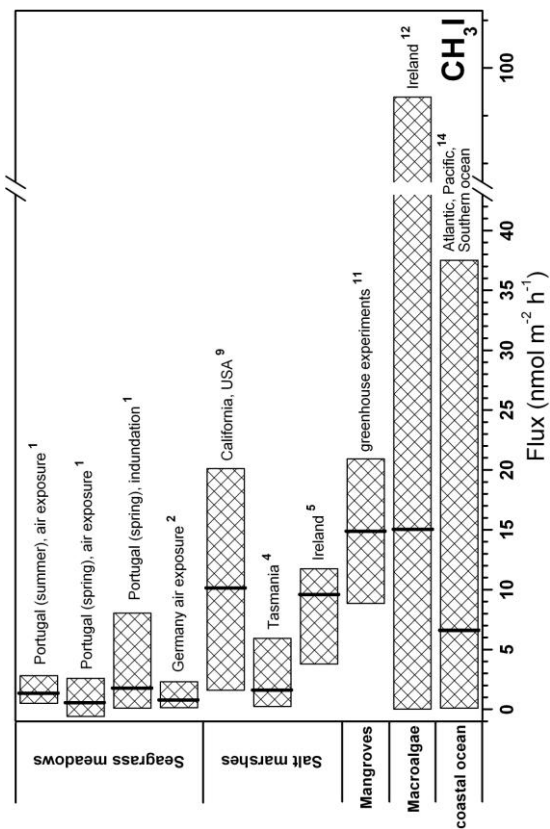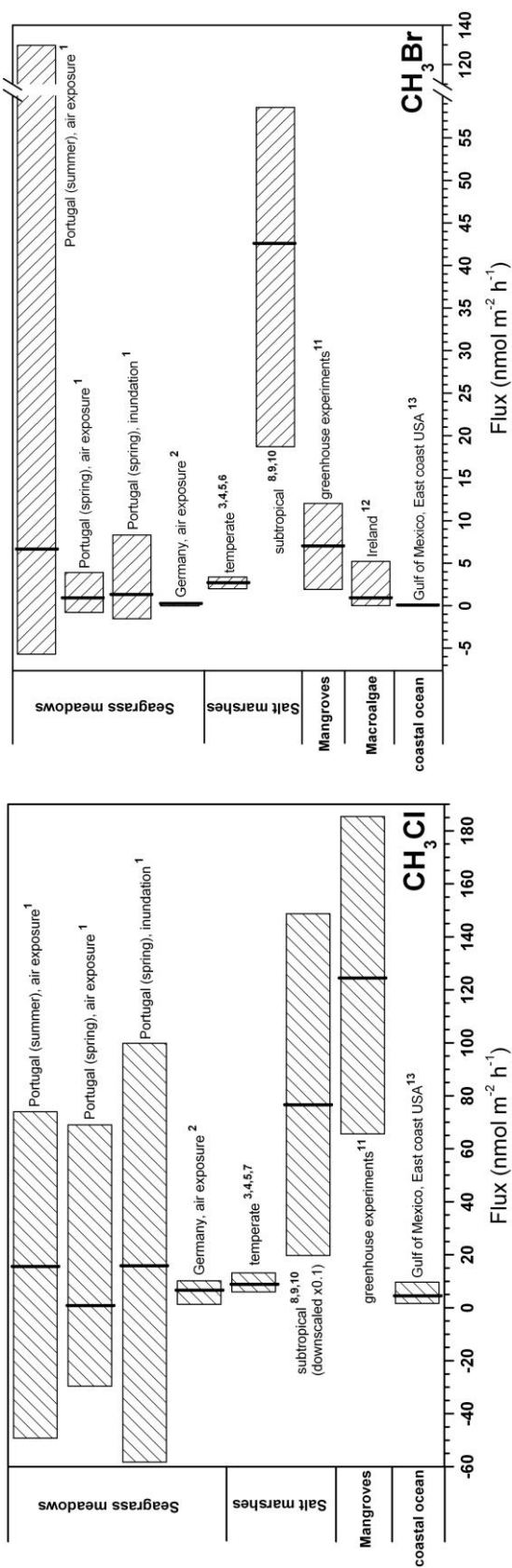
Figure 15: Compilation of mean emissions (bold black vertical lines) and ranges from different sources in coastal environments for CH_3Cl (upper left panel), CH_3Br (upper right panel) and CH_3I (lower left panel). Note the different scales. Published data adopted from: [1] this study; [2] Weinberg et al. (2013); [3] Blei et al. (2010a); [4] Cox et al. (2004); [5] Dimmer et al. (2001); [6] Drewer et al. (2006); [7] Valtanen et al. (2009); [8] Rhew and Mazéas (2010); [9] Manley et al. (2006); [10] Rhew et al. (2000); [11] Manley et al. (2007); [12] Carpenter et al. (2000); [13] Leedham et al. (2013). **Note that the data of CH_3Cl from subtropical salt marshes are downscaled by a factor of 10 for visualization reasons. Where multiple references were used, the individual study means were averaged and presented along with the resulting ranges. Thus, ranges of halocarbon fluxes in each single study are not covered. Studies reporting a strong species dependency in magnitude of fluxes were averaged over all species for simplicity reasons. Macroalgae emissions given in g fresh weight per hour were converted by using the species' fresh weights and spatial coverage in the coastal belt in Mace Head, Ireland for CH_3Br (Carpenter et al., 2000) and the Malaysian coastline for CH_3I (Leedham et al., 2013), respectively.**

Many uncertainties arise from a limited number of emission data to estimate the global relevance of seagrass meadows. Those may be high variation in space and time, high heterogeneity of seagrass meadows, species dependent emission potential, and errors regarding the global seagrass abundance. Therefore, the scale-up of our data gives only a first rough approximation; it was undertaken as follows. Since we did not measure a full annual cycle, we assumed that seagrass measurements during the summer campaign represent emissions from the reproductive season (May - September). The remaining period of the year (October - April) was calculated with emission data from the spring campaign. The emission data were weighted to tidal states using 8 hours and 16 hours per day as durations when seagrass meadows are air-exposed or submerged, respectively. Due to the lack of flood tide emission data in summer, we used those derived from the sea-air exchange. The resulting average annual emissions from seagrass meadows of 150 μmol m^{-2} yr^{-1} (CH$_3$Cl), 18 μmol m^{-2} yr^{-1} (CH$_3$Br), 14 μmol m^{-2} yr^{-1} (CH$_3$I), and 25 μmol m^{-2} yr^{-1} (CHBr$_3$) were scaled-up with the current estimates of a global seagrass area ranging from 0.3×10^{12} m^2 (Duarte et al., 2005) to 0.6×10^{12} m^2 (Charpy-Roubaud and Sournia, 1990).

The tentative estimate yields annual emissions of 2.3-4.5 Gg yr^{-1} for CH$_3$Cl, 0.5-1.0 Gg yr^{-1} for CH$_3$Br, 0.6-1.2 Gg yr^{-1} for CH$_3$I, and 1.9-3.7 Gg yr^{-1} for CHBr$_3$. Based on the recent global budget calculations (Xiao et al., 2010; WMO, 2011), these ranges are equivalent to 0.06-0.11% and 0.45-0.89%, for CH$_3$Cl and CH$_3$Br, respectively. Seagrass meadows would therefore cover a portion of 1.4-2.8% of the missing sources for CH$_3$Br reported in the most recent WMO report (36.1 Gg yr^{-1}; WMO, 2011). Given the emissions from oceanic sources (e.g. Quack and Wallace, 2003 and references therein; Butler et al., 2007), CH$_3$I and CHBr$_3$ emissions from seagrass meadows are rather insignificant on a global scale.

5.5 Conclusions

We presented the first detailed study of halocarbon fluxes from seagrass meadows. The data were obtained from a subtropical mesotidal lagoon in Southern Portugal. During air exposure, fluxes of CH$_3$Cl and CH$_3$Br were highly variable with increasing fluxes at midday and afternoon while deposition fluxes were predominantly observed in periods of low radiation and at nighttimes. Diurnal fluctuations were less obvious for CH$_3$I and CHBr$_3$, though their emission maxima were also shifted to the afternoon. Generally, diurnal variations and emission rates were minor in spring than in summer, suggesting a considerable seasonality. This is supported by distinctively lower atmospheric mixing ratios in spring. Distinct emission peaks occurred in the certain moments when lagoon waters were just arriving or leaving the sampling site. Moreover, a comparison between chamber measurements during air exposure and tidal inundation revealed elevated emission rates during flooding. Overall, seagrass meadows are highly diverse regarding their potential halocarbon sources which might be responsible for the observed high variations of emission fluxes. For example, we could show that the sediments were also able to emit halocarbons, though in low quantities on per area basis.

The results from a transect cruise along the mid and western part of the lagoon clearly revealed a significant halocarbon production within lagoon waters. This finding corresponds to high halocarbon concentrations in the lagoon water above submerged seagrass meadows. This was especially pronounced for CH_3Cl exhibiting the highest water concentration as compared to other measurements from Atlantic waters. However, CH_3I and $CHBr_3$ water concentrations were well below those reported from macroalgae-dominated coastlines.

To obtain further information on sources and sinks in the lagoon, stable carbon isotopes of halocarbons from the air and water phase along with source signatures were studied. Results suggest that CH_3Cl more originates from the water column and/or seagrass meadows than from adjacent salt marshes or abiotic formation processes. Atmospheric and aqueous CH_3Br in the lagoon was substantially enriched in ^{13}C pointing towards degradation processes and re-emission into the atmosphere. Furthermore, we presented isotopic data of CH_3I and $CHBr_3$ from the water phase.

Monohalomethane emissions from seagrass meadows fall in-between those from temperate salt marshes and mangroves. For $CHBr_3$, seagrass-based emissions are distinctively below those of macroalgae. On a global scale, seagrass meadows are rather a minor source for halocarbons but will have a certain imprint on the local and regional budgets. This holds in particular true for subtropical coastlines where seagrass meadows belong to the most abundant ecosystems.

Future studies should focus on emission from seagrass-based systems from different regions in order to refine the global relevance. Likewise, since magnitudes of fluxes are often species-dependent, budgets calculations will certainly benefit from a more detailed view on different seagrass species. Furthermore, while this study focused on halocarbon dynamics from seagrass meadows on the level of the benthic community, it is worthwhile to identify the specific sources in these ecosystems. The sediments being capable to act as both, a sink and a source, should be further studied. Though our results suggest sediments being a weak producer on a per area basis which corroborates other studies from e.g. salt marshes (Manley et al., 2006), they may have a significant impact in view of their high area coverage in coastal zones exceeding by far all other macrophytic systems (see Duarte et al., 2005).

6. Tidal controls on trace gas dynamics in a subtropical seagrass meadow of Ria Formosa lagoon (southern Portugal)

Enno Bahlmann, Ingo Weinberg, Rui Santos, Tim Eckhardt, Jost Valentin Lavric, Walter Michaelis, and Richard Seifert

Manuscript

Abstract

Coastal zones are important source regions for a variety of trace gases including halocarbons and sulphur bearing species. While salt marshes, macroalgae and phytoplankton communities have been intensively studied, little is known about trace gas fluxes in seagrass meadows. Here we report results of a newly developed dynamic flux chamber system that can be deployed in intertidal areas over full tidal cycles allowing for high time resolved measurements. The trace gases measured in this study included CO_2, methane, a variety of hydrocarbons, halocarbons, and sulphur bearing compounds. The high time resolved CO_2 and methane flux measurements revealed a complex dynamic. In contrast to most previous studies our data indicate significantly enhanced fluxes during tidal immersion relative to periods of air exposure. In particular for methane, we observed short emission peaks with the feeder current just arriving at the sampling site. We suggest an overall strong effect of advective transport processes to explain the elevated fluxes during tidal immersion. Still many emission estimates from tidally influenced coastal areas rely on measurements carried out during low tide. Hence, our results may have significant implications for budgeting trace gases in coastal areas.

6.1 Introduction

Coastal zones are hot spots for a variety of volatile organic compounds (VOCs) including halogenated compounds (Gschwend et al., 1985; Moore et al., 1995b; Baker et al., 1999; Rhew et al., 2000; Christof et al., 2002; Manley et al., 2006; Valtanen et al., 2009) and sulphur bearing compounds (Cooper et al., 1987a, b; Dacey et al., 1987; De Mello et al., 1987; Turner et al., 1989; Leck and Rodhe, 1991), but a minor source for hydrocarbons such as methane (Van der Nat and Middelburg, 2000; Middelburg et al., 2002). While coastal ecosystems, such as salt marshes, macroalgae and phytoplankton communities have been intensively studied, little is known about trace gas fluxes from seagrass meadows. Seagrass meadows are amongst the most productive coastal ecosystems with an average net primary production of 900 g carbon per year (Mateo et al., 2006). They cover a considerable portion of global coastal zones with conservative estimates of 300.000 km^2 (Duarte et al., 2005). Most previous studies in seagrass meadows have focussed on carbon dynamics (e.g. Migné et al., 2004; Silva et al., 2005; Spilmont et al., 2005; Hubas et al., 2006) and were often restricted to

periods of air exposure. More recently, benthic chambers for underwater incubations were developed (Barron et al., 2006; Silva et al., 2008). There is some evidence that seagrass meadows *(Zostera spec.).* are capable to form and/or release a variety of trace gases (Urhahn, 2003; Weinberg et al., 2013). Furthermore, seagrass meadows may foster dimethyl sulfide (DMS) emissions (Jonkers et al., 2000; Lopez and Duarte, 2004).

As other higher plants rooting in anoxic soils and sediments, seagrasses have an aerenchymatic tissue for supplying oxygen to their root system. This aerenchymatic tissue in turn may provide an effective transport pathway for trace gases from the sediment to the atmosphere. The importance of this transport pathway has been shown for methane emissions from a variety of vegetation types (Laanbroek, 2010). However, early incubation experiments have indicated fairly low emission rates from *Thalassia testudinum* beds (Oremland, 1975). More recently, Deborde et al. (2010) reported methane fluxes from *Z. noltii* meadows in the Arcachon lagoon (SW France) being below 1.6 µmol m^{-2} h^{-1}, which was actually the detection limit.

So far, mainly static chambers have been used for measuring fluxes of trace gases in coastal environments, mainly of methane and CO_2 (e.g. Delaune et al., 1983; Bartlett et al., 1987; Van der Nat and Middelburg, 2000; Migné et al., 2002, 2004; Silva et al., 2005; Spilmont et al., 2005; Hubas et al., 2006). There are several problems arising from chamber based flux measurements such as pertubations of the turbulent fields on the air and water side, introduction of artificial gradients, pertubations of the thermal environment, and the gas composition inside the chamber. In particular solid static chambers will most likely introduce stagnant conditions and thus suppress advective exchange (Cook et al., 2007). For this study we used a dynamic chamber modified to enable flux measurements over full tidal cycles. During tidal immersion the chamber is continiously purged whereby the purging introduces an advective flow inside the chamber. Though artificial, this turbulent motion inside the chamber may to some extent mimic the turbulent flow outside the chamber. The system allows continous methane and CO_2 flux measurements with a time resolution of 10 minutes as well as the determination of VOC fluxes by discrete sampling. Here we provide a detailed description of the flux chamber system and first results of a field study conducted in a subtropical seagrass meadow in Faro, Portugal. We report fluxes of CO_2, methane, propane, butane, propene, chloromethane (CH_3Cl), bromomethane (CH_3Br), iodomethane (CH_3I), chloroform ($CHCl_3$), bromoform ($CHBr_3$), carbondisulfide (CS_2), carbonyl silfide (COS), as well as DMS and discuss them in terms of factors controlling trace gas dynamics in intertidal seagrass meadows.

6.2 Methods

6.2.1 Flux chamber design

Dynamic flux chambers have been widely used in trace gas studies in terrestrial systems (Kim and Lindberg, 1995; Gao et al., 1997; Gao and Yates, 1998; Zhang et al., 2002; Pape et al., 2009). Details on the theory of dynamic flux chamber measurements are given in Gao et al. (1997) and Meixner et al.

(1997). Briefly, the surface of interest is enclosed by a chamber and air is drawn through the chamber at a predefined flow rate. Net fluxes above the covered surface are commonly calculated from the concentration difference between the inlet and outlet of the chamber:

$$F_{Net} = \frac{Q_N \times (C_{out} - C_{in})}{A \times V_N \times 1000} \qquad (1)$$

Here F_{net} is the net flux (nmol m^{-2} h^{-1}), Q_N is the flushing flow rate through the chamber (L min^{-1}, at 1013.25 mbar and 298.15 K), C_{out} and C_{in} are the air mixing ratios of target compounds (ppt) at the outlet and the inlet of the flux chamber, respectively, A is the bottom surface area of the flux chamber (m^2), and V_N is the molar volume at 1013.25 mbar and 298.15 K.

A scheme of the flux chamber used here is depicted in figure 16. The chamber was made from a 10 L Duran glass bottle with the bottom being cut off. The chamber dimensions were a volume of 8 L, a bottom surface area of 0.037 m^2, and a height of 0.3 m.
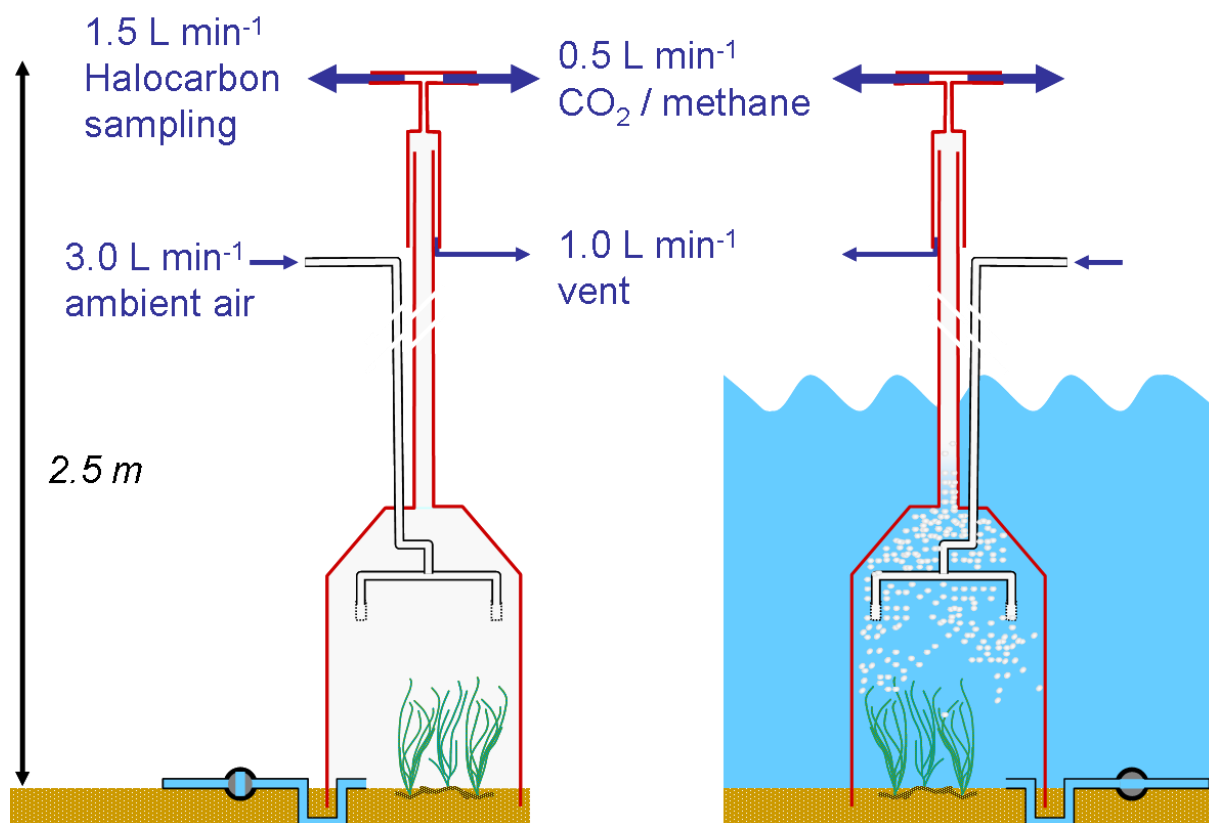
Figure 16: Scheme of the dynamic flux chamber system. During air exposure the chamber acts as a conventional dynamic flux chamber. During tidal immersion the enclosed water is continuously purged with ambient air.

Prior to the sampling, the chamber is pressed 5 cm into the sediment resulting in a final headspace volume of approximately 6 L. During tidal change water entered and left the chamber through a U-tube at the bottom (stainless steel tube 50 cm length, 4 mm inner diameter). The tube was connected to a valve that was closed during air exposure and open during tidal immersion. During sampling,

ambient air is pumped through the chamber with a membrane pump (KNF-Neuberger, Germany) at a flow rate between 3.0 and 3.5 L min^{-1}. The air enters the chamber through a PFA-tube at the top of the chamber and is further distributed to two metal frits (10 µm pore size). The frits are placed 12 cm above the sediment surface preventing visible dispersion of surface sediments. The outlet of the chamber is connected to an open split in 2.5 m height via a ½' PFA-tube. The tube is inserted 30 cm into a stainless steel tube (50 cm long, ¾' inner diameter) that is open at the bottom and has to sampling ports at the top. Typically, about 0.5 L min^{-1} are directed to the CO_2 / methane analyzer and 1.5 L min^{-1} are directed to the trace gas sampling system. The excess air with water droplets and aerosols is vented into the atmosphere via the open split. Two Teflon membrane filters are used to further protect the sampling systems from water and aerosols. The U-tube at the bottom and the open split ensured pressure equilibrium between the chamber and the ambient water body.

6.2.2 Sampling site

The sampling was conducted in an intertidal seagrass meadow of *Zostera noltii Hornem.* in the Ria Formosa lagoon, a mesotidal system located in southern Portugal. The lagoon has a surface area of 84 km^2 with about 80% of it being intertidal. It is separated from the open ocean by a system of sand barrier islands. Six inlets allow exchanges of water with the Atlantic Ocean. The tidal amplitude ranges from 3.5 m on spring tides to 1.3 m on neap tides. In each tidal cycle about 50% to 75% of the water in the lagoon is renovated. Salinity ranges from 35.5 to 36 psu throughout the year, except during the sporadic periods of heavy rainfall; water temperature varies between 12 ºC in winter and 27 ºC in summer.

Z. noltii is the most abundant seagrass species in Ria Formosa, covering about 45% of the intertidal area (Guimarães et al., 2012). The species plays a major role in the whole ecosystem metabolism of the lagoon (Santos et al., 2004). The range of *Z. noltii* biomass variation at the sampling site is 229-310 g DW m^{-2} (Cabaço et al., 2008).

6.2.3 Sampling and measurement

The CO_2 and methane flux measurements were performed between April 23th and April 27th 2012. VOC fluxes were measured between April 17th and April 28th 2012. Therefore, the time base of the VOC sampling does not fully overlap the time base of the CO_2 and methane sampling. The sampled seagrass patches (*Zostera noltii*) were free of visible epiphytes and macroalgae. The canopy coverage was estimated to >95%.

CO_2 and methane were measured on site with a Picarro 1701-G cavity ring down spectrometer. A six port Valco valve was used to switch between 3 different sampling lines. The first sampling line was directly connected to the dynamic flux chamber and the two other sampling lines were used to sample ambient air from two different heights (e.g. 2 m and 4 m). The air mixing ratios from both sampling lines were averaged to calculate the inlet concentration of the chamber. The sampling lines were consecutively sampled for 5 minutes and each line was connected to an additional membrane pump for

continuously flushing (flow rate: 0.5 L min^{-1}). Discrete gas samples were taken from the second sampling port to determine the outlet concentration of the VOCs. In parallel, discrete samples were taken from the feeding line to the flux chamber via a T-union to determine the inlet concentration of the VOCs. Details of the VOC sampling system are given in chapter 5 and in the Appendix. Briefly, 28±5 L of ambient air were drawn through a cryotrap at a flow rate of 1.0±0.2 L min^{-1}. The samples were thermally desorbed from the cryotrap (310°C) using a flow of helium (30 mL min^{-1} for 15 min) and recollected on peltier-cooled adsorption tubes maintained at –15°C. From the adsorption tube the samples were again desorbed into a flow of helium and refocused on a quartz capillary (0.32 i.d., 60 cm length) immersed in liquid nitrogen. The analytes were desorbed from the quartz capillary at ambient temperature and transferred to a GC-MS system (6890N/5975B, Agilent). VOCs were separated on a CP-PorabondQ column (Varian, 25m, 0.25 µm i.d.) with helium as a carrier gas. Quantification of CH_3Cl, CH_3Br, CH_3I, $CHCl_3$, $CHBr_3$, propene, and CS_2 was performed against a working standard. The overall precision of this method is better then ± 6%. For COS, propane, butane, and DMS not present in the standard, relative fluxes were calculated from the measured intensities.

6.3 Results

The high time resolution of our measurements provided detailed insights into the complex dynamics of the methane and CO_2 fluxes. The flux patterns of CO_2 and methane are displayed in figure 17 (seagrass meadows) and figure 18 (sediment). Table 13 provides an overview over the time averaged fluxes for different stages of the tidal cycle. It should be noted that by definition emission fluxes are positive and deposition fluxes are negative. In general, much higher CO_2 and methane fluxes were observed for the seagrass covered areas than for the bare sediment. The fluxes of both compounds showed clear diurnal variations with similar patterns above the seagrass and the bare sediment. We observed a strong imprint of the tidal cycle on both gases with more pronounced emission fluxes generally occurring during tidal inundation. At daytime, CO_2 assimilation dominated over benthic respiration resulting in a net uptake, regardless of the tidal state. Elevated fluxes during tidal immersion were also observed for all non methane VOCs studied here.
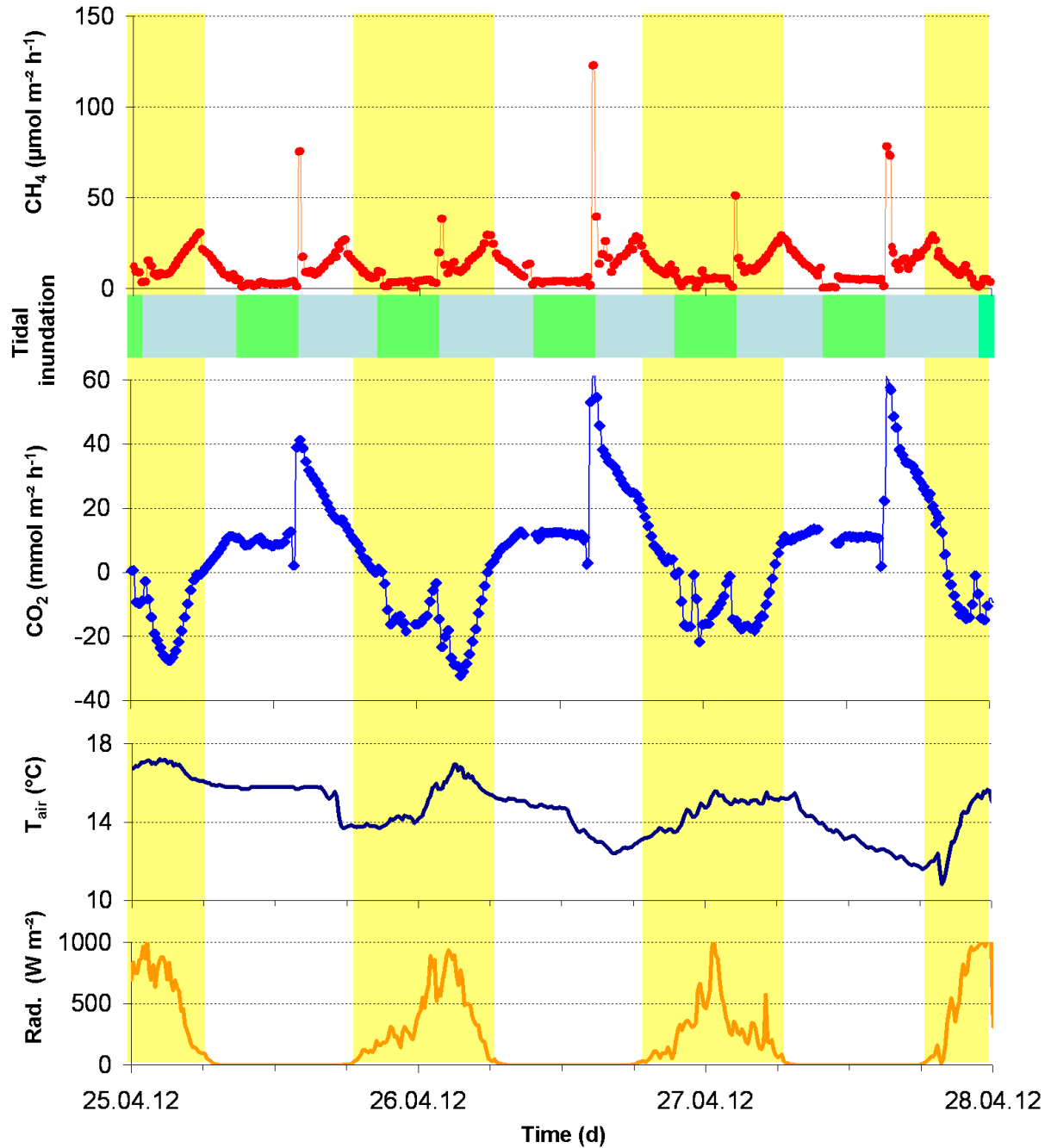
Figure 17: Diurnal variations of the methane (red) and CO₂ fluxes (blue) along with air temperatures and light intensity above a meadow of the seagrass *Z. noltii*. Air temperature and light intensity are also displayed. The measurements were carried out from April 25ᵗʰ to April 28ᵗʰ 2012. Yellow shades: daylight periods; green bars: periods of air exposure; blue bars: periods of tidal immersion.

Table 13: Averaged CO_2 and methane fluxes above seagrass for different periods of the tidal cycle. The fluxes were calculated from the measurements of day 2 and 3.

tidal stage	CO_2 (mmol m^{-2} h^{-1})		CH_4 (µmol m^{-2} h^{-1})	
	sediment	seagrass	sediment	seegrass
low tide day	-1.1	-9.1	0.4	6.9
low tide night	1.0	8.4	0.2	4.4
high tide day	-2.0	-16.4	6.6	14.3
high tide night	6.4	20.1	5.2	16.6
peak (water just arriving)	14.8	55.0	10.8	71.0
time averaged mean	2.1	4.2	3.0	12.8

6.3.1 Methane

During air exposure at low tide methane fluxes averaged 4.4 µmol m^{-2} h^{-1} at night and 6.9 µmol m^{-2} h^{-1} at day. With the feeder current just arriving at the sampling site the fluxes dropped almost to zero for 5 to 10 minutes. This drop was followed by a sharp emission peak observed for 15 minutes. Accounting for the integration time and the response time of the chamber system we deduce that these events may have actually lasted for two to five minutes. During these peak events the fluxes averaged 71 µmol m^{-2} h^{-1}. The peaks were more pronounced during the night (76 and 123 µmol m^{-2} h^{-1}) than during daytime (38 and 51 µmol m^{-2} h^{-1}). Afterwards the fluxes rapidly decreased to values below 9±1 µmol m^{-2} h^{-1}.

During tidal immersion the methane fluxes increased with rising height of the water and showed a second maximum of 30 ±1 µmol m^{-2} h^{-1} at high tide. With the ebb flow the methane fluxes decreased constantly to values about 9±1 µmol m^{-2} h^{-1} at water levels below 10 cm. The change from tidal immersion to air exposure is marked by a slightly elevated flux observed for about 15 minutes again followed by a drop close to zero before the flux stabilized on the low tide level again. In contrast to the peak events observed during the incoming tide, the increase in the flux during the ebb flow was rather small with 4 to 6 µmol m^{-2} h^{-1}.

The diurnal flux cycles observed above the sediment were similar to the diurnal cycles above the seagrass but, with much lower values (table 13 and figure 18). The methane fluxes averaged 0.3 µmol m^{-2} h^{-1} during low tide, and 6 µmol m^{-2} h^{-1} (5.2 µmol m^{-2} h^{-1} at daytime and 6.4 µmol m^{-2} h^{-1} at night time) during tidal inundation.
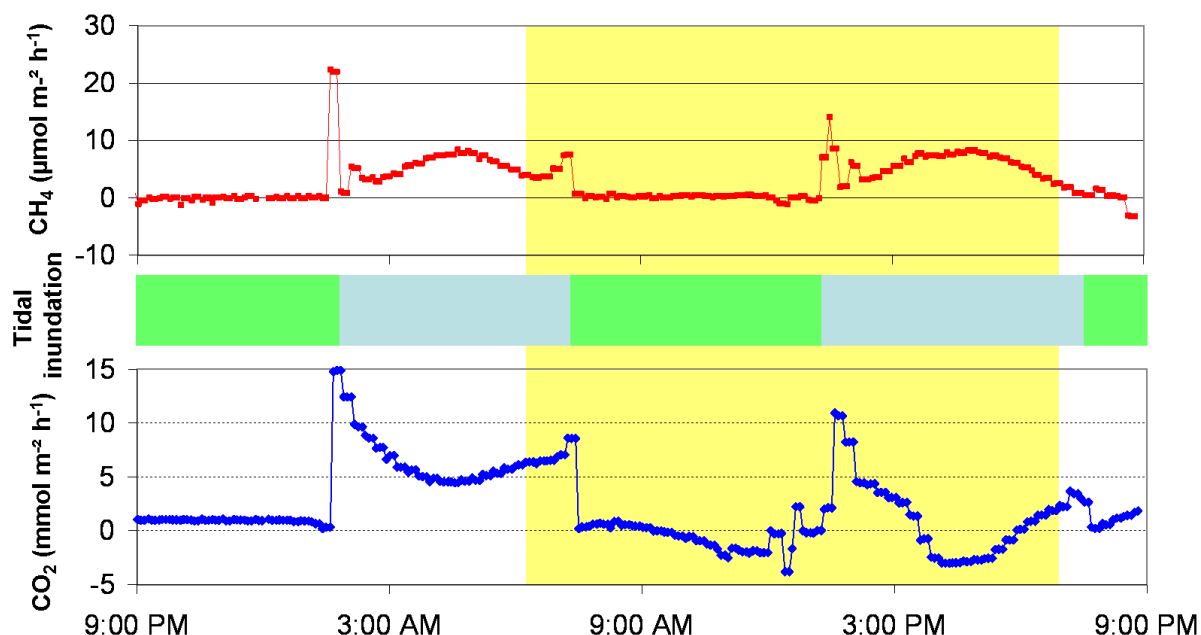
Figure 18: Methane and CO$_2$ fluxes above a bare sediment patch recorded on April 23th 2012. Upper graph (red): methane fluxes in µmol m^{-2} h^{-1}. Lower graph (blue): CO$_2$ fluxes in mmol m^{-2} h^{-1}. Yellow shades: daylight period; green bars: periods of air exposure; blue bars: periods of tidal immersion.

6.3.2 CO$_2$

In contrast to methane, the CO$_2$ flux was strongly influenced by both, the time of day and the tidal cycle. Deposition fluxes were observed during the day resulting from photosynthetic uptake while positive fluxes were observed during the night due to respiration. At air exposure during night, the emissions were relatively constant and averaged 8.4±0.5 mmol m^{-2} h^{-1}. Simultaneously to methane, with the incoming tide arriving at the sampling site, the flux dropped to zero for about 10 minutes and then rapidly increased to highest CO$_2$ emissions of up to 62 mmol m^{-2} h^{-1}. Thereafter, the CO$_2$ flux decreased rapidly to 38±4 mmol m^{-2} h^{-1} and then further declined slowly over the period of tidal inundation with a short plateau at high tide, which is somewhat different to methane. After sunrise, roughly coinciding with high tide, the CO$_2$ fluxes declined more rapidly due to the beginning of photosynthetic CO$_2$ assimilation. During the daylight period, CO$_2$ assimilation dominated over benthic CO$_2$ respiration resulting in a net uptake of CO$_2$ with average fluxes of -9.1 mmol m^{-2} h^{-1} during air exposure and of -16.4 mmol m^{-2} h^{-1} during immersion.

At night, the average sedimentary CO$_2$ fluxes were 1.0 mmol m^{-2} h^{-1} during air exposure and 6.4 mmol m^{-2} h^{-1} during tidal inundation. The CO$_2$ night time flux during inundation decreased until high tide and increased again with the onset of ebb flow indicating an inverse relation with the height of the water table. The daytime average CO$_2$ fluxes from sediment were -1 mmol m^{-2} h^{-1} during low tide and -2.1 mmol m^{-2} h^{-1} during tidal inundation.

6.3.3 VOCs

Relative fluxes of COS, CS_2, DMS, CH_3Cl, CH_3Br, CH_3I, $CHCl_3$, $CHBr_3$, propane, butane and propene are shown in figure 19. For those, which have been quantified against the Scott TOC 15/17 standard, mean fluxes and ranges are provided in table A3 (Appendix). It has to be noted that for most of the VOC flux data the sampling time does not agree with the sampling time for the CO_2 and methane data shown above. However, as observed for CO_2 and methane, the emission rates during tidal immersion significantly exceeded those measured during air exposure. The average enrichment ranged from 4 to 6 for CS_2, COS, propane, and the halocarbons CH_3Br, CH_3I, $CHCl_3$, and $CHBr_3$. A somewhat higher enhancement was observed for CH_3Cl. A less pronounced enhancement ranging from 1 to 3 is observed for DMS, propene, and butane. Except for CH_3Cl, our data indicate no similar drastic increase in the fluxes with the feeder current arriving at the sampling site as observed for methane. However, in this context it is important to note that the sampling time for the VOCs was 30 minutes followed by a break of 15 minutes required to change the cryotraps. Hence, it is possible that peak flux, lasting 3 to 5 minutes for methane, is not or not fully captured or diluted by our VOC sampling. For some compounds, notably propane, $CHBr_3$, and butane, our data also indicate a small enhancement when falling dry.

The temporal flux patterns demonstrate some remarkable differences between individual VOCs during tidal immersion. Strongly enhanced fluxes during high tide were observed for propane, COS and CS_2, indicating a similar pattern as for methane. In contrast the fluxes of the other compounds decreased or even turned from emission to uptake during high tide as observed for CH_3Cl, CH_3Br and $CHCl_3$ and thus are more similar to CO_2.
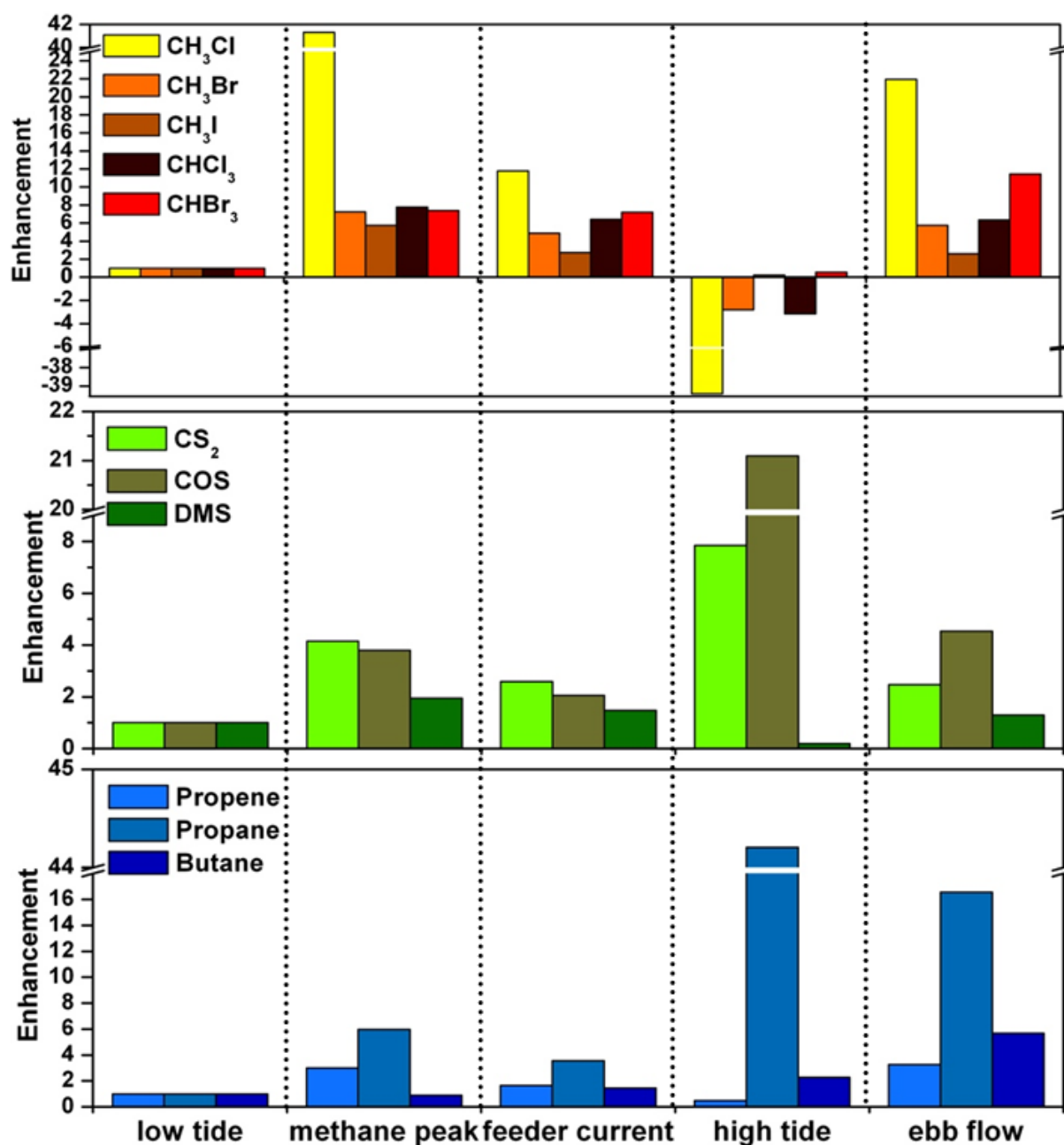
Figure 19: Relative enhancement of selected VOC fluxes from a tidally influenced seagrass bed. All fluxes were normalized to the respective mean fluxes during low tide. CS_2, CH_3Cl, CH_3Br, CH_3I, $CHCl_3$, $CHBr_3$, and propene were quantified against a Scott TOC 15/17 standard. Relative fluxes for COS, propane, butane and DMS were calculated from the measured intensities. For clarity reasons the variability of the VOC fluxes is not shown here. Mean and ranges are provided in the Appendix (table A3).

6.4 Discussion

6.4.1 Temporal flux pattern

The most striking feature of our results is the pronounced effect of the tidal cycle on the fluxes of all trace gases with significantly enhanced fluxes during periods of immersion as compared to periods of air exposure. Additionally, strong emission peaks of methane and CO_2 among other VOCs occurred during the transition from air exposure to immersion.

To the best of our knowledge, only one study has reported a positive correlation of the CO_2 and methane fluxes with the height of the water table from a brackish coastal lake in Japan (Yamamoto et al., 2009). The authors of this study did not present a conclusive explanation for the elevated fluxes, but suggested either lateral transport in the sediment in combination with salinity gradients affecting the source strength and/or enhanced gas ebullition due to increased pressure from the water column to be responsible for the enhanced emissions during high tide. A correlation between bubble ebullition and pressure change has been reported in some previous studies (Chanton et al., 1989; Baird et al., 2004; Glaser et al., 2004). However, the only study carried out in a tidally influenced system we are aware of suggests an inverse correlation between tidal height and bubble ebullition (Chanton et al., 1989). Due to a negligible inflow of freshwater, the Ria Formosa has a fairly constant salinity close to that of the open ocean. Thus, significant salinity driven lateral changes in methanogenesis and benthic respiration as suggested by Yamamoto et al. (2009) are implausible. Nevertheless, spatial variations in the source strength may occur due to variations in the benthic communities and in the supply of substrate by litter production and root exudates. The benthic vegetation around the sampling site consisted almost exclusively of *Z. noltii* and was quite homogeneous with variations in the above ground biomass being clearly below a factor of 2 and thus, do not support a change in the source strength by a factor of 6 as observed for methane during tidal immersion.

Most previous studies on trace gas fluxes in tidally influenced systems have reported higher fluxes during low tide than during high tide. These higher emissions during low tide were attributed to reduced gas diffusion during inundation (Heyer and Berger, 2000; Van der Nat and Middelburg, 2000) or to deep pore water circulation in tidal flats. Since the pioneering work of Riedl et al. (1972) there is rising evidence that advective exchange processes at the sediment-water interface strongly affect the fluxes and concentrations of trace constituents. Billerbeck et al. (2006b) proposed two different pathways for pore water circulation in intertidal sediments. Firstly, "body circulation" is generated by the hydraulic gradient between the sea water level and the pore water level in the sediment and leads to seepage of pore water close to the low water line at low tide. Several studies have attributed elevated levels of pCO_2 (Barnes et al., 2006; de la Paz et al., 2008; Deborde et al., 2010) and dissolved methane (Grunwald et al., 2009) during low tide to this kind of deep pore water advection.

Secondly, "skin circulation" (Billerbeck et al., 2006b) refers to the advective exchange in surface sediments and is driven by bottom current induced pressure gradients at the sediment surface. Several

studies have shown a prominent effect of advective exchange processes on the exchange of organic matter and nutrients in tidal sand flats (Huettel et al., 1996; Precht and Huettel, 2004; Billerbeck et al., 2006a; Werner et al., 2006). Werner et al. (2006) found a more intense and deeper transport of oxygen into the sediment due to advective exchange during tidal immersion than during air exposure, when the exchange is presumably driven by gas diffusion. This is also supported by a study of Kim and Kim (2007), who reported total oxygen fluxes exceeding diffusive fluxes by a factor of 2 to 3 for intertidal sediments from Taean Bay located in the Midwestern part of the Korean peninsula. Cook et al. (2007) reported a concurrent increase of total oxygen and TIC fluxes at the sediment surface by a factor of up to 2.5 under turbulent conditions relative to stagnant (diffusive) conditions. During measurements in the back barrier area of the island of Spiekeroog (Billerbeck et al., 2006b; Jansen et al., 2009), the highest oxygen penetration rates were observed immediately after high tide. In particular our methane fluxes may provide a mirror image of these oxygen dynamics. This is in accordance with Yamamoto et al. (2009), who noted a concurrent increase of the redox potential of the sediment with increasing methane and CO_2 fluxes during tidal inundation. Given this, we suppose an overall strong effect of advective solute transport at the sediment water interface on trace gas fluxes to explain the elevated fluxes during tidal immersion. Furthermore, the similarities in the flux pattern among all trace gases in our study suggests rather a change in the physical forcing than in the biogeochemical processes controlling the formation of the trace gases.

During each period of air exposure at night time, the CO_2/CH_4 ratios remained fairly constant and both fluxes dropped to zero for 15 minutes when the incoming tide reached the sampling site. This further suggests that the flux patterns rather mirror changes in the physical forcing towards the end of the period of air exposure than changes in the biogeochemical processes controlling the formation of both gases.

It is commonly thought that the fluxes during air exposure are most likely driven by gas evasion across the sediment-air and plant-air interface, respectively, and are hence controlled by the transfer resistance across these interfaces (Yamamoto et al., 2009 and references therein). However, this model cannot explain the observed drop in the fluxes. In waterlogged sediments trace gases have to be transported to the sites of gas diffusion, such as to a water gas interface or to the root systems of higher plants. Werner et al. (2006) observed a constant flow velocity of pore water over the entire period of air exposure and noted a decreasing flow velocity in the top 2 cm shortly before the feeder current reached the sampling site and the flow direction reversed. This decrease may explain the observed drop in the emission fluxes.

The drop in the fluxes is followed by a dramatic increase in CO_2 and methane emissions with methane showing a distinct peak and the respiratory CO_2 flux (during night) showing a more gradual decline. A similar increase of the fluxes has previously been reported for biogenic sulphur compounds (Aneja et al., 1986; Cooper et al., 1987a, b) and ammonia (Falcão and Vale, 2003) and has been attributed to a changing hydrodynamic pressure. In contrast to these studies, we did not observe a similarly

pronounced peak for any of the VOCs other than methane. However, it is quite reasonable that the peak events were not captured by the VOC sampling due to the discrete sampling strategy.

We suggest, air being trapped in the pore space becomes enriched in methane and CO_2 over the period of air exposure and is then displaced by the water reaching the sampling site causing a distinct peak. Due to the tortuosity of the air filled pores the release of trapped air from the sediment may be fostered by the aforementioned reverse of flow direction (Werner et al., 2006). Such a bubble ebullition mechanism is further supported by the fact that in particular for methane a similar drop in the emission is also observed for the transition from tidal immersion to air exposure, but not followed by a peak in the emission, which is simply due to the lack of air bubbles in the sediment at this stage of the tidal cycle. Furthermore, the higher fluxes during tidal inundation may limit the enrichment of trace gases in the surface sediment. The short and sharp emission peak for methane suggests that the methane has been accumulated close to the sediment surface or close to the roots of the seagrass from where it can be readily transferred into the atmosphere. In agreement with this, our data clearly show higher methane emission peaks during night than during daytime indicating a trapping of methane in a zone of the sediment where the methane oxidation capacity is affected by the diurnal changes in the sediment oxygenation.

As evident from the night time measurements, the respiratory CO_2 flux and the methane flux show a fairly constant ratio during air exposure but a different evolution during tidal immersion. In contrast to methane showing a distinct peak with the feeder current arriving at the sample site the CO_2 flux declines much slower. Methane has a fairly low water solubility and is strongly enriched in the entrapped gas relative to the pore water solution, whereas CO_2 is always close to equilibrium with the pore water DIC. Hence, after the transition from a bubble ebullition driven emission as suggested for the "methane peak" to an advective transport of pore water as suggested for the period of tidal immersion, the CO_2 flux is driven by the exchange of enriched pore water DIC and the observed gradual decline in the CO_2 flux reflects the dilution of the pore water DIC. While the seagrass measurements suggest a continuous decline of the CO_2 flux during tidal immersion, the experiment above the sediment suggests a partial recovery of the CO_2 flux after high tide and thus an inverse correlation with the height of the water table. As outlined before, this difference may result from the beginning CO_2 assimilation at the end of the tidal cycle which has a more pronounced impact during the seagrass incubations. In any case, this is in contrast to methane showing a second distinct peak during high tide. We can currently not elucidate the differences between the methane flux and the respiratory CO_2 flux during high tide. However, we speculate that the different emission pattern may result from different concentration profiles of both compounds in the sediment. Further the decline of the respiratory CO_2 flux may reflect competing processes such as H_2S oxidation.

6.4.2 Magnitude of methane fluxes

Methane fluxes above the seagrass averaged 0.31 mmol m^{-2} d^{-1} with ~76% being released during tidal immersion and the fluxes above the adjacent bare sediment patch were 0.07 mmol m^{-2} d^{-1} with ~93% being released during tidal immersion.

It is well recognized that sulphate reduction precludes methane generation in anoxic coastal sediments as the more energy efficient sulphate reduction can impose a substrate limitation on methanogenic bacteria (Martens and Berner, 1974; Oremland et al., 1982). Concordantly, Bartlett et al. (1987) and Delaune et al. (1983) reported decreasing methane fluxes with increasing salinity. Methane fluxes decreased from 100 to 200 g m^{-2} yr^{-1} at salinities around 1 psu to 1 to 5 g m^{-2} yr^{-1} at salinities above 18 psu. A direct comparison of our data to previous reported data is difficult due to the differences in salinity. However, Middelburg et al. (2002) have estimated the average methane flux from European estuarine waters to 0.13 mmol m^{-2} d^{-1}. The authors moreover suggested tidal flats as important methane sources in estuaries. Our data suggest that apart from body circulation (Jansen et al., 2009; Grunwald et al., 2009), skin circulation may substantially contribute to methane fluxes.

Our methane flux of 0.3 mmol m^{-2} d^{-1} from seagrass meadows are by about one magnitude higher than those reported by Deborde et al. (2010). Anyhow, based on a global seagrass coverage area of 300.000 km² (Duarte et al., 2005) this corresponds to a methane flux of ~ 0.5 Tg CH_4 yr^{-1} suggesting seagrass meadows being a minor global source of methane.

6.4.3 Magnitude of CO_2 fluxes

Seagrass meadows have been suggested to be only marginally autotrophic systems due to the high input of allochthonous organic matter (Hemminga and Duarte, 2000). Santos et al. (2004) found heterotrophic and autotrophic processes being close to balance in seagrass beds of the Ria Formosa. Our data suggest an overall net community production (NCP) of 4.2 mmol m^{-2} h^{-1} (101 mmol m^{-2} d^{-1}) over the course of the experiment, demonstrating heterotrophic metabolism do dominate within the seagrass community. The average net CO_2 emissions (community respiration, CR) during night were 10.2 mmol m^{-2} h^{-1} (air exposure), 23.2 mmol m^{-2} h^{-1} (tidal immersion) and 55.0 mmol m^{-2} h^{-1} (peak event) (table 13). With an average daylight period of 12 h and an average period of tidal inundation of 15.30 h d^{-1}, the community respiration is estimated to 233 mmol m^{-2} during night time. It is quite reasonable that, as observed for methane, the respiratory CO_2 production during the day is in the same order as during night but is immediately recycled, i.e. assimilated by the seagrass community. In particular the accelerated decrease in the CO_2 flux, coinciding with sunrise during tidal inundation on the 27th, provides some evidence for this hypothesis. Further the CO_2 peaks occurring during the transition from air exposure to inundation further substantiate this hypothesis. Given this, we speculate that the community respiration may double to 466 mmol m^{-2} d^{-1} with roughly the half being immediately being recycled. Over the course of the experiment a net CO_2 assimilation occurred roughly between 9:00 am and 6:00 pm with average assimilation rates of 9.1 mmol m^{-2} h^{-1} during air exposure and 16.4 mmol m^{-2} h^{-1} during immersion summing up to a net CO_2 assimilation of 125 mmol

m^{-2} d^{-1}. Accounting for the internal recycling of CO_2 the average assimilation rates may increase to 20.9 mmol m^{-2} h^{-1} during air exposure and 39.2 mmol m^{-2} h^{-1} during immersion. Based on this we estimate that the gross community production (GCP) may be as high as 358 mmol m^{-2} d^{-1} (4.3 g C m^{-2} d^{-1}). Without accounting for the internal recycling the assimilation rate during air exposure (9.1 mmol m^{-2} h^{-1}) found in our study compares well to the previous reported assimilation rates ranging from 10 to 15 mmol m^{-2} h^{-1} (Santos et al., 2004; Silva et al., 2005), while our net assimilation rate during tidal immersion (16.4 mmol m^{-2} h^{-1}) significantly exceeds previously reported rates of less than 5 mmol m^{-2} h^{-1} (Santos et al., 2004, Silva et al., 2005, 2008). These earlier studies used static chambers prone to introduce stagnant condition. In contrast, the bubbling in our chamber introduces turbulent mixing and hence may facilitate the transport of CO_2 across the water leaf interface. In conclusion, these differences can be mainly attributed to the introduction of advection in our chamber system. As already outlined in Silva et al. (2005), the available data on the aerial versus submerged photosynthesis of *Z. noltii* are not consistent. While Leuschner and Rees (1993) and Leuschner et al. (1998) measured comparable rates of CO_2 assimilation in air and water, Pérez-Llorens and Niell (1994) found CO_2 uptake rates in air 10 to 20 times lower than in water. As the strength of advection in our chamber system relative to ambient conditions is unknown we can currently not appraise the quality and reliability of the difference chamber systems. However, these differences highlight the importance of accurately addressing the perturbations of turbulent flows in benthic flux chambers.

When accounting for the internal recycling of CO_2 the rates estimated here (20.9 mmol m^{-2} h^{-1} during air exposure and 39.2 mmol m^{-2} h^{-1} during immersion) significantly exceed those from previous flux chamber studies (Santos et al., 2004, Silva et al., 2005, 2008). The GCP obtained from our corrected rates (4.3 g C m^{-2} d^{-1}) is close to that (~ 5 g C m^{-2} d^{-1}) reported by Cabaço et al. (2012) for established meadows of *Z. noltii* in the Ria Formosa for this time (late spring) of the year, whereas it should be noted that the latter refers to the species level and not to the community level.

6.4.4 VOCs

The overall focus of this section is the temporal evolution of the VOC fluxes over a tidal cycle. A quantitative discussion of the VOC data and an assessment of potential intrinsic sources are beyond the scope of this paper. For the halocarbons CH_3Cl, CH_3Br, CH_3I, and $CHBr_3$ this is reported elsewhere (Weinberg et al., in prep., chapter 5). COS, CS_2, and propane, having a known sedimentary source (Claypool and Kvenvolden, 1983; Bodenbender et al., 1999), show a similar temporal pattern as methane during high tide. Thus, we conclude that the emission of these compounds is in analogy to methane mainly controlled by advective transport across the sediment water interface.

Halocarbon production in the marine environment is generally attributed to photoautotrophic sources (Gschwend et al., 1985; Moore et al., 1995b; Manley et al., 2006), though there is some evidence of a sedimentary bacterial source for iodomethane (Amachi et al., 2001). In seagrass meadows halocarbons are presumably produced by the seagrass or by the microphytobenthos. Only in the latter case porewater flow across the sedimentary interface can directly affect the emission. However, the

elevated halocarbon fluxes during tidal immersion may reflect an enhanced transport across the leave water interface and/or result from the enhanced net primary production during immersion. Sediments may also act as a sink for monohalomethanes (Miller et al., 2001; Bill et al., 2002) and trihalomethanes are known to be degraded by a variety of microorganisms (Neilson and Allard, 2008). Thus, the remarkable decrease and the uptake of the halocarbons may simply reflect sedimentary degradation processes. We further noted remarkable levels of H_2S and methanethiol in our samples during high tide. In particular H_2S is a very reactive nucleophile, readily reacting with monohalomethanes (Barbash and Reinhard, 1989) and thus may additionally foster the degradation of monohalomethanes. In summary, similarly to methane and CO_2, the VOC fluxes are more pronounced during tidal immersion than during air exposure but further show some remarkable differences resulting from their different sources and sinks.

6.5 Conclusions

We presented flux measurements for a variety of trace gases in a tidally influenced seagrass bed (*Z. noltii*) using a newly developed flux dynamic chamber system that can be deployed over full tidal cycles. In particular the CO_2 and methane data illustrate the need for high time resolution measurements to accurately address the fluxes and dynamics of trace gases in tidally controlled systems. In particular for methane we observed short emission peaks with the feeder current just arriving at the sampling site. While previous studies have demonstrated the importance of advective transport processes for the oxygenation of sediments, our results emphasize a general strong control of advective transport processes on trace gas fluxes in tidal systems. We are currently aware of only quite a few earlier studies indicating elevated fluxes during tidal immersion or periods of tidal change. Contrasting most previous flux chamber studies, our data indicate significant enhanced fluxes during tidal immersion relative to periods of air exposure for all trace gases measured in this study. The main difference to most of the previous studies is the introduction of an advective flow in our flux chamber system resulting in substantially higher fluxes during immersion. Hence, our results highlight the importance of accurately addressing the perturbations of turbulent flows in flux chamber studies. If the observed flux enhancements are more than just episodic events this may have fundamental implications for our understanding of the carbon and trace gas cycling in coastal environments.

7. Estimation of the annual halocarbon budget in the Ria Formosa

The last chapters presented seagrass meadows as a vital source for halocarbons to the atmosphere in the lagoon. However, additional sources are suggested to have a significant impact on the halocarbon budget in this system due their spatial abundances and/or specific emission potentials. These potentially significant sources comprise salt marshes, phytoplankton, macroalgae, and sediments. Thus, this chapter tries to elucidate the halocarbon budget by integrating the emission data from distinct sources using data from own field measurements (seagrass meadows and sediments) as well as from the literature (salt marshes, phytoplankton, and macroalgae) along with their respective abundance in the lagoon. The estimate relies on several simplifications and assumptions which are as follows:

In general, mean emission of individual studies from incubation and field experiments were used neglecting possible diurnal patterns. Except for salt marshes, all potential sources are subject to the tidal regime and thus the emission rates might shift significantly from air exposure to inundation. However, such data is hardly available in the literature and thus, it was not possible to account for these circumstances other than for seagrass meadows. The specific assumptions and procedures for data treatment for each source were:

i) Seagrass meadows. The extent of coverage by the seagrass species *Z. noltii* in the lagoon is 13.04 km^2 (Guimarães et al., 2012; Rui Santos pers. comm.). Other species comprise *Zostera marina* and *Cymodocea nodosa* with a combined abundance of 0.96 km^2 (Cunha et al., 2009). Accordingly, a total seagrass coverage of 14 km^2 was adopted for the annual estimate.

Seasonal and tidally weighted flux data of halocarbons from seagrass meadows was obtained from chamber based measurements and sea-air flux calculations from chapter 5. Two emission scenarios for the annual halocarbon production were calculated: In Scenario A, the halocarbon emissions during air exposure and tidal inundation emanate directly into the atmosphere and only from the areas covered by seagrass meadows (14 km^2). Secondly, it was assumed that the halocarbons produced under submerged conditions are transported and emitted downstream in the entire lagoon (Scenario B). Therefore, the emissions above inundated seagrass meadows (sea-air exchange) were taken as representative for the seagrass emissions along the entire inundated parts of the lagoon (53 km^2). To our observation the water concentrations of halocarbons at the sampling spot fell roughly in the middle range to those determined at the sampling position most distant from the inlet which in turn supports this assumption. Scenario B implies that entire emissions from the water phase originate solely from seagrass meadows and contributions from other sources are negligible. Thus, this approach depicts an upper limit of seagrass production from this single source.

ii) Sediments. Bare sediments in the Ria Formosa cover 35.96 km^2 (Rui Santos pers.comm.). Firstly, annual emissions from the sediment were estimated from the field incubations in summer during low tide (chapter 5). Secondly, the sandy to muddy sediments in the lagoon were reported to exhibit high

amounts of benthic chlorophyll a (microphytobenthos) with 269 mg m^{-2} which is equivalent to about 99% of the total pelagic chlorophyll a concentration in the lagoon (Brito et al., 2010). Therefore, the estimate for sedimentary emissions by microphytobenthos was further complemented by phytoplankton production data of Smythe-Wright et al. (2010) for monohalomethanes and Tokarczyk and Moore (1994) for CHBr$_3$ using the abundance of sediments with the microphytobenthos concentration per unit area. Thereby it was assumed that pelagic phytoplankton composition is similar to benthic microphytobenthos.

iii) Salt marshes. Reported halocarbon emissions from salt marshes are characterized by high variation depending on species distribution and regional climate. The lagoon comprises in total 13 different salt marsh plant species (Rui Santos, pers. comm.). Most of these species were not yet determined with regard to halocarbon emissions. Thus, the estimated annual emissions should be handled with great care. The salt marsh species *Spartina maritima* and three species from the family of Amaranthaceae (*Salicornia ramosissima, Sarcocornia fruticosa, Sarcocornia perennis*) cover 14.5 km^2 roughly representing 60% of the total salt marsh area of the lagoon. To extrapolate the emissions, average production rates were taken from Manley et al. (2006) (seasonal emissions of CH$_3$Cl, CH$_3$Br, CH$_3$I) and Rhew et al. (2000) (mean emissions of CH$_3$Cl and CH$_3$Br) for *Spartina* and Amaranthaceae family (there, represented by two *Salicornia* subspecies). Extraordinary high emitting species in their study areas such as *Batis* and *Frankenia* (Manley et al., 2006) are absent in the Ria Formosa, and thus are not considered. Yearly emissions from the lagoon were upscaled with emission data from salt marsh plants of temperate regions (Cox et al. (2004) for CH$_3$I and Blei et al. (2010) for CH$_3$Cl and CH$_3$Br). For both estimates the areal coverage of 24.95 km^2 was used (Rui Santos, pers. comm.).

iv) Phytoplankton. A chlorophyll a concentration of 3.06 μg L^{-1} adopted from long-term measurements in the Ria Formosa (Brito et al., 2012) was assumed for the extrapolation. The water volume in the lagoon was estimated using the mean water depth of 1.5 m (Tett et al., 2003) and the areal extension as given by Brito et al. (2010) during high tide (55 km^2) and low tide (22 km^2). The emission rates from phytoplankton were taken from incubation experiments of Smythe-Wright et al. (2010) and Tokarczyk and Moore (1994) for monohalomethanes and CHBr$_3$, respectively. In analogy to the estimate for seagrass meadows, the emissions during low tide and high tide were weighted by 8 hours and 16 hours, respectively.

v) Macroalgae. The macroalgae species in the lagoon are mainly composed of *Ulva spp.* and *Entereomorpha spp.*. Since their abundance varies considerable between seasons and years (Rui Santos, pers. comm.), mean annual dry weights derived from monthly means for both species were adopted (Anibal et al., 2007). The best estimate of macroalgal abundance in the lagoon is 2.5 km^2 (Duarte et al., 2008). The species-based emissions were calculated according to mean production rates of Baker et al. (2001) for monohalomethanes and Nightingale et al. (1995) for CHBr$_3$, respectively.

The resulting annual emission inventory of seagrass meadows and other sources in the lagoon is presented in table 14.

Table 14: Estimated annual halocarbons emission (Mol yr^{-1}) from seagrass meadows in comparison to other sources in the Ria Formosa. Numbers are rounded to two significant digits. Sources other than seagrass meadows and sediment were calculated from published emission rates. For more information see text.

Source	lagoon area covered km^2	CH$_3$Cl Mol yr^{-1}	CH$_3$Br Mol yr^{-1}	CH$_3$I Mol yr^{-1}	CHBr$_3$ Mol yr^{-1}
Seagrass meadows (Scenario A)	14	2100	250	200	340
Seagrass meadows (Scenario B)	14, ~53	6900	540	550	2200
Phytoplankton	~53 (~22)	26	3	4	83
Macroalgae	2.5	7	14	6	56
Sediment (microphytobenthos)	35.96	1100-1300	150-180	80-180	270-4100
Salt marshes [a]	24.95	4700	910	390	-
Salt marshes [b]		25000	1800	840	-

[a] calculated using mean emission data from temperate salt marshes (Cox et al., 2004; Blei et al., 2010)
[b] estimated using mean emission data from subtropical salt marshes (Rhew et al., 2002; Manley et al., 2006); for more information, see text.

The obtained seagrass-derived emission estimate ranged from 2100-6900 Mol yr^{-1} for CH$_3$Cl, 250-540 Mol yr^{-1} for CH$_3$Br, 200-550 Mol yr^{-1} for CH$_3$I, and 340-2200 Mol yr^{-1} for CHBr$_3$. Obviously, there is a huge difference between the two scenarios with substantially enhanced emissions in Scenario B. This discrepancy may relate to a large spatial variation of seagrass meadows which are not sufficiently resolved by the measurements at a definite sampling spot (Scenario A). Furthermore, in particular for CHBr$_3$, the chamber measurements during tidal inundation underestimate the production rates due to the low purge efficiency for this compound (see chapter 5). Thus, when accounting for the purge efficiency, the annual CHBr$_3$ fluxes may actually increase to 600 Mol yr^{-1} in Scenario A. Despite these potential uncertainties, the emission scenario B suggests that other abundant sources in the water phase contributing to the overall emissions.

Accordingly, neither pelagic phytoplankton nor macroalgae are able to close the gap between the two scenarios, as they only reassemble a small fraction of the total halocarbon budget. The small emissions from phytoplankton can most likely be explained by the low amount of water masses within the lagoon in combination with the low chlorophyll a concentration. Similarly, the abundance of macroalgae and their areal biomass is too low in the lagoon to have a significant impact. Otherwise, the difference between the two scenarios may be closed by CH$_3$Br and CH$_3$I emissions from the sediments. This also holds true for CHBr$_3$, when using reported phytoplanktonic production rates to estimate the production rates for the microphytobenthos. In contrast, the sediments seem unlikely to close the gap by additional CH$_3$Cl emissions. Recently, photochemical production pathways for CH$_3$Cl from dissolved organic matter were discovered (Moore, 2008; Dallin et al., 2009).

The estimate of monohalomethane emissions of salt marshes is highly uncertain due to the very variable emission rates reported in the literature. Using emission data from subtropical studies (Rhew et al., 2000; Manley et al., 2006), in particular CH$_3$Cl production is by far greater than all other sources

in the lagoon. However, as pointed out in chapter 5, atmospheric $\delta^{13}C$ values did not mirror such high contributions from this source. Accordingly, this suggests a lower contribution from salt marsh plants as rather represented by the emission rates from temperate salt marshes (Cox et al., 2004; Blei et al., 2010).

Overall, while salt marshes presumably play a significantly role, their actual contribution to the lagoons' halocarbon budget cannot sufficiently clarified without detailed field studies. Despite of the mentioned uncertainties, seagrass meadows and the sediments (microphytobenthos) appear as the most important halocarbon sources within the Ria Formosa rather than phytoplankton and macroalgae. Therefore, on local and perhaps regional scales the emission of halocarbons, notably of $CHBr_3$, are not necessarily linked to phytoplanktonic and macroalgae sources as commonly believed. Other sources such as seagrass meadows and sediments may reassemble a significant portion in these coastal areas.

8. Determination of seagrass emissions and stable carbon isotope composition of halocarbons from incubation experiments

8.1 Introduction

The results presented in the last chapters revealed the capability of seagrass meadows to produce halocarbons. As the net emissions during field studies definitely depict the emission potential of the entire ecosystem, it is still questionable whether the seagrass itself or other sources, e.g. sedimentary microphytobenthos, are responsible for this production. Up to date, there is no direct evidence for the ability of seagrass to produce halocarbons. Biosynthesis of monohalomethanes generally proceeds enzymatically (methyltransferase) by utilizing S-adenosyl-L-methionine (SAM) as methyl donor (Wuosmaa and Hager, 1990; Ni and Hager, 1999); the respective being also reported for higher plants (Attieh et al., 1995; Saini et al., 1995; Yokouchi et al., 2002; Saito and Yokouchi, 2006). Therefore, it is likely that also seagrass species generate monohalomethanes as part of their metabolism by this pathway.

Thus, to get first information whether the seagrass itself produces halocarbons, a lab incubation study with solely seagrass was performed. Along with the emissions, the stable carbon isotope signatures were determined. It should be noted that seagrasses are generally colonized with epiphytes (Borowitzka et al., 2006) representing an additional possible source for halocarbons. Thus, emissions presented here are presumably brought by a combination of both sources (source organisms).

Incubation studies are frequently used to study halocarbon emissions. For example, almost all emission estimates for coastal macroalgae rely on this type of experiments (e.g. Gschwend et al., 1985; Baker et al., 2001; Laturnus et al., 2004; Leedham et al., 2013). This is primarily a consequence of the relatively low complexity of experimental design making it a logistically more convenient and cost-effective method to cover a broad range of different species. Furthermore, potentially emission-driving parameters such as radiation, temperature, and salinity can be adjusted. The design and operation of the incubations varies between different studies. Principally, the organism of choice is enclosed in a suitable vessel and the produced compounds are analyzed in the vessels' air or water after certain times of incubation.

8.2 Experimental design and operation

The seagrass (*Z. noltii*) was collected from a dense seagrass meadow in Dagebüll, Northern Germany on 10th September 2010. The seagrass was gently removed from the ground minimizing plant damage and washed on-site with seawater. Furthermore, seawater was sampled in order to cultivate the seagrass for the duration of incubation experiments and to use it for the incubation experiments as control experiment. The incubation system is presented in figure 20.
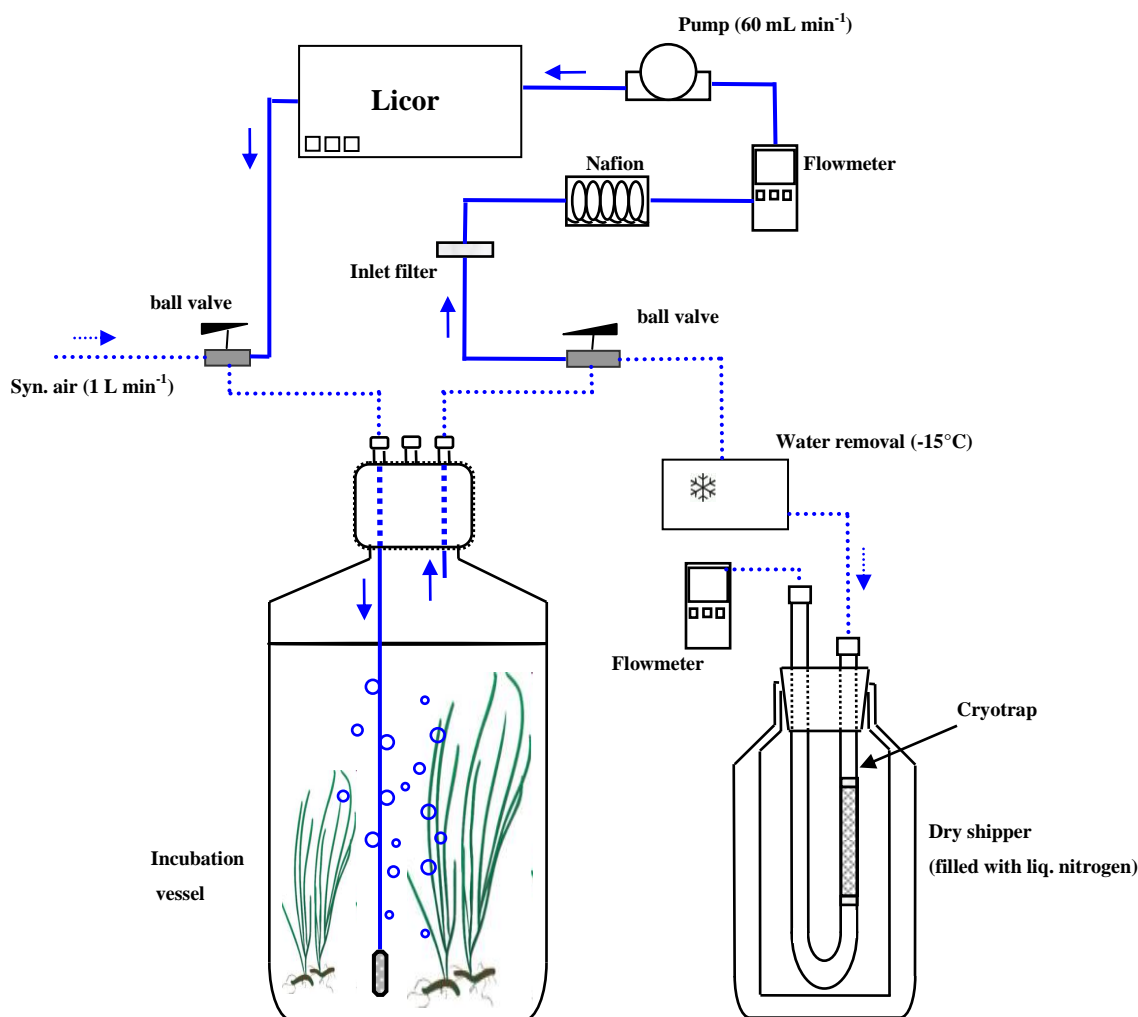
Figure 20: Scheme of the incubation system for the determination of emission and stable isotope composition of halocarbons

The incubation system consists of a purge vessel (Duran glass bottle, 1L volume, Schott, Germany) in which seawater and the seagrass is filled. All connections were made with PFA tubes (1/2", 1/8") and Swagelok fittings. The cap of the vessel has three connections. One is generally closed by a septum for injection of CO_2 during the incubations and is assembled by a temperature sensor to determine the water temperature (mean 22.7°C). The other two connections are the inlet and outlets for the purge gas/circulating gas. The gas is thereby introduced through the inlet by a stainless steel frit. Two different stages of this system exist: Firstly, during incubation time, the system is a closed system whereby a pump maintains a constant flow of 60 mL min^{-1}. The purged gas passes an inlet filter to scavenge the salt aerosols and water is removed by a Nafion dryer. The CO_2 content of the gas stream is measured using a CO_2 analyzer (Li-840, LICOR Biosciences, Germany). The outgoing gas is then reintroduced into the purge vessel. This circulation in this closed system enabling the continuous measurement of CO_2 as representative for production and consumption of the seagrass/seawater and thus, the primary productivity. Furthermore, it ensures a well mixed system. Secondly, after each incubation cycle the pump is shut off and thus the internal cycling is stopped. By switching the two

ball valves synthetic air (Westfalen, Germany) is introduced into the purge vessel at a flow of 1 L min⁻¹(dashed line) (final volume 30L). The produced halocarbons are stripped from the gas/water phase into the cryotrapping system which is the same as used during our field campaigns and is in detail described in chapter 5. Thus, during this stage the incubation system operates like an ordinary purge and trap system. Measurement and quantification was done as presented in chapter 5 for concentration and in chapter 3 for the determination of stable carbon isotopes.

Prior to the incubation, 600-700 mL of seawater was filtered (glass fibre filter, 110 mm, 0.7µm, Whatman, USA) ensuring the elimination of phytoplankton, though bacteria may remain in the water. The seawater was purged for about one hour with synthetic air in order to eliminate the halocarbons already dissolved in the seawater. Afterwards, the seagrass was filled into the incubation vessel, the system was closed, and the incubation cycle was started. CO_2 concentration in the system was monitored and CO_2 was injected by a gas-tight syringe when the concentration fell below 370 ppm. Daytime was simulated by using two lamps (500W) positioned near to the vessel that were turned off during night. The duration of the daytime incubation cycles were 1-3 hours during initial tests and finally set to two hours. Nighttime incubations were 14-16 hours. The measurements of the incubation samples were performed as described in chapter 5. After each incubation experiment, the seagrass was gently removed from the vessel and the fresh weight and dry weights (after air drying) were determined. For seawater controls either the seawater from the seagrass incubation or from the seagrass cultivation basins were taken.

Since synthetic air and cryotraps contain small amounts of CH_3Cl, CH_3Br, and CH_3I the contribution was determined by trapping 30 L of this gas on cryotraps and subsequently measured. The contribution to the seagrass incubation samples was usually found to be lower than 7% for each of the monohalomethanes. Since in seawater incubations (controls) the blank contribution was higher, all values given in the next section are blank-corrected. Extraction efficiency of halocarbons from the incubation vessel was evaluated during each incubation cycle. The average efficiency for a seawater volume of 700 mL and a purge rate of 1 L min⁻¹ (purge volume 30L) was 97% for CH_3Cl, 93% for CH_3Br, 87% for CH_3I, and 70% for $CHBr_3$. Since for the halocarbon extraction of seawater controls a magnetic stir bar was used, the average efficiencies were higher for all compounds with 96% (CH_3Cl), 95% (CH_3Br), 92% (CH_3I), and 82% ($CHBr_3$). The individual purge efficiencies were used to calculate the final emissions. Emissions in the next sections are commonly reported as pmoles per grams fresh weight and hour (pmol g FW⁻¹ h⁻¹) and pmoles per grams dry weight and hour (pmol g DW⁻¹ h⁻¹) for seagrass experiments.

8.3 Results

8.3.1 Halocarbon emissions from seagrass and seawater incubations

The biomass-normalized results of two incubation experiments are given in table 15. During all incubation periods the seagrass emitted halocarbons. The ranges were 3.0 to 16.2 pmol g FW^{-1} h^{-1} for CH_3Cl, 0.3 to 3.7 pmol g FW^{-1} h^{-1} for CH_3Br, 0.02 to 1.0 pmol g FW^{-1} h^{-1} for CH_3I, and 0.5 to 20.9 pmol g FW^{-1} h^{-1} for $CHBr_3$.

Table 15: Biomass-normalized halocarbon emissions of *Z. noltii* submerged in filtrated seawater over the course of two incubation experiments. Fresh/dry weights were 28.2/4.0 g in experiment 1 and 29.1/2.8 g in experiment 2, respectively. Samples with longer incubation times than three hours are nighttime incubations. SD: standard deviation. n.a.: not available due to analytical problems.

Sample	time hours	CH_3Cl	CH_3Br pmol g FW^{-1} h^{-1}	CH_3I	$CHBr_3$	CH_3Cl	CH_3Br pmol g DW^{-1} h^{-1}	CH_3I	$CHBr_3$
Experiment 1									
Z. Noltii 1	14	8.0	1.1	0.2	0.6	56.4	8.0	1.2	4.2
Z. Noltii 2	1	16.2	3.7	0.8	9.8	113.9	25.8	5.7	69.0
Z. Noltii 3	1	8.7	2.1	0.6	11.6	61.1	14.9	4.0	81.6
Z. Noltii 4	3	10.1	1.5	0.4	9.4	71.3	10.3	2.8	66.2
Z. Noltii 5	2	13.3	1.6	0.4	20.9	93.7	11.3	3.0	147.2
Z. Noltii 6	15	6.5	0.8	0.1	1.9	45.9	5.4	0.4	13.7
Mean		10.5	1.8	0.4	9.0	73.7	12.6	2.9	63.6
SD		3.6	1.0	0.3	7.3	25.5	7.2	1.9	51.7
Experiment 2									
Z. Noltii 1	2	4.6	1.3	1.0	3.6	48.2	13.6	10.0	37.4
Z. Noltii 2	2	6.5	0.5	0.2	-	67.1	4.9	1.7	n.a.
Z. Noltii 3	14	3.9	0.4	0.1	0.9	41.0	4.4	0.6	9.0
Z. Noltii 4	2	6.2	1.1	0.3	5.3	64.6	11.1	3.3	55.0
Z. Noltii 5	2	7.4	0.8	0.3	5.5	76.4	8.0	3.3	57.2
Z. Noltii 6	2	3.0	0.5	0.3	4.5	31.1	5.5	3.0	46.9
Z. Noltii 7	15	4.0	0.4	<0.1	0.8	41.9	3.9	0.3	8.2
Z. Noltii 8	2	6.3	1.1	0.2	5.9	65.2	11.5	2.5	61.7
Z. Noltii 9	2	6.7	0.7	0.2	3.8	70.1	7.1	2.2	39.0
Z. Noltii 10	2	7.3	n.a.	n.a.	n.a.	75.8	n.a.	n.a.	n.a.
Z. Noltii 11	16	3.9	0.3	<0.1	0.5	40.3	3.4	0.2	5.6
Mean	-	5.4	0.7	0.3	3.4	56.5	7.3	2.7	35.6
SD	-	1.6	0.3	0.3	2.2	16.2	3.6	2.8	22.4
All									
Mean	-	7.2	1.1	0.3	5.7	62.6	9.3	2.8	46.8
SD	-	3.4	0.8	0.3	5.5	21.0	5.7	2.4	38.0

The average variabilities between both experiments were usually within a factor of 2 for all compounds reflecting a good reproducibility of this incubation approach. The first experiment, where partly short incubations times (1 hour) were applied, revealed that the seagrass emits halocarbons quite rapidly. Furthermore, there seems to be no clear difference between incubation lengths under light

conditions lasting between one to three hours. However, the comparison between day and nighttime measurements indicate certain differences (figure 21, left panel).
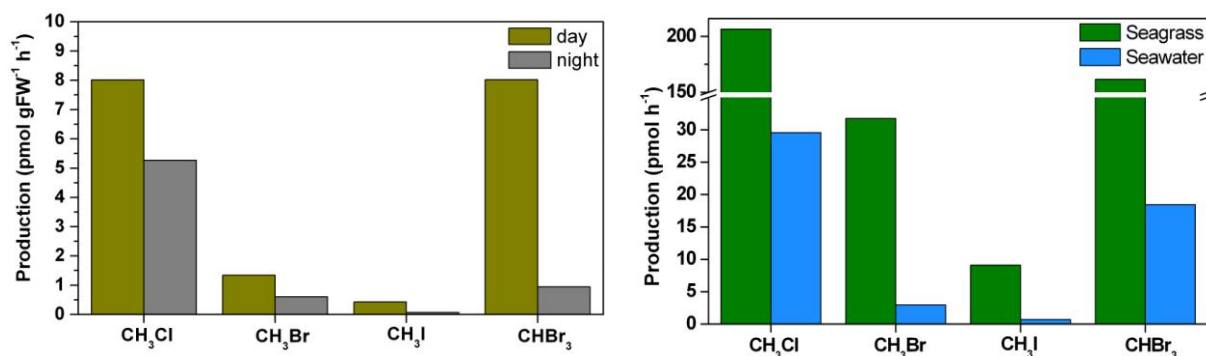
Figure 21: Left panel: average daytime (n=12) versus average nighttime emissions (n=5) of halocarbons from two incubation experiments with the seagrass *Z. noltii*. Right panel: Comparison of average emissions of halocarbons from two incubation experiments with seagrass (n= 17) and seawater controls (n=11).

Average daytime measurements revealed actually higher emissions reassembling factors of 1.5 (CH_3Cl), 2.2 (CH_3Br), 6.2 (CH_3I), and 8.5 ($CHBr_3$) in comparison to periods of darkness. Thus, light seems to stimulate halocarbon production which is concordant to the higher primary productivity of the seagrass or seagrass-attached epiphytes. This effect was especially pronounced for CH_3I and $CHBr_3$.

Some halocarbon production was also observed in seagrass free seawater controls, but at much lower levels. There, halocarbon emissions ranged from 4.0 to 88.3 pmol h^{-1}, 0.4 to 8.2 pmol h^{-1} for CH_3Br, 0.1 to 1.6 pmol h^{-1} for CH_3I, and 1.8 to 57.3 pmol h^{-1} for $CHBr_3$. As for the seagrass experiments, higher emissions by factors of 4 to 8 were observed under light irradiance. For better comparison, seagrass emissions from table 15 are converted to pmol h^{-1}. Results are depicted in figure 21 (right panel). On average, the seagrass emissions were higher than seawater controls by factors 8, 12, 14, and 10 for CH_3Cl, CH_3Br, CH_3I, and $CHBr_3$.

8.3.2 Isotopic composition of halocarbons

Aiming to calculate seagrass isotopic source signatures for halocarbons, the contribution of seawater controls must be accounted for, since both experiments revealed emission. It was assumed that during seagrass experiments emissions fluxes and $\delta^{13}C$ values of seawater were the same as without seagrass. As the best estimate for the seawater source the respective means of fluxes and isotope values were used, if available. Thus, the isotopic signature for the seagrass ($\delta^{13}C_{seagrass-em}$) was calculated using a coupled isotope and mass balance:

$$\delta^{13}C_{seagrass-em} = \frac{(\delta^{13}C_{seagrass} \times F_{seagrass} - \delta^{13}C_{seawater} \times F_{seawater})}{(F_{seagrass} - F_{seawater})}$$

where $\delta^{13}C_{seagrass}$ and $\delta^{13}C_{seawater}$ (‰) as well as $F_{seagrass}$ and $F_{seawater}$ (nmol h^{-1}) are the isotope values and fluxes of seagrass and seawater, respectively. The final stable carbon isotope values along with the uncorrected values from seagrass and seawater incubation are given in table 16. Due to the small contribution of seawater to the emitted halocarbons in seagrass incubations, the applied corrections shift the final seagrass-derived source signature usually not more than ±2‰. However, in nighttime samples were the contribution of CHBr$_3$ in the seawater were presumably higher, the seagrass emission of this compound must have been more depleted in ^{13}C.

Table 16: Stable carbon isotopes of halocarbons emitted from seawater and *Z. Noltii*. Samples with longer incubation times than three hours are nighttime incubations. Number in parenthesis are the uncorrected, measured values; for further information, see text. SD: standard deviation. n.a.: not available due to analytical problems. n.d.: not detected, below limit of detection.

Sample	time	CH$_3$Cl	CH$_3$Br	CH$_3$I	CHBr$_3$
	hours	‰	‰	‰	‰
Seawater 1	3	-37.5	-33.8	n.d.	-2.7
Seawater 2	16	-42.1	n.d.	n.d.	-0.6
Seawater 3	3	-47.2	n.d.	n.d.	-5.0
Seawater 4	2	-44.8	n.d.	n.d.	0.7
Seawater 5	17	-46.4	n.d.	n.d.	1.8
Mean	-	-43.6	-	-	-1.2
SD	-	3.9	-	-	2.7
Z. Noltii 1	2	-51.6 (-50.3)	-51.5 (-50.5)	-44.4	-8.8 (-7.9)
Z. Noltii 2	2	-49.1 (-48.5)	-50.9- (-48.0)	-40.8	n.a.
Z. Noltii 3	14	-54.2 (-52.2)	-30.5 (-31.1)	-34.7	-17.6 (-10.2)
Z. Noltii 4	2	-49.5 (-48.8)	-43.0 (-42.7)	-33.9	-8.4 (-7.8)
Z. Noltii 5	2	-49.8 (-49.2)	-51.6 (-49.8)	-27.9	-3.3 (-3.2)
Z. Noltii 6	2	-50.9 (-49.1)	-43.0 (-41.6)	-30.4	-4.9 (-4.6)
Z. Noltii 7	15	-52.9 (-51.2)	-20.1 (-23.0)	-40.8	-15.7 (-8.5)
Z. Noltii 8	2	-49.8 (-49.1)	-40.9 (-40.4)	-42.8	-9.5 (-8.9)
Z. Noltii 9	2	-49.7 (-49.1)	-41.0 (-40.2)	-35.9	-5.1 (-4.7)
Z. Noltii 10	2	-47.1 (-46.8)	n.a.	n.a.	n.a.
Z. Noltii 11	16	-55.4 (-53.1)	-25.2 (-27.2)	-27.8	-21.8 (-6.8)
Mean	-	-50.9 (-49.8)	-39.8 (-39.5)	-35.9	-10.6 (-6.3)
SD	-	2.4 (1.8)	11.1 (9.5)	6.1	6.4 (3.0)

The δ^{13}C values of CH$_3$Cl emitted from seagrass were on average more depleted in ^{13}C as those of seawater incubation by about 7‰. CH$_3$Cl and CHBr$_3$ exhibited a diurnal isotopic shift in the seagrass incubations with more ^{13}C depleted values during night. This is in contrast to CH$_3$Br from the seagrass incubations, where nighttime measurements revealed an isotopic enrichment of about 21‰ in comparison to daytime emissions. For CH$_3$I the δ^{13}C values ranged from -27.9 to -44.4‰ without any clear diurnal pattern.

8.4 Discussion

Halocarbon production was strongly elevated in incubations with seagrass in comparison to those with pure filtered seawater. Thus, the experiments clearly show that the seagrass or attached epiphytes are able to produce these compounds more effectively. This is further evidenced by certain differences in

δ^{13}C values between seawater and seagrass experiments (table 16). The seagrass experiments clearly revealed higher emissions during day than during night. This suggests light induced production in this setting which corroborates the findings during the summer campaign in Faro as well as results of other studies from tropical plants (Saito and Yokouchi, 2006) and peatland plants (Khan et al., 2013). Since halocarbon production is not primarily linked to the plants' photosynthesis, light is not a prerequisite for elevated emissions (Manley, 2002), but may foster emissions by general higher primary productivity. Likewise, the seawater incubations revealed similar diurnal pattern suggesting that bacterial activity or abiotic processes are regulating the emissions (see below).

The δ^{13}C values of CH_3Br were strikingly enriched in ^{13}C at darkness. This strongly suggests degradation processes in the incubation vessel during nighttime where the residence time is longer in comparison to daytime incubations (14h–16h vs. 2h). CH_3Br as the most labile monohalomethane in the dissolved phase can undergo several transformation processes. Most prominent destruction mechanisms are the hydrolysis and transhalogenation with high degradation rates (10% d^{-1} at 21.3°C) and strong kinetic isotope effects (63-75‰) (Elliott and Rowland, 1993, 1995; King and Saltzman, 1997; Tokarczyk and Saltzman, 2001). Furthermore, high fractionating microbial destructions could further have resulted in the enriched isotopic values of this compound (King and Saltzman, 1997; Tokarczyk and Saltzman, 2001; Schäfer et al., 2005).

Excluding the nighttime measurements of CH_3Br, the δ^{13}C values of CH_3Cl (-50.9± 2.4‰) and CH_3Br (-46.0± 5.0‰) fit well to those determined during the field campaigns and subsequent recalculations using the isotopic mass balance approach (chapter 4 and 5). The stable carbon isotopes of $CHBr_3$ are also strongly enriched in ^{13}C in comparison to the monohalomethanes which confirms the field measurements from the Sylt campaign. However, the δ^{13}C values of CH_3I are more enriched in ^{13}C as compared to the field measurements in Sylt. As pointed out in chapter 4, CH_3I may additionally be produced in the sediments and thus potentially explaining the different source signature between field measurements and incubation experiments.

Despite the seagrass/epiphytes derived emission, several other possible production pathways exist for halocarbons. Bacteria are reported to produce monohalomethanes. This was reported for CH_3I by Amachi et al. (2001) in various strains of marine bacteria in the presence of iodine with concurrent methylation. Further investigations revealed microbial production potential for CH_3Cl and CH_3Br in brackish water (Fujimori et al., 2012). Since the seawater in the incubations was not sterilized, a bacterial production cannot finally denied. Furthermore, abiotic mechanisms are currently under broad discussion regarding their environmental relevance to halocarbons budgets. One was postulated by Hamilton et al. (2003) where CH_3Cl is produced from senescent and or dead plant material by using pectin as methyl donor and chloride. This mechanism was further studied in laboratory experiments by means of stable carbon isotopes (Keppler et al., 2004). The resulting CH_3Cl emitted by these abiotic processes were extremely depleted in ^{13}C by up to -147‰. Furthermore, these formations are most effective at high temperatures and low water content. Since the measured δ^{13}C values of

monohalomethanes were much more enriched in ^{13}C and temperatures and water contents were high, this mechanism seems to be negligible in the incubation experiments. Other abiotic processes which can take place are photochemically induced productions of CH_3I and CH_3Cl (Moore and Zafiriou, 1994; Moore, 2008). Since higher emissions during daytime for seagrass and seawater as during night were observed, this mechanism could also apply to the incubation experiments. Moreover, the $\delta^{13}C$ values of CH_3Cl determined during daytime incubations were different to those during night and thus may further mirror photochemical production. However, in the light of the number of potential biological sources in the incubations, the contribution of photochemical production of CH_3I and CH_3Cl can not be clearly assessed. The reason for the more depleted $\delta^{13}C$ values of $CHBr_3$ from the seagrass incubations during nightime remained unclear.

Additionally to the global estimate presented in chapter 5, seagrass emissions were further upscaled using the emission data from the incubation experiments. For this estimate mean emission data from incubation experiments was used (table 15) and hourly emission rates were converted to yearly emissions. Duarte and Chiscano (1999) and Fourqurean et al. (2012) presented the most comprehensive compilations of the global areal seagrass biomass (above + below-ground) which were 461 g DW m^{-2} and 495 g DW m^{-2}. For the estimate a mean value of 478 g DW m^{-2} was used. Due to the lack of emission data during air exposure, this estimate assumes that seagrass are never air-exposed in the coastal zone. The results are presented in table 17. Although the two datasets are based on two different approaches regarding their sampling and upscaling methodologies, they yield similar annual emissions for the monohalomethanes. This in particular holds true for CH_3I exhibiting almost identical annual emissions from seagrass meadows. For CH_3Cl and CH_3Br the incubation data revealed higher production by factors of 1.7 and 2.2, respectively. For $CHBr_3$, there is a strong discrepancy between the two estimates as represented by an about eight-fold higher annual production using data from the incubation study. Numerous factors could have

Table 17: Global emission estimate of halocarbons from seagrass meadows based on laboratory incubation data and field data (from chapter 5). Values are given in Gg yr^{-1}.

	incubation data	field data
CH$_3$Cl	4.0 - 7.9	2.3 - 4.5
CH$_3$Br	1.1 - 2.2	0.5 - 1.0
CH$_3$I	0.5 - 1.0	0.6 - 1.2
CHBr$_3$	14.9 - 29.7	1.9 - 3.7

influenced the individual discrepancies. At least three of them seem to be noteworthy: Firstly, during field experiments net fluxes were determined. Thus, the dataset of the field campaigns likely includes sink functions which are only to a lesser extent covered by the incubation data. Secondly, the difference between both estimates may simply stem from the assumed global standing stock of seagrass biomass (478 g DW m^{-2}) used for the estimate using incubation data. In contrast, seagrass biomass during field sampling in the Ria Formosa was lower (229-310 g DW m^{-2}) than on global average. Thirdly, the huge discrepancy for $CHBr_3$ may, as discussed in chapter 5, result from the underestimation of $CHBr_3$ production in the Ria Formosa during tidal inundation. On the other hand, it can be attributed to the emissions of epiphytic algae that were attached to the seagrass in the

incubation experiments, while the seagrass sampled in the Ria Formosa was free from visible epiphytes.

8.5 Conclusions

The field campaigns revealed seagrass ecosystem as a net source for halocarbons. However, within this thesis the question arised whether the seagrass itself is generally able to emit these compounds or whether these emissions are brought by sedimentary production processes. Therefore the main objective was to get further insights regarding this topic. Accordingly, the stable carbon isotope values may differ from those measured in the field by eliminating the sedimentary influences. The results of the incubation experiments with submerged seagrass clearly show that seagrass or attached epiphytes do produce halocarbons. The emissions were strongly increased in comparison to those of seawater controls and during daytime which indicate plant-derived emissions and/or other photoautotrophic source organisms. Thus, sedimentary production is not the only driving factor within these complex coastal systems. Moreover, $\delta^{13}C$ values of the emitted CH_3Cl and CH_3Br, and $CHBr_3$ are similar to those measured in the field and calculated with the newly developed isotope and mass balance. Production mechanisms for $CHBr_3$ in plants are not known yet and therefore, strongly indicating epiphytic emission at least for this compound. A global estimate using the emission data from incubation studies revealed similar ranges for the monohalomethanes as derived from field data. The elevated production of $CHBr_3$ in incubation studies underlines the need for detailed studies on the particular constituents comprising the ecosystem seagrass meadows in order to refine emission estimates.

9. General conclusions

9.1 Synthesis

This thesis focuses on the emission and dynamics of halocarbons (CH_3Cl, CH_3Br, CH_3I, and $CHBr_3$) from seagrass meadows. Thereby, stable carbon isotopes of halocarbons were used to gain a better understanding of the underlying biogeochemistry in this ecosystem. An analytical field suitable cryogenic sampling method for the determination of stable carbon isotopes of halocarbons from ambient air was successfully developed. Due to the high air volume and thus, high compound enrichment, even low concentrated compounds usually found in the range of 1 to 10 ppt can be determined isotopically. Furthermore, this method is applicable for other groups of trace gases such as hydrocarbons. Good chromatographic separation is a prerequisite for the determination of stable carbon isotopes which was finally achieved by using two GC systems in parallel (2D GC) equipped with two different GC columns, column flow rates, and temperature programs as well as external fractionation of compounds (compound groups). The cryogenic sampling device was complemented by using smaller-scaled cryotraps in order to reduce the sample processing times. Furthermore, the systems are also suitable for the pre-concentration of halocarbons from the water phase (purge and trap). Therefore, this thesis presents the first report of isotopic CH_3I in the atmosphere and CH_3Br in seawater. Though few data of isotopic composition of CH_3Br, CH_3I, and $CHBr_3$ were already available, this thesis extends the existing dataset by source-related isotope values.

Three measurement campaigns were conducted to evaluate the source strength of seagrass meadows, one located at a temperate site (Sylt, Germany) and two in a subtropical site during summer and spring (lagoon Ria Formosa, Faro, Portugal). Dynamic flux chambers were used to obtain halocarbon fluxes and isotopic composition of halocarbons during air exposure and tidal inundation. These measurements were complemented by discrete in-situ water sampling for dissolved halocarbons and atmospheric sampling. Further efforts have been made to record the halocarbon production of seagrass in laboratory incubations.

During all sampling campaigns seagrass meadows were a net source for the halocarbons CH_3Cl, CH_3Br, CH_3I, and $CHBr_3$ to the atmosphere. The observed fluxes were characterized by a high variability which is commonly found in other coastal ecosystems. The following environmental controls on the halocarbon fluxes from seagrass meadows could be figured out:

During periods of air exposure in summer the emissions of halocarbons showed a certain diurnal cycle, though fluxes did not correlate with radiation. They were elevated at midday and afternoon while at night and/or low light intensities the emissions declined or halocarbon fluxes were even negative. These diurnal pattern was most obvious for CH_3Cl and CH_3Br rather than for CH_3I and $CHBr_3$. This is further supported by the results during incubation experiments where seagrass-derived emissions were significantly higher during daytime than during night also under submerged conditions. Although the halocarbon synthesis in plants is not primarily linked to the primary

metabolism (photosynthesis), there is overall strong evidence that light is one of the driving parameters stimulating halocarbon emissions from these ecosystems.

Although a full annual cycle was not performed, the flux data obtained in summer and spring point towards a strong seasonality. Significantly higher emission fluxes at air exposure were measured during summer as compared to the spring period. This went along with higher correlation coefficients of the monohalomethanes, higher emission fluxes at increased irradiance, and higher mixing ratios in the atmosphere in summer. These findings may be rather of regional importance in higher latitudes, since the highest abundance of seagrass meadows is situated in tropical regions (e.g. Indo-Pacific) where no strong seasonality occurs.

As seagrass meadows cover intertidal and subtidal areas, it was worthwhile to evaluate the halocarbon production along the tidal regime. During the summer campaign in the Ria Formosa, strongly elevated emission fluxes in particular for CH_3Br from seagrass meadows were observed during tidal changes from air exposure to inundation and conversely. During these periods the atmospheric mixing ratios were strongly elevated as compared to those during other periods. Supported by continuous CO_2 and methane measurements with high temporal resolution these elevated fluxes of halocarbons were attributed to an advective mechanism (bubble ebullition) when the water reaches the sampling site. Enhanced in-situ production of all trace gases studied was observed during tidal inundation in comparison to measurements during air exposure. These results suggest advective transport processes across the sediment-water and/or the plant-water interface as an important factor regulating the emission of trace gases in seagrass meadows. This is in contrast to most other studies in coastal areas stating that the trace gas emissions are mainly driven by gas diffusion during air exposure which is in turn inhibited by the water column during tidal inundation. Since most of trace gas emission estimates rely on measurements during low tide, the new results may have important implications for reassessing the coastal trace gas budgets.

Using the obtained concentration and isotopic data of halocarbons from seagrass meadows a coupled mass and isotope balance was developed which integrates source and sink functions for trace gases. It was demonstrated that the isotopic fingerprint of CH_3Cl and CH_3Br can be substantially improved by integrating production and degradation processes. Since the dynamics of halocarbons in most natural systems includes mostly both processes, it underlines the importance of this approach. The source signatures of CH_3Cl and CH_3Br determined during the field campaigns and incubation experiments revealed similar isotopic values suggesting the same production mechanism of the two compounds. $CHBr_3$, derived from flux chamber and laboratory experiments as well as from air and water samples was strikingly enriched in ^{13}C as compared to the monohalomethanes. The most conclusive explanation is the different enzymatic production mechanism by which polyhalomethanes are formed.

The isotopic source signatures of CH_3Cl and CH_3Br from seagrass meadows are certainly different to other natural sources yet reported. Therefore, this opens the way to integrate these values in isotope and mass budget considerations. Accordingly, the isotopic source signatures were used to evaluate the

sources and sinks in the Ria Formosa. For CH_3Cl, results suggest rather a contribution of seagrass meadows and the water column to the atmosphere than from salt marshes. On the other hand, CH_3Br was substantially enriched in the lagoons' atmosphere compared to those outside the lagoon. CH_3Br is rapidly degraded in the water phase by chemical and/or microbial destruction along with strong isotopic fractionation. This strongly suggest a higher contribution of CH_3Br from the water column to the atmospheric burden than directly from seagrass meadows or salt marshes whose isotopic signatures are generally more depleted in ^{13}C. Other processes such as the abiotic production of monohalomethanes during the degradation of organic matter as well as the photochemical formation of CH_3I from seawater DOM may further have a certain impact on the isotopic values found in the atmosphere. While a detailed consideration on these mechanisms is beyond the scope of this thesis, it became clear that the contribution of abiotic production of CH_3Cl from senescent plants is a negligible source in seagrass meadows since the strong fractionation connected to this mechanism was not observed at all.

A quantitative estimate of halocarbon sources in the lagoon revealed a strong contribution of seagrass meadows and sediments to the annual budget. Though the sediments reassembling high microphytobenthos contents were determined as low producer of halocarbons in comparison to seagrass meadows on per area basis, they cover a significant portion of the halocarbon production in this system due to the high abundance. In contrast, the macroalgae and phytoplankton abundance were distinctively lower and thus, their impact on the halocarbon budget is presumably rather low. This is in particular an important finding for $CHBr_3$ and CH_3I, since these compounds were often reported to stem mainly from either macroalgae and/or phytoplankton communities in coastal areas.

In comparison to other coastal macrophytic sources, the emission rates from seagrass meadows fall in-between those of temperate salt marshes and mangroves. On a global scale, seagrass meadows are a minor source for halocarbons. This in particular holds true for CH_3Cl for which emissions from seagrass meadows are substantially lower than those from tropical plants which were reported as the most dominant source. Seagrass meadows only partly fill the gap in the current atmospheric budgets for CH_3Br. Short-lived CH_3I and $CHBr_3$ produced within seagrass meadows are insignificant in comparison to oceanic sources yet identified. Overall, seagrass meadows are important production sites of halocarbons rather on local and regional than on global scales.

9.2 Outlook

This thesis presents the first data on halocarbon emission and dynamics from seagrass meadows. Accordingly, there are still some issues that require future research. Since the current work in seagrass meadows was mainly performed on the community level it is worthwhile to identify which particular constituents of the seagrass meadows are responsible for halocarbon emissions. Though the results from the incubation experiments suggest the seagrass itself to produce halocarbons, there is still some uncertainty regarding the role of epiphytic organisms. One possible step to clarify this issue would be to identify the occurrence and activity of the enzyme methyltransferase in seagrass tissue which is

generally involved in the halocarbon generation in higher plants. Additionally, the role of epiphytic organisms should be further clarified that prevail in the respective seagrass meadows.

Since the emission potential of natural produced halocarbons is often species dependent, additional investigations should be performed on other seagrass species to elucidate the regional and global relevance seagrass meadows as halocarbon emitting ecosystem. This is of particular importance, as seagrass meadows in the subtropics exhibit significantly higher biomass per unit area than during the field studies in the Ria Formosa and thus, the emission potential of halocarbons might be stronger than actually determined. These experiments could be performed using incubation experiments which are less time-consuming and logistically more convenient than field studies.

As trace gas fluxes substantially rely on the tidal processes, it will be necessary to further elucidate the dynamics caused by the tides on longer time scales. Those investigations should clarify how the flux dynamics and the physical forcing will change during a full tidal cycle including spring and neep tides. Sediments, comprising vast areas of the global coastal zones, should urgently be further evaluated as source for halocarbons. Additional marine sources for halocarbons with potentially global relevance are coral reefs. Class and Ballschmiter (1987) found considerable elevated water concentrations of polyhalomethanes in the surroundings of coral reefs. Recently, elevated atmospheric mixing ratios of CH_3Cl and CH_3Br from a coral beach in Japan were reported (Yokouchi et al., 2010).

This thesis has successfully applied stable carbon isotopes to trace halocarbon dynamics in the atmosphere, the water phase, and by evaluating the intrinsic sources and sinks in a seagrass-based system. For some compounds the obtained $\delta^{13}C$ values were among the first reported and thus the interpretation remained rather crucial; in particular for the short-lived CH_3I and $CHBr_3$. In future, stable carbon isotopes of halocarbons will certainly have the potential to unravel the major issues of halocarbon cycles in marine environments in addition to quantitative approaches predominantly applied. Among those, stable carbon isotopes could help to clarify the turnover of CH_3Br in ocean surface waters and the impact on the marine boundary layer. Furthermore, the contribution of photochemical production of CH_3I versus the production from biological sources in ocean surface waters is one of the emergent issues in halocarbon research. Since both formation mechanisms rely on fundamentally different (bio-)chemical reactions, stable carbon isotopes may help to distinct these two production pathways in the marine environment.

Overall, further research on environmentally significant isotopic fractionation factors, reaction rates, and source signatures along with ocean-atmosphere modelling is essential to further elucidate the complex nature of halocarbons when using isotopic measurements. Some of these tasks are currently under investigation and will be further examined within the framework of the SOPRAN project.

10. References

Amachi, S., Kamagata, Y., Kanagawa, T., and Muramatsu, Y. (2001): Bacteria mediate methylation of iodine in marine and terrestrial environments, *Applied and Environmental Microbiology*, 67, 2718-2722, doi: 10.1128/aem.67.6.2718-2722.2001.

Amachi, S., Kasahara, M., Hanada, S., Kamagata, Y., Shinoyama, H., Fujii, T., and Muramatsu, Y. (2003): Microbial participation in iodine volatilization from soils, *Environmental Science & Technology*, 37, 3885-3890, doi: 10.1021/es0210751.

Andreae, M. O., Atlas, E., Harris, G. W., Helas, G., deKock, A., Koppmann, R., Maenhaut, W., Mano, S., Pollock, W. H., Rudolph, J., Scharffe, D., Schebeske, G., and Welling, M. (1996): Methyl halide emissions from savanna fires in southern Africa, *Journal of Geophysical Research-Atmospheres*, 101, 23603-23613, doi: 10.1029/95jd01733.

Aneja, V. P. (1986): Characterization of emissions of biogenic atmospheric hydrogen sulfide, *Tellus Series B Chemical and Physical Meteorology*, 38, 81-86, doi: 10.1111/j.1600-0889.1986.tb00091.x.

Anibal, J., Rocha, C., and Sprung, M. (2007): Mudflat surface morphology as a structuring agent of algae and associated macroepifauna communities: A case study in the Ria Formosa, *Journal of Sea Research*, 57, 36-46, doi: 10.1016/j.seares.2006.07.002.

Archbold, M. E., Redeker, K. R., Davis, S., Elliot, T., and Kalin, R. M. (2005): A method for carbon stable isotope analysis of methyl halides and chlorofluorocarbons at pptv concentrations, *Rapid Communications in Mass Spectrometry*, 19, 337-342, doi: 10.1002/rcm.1791.

Attieh, J. M., Hanson, A. D., and Saini, H. S. (1995): Purification and characterization of a novel methyltransferase responsible for biosynthesis of halomethanes and methanethiol in Brassica oleracea, *Journal of Biological Chemistry*, 270, 9250-9257, doi: 10.1074/jbc.270.16.9250.

Auer, N. (2005): Stable carbon isotope analysis of volatile halogenated organic compounds (VHOCs) in the marine environment, PhD thesis, University of Rostock, Rostock, Germany.

Auer, N. R., Manzke, B. U., and Schulz-Bull, D. E. (2006): Development of a purge and trap continuous flow system for the stable carbon isotope analysis of volatile halogenated organic compounds in water, *Journal of Chromatography A*, 1131, 24-36, doi: 10.1016/j.chroma.2006.07.043.

Bahlmann, E., Weinberg, I., Seifert, R., Tubbesing, C., and Michaelis, W. (2011): A high volume sampling system for isotope determination of volatile halocarbons and hydrocarbons, *Atmospheric Measurement Techniques*, 4, 2073-2086, doi: 10.5194/amt-4-2073-2011.

Bahlmann, E., Weinberg, I., Santos, R., Eckhardt, T., Lavric, J.V., Michaelis, W., and Seifert, R.: Tidal controls on trace gas dynamics in a subtropical seagrass meadows in the Ria Formosa (Portugal), *in prep*.

Baird, A. J., Beckwith, C. W., Waldron, S., and Waddington, J. M. (2004): Ebullition of methane-containing gas bubbles from near-surface Sphagnum peat, *Geophysical Research Letters*, 31, L21505, doi: 10.1029/2004gl021157.

Baker, J. M., Reeves, C. E., Nightingale, P. D., Penkett, S. A., Gibb, S. W., and Hatton, A. D. (1999): Biological production of methyl bromide in the coastal waters of the North Sea and open ocean of the northeast Atlantic, *Marine Chemistry*, 64, 267-285, doi: 10.1016/s0304-4203(98)00077-2.

Baker, J. M., Sturges, W. T., Sugier, J., Sunnenberg, G., Lovett, A. A., Reeves, C. E., Nightingale, P. D., and Penkett, S. A. (2001): Emissions of CH3Br, organochlorines, and organoiodines from temperate macroalgae, *Chemosphere - Global Change Science*, 3, 93-106, doi: 10.1016/S1465-9972(00)00021-0.

Barbash J. E. and Reinhard, M. (1989): Reactivity of Sulfur Nucleophiles Toward Halogenated Organic Compounds in Natural Waters, in: *Biogenic Sulfur in the Environment*, ACS Symposium Series, 393, American Chemical Society, 101-138.

Barnes, J., Ramesh, R., Purvaja, R., Rajkumar, A. N., Kumar, B. S., Krithika, K., Ravichandran, K., Uher, G., and Upstill-Goddard, R. (2006): Tidal dynamics and rainfall control N2O and CH4 emissions from a pristine mangrove creek, *Geophysical Research Letters*, 33, L15405, doi: 10.1029/2006gl026829.

Barron, C., Duarte, C. M., Frankignoulle, M., and Borges, A. V. (2006): Organic carbon metabolism and carbonate dynamics in a Mediterranean seagrass (Posidonia oceanica) meadow, *Estuaries and Coasts*, 29, 417-426.

Bartlett, K. B., Bartlett, D. S., Harriss, R. C., and Sebacher, D. I. (1987): Methane emissions along a salt-marsh salinity gradient, *Biogeochemistry*, 4, 183-202, doi: 10.1007/bf02187365.

Bell, N., Hsu, L., Jacob, D. J., Schultz, M. G., Blake, D. R., Butler, J. H., King, D. B., Lobert, J. M., and Maier-Reimer, E. (2002): Methyl iodide: Atmospheric budget and use as a tracer of marine convection in global models, *Journal of Geophysical Research-Atmospheres*, 107, 4340, doi: 10.1029/2001jd001151.

REFERENCES

Bill, M., Miller, L. G., and Goldstein, A. H. (2002a): Carbon Isotope Fractionation of Methyl Bromide during Agricultural Soil Fumigations, *Biogeochemistry*, 60, 181-190, doi: 10.2307/1469818.

Bill, M., Rhew, R. C., Weiss, R. F., and Goldstein, A. H. (2002b): Carbon isotope ratios of methyl bromide and methyl chloride emitted from a coastal salt marsh, *Geophysical Research Letters*, 29, 1045, doi: 10.1029/2001gl012946.

Bill, M., Conrad, M. E., and Goldstein, A. H. (2004): Stable carbon isotope composition of atmospheric methyl bromide, *Geophysical Research Letters*, 31, L04109, doi: 10.1029/2003gl018639.

Billerbeck, M., Werner, U., Bosselmann, K., Walpersdorf, E., and Huettel, M. (2006a): Nutrient release from an exposed intertidal sand flat, *Marine Ecology Progress Series*, 316, 35-51, doi: 10.3354/meps316035.

Billerbeck, M., Werner, U., Polerecky, L., Walpersdorf, E., deBeer, D., and Huettel, M. (2006b): Surficial and deep pore water circulation governs spatial and temporal scales of nutrient recycling in intertidal sand flat sediment, *Marine Ecology Progress Series*, 326, 61-76, doi: 10.3354/meps326061.

Blei, E., Hardacre, C. J., Mills, G. P., Heal, K. V., and Heal, M. R. (2010a): Identification and quantification of methyl halide sources in a lowland tropical rainforest, *Atmospheric Environment*, 44, 1005-1010, doi: 10.1016/j.atmosenv.2009.12.023.

Blei, E., Heal, M. R., and Heal, K. V. (2010b): Long-term CH3Br and CH3Cl flux measurements in temperate salt marshes, *Biogeosciences*, 7, 3657-3668, doi: 10.5194/bg-7-3657-2010.

Blei, E. and Heal, M. R. (2011): Methyl bromide and methyl chloride fluxes from temperate forest litter, *Atmospheric Environment*, 45, 1543-1547, doi: 10.1016/j.atmosenv.2010.12.044.

Bloom, Y., Aravena, R., Hunkeler, D., Edwards, E., and Frape, S. K. (2000): Carbon isotope fractionation during microbial dechlorination of trichloroethene, cis-1,2-dichloroethene, and vinyl chloride: implications for assessment of natural attenuation, *Environmental Science & Technology*, 34, 2768-2772, doi: 10.1021/es991179k.

Bodenbender, J., Wassmann, R., Papen, H., and Rennenberg, H. (1999): Temporal and spatial variation of sulfur-gas-transfer between coastal marine sediments and the atmosphere, *Atmospheric Environment*, 33, 3487-3502, doi: 10.1016/s1352-2310(98)00351-3.

Borges, A. V., Vanderborght, J. P., Schiettecatte, L. S., Gazeau, F., Ferron-Smith, S., Delille, B., and Frankignoulle, M. (2004): Variability of the gas transfer velocity of CO2 in a macrotidal estuary (the Scheldt), *Estuaries*, 27, 593-603, doi: 10.1007/bf02907647.

Borowitzka, M. A., Lavery, P. S., and van Keulen, M. (2006): Epiphytes of seagrasses, in: *Seagrasses: Biology, Ecology and Conservation*, edited by: Larkum, A. W., Orth, R. J., and Duarte, C. M., Springer Netherlands, 441-461.

Bravo-Linares, C. M. and Mudge, S. M. (2009): Temporal trends and identification of the sources of volatile organic compounds in coastal seawater, *Journal of Environmental Monitoring*, 11, 628-641, doi: 10.1039/b814260m.

Brenchley, J. L., Raven, J. A., and Johnston, A. M. (1997): Resource acquisition in two intertidal fucoid seaweeds, Fucus serratus and Himanthalia elongata: seasonal variation and effects of reproductive development, *Marine Biology*, 129, 367-375, doi: 10.1007/s002270050177.

Brito, A., Newton, A., Tett, P., and Fernandes, T. F. (2010): Sediment and water nutrients and microalgae in a coastal shallow lagoon, Ria Formosa (Portugal): Implications for the Water Framework Directive, *Journal of Environmental Monitoring*, 12, 318-328, doi: 10.1039/b909429f.

Brito, A. C., Quental, T., Coutinho, T. P., Branco, M. A. C., Falcao, M., Newton, A., Icely, J., and Moita, T. (2012): Phytoplankton dynamics in southern Portuguese coastal lagoons during a discontinuous period of 40 years: An overview, *Estuarine Coastal and Shelf Science*, 110, 147-156, doi: 10.1016/j.ecss.2012.04.014.

Brownell, D. K., Moore, R. M., and Cullen, J. J. (2010): Production of methyl halides by Prochlorococcus and Synechococcus, *Global Biogeochemical Cycles*, 24, Gb2002, doi: 10.1029/2009gb003671.

Butler, J., Elkins, J., Lobert, J., Montzka, S., and Koropolov, V. (1997): Significant global loss of atmospheric CCl4 to the ocean, AGU Fall meeting.

Butler, J. H. (2000): Atmospheric chemistry - Better budgets for methyl halides?, *Nature*, 403, 260-261, doi: 10.1038/35002232.

Butler, J. H., King, D. B., Lobert, J. M., Montzka, S. A., Yvon-Lewis, S. A., Hall, B. D., Warwick, N. J., Mondeel, D. J., Aydin, M., and Elkins, J. W. (2007): Oceanic distributions and emissions of short-lived halocarbons, *Global Biogeochemical Cycles*, 21, GB1023, doi: 10.1029/2006gb002732.

Cabaço, S., Machas, R., Vieira, V., and Santos, R. (2008): Impacts of urban wastewater discharge on seagrass meadows (Zostera noltii), *Estuarine, Coastal and Shelf Science*, 78, 1-13, doi: 10.1016/j.ecss.2007.11.005.

Cabaço, S., Machás, R., and Santos, R. (2009): Individual and population plasticity of the seagrass Zostera noltii along a vertical intertidal gradient, *Estuarine, Coastal and Shelf Science*, 82, 301-308, doi: 10.1016/j.ecss.2009.01.020.

Cabaço, S., Santos, R., and Sprung, M. (2012): Population dynamics and production of the seagrass Zostera noltii in colonizing versus established meadows, *Marine Ecology*, 33, 280-289, doi: 10.1111/j.1439-0485.2011.00494.x.

Carpenter, L. J., Sturges, W. T., Penkett, S. A., Liss, P. S., Alicke, B., Hebestreit, K., and Platt, U. (1999): Short-lived alkyl iodides and bromides at Mace Head, Ireland: Links to biogenic sources and halogen oxide production, *Journal of Geophysical Research*, 104, 1679-1689, doi: 10.1029/98jd02746.

Carpenter, L. J. and Liss, P. S. (2000): On temperate sources of bromoform and other reactive organic bromine gases, *Journal of Geophysical Research-Atmospheres*, 105, 20539-20547, doi: 10.1029/2000jd900242.

Carpenter, L. J., Malin, G., Liss, P. S., and Küpper, F. C. (2000): Novel biogenic iodine-containing trihalomethanes and other short-lived halocarbons in the coastal east Atlantic, *Global Biogeochemical Cycles*, 14, 1191-1204, doi: 10.1029/2000gb001257.

Carpenter, L. J. (2003): Iodine in the marine boundary layer, *Chemical Reviews*, 103, 4953-4962, doi: 10.1021/cr0206465.

Carpenter, L. J., Jones, C. E., Dunk, R. M., Hornsby, K. E., and Woeltjen, J. (2009): Air-sea fluxes of biogenic bromine from the tropical and North Atlantic Ocean, *Atmospheric Chemistry and Physics*, 9, 1805-1816, doi: 10.5194/acp-9-1805-2009.

Chanton, J. P., Martens, C. S., and Kelley, C. A. (1989): Gas-transport from methane-saturated, tidal fresh-water and wetland sediments, *Limnology and Oceanography*, 34, 807-819.

Charpy-Roubaud, C. and Sournia, A. (1990): The comparative estimation of phytoplanktonic microphytobenthic and macrophytobenthic primary production in the oceans, *Marine Microbial Food Webs*, 4, 31-58.

Chitwood, D. E. and Deshusses, M. A. (2001): Development of a methyl bromide collection system for fumigated farmland, *Environmental Science & Technology*, 35, 636-642, doi: 10.1021/es001440t.

Christof, O., Seifert, R., and Michaelis, W. (2002): Volatile halogenated organic compounds in European estuaries, *Biogeochemistry*, 59, 143-160, doi: 10.1023/a:1015592115435.

Class, T. and Ballschmiter, K.: Chemistry of organic traces in air IX (1987): Evidence of natural marine sources for chloroform in regions of high primary production, *Fresenius Zeitschrift für analytische Chemie*, 327, 40-41, doi. 10.1007/bf00474552.

Claypool, G. E., and Kvenvolden, K. A. (1983): Methane and other hydrocarbon gases in marine sediment, *Annual Review of Earth and Planetary Sciences*, 11, 299-327, doi: 10.1146/annurev.ea.11.050183.001503.

Cook, P. L. M., Wenzhofer, F., Glud, R. N., Janssen, F., and Huettel, M. (2007): Benthic solute exchange and carbon mineralization in two shallow subtidal sandy sediments: Effect of advective pore-water exchange, *Limnology and Oceanography*, 52, 1943-1963, doi: 10.4319/lo.2007.52.5.1943.

Cooper, D. J., Demello, W. Z., Cooper, W. J., Zika, R. G., Saltzman, E. S., Prospero, J. M., and Savoie, D. L. (1987a): Short-term variability in biogenic sulfur emissions from a Florida Spartina alterniflora marsh, *Atmospheric Environment*, 21, 7-12, doi: 10.1016/0004-6981(87)90264-2.

Cooper, W. J., Cooper, D. J., Saltzman, E. S., Demello, W. Z., Savoie, D. L., Zika, R. G., and Prospero, J. M. (1987b): Emissions of biogenic sulfur-compounds from several wetland soils in Florida, *Atmospheric Environment*, 21, 1491-1495, doi: 10.1016/0004-6981(87)90311-8.

Cotter, E. S. N., Booth, N. J., Canosa-Mas, C. E., and Wayne, R. P. (2001): Release of iodine in the atmospheric oxidation of alkyl iodides and the fates of iodinated alkoxy radicals, *Atmospheric Environment*, 35, 2169-2178, doi: 10.1016/S1352-2310(00)00479-9.

Cox, M. L., Fraser, P. J., Sturrock, G. A., Siems, S. T., and Porter, L. W. (2004): Terrestrial sources and sinks of halomethanes near Cape Grim, Tasmania, *Atmospheric Environment*, 38, 3839-3852, doi: 10.1016/j.atmosenv.2004.03.050.

Craig, H. (1953): The geochemistry of the stable carbon isotopes, *Geochimica et Cosmochimica Acta*, 3, 53-92, doi: 10.1016/0016-7037(53)90001-5.

Crutzen, P. J. and Gidel, L. T. (1983): A two-dimensional photochemical model of the atmosphere 2: The tropospheric budgets of the anthropogenic chlorocarbons CO, CH4, CH3Cl and the effect of various NOx sources on tropospheric ozone, *Journal of Geophysical Research*, 88, 6641-6661, doi: 10.1029/JC088iC11p06641.

Cunha, A. H., Assis, J., and Serrao, E. A. (2009): Estimation of available seagrass meadow area in Portugal for transplanting purposes, *Journal of Coastal Research*, 1100-1104.

REFERENCES

Dacey, J. W. H., King, G. M., and Wakeham, S. G. (1987): Factors controlling emission of dimethyldulfide from salt marshes, *Nature*, 330, 643-645, doi: 10.1038/330643a0.

Dallin, E., Wan, P., Krogh, E., Gill, C., and Moore, R. M. (2009): New pH-dependent photosubstitution pathways of syringic acid in aqueous solution: Relevance in environmental photochemistry, *Journal of Photochemistry and Photobiology A-Chemistry*, 207, 297-305, doi: 10.1016/j.jphotochem. 2009.07.023.

Daniel, J. S., Solomon, S., Portmann, R. W., and Garcia, R. R. (1999): Stratospheric ozone destruction: The importance of bromine relative to chlorine, *Journal of Geophysical Research - Atmospheres*, 104, 23871-23880, doi: 10.1029/1999jd900381.

Deborde, J., Anschutz, P., Guerin, F., Poirier, D., Marty, D., Boucher, G., Thouzeau, G., Canton, M., and Abril, G. (2010): Methane sources, sinks and fluxes in a temperate tidal Lagoon: The Arcachon lagoon (SW France), *Estuarine Coastal and Shelf Science*, 89, 256-266, doi: 10.1016/j.ecss.2010.07.013.

De Bruyn, W. J. and Saltzman, E. S. (1997): The solubility of methyl bromide in pure water, 35 parts per thousand sodium chloride and seawater, *Marine Chemistry*, 56, 51-57, doi: 10.1016/s0304-4203(96)00089-8.

de la Paz, M., Gomez-Parra, A., and Forja, J. (2008): Variability of the partial pressure of CO2 on a daily-to-seasonal time scale in a shallow coastal system affected by intensive aquaculture activities (Bay of Cadiz, SW Iberian Peninsula), *Marine Chemistry*, 110, 195-204, doi: 10.1016/j.marchem.2008.03.002.

Delaune, R. D., Smith, C. J., and Patrick, W. H. (1983): Methane release from gulf-coast wetlands, *Tellus Series B-Chemical and Physical Meteorology*, 35, 8-15.

De Mello, W. Z., Cooper, D. J., Cooper, W. J., Saltzman, E. S., Zika, R. G., Savoie, D. L., and Prospero, J. M. (1987): Spatial and diel variability in the emissions of some biogenic sulfur-compounds from a Florida Spartina-alterniflora coastal zone, *Atmospheric Environment*, 21, 987-990, doi: 10.1016/0004-6981(87)90095-3.

den Hartog, C. and Kuo, J. (2006): Taxonomy and biogeography of seagrasses, in: *Seagrasses: Biology, Ecology, and Conservation*, edited by: Larkum, A. W., Orth, R. J., and Duarte, C. M., Springer Netherlands, 1-23.

Dimmer, C. H., Simmonds, P. G., Nickless, G., and Bassford, M. R. (2001): Biogenic fluxes of halomethanes from Irish peatland ecosystems, *Atmospheric Environment*, 35, 321-330, doi: 10.1016/s1352-2310(00)00151-5.

Draxler, R.R. and Rolph, G.D. (2011): HYSPLIT (Hybrid Single- Particle Lagrangian Integrated Trajectory), NOAA Air Resources Laboratory, Silver Spring, USA.

Drewer, J., Heal, M. R., Heal, K. V., and Smith, K. A. (2006): Temporal and spatial variation in methyl bromide flux from a salt marsh, *Geophysical Research Letters*, 33, L16808, doi: 10.1029/2006gl026814.

Drewer, J., Heal, K. V., Smith, K. A., and Heal, M. R. (2008): Methyl bromide emissions to the atmosphere from temperate woodland ecosystems, *Global Change Biology*, 14, 2539-2547, doi: 10.1111/j.1365-2486.2008.01676.x.

Duarte, C. M. (1991): Seagrass depth limits, *Aquatic Botany*, 40, 363-377, doi: 10.1016/0304-3770(91)90081-F.

Duarte, C. M. and Chiscano, C. L. (1999): Seagrass biomass and production: a reassessment, *Aquatic Botany*, 65, 159-174, doi: 10.1016/s0304-3770(99)00038-8.

Duarte, C. M. (2002): The future of seagrass meadows, *Environmental Conservation*, 29, 192-206, doi: 10.1017/s0376892902000127.

Duarte, C. M., Middelburg, J. J., and Caraco, N. (2005): Major role of marine vegetation on the oceanic carbon cycle, *Biogeosciences*, 2, 1-8, doi: 10.5194/bg-2-1-2005.

Duarte, P., Azevedo, B., Guerreiro, M., Ribeiro, C., Bandeira, R., Pereira, A., Falcao, M., Serpa, D., and Reia, J. (2008): Biogeochemical modelling of Ria Formosa (South Portugal), *Hydrobiologia*, 611, 115-132, doi: 10.1007/s10750-008-9464-3.

Duce, R. A., Winchester, J. W., and van Nahl, T. W. (1965): Iodine bromine and chlorine in Hawaiian marine atmosphere, *Journal of Geophysical Research*, 70, 1775-&, doi: 10.1029/JZ070i008p01775.

Durham, L. (2000): A kinematic study of the Ancão Basin in the Ria Formosa lagoon, Algarve, MSc thesis, School of Ocean Sciences, University of Wales, Bangor, UK.

Dvortsov, V. L., Geller, M. A., Solomon, S., Schauffler, S. M., Atlas, E. L., and Blake, D. R. (1999): Rethinking reactive halogen budgets in the midlatitude lower stratosphere, *Geophysical Research Letters*, 26, 1699-1702, doi: 10.1029/1999gl900309.

Elliott, S. and Rowland, F. S. (1993): Nucleophilic-substitution rates and solubilities for methyl halides in seawater, *Geophysical Research Letters*, 20, 1043-1046, doi: 10.1029/93gl01081.

Elliott, S. and Rowland, F. S. (1995): Methyl halide hydrolysis rates in natural-waters, *Journal of Atmospheric Chemistry*, 20, 229-236, doi: 10.1007/bf00694495.

106

Falcão, M., and Vale, C. (2003): Nutrient dynamics in a coastal lagoon (Ria Formosa, Portugal): The importance of lagoon-sea water exchanges on the biological productivity, *Ciencias Marinas*, 29, 425-433.

Fourqurean, J. W., Duarte, C. M., Kennedy, H., Marba, N., Holmer, M., Angel Mateo, M., Apostolaki, E. T., Kendrick, G. A., Krause-Jensen, D., McGlathery, K. J., and Serrano, O. (2012): Seagrass ecosystems as a globally significant carbon stock, *Nature Geoscience*, 5, 505-509, doi: 10.1038/ngeo1477.

Fujimori, T., Yoneyama, Y., Taniai, G., Kurihara, M., Tamegai, H., and Hashimoto, S. (2012): Methyl halide production by cultures of marine proteobacteria Erythrobacter and Pseudomonas and isolated bacteria from brackish water, *Limnology and Oceanography*, 57, 154-162, doi: 10.4319/lo.2012.57.1.0154.

Gao, F., Yates, S. R., Yates, M. V., Gan, J. Y., and Ernst, F. F. (1997): Design, fabrication, and application of a dynamic chamber for measuring gas emissions from soil, *Environmental Science & Technology*, 31, 148-153, doi: 10.1021/es9602511.

Gao, F. and Yates, S. R. (1998): Simulation of enclosure-based methods for measuring gas emissions from soil to the atmosphere, *Journal of Geophysical Research-Atmospheres*, 103, 26127-26136, doi: 10.1029/98jd01345.

Gebhardt, S., Colomb, A., Hofmann, R., Williams, J., and Lelieveld, J. (2008): Halogenated organic species over the tropical South American rainforest, *Atmospheric Chemistry and Physics*, 8, 3185-3197, doi: 10.5194/acp-8-3185-2008.

Giebel, B. M., Swart, P. K., and Riemer, D. D. (2010): Delta C-13 stable isotope analysis of atmospheric oxygenated volatile organic compounds by gas chromatography-isotope ratio mass spectrometry, *Analytical Chemistry*, 82, 6797-6806, doi: 10.1021/ac1007442.

Giese, B., Laturnus, F., Adams, F. C., and Wiencke, C. (1999): Release of volatile iodinated C(1)-C(4) hydrocarbons by marine macroalgae from various climate zones, *Environmental Science & Technology*, 33, 2432-2439, doi: 10.1021/es980731n.

Gillanders, B. (2006): Seagrasses, fish, and fisheries, in: *Seagrasses: Biology, Ecology, and Conservation*, edited by: Larkum, A. W., Orth, R. J., and Duarte, C. M., Springer Netherlands, 503-505.

Glaser, P. H., Chanton, J. P., Morin, P., Rosenberry, D. O., Siegel, D. I., Ruud, O., Chasar, L. I., and Reeve, A. S. (2004): Surface deformations as indicators of deep ebullition fluxes in a large northern peatland, *Global Biogeochemical Cycles*, 18, Gb1003, doi: 10.1029/2003gb002069.

Glew, D. N. and Moelwyn-Hughes, E. A. (1953): Chemical statics of the methyl halides in water, *Discussions of the Faraday Society*, 15, 150-161, doi: 10.1039/df9531500150.

Gola, A. A., D'Anna, B., Feilberg, K. L., Sellevag, S. R., Bache-Andreassen, L., and Nielsen, C. J. (2005): Kinetic isotope effects in the gas phase reactions of OH and Cl with CH3Cl, CD3Cl, and (CH3Cl)-C-13, *Atmospheric Chemistry and Physics*, 5, 2395-2402, doi: 10.5194/acp-5-2395-2005.

Goldstein, A. H. and Shaw, S. L. (2003): Isotopes of volatile organic compounds: an emerging approach for studying atmospheric budgets and chemistry, *Chemical Reviews*, 103, 5025-5048, doi: 10.1021/cr0206566.

Green, E. and Short, F. (2003): World atlas of seagrasses, prepared by the UIMEP World Conservation Monitoring Centre, University of California Press, Berkeley, USA.

Gribble, G. W. (2003): The diversity of naturally produced organohalogens, *Chemosphere*, 52, 289-297, doi: 10.1016/s0045-6535(03)00207-8.

Gribble, G. W. (2009): Naturally occurring organohalogen compounds: A comprehensive update, Springer, Vienna.

Grunwald, M., Dellwig, O., Beck, M., Dippner, J. W., Freund, J. A., Kohlmeier, C., Schnetger, B., and Brumsack, H. J. (2009): Methane in the southern North Sea: Sources, spatial distribution and budgets, *Estuarine Coastal and Shelf Science*, 81, 445-456, doi: 10.1016/j.ecss.2008.11.021.

Gschwend, P. M., Macfarlane, J. K., and Newman, K. A. (1985): Volatile Halogenated Organic Compounds Released to Seawater from Temperate Marine Macroalgae, *Science*, 227, 1033-1035, doi: 10.1126/science.227.4690.1033.

Guimarães, M. H. M. E., Cunha, A. H., Nzinga, R. L., and Marques, J. F. (2012): The distribution of seagrass (Zostera noltii) in the Ria Formosa lagoon system and the implications of clam farming on its conservation, *Journal for Nature Conservation*, 20, 30-40, doi: 10.1016/j.jnc.2011.07.005.

Hamilton, J. T. G., McRoberts, W. C., Keppler, F., Kalin, R. M., and Harper, D. B. (2003): Chloride methylation by plant pectin: An efficient environmentally significant process, *Science*, 301, 206-209, doi: 10.1126/science.1085036.

Harper, D. B., Kalin, R. M., Hamilton, J. T. G., and Lamb, C. (2001): Carbon isotope ratios for chloromethane of biological origin: Potential tool in determining biological emissions, *Environmental Science & Technology*, 35, 3616-3619, doi: 10.1021/es0106467.

REFERENCES

Harper, D. and Hamilton, J. T. G. (2003): The global cycles of the naturally-occurring monohalomethanes, in: *Natural Production of Organohalogen Compounds*, edited by: Gribble, G., The Handbook of Environmental Chemistry, Springer Berlin Heidelberg, 17-41.

Harper, D. B., Hamilton, J. T. G., Ducrocq, V., Kennedy, J. T., Downey, A., and Kalin, R. M. (2003): The distinctive isotopic signature of plant-derived chloromethane: possible application in constraining the atmospheric chloromethane budget, *Chemosphere*, 52, 433-436, doi: 10.1016/s0045-6535(03)00206-6.

Hayes, J. (1983): Practice and principles of isotopic measurements in organic geochemistry, in: *Organic geochemistry of contemporaneous and ancient sediments*, edited by: Meinschein, W. G., Great Lakes Section, Society of Economic Paleontologists and Mineralogists, Bloomington, Ind.

Hayes, J. M. (2001): Fractionation of carbon and hydrogen isotopes in biosynthetic processes, *Stable Isotope Geochemistry*, 43, 225-277, doi: 10.2138/gsrmg.43.1.225.

Hemminga, M. and Duarte, C. M. (2000): Seagrass ecology, Cambridge University Press, Cambridge, UK.

Heyer, J. and Berger, U. (2000): Methane emission from the coastal area in the southern Baltic Sea, *Estuarine, Coastal and Shelf Science*, 51, 13-30, doi: 10.1006/ecss.2000.0616.

Hines, M. E., Crill, P. M., Varner, R. K., Talbot, R. W., Shorter, J. H., Kolb, C. E., and Harriss, R. C. (1998): Rapid consumption of low concentrations of methyl bromide by soil bacteria, *Applied and Environmental Microbiology*, 64, 1864-1870.

Hoeft, S. E., Rogers, D. R., and Visscher, P. T. (2000): Metabolism of methyl bromide and dimethyl sulfide by marine bacteria isolated from coastal and open waters, *Aquatic Microbial Ecology*, 21, 221-230, doi: 10.3354/ame021221.

Horvath, A. (1982): Halogenated hydrocarbons: Solubility-miscibility with water, M. Dekker, New York.

Hu, L., Yvon-Lewis, S. A., Liu, Y., Salisbury, J. E., and O'Hern, J. E. (2010): Coastal emissions of methyl bromide and methyl chloride along the eastern Gulf of Mexico and the east coast of the United States, *Global Biogeochemical Cycles*, 24, GB1007, doi: 10.1029/2009gb003514.

Hubas, C., Davoult, D., Cariou, T., and Artigas, L. F. (2006): Factors controlling benthic metabolism during low tide along a granulometric gradient in an intertidal bay (Roscoff Aber Bay, France), *Marine Ecology Progress Series*, 316, 53-68, doi: 10.3354/meps316053.

Huettel, M., Ziebis, W., and Forster, S. (1996): Flow-induced uptake of particulate matter in permeable sediments, *Limnology and Oceanography*, 41, 309-322.

Hughes, C., Franklin, D. J., and Malin, G. (2011): Iodomethane production by two important marine cyanobacteria: Prochlorococcus marinus (CCMP 2389) and Synechococcus sp (CCMP 2370), *Marine Chemistry*, 125, 19-25, doi: 10.1016/j.marchem.2011.01.007.

Hughes, C., Johnson, M., Utting, R., Turner, S., Malin, G., Clarke, A., and Liss, P. S. (2013): Microbial control of bromocarbon concentrations in coastal waters of the western Antarctic Peninsula, *Marine Chemistry*, 151, 35-46, doi: 10.1016/j.marchem.2013.01.007.

Itoh, N., Tsujita, M., Ando, T., Hisatomi, G., and Higashi, T. (1997): Formation and emission of monohalomethanes from marine algae, *Phytochemistry*, 45, 67-73, doi: 10.1016/s0031-9422(96)00786-8.

Jansen, S., Walpersdorf, E., Werner, U., Billerbeck, M., Bottcher, M. E., and de Beer, D. (2009): Functioning of intertidal flats inferred from temporal and spatial dynamics of O-2, H2S and pH in their surface sediment, *Ocean Dynamics*, 59, 317-332, doi: 10.1007/s10236-009-0179-4.

Jones, C. E., Hornsby, K. E., Dunk, R. M., Leigh, R. J., and Carpenter, L. J. (2009): Coastal measurements of short-lived reactive iodocarbons and bromocarbons at Roscoff, Brittany during the RHaMBLe campaign, *Atmospheric Chemistry and Physics*, 9, 8757-8769, doi: 10.5194/acp-9-8757-2009.

Jonkers, H. M., van Bergeijk, S. A., and van Gemerden, H. (2000): Microbial production and consumption of dimethyl sulfide (DMS) in a sea grass (Zostera noltii)-dominated marine intertidal sediment ecosystem (Bassin d'Arcachon, France), Fems Microbiology Ecology, 31, 163-172, doi: 10.1111/j.1574-6941.2000.tb00681.x.

Keppler, F., Eiden, R., Niedan, V., Pracht, J., and Schöler, H. F. (2000): Halocarbons produced by natural oxidation processes during degradation of organic matter, *Nature*, 403, 298-301, doi: 10.1038/35002055.

Keppler, F., Kalin, R. M., Harper, D. B., McRoberts, W. C., and Hamilton, J. T. G. (2004): Carbon isotope anomaly in the major plant C1 pool and its global biogeochemical implications, *Biogeosciences*, 1, 123-131, doi: 10.5194/bg-1-123-2004.

Keppler, F., Harper, D. B., Rockmann, T., Moore, R. M., and Hamilton, J. T. G. (2005): New insight into the atmospheric chloromethane budget gained using stable carbon isotope ratios, *Atmospheric Chemistry and Physics*, 5, 2403-2411, doi: doi:10.5194/acp-5-2403-2005.

Khan, M. A. H., Rhew, R. C., Whelan, M. E., Zhou, K., and Deverel, S. J. (2011): Methyl halide and chloroform emissions from a subsiding Sacramento–San Joaquin Delta island converted to rice fields, *Atmospheric Environment*, 45, 977-985, doi: 10.1016/j.atmosenv.2010.10.053.

Khan, M. A. H., Rhew, R. C., Zhou, K., and Whelan, M. E. (2013): Halogen biogeochemistry of invasive perennial pepperweed (Lepidium latifolium) in a peatland pasture, *Journal of Geophysical Research-Biogeosciences*, 118, 239-247, doi: 10.1002/jgrg.20020.

Kim, K. H. and Lindberg, S. E. (1995): Design and initial tests of a dynamic enclosure chamber for measurements of vapor-phase mercury fluxes over soils, *Water, Air, & Soil Pollution*, 80, 1059-1068, doi: 10.1007/bf01189766.

Kim, K. H. and Kim, D. (2007): Seasonal and spatial variability of sediment oxygen fluxes in the Beobsan intertidal flat of Taean Bay, mid-western Korean Peninsula, *Geosciences Journal*, 11, 323-329, doi: 10.1007/bf02857049.

King, D. B. and Saltzman, E. S. (1997): Removal of methyl bromide in coastal seawater: Chemical and biological rates, *Journal of Geophysical Research-Oceans*, 102, 18715-18721, doi: 10.1029/97jc01214.

Kokil, P. B. and Fry, A. (1986): Isotope effects and mechanisms in the bromination of alpha-carbon-14 and beta-carbon-14 labelled 4-nitro-4'-methylstilbenes, *Tetrahedron Letters*, 27, 5051-5054, doi: 10.1016/s0040-4039(00)85130-8.

Komatsu, D. D., Tsunogai, U., Yamaguchi, J., Nakagawa, F., Yokouchi, Y., and Noijiri, Y. (2004): The budget of atmospheric methyl chloride using stable carbon isotopic massbalance, Poster A51C-0784, AGU Fall Meeting, San Francisco.

Laanbroek, H. J. (2010): Methane emission from natural wetlands: interplay between emergent macrophytes and soil microbial processes. A mini-review, *Annals of Botany*, 105, 141-153, doi: 10.1093/aob/mcp201.

Laturnus, F., Giese, B., Wiencke, C., and Adams, F. C. (2000): Low-molecular-weight organoiodine and organobromine compounds released by polar macroalgae - The influence of abiotic factors, *Fresenius Journal of Analytical Chemistry*, 368, 297-302, doi: 10.1007/s002160000491.

Laturnus, F., Svensson, T., Wiencke, C., and Oberg, G. (2004): Ultraviolet radiation affects emission of ozone-depleting substances by marine macroalgae: Results from a laboratory incubation study, *Environmental Science & Technology*, 38, 6605-6609, doi: 10.1021/es0449527s.

Leck, C. and Rodhe, H. (1991): Emissions of marine biogenic sulfur to the atmosphere of Northern Europe, *Journal of Atmospheric Chemistry*, 12, 63-86, doi: 10.1007/bf00053934.

Leedham, E. C., Hughes, C., Keng, F. S. L., Phang, S. M., Malin, G., and Sturges, W. T. (2013): Emission of atmospherically significant halocarbons by naturally occurring and farmed tropical macroalgae, *Biogeosciences*, 10, 3615-3633, doi: 10.5194/bg-10-3615-2013.

Lee-Taylor, J. and Redeker, K. R. (2005): Reevaluation of global emissions from rice paddies of methyl iodide and other species, *Geophysical Research Letters*, 32, L15801, doi: 10.1029/2005gl022918.

Leuschner, C. and Rees, U. (1993): CO2 gas-exchange of 2 intertidal seagrass species, Zostera-marina L and Zostera noltii Hornem during emersion, *Aquatic Botany*, 45, 53-62, doi: 10.1016/0304-3770(93)90052-x.

Leuschner, C., Landwehr, S., and Mehlig, U. (1998): Limitation of carbon assimilation of intertidal Zostera noltii and Z-marina by desiccation at low tide, *Aquatic Botany*, 62, 171-176, doi: 10.1016/s0304-3770(98)00091-6.

Lopez, N. I. and Duarte, C. M. (2004): Dimethyl sulfoxide (DMSO) reduction potential in mediterranean seagrass (Posidonia oceanica) sediments, *Journal of Sea Research*, 51, 11-20, doi: 10.1016/j.seares.2003.03.001.

Lovelock, J. E. and Maggs, R. J. (1973): Halogenated hydrocarbons in and over Atlantic, *Nature*, 241, 194-196, doi: 10.1038/241194a0.

Lovelock, J. E. (1975): Natural halocarbons in air and in sea, *Nature*, 256, 193-194, doi: 10.1038/256193a0.

MacDonald, S. and Moore, R. M. (2007): Seasonal and spatial variations in methyl chloride in NW Atlantic waters, *Journal of Geophysical Research-Oceans*, 112, C05028, doi: 10.1029/2006jc003812.

Mackay, D. and Shiu, W. Y. (1981): A critical review of Henry's law constants for chemicals of environmental interest, *Journal of Physical and Chemical Reference Data*, 10, 1175-1199.

Mackay, D., Ma, K.-C., Lee, S. C., and Shiu, W.-Y. (2006): Halogenated Aliphatic Hydrocarbons, in: *Handbook of Physical-Chemical Properties and Environmental Fate for Organic Chemicals*, Second Edition, CRC Press, 921-1256.

Manley, S. L. and Dastoor, M. N. (1987): Methyl halide (CH3X) production from the giant kelp, Macrocystis, and estimates of global CH3X production by kelp, *Limnology and Oceanography*, 32, 709-715.

REFERENCES

Manley, S. L. and Dastoor, M. N. (1988): Methyl-Iodide (CH3I) production by kelp and associated microbes, *Marine Biology*, 98, 477-482, doi: 10.1007/bf00391538.

Manley, S. L., Goodwin, K., and North, W. J. (1992): Laboratory production of bromoform, methylene bromide, and methyl iodide by macroalgae and distribution in nearshore Southern California waters, *Limnology and Oceanography*, 37, 1652-1659.

Manley, S. L. and de la Cuesta, J. L. (1997): Methyl iodide production from marine phytoplankton cultures, *Limnology and Oceanography*, 42, 142-147.

Manley, S. L. (2002): Phytogenesis of halomethanes: A product of selection or a metabolic accident?, *Biogeochemistry*, 60, 163-180, doi: 10.1023/a:1019859922489.

Manley, S. L., Wang, N.-Y., Walser, M. L., and Cicerone, R. J. (2006): Coastal salt marshes as global methyl halide sources from determinations of intrinsic production by marsh plants, *Global Biogeochemical. Cycles*, 20, GB3015, doi: 10.1029/2005gb002578.

Manley, S. L., Wang, N.-Y., Walser, M. L., and Cicerone, R. J. (2007): Methyl halide emissions from greenhouse-grown mangroves, *Geophysical Research Letters*, 34, L01806, doi: 10.1029/2006gl027777.

Manö, S., and Andreae, M. O. (1994): Emission of methyl bromide from biomass burning, *Science*, 263, 1255-1257, doi: 10.1126/science.263.5151.1255.

Martens, C. S. and Berner, R. A. (1974): Methane production in interstitial waters of sulfate-depleted marine sediments, *Science*, 185, 1167-1169, doi: 10.1126/science.185.4157.1167.

Mateo, M., Cebrián, J., Dunton, K., and Mutchler, T. (2006): Carbon flux in seagrass ecosystems, in: *Seagrasses: Biology, Ecology, and Conservation*, edited by: Larkum, A. W., Orth, R. J., and Duarte, C. M., Springer Netherlands, 159-192.

McCauley, S. E., Goldstein, A. H., and DePaolo, D. J. (1999): An isotopic approach for understanding the CH3Br budget of the atmosphere, *Proceedings of the National Academy of Sciences of the United States of America*, 96, 10006-10009, doi: 10.1073/pnas.96.18.10006.

McCulloch, A., Aucott, M. L., Benkovitz, C. M., Graedel, T. E., Kleiman, G., Midgley, P. M., and Li, Y. F. (1999): Global emissions of hydrogen chloride and chloromethane from coal combustion, incineration and industrial activities: Reactive Chlorine Emissions Inventory, *Journal of Geophysical Research-Atmospheres*, 104, 8391-8403, doi: 10.1029/1999jd900025.

McKenzie, L. (2008): Seagrass Educators Handbook, available at: http://www.seagrasswatch.org/ Info_centre/ education/Seagrass_Educators_Handbook.pdf.

McKinney, C. R., McCrea, J. M., Epstein, S., Allen, H. A., and Urey, H. C. (1950): Improvements in mass spectrometers for the measurement of small differences in isotope abundance ratios, *Review of Scientific Instruments*, 21, 724-730, doi: 10.1063/1.1745698.

Mead, M. I., Khan, M. A. H., Bull, I. D., White, I. R., Nickless, G., and Shallcross, D. E. (2008a): Stable carbon isotope analysis of selected halocarbons at parts per trillion concentration in an urban location, *Environmental Chemistry*, 5, 340-346, doi: 10.1071/en08037.

Mead, M. I., Khan, M. A. H., White, I. R., Nickless, G., and Shallcross, D. E. (2008b): Methyl halide emission estimates from domestic biomass burning in Africa, *Atmospheric Environment*, 42, 5241-5250, doi: 10.1016/j.atmosenv.2008.02.066.

Meixner, F. X., Fickinger, T., Marufu, L., Serca, D., Nathaus, F. J., Makina, E., Mukurumbira, L., and Andreae, M. O. (1997): Preliminary results on nitric oxide emission from a southern African savanna ecosystem, *Nutrient Cycling in Agroecosystems*, 48, 123-138, doi: 10.1023/a:1009765510538.

Middelburg, J. J., Nieuwenhuize, J., Iversen, N., Hogh, N., De Wilde, H., Helder, W., Seifert, R., and Christof, O. (2002): Methane distribution in European tidal estuaries, *Biogeochemistry*, 59, 95-119, doi: 10.1023/a:1015515130419.

Migné, A., Davoult, D., Spilmont, N., Menu, D., Boucher, G., Gattuso, J. P., and Rybarczyk, H. (2002): A closed-chamber CO2-flux method for estimating intertidal primary production and respiration under emersed conditions, *Marine Biology*, 140, 865-869, doi: 10.1007/s00227-001-0741-1.

Migné, A., Spilmont, N., and Davoult, D. (2004): In situ measurements of benthic primary production during emersion: seasonal variations and annual production in the Bay of Somme (eastern English Channel, France), *Continental Shelf Research*, 24, 1437-1449, doi: 10.1016/j.csr.2004.06.002.

Miller, L. G., Kalin, R. M., McCauley, S. E., Hamilton, J. T. G., Harper, D. B., Millet, D. B., Oremland, R. S., and Goldstein, A. H. (2001): Large carbon isotope fractionation associated with oxidation of methyl halides by methylotrophic bacteria, *Proceedings of the National Academy of Sciences of the United States of America*, 98, 5833-5837, doi: 10.1073/pnas.101129798.

Miller, L. G., Warner, K. L., Baesman, S. M., Oremland, R. S., McDonald, I. R., Radajewski, S., and Murrell, J. C. (2004): Degradation of methyl bromide and methyl chloride in soil microcosms: Use of stable C isotope fractionation and stable isotope probing to identify reactions and the responsible microorganisms, *Geochimica et Cosmochimica Acta*, 68, 3271-3283, doi: 10.1016/j.gca.2003.11.028.

Miller, B. R., Weiss, R. F., Salameh, P. K., Tanhua, T., Greally, B. R., Muhle, J., and Simmonds, P. G. (2008): Medusa: A sample preconcentration and GC/MS detector system for in situ measurements of atmospheric trace halocarbons, hydrocarbons, and sulfur Compounds, *Analytical Chemistry*, 80, 1536-1545, doi: 10.1021/ac702084k.

Moore, R. M. and Zafiriou, O. C. (1994): Photochemical production of methyl iodide in seawater, *Journal of Geophysical Research: Atmospheres*, 99, 16415-16420, doi: 10.1029/94jd00786.

Moore, R. M., Geen, C. E., and Tait, V. K. (1995a): Determination of Henry's Law constants for a suite of naturally occurring halogenated methanes in seawater, *Chemosphere*, 30, 1183-1191, doi: 10.1016/0045-6535(95)00009-W.

Moore, R. M., Tokarczyk, R., Tait, V. K., Poulin, M., and Geen, C. (1995b): Marine phytoplankton as a natural source of volatile organohalogens, in: *Naturally-Produced Organohalogens*, edited by: Grimvall, A. and Leer, E. B., Environment & Chemistry, Springer Netherlands, 283-294.

Moore, R. M., Webb, M., Tokarczyk, R., and Wever, R. (1996): Bromoperoxidase and iodoperoxidase enzymes and production of halogenated methanes in marine diatom cultures, *Journal of Geophysical Research-Oceans*, 101, 20899-20908, doi: 10.1029/96jc01248.

Moore, R. M. and Groszko, W. (1999): Methyl iodide distribution in the ocean and fluxes to the atmosphere, *Journal of Geophysical Research-Oceans*, 104, 11163-11171, doi: 10.1029/1998jc900073.

Moore, R. M. (2000): The solubility of a suite of low molecular weight organochlorine compounds in seawater and implications for estimating the marine source of methyl chloride to the atmosphere, *Chemosphere - Global Change Science*, 2, 95-99, doi: 10.1016/S1465-9972(99)00045-8.

Moore, R. M. (2008): A photochemical source of methyl chloride in saline waters, *Environmental Science & Technology*, 42, 1933-1937, doi: 10.1021/es071920I.

Morasch, B. and Hunkeler, D. (2009): Isotope fractionation during transformation processes, in: *Environmental Isotopes in Biodegradation and Bioremediation*, edited by: Aelion, C.M., Aravena, R., Hunkeler, D., Höhener, P., CRC Press, 79-125.

Moyes, A. B., Schauer, A. J., Siegwolf, R. T. W., and Bowling, D. R. (2010): An injection method for measuring the carbon isotope content of soil carbon dioxide and soil respiration with a tunable diode laser absorption spectrometer, *Rapid Communications in Mass Spectrometry*, 24, 894-900, doi: 10.1002/rcm.4466.

Neilson, A. H. and Allard, A.-S. (2008): Environmental degradation and transformation of organic chemicals, CRC Press/Taylor & Francis, Boca Raton, USA.

Ni, X. H. and Hager, L. P. (1999): Expression of Batis maritima methyl chloride transferase in Escherichia coli, *Proceedings of the National Academy of Sciences of the United States of America*, 96, 3611-3615, doi: 10.1073/pnas.96.7.3611.

Nightingale, P. D., Malin, G., and Liss, P. S. (1995): Production of chloroform and other low-molecular-weight halocarbons by some species of macroalgae, Limnology and Oceanography, 40, 680-689.

Nightingale, P. D., Malin, G., Law, C. S., Watson, A. J., Liss, P. S., Liddicoat, M. I., Boutin, J., and Upstill-Goddard, R. C. (2000): In situ evaluation of air-sea gas exchange parameterizations using novel conservative and volatile tracers, *Global Biogeochemical Cycles*, 14, 373-387, doi: 10.1029/1999gb900091.

O'Dowd, C. D., Jimenez, J. L., Bahreini, R., Flagan, R. C., Seinfeld, J. H., Hameri, K., Pirjola, L., Kulmala, M., Jennings, S. G., and Hoffmann, T. (2002): Marine aerosol formation from biogenic iodine emissions, *Nature*, 417, 632-636, doi: 10.1038/nature00775.

Oremland, R. S. (1975): Methane production in shallow-water, tropical marine sediments, *Applied Microbiology*, 30, 602-608.

Oremland, R. S., Marsh, L. M., and Polcin, S. (1982): Methane production and simultaneous sulfate reduction in anoxic, salt-marsh sediments, *Nature*, 296, 143-145, doi: 10.1038/296143a0.

Oremland, R. S., Miller, L. G., and Strohmaier, F. E. (1994): Degradation of methyl bromide in anaerobic sediments, *Environmental Science & Technology*, 28, 514-520, doi: 10.1021/es00052a026.

Orth, R. J., Carruthers, T. J. B., Dennison, W. C., Duarte, C. M., Fourqurean, J. W., Heck, K. L., Jr., Hughes, A. R., Kendrick, G. A., Kenworthy, W. J., Olyarnik, S., Short, F. T., Waycott, M., and Williams, S. L. (2006): A global crisis for seagrass ecosystems, *Bioscience*, 56, 987-996, doi: 10.1641/0006-3568(2006)56[987:agcfse]2.0.co;2.

REFERENCES

Pape, L., Ammann, C., Nyfeler-Brunner, A., Spirig, C., Hens, K., and Meixner, F. X. (2009): An automated dynamic chamber system for surface exchange measurement of non-reactive and reactive trace gases of grassland ecosystems, *Biogeosciences*, 6, 405-429, doi:10.5194/bg-6-405-2009.

Paul, C. and Pohnert, G. (2011): Production and role of volatile halogenated compounds from marine algae, *Natural Product Reports*, 28, 186-195, doi: 10.1039/c0np00043d.

Pérez-Llorens, J. L. and Niell, F. X. (1994): Photosynthesis in air: comparative responses to different temperatures of two morphotypes of Zostera noltii Hornem. from Palmones River estuary (southern Spain), *Verhandlungen des Internationalen Verein Limnologie*, 25, 2265- 2269.

Pfeilsticker, K., Sturges, W. T., Bosch, H., Camy-Peyret, C., Chipperfield, M. P., Engel, A., Fitzenberger, R., Muller, M., Payan, S., and Sinnhuber, B. M. (2000): Lower stratospheric organic and inorganic bromine budget for the Arctic winter 1998/99, *Geophysical Research Letters*, 27, 3305-3308, doi: 10.1029/2000gl011650.

Platt, U. and Hönninger, G. (2003): The role of halogen species in the troposphere, *Chemosphere*, 52, 325-338, doi: 10.1016/s0045-6535(03)00216-9.

Powers, H. H., Hunt, J. E., Hanson, D. T., and McDowell, N. G. (2010): A dynamic soil chamber system coupled with a tunable diode laser for online measurements of delta(13)C, delta(18)O, and efflux rate of soil-respired CO(2), *Rapid Communications in Mass Spectrometry*, 24, 243-253, doi: 10.1002/rcm.4380.

Precht, E. and Huettel, M. (2004): Rapid wave-driven advective pore water exchange in a permeable coastal sediment, *Journal of Sea Research*, 51, 93-107, doi: 10.1016/j.seares.2003.07.003.

Pupek, M., Assonov, S. S., Muhle, J., Rhee, T. S., Oram, D., Koeppel, C., Slemr, F., and Brenninkmeijer, C. A. M. (2005): Isotope analysis of hydrocarbons: trapping, recovering and archiving hydrocarbons and halocarbons separated from ambient air, *Rapid Communications in Mass Spectrometry*, 19, 455-460, doi: 10.1002/rcm.1812.

Quack, B. and Wallace, D. W. R. (2003): Air-sea flux of bromoform: Controls, rates, and implications, *Global Biogeochemical Cycles*, 17, 1023, doi: 10.1029/2002gb001890.

Quack, B., Peeken, I., Petrick, G., and Nachtigall, K. (2007): Oceanic distribution and sources of bromoform and dibromomethane in the Mauritanian upwelling, *Journal of Geophysical Research*, 112, C10006, doi: 10.1029/2006jc003803.

Raymond, P. A. and Cole, J. J. (2001): Gas exchange in rivers and estuaries: Choosing a gas transfer velocity, *Estuaries*, 24, 312-317, doi: 10.2307/1352954.

Read, K. A., Mahajan, A. S., Carpenter, L. J., Evans, M. J., Faria, B. V. E., Heard, D. E., Hopkins, J. R., Lee, J. D., Moller, S. J., Lewis, A. C., Mendes, L., McQuaid, J. B., Oetjen, H., Saiz-Lopez, A., Pilling, M. J., and Plane, J. M. C. (2008): Extensive halogen-mediated ozone destruction over the tropical Atlantic Ocean, *Nature*, 453, 1232-1235, doi: 10.1038/nature07035.

Redeker, K. R., Wang, N. Y., Low, J. C., McMillan, A., Tyler, S. C., and Cicerone, R. J. (2000): Emissions of methyl halides and methane from rice paddies, *Science*, 290, 966-969, doi: 10.1126/science.290.5493.966.

Redeker, K. R. and Cicerone, R. J. (2004): Environmental controls over methyl halide emissions from rice paddies, *Global Biogeochemical Cycles*, 18, GB1027, doi: 10.1029/2003gb002092.

Redeker, K. R., Manley, S. L., Brothers, L., McDuffee, K., Walser, M., and Cicerone, R. J. (2004): Seasonal mass balance of halogens in simulated rice paddies, *Geophysical Research Letters*, 31, L11504, doi: 10.1029/2004gl019579.

Redeker, K. R., Davis, S., and Kalin, R. M. (2007): Isotope values of atmospheric halocarbons and hydrocarbons from Irish urban, rural, and marine locations, *Journal of Geophysical. Research*, 112, D16307, doi: 10.1029/2006jd007784.

Redeker, K. R., and Kalin, R. M. (2012): Methyl chloride isotopic signatures from Irish forest soils and a comparison between abiotic and biogenic methyl halide soil fluxes, *Global Change Biology*, 18, 1453-1467, doi: 10.1111/j.1365-2486.2011.02600.x.

Rhew, R. C., Miller, B. R., and Weiss, R. F. (2000): Natural methyl bromide and methyl chloride emissions from coastal salt marshes, *Nature*, 403, 292-295, doi: 10.1038/35002043.

Rhew, R. C., Miller, B. R., Bill, M., Goldstein, A. H., and Weiss, R. F. (2002): Environmental and biological controls on methyl halide emissions from southern California coastal salt marshes, *Biogeochemistry*, 60, 141-161, doi: 10.1023/a:1019812006560.

Rhew, R. C., Aydin, M., and Saltzman, E. S. (2003): Measuring terrestrial fluxes of methyl chloride and methyl bromide using a stable isotope tracer technique, *Geophysical Research. Letters*, 30, 2103, doi: 10.1029/2003gl018160.

Rhew, R. and Mazéas, O. (2010): Gross production exceeds gross consumption of methyl halides in northern California salt marshes, *Geophysical Research Letters*, 37, L18813, doi: 10.1029/2010gl044341.

Riedl, R. J., Machan, R., and Huang, N. (1972): Subtidal pump - mechanisms of interstitial water exchange by wave action, *Marine Biology*, 13, 210-&, doi: 10.1007/bf00391379.

Rudolph, J., Lowe, D. C., Martin, R. J., and Clarkson, T. S. (1997): A novel method for compound specific determination of delta C-13 in volatile organic compounds at ppt levels in ambient air, *Geophysical Research Letters*, 24, 659-662, doi: 10.1029/97gl00537.

Rudolph, J. and Czuba, E. (2000): On the use of isotopic composition measurements of volatile organic compounds to determine the "photochemical age" of an air mass, *Geophysical Research Letters*, 27, 3865-3868, doi: 10.1029/2000gl011385.

Rudolph, J., Czuba, E., and Huang, L. (2000): The stable carbon isotope fractionation for reactions of selected hydrocarbons with OH-radicals and its relevance for atmospheric chemistry, *Journal of Geophysical Research-Atmospheres*, 105, 29329-29346, doi: 10.1029/2000JD900447.

Sachs, J. P., Repeta, D. J., and Goericke, R. (1999): Nitrogen and carbon isotopic ratios of chlorophyll from marine phytoplankton, *Geochimica et Cosmochimica Acta*, 63, 1431-1441, doi: 10.1016/s0016-7037(99)00097-6.

Saemundsdottir, S. and Matrai, P. A. (1998): Biological production of methyl bromide by cultures of marine phytoplankton, *Limnology and Oceanography*, 43, 81-87.

Saini, H. S., Attieh, J. M., and Hanson, A. D. (1995): Biosynthesis of halomethanes and methanethiol by higher plants via a novel methyltransferase reaction, *Plant, Cell & Environment*, 18, 1027-1033, doi: 10.1111/j.1365-3040.1995.tb00613.x.

Saito, T., and Yokouchi, Y. (2006): Diurnal variation in methyl halide emission rates from tropical ferns, *Atmospheric Environment*, 40, 2806-2811, doi: 10.1016/j.atmosenv.2006.01.016.

Saito, T. and Yokouchi, Y. (2008): Stable carbon isotope ratio of methyl chloride emitted from glasshouse-grown tropical plants and its implication for the global methyl chloride budget, *Geophysical Research Letters*, 35, L08807, doi: 10.1029/2007gl032736.

Saiz-Lopez, A. and von Glasow, R. (2012): Reactive halogen chemistry in the troposphere, *Chemical Society Reviews*, 41, 6448-6472, doi: 10.1039/c2cs35208g.

Sander, R., Vogt, R., Harris, G. W., and Crutzen, P. J. (1997): Modelling the chemistry of ozone, halogen compounds, and hydrocarbons in the arctic troposphere during spring, *Tellus B*, 49, 522-532, doi: 10.1034/j.1600-0889.49.issue5.8.x.

Santos, R., Silva, J., Alexandre, A., Navarro, N., Barron, C., and Duarte, C. M. (2004): Ecosystem metabolism and carbon fluxes of a tidally-dominated coastal lagoon, *Estuaries*, 27, 977-985, doi: 10.1007/bf02803424.

Saxena, D., Aouad, S., Attieh, J., and Saini, H. S. (1998): Biochemical characterization of chloromethane emission from the wood-rotting fungus Phellinus pomaceus, *Applied and Environmental Microbiology*, 64, 2831-2835.

Scarratt, M. G. and Moore, R. M. (1996): Production of methyl chloride and methyl bromide in laboratory cultures of marine phytoplankton, *Marine Chemistry*, 54, 263-272, doi: 10.1016/0304-4203(96)00036-9.

Scarratt, M. G. and Moore, R. M. (1998): Production of methyl bromide and methyl chloride in laboratory cultures of marine phytoplankton II, *Marine Chemistry*, 59, 311-320, doi: 10.1016/s0304-4203(97)00092-3.

Schäfer, H., McDonald, I. R., Nightingale, P. D., and Murrell, J. C. (2005): Evidence for the presence of a CmuA methyltransferase pathway in novel marine methyl halide-oxidizing bacteria, *Environmental Microbiology*, 7, 839-852, doi: 10.1111/j.1462-2920.2005.00757.x.

Schäfer, H., Miller, L. G., Oremland, R. S., and Murrell, J. C. (2007): Bacterial cycling of methyl halides, in: *Advances in Applied Microbiology*, edited by: Laskin, A. I., Sariaslani, S., and Gadd, G. M., Academic Press, 307-346.

Shorter, J. H., Kolb, C. E., Crill, P. M., Kerwin, R. A., Talbot, R. W., Hines, M. E., and Harriss, R. C. (1995): Rapid degradation of atmospheric methyl bromide in soils, *Nature*, 377, 717-719, doi: 10.1038/377717a0.

Silva, J., Santos, R., Calleja, M. L., and Duarte, C. M. (2005): Submerged versus air-exposed intertidal macrophyte productivity: from physiological to community-level assessments, *Journal of Experimental Marine Biology and Ecology*, 317, 87-95, doi: 10.1016/j.jembe.2004.11.010.

Silva, J., Feijoo, P., and Santos, R. (2008): Underwater measurements of carbon dioxide evolution in marine plant communities: A new method, *Estuarine, Coastal and Shelf Science*, 78, 827-830, doi: 10.1016/j.ecss.2008.02.019.

Sive, B. C., Varner, R. K., Mao, H., Blake, D. R., Wingenter, O. W., and Talbot, R. (2007): A large terrestrial source of methyl iodide, *Geophysical Research Letters*, 34, L17808, doi: 10.1029/2007gl030528.

REFERENCES

Smith, R. D., Dennison, W. C., and Alberte, R. S. (1984): Role of seagrass photosynthesis in root aerobic processes, *Plant Physiology*, 74, 1055-1058, doi: 10.1104/pp.74.4.1055.

Smythe-Wright, D., Boswell, S. M., Breithaupt, P., Davidson, R. D., Dimmer, C. H., and Diaz, L. B. E. (2006): Methyl iodide production in the ocean: Implications for climate change, *Global Biogeochemical Cycles*, 20, Gb3003, doi: 10.1029/2005gb002642.

Smythe-Wright, D., Peckett, C., Boswell, S., and Harrison, R. (2010): Controls on the production of organohalogens by phytoplankton: Effect of nitrate concentration and grazing, *Journal of Geophysical Research-Biogeosciences*, 115, G03020, doi: 10.1029/2009jg001036.

Solomon, S., Garcia, R. R., and Ravishankara, A. R. (1994): On the role of iodine in ozone depletion, *Journal of Geophysical Research-Atmospheres*, 99, 20491-20499, doi: 10.1029/94jd02028.

Spilmont, N., Migné, A., Lefebvre, A., Artigas, L. F., Rauch, M., and Davoult, D. (2005): Temporal variability of intertidal benthic metabolism under emersed conditions in an exposed sandy beach (Wimereux, eastern English Channel, France), *Journal of Sea Research*, 53, 161-167, doi: 10.1016/j.seares.2004.07.004.

Sturges, W. T., Oram, D. E., Carpenter, L. J., Penkett, S. A., and Engel, A. (2000): Bromoform as a source of stratospheric bromine, *Geophysical Research Letters*, 27, 2081-2084, doi: 10.1029/2000gl011444.

Tait, V. K., Moore, R. M., and Tokarczyk, R. (1994): Measurements of methyl-chloride in the Northwest Atlantic, *Journal of Geophysical Research-Oceans*, 99, 7821-7833, doi: 10.1029/93jc03582.

Tait, V. K. (1995): An investigation of the oceanic source of methyl chloride, PhD thesis, Dalhousie University, Halifax, Canada.

Tait, V. K. and Moore, R. M. (1995): Methyl-chloride (CH3Cl) production in phytoplankton cultures, *Limnology and Oceanography*, 40, 189-195.

Tegtmeier, S., Krüger, K., Quack, B., Atlas, E., Blake, D. R., Boenisch, H., Engel, A., Hepach, H., Hossaini, R., Navarro, M. A., Raimund, S., Sala, S., Shi, Q., and Ziska, F. (2013): The contribution of oceanic methyl iodide to stratospheric iodine, *Atmospheric Chemistry and Physics Discussions*, 13, 11427-11471, doi: 10.5194/acpd-13-11427-2013.

Tett, P., Gilpin, L., Svendsen, H., Erlandsson, C. P., Larsson, U., Kratzer, S., Fouilland, E., Janzen, C., Lee, J. Y., Grenz, C., Newton, A., Ferreira, J. G., Fernandes, T., and Scory, S. (2003): Eutrophication and some European waters of restricted exchange, *Continental Shelf Research*, 23, 1635-1671, doi: 10.1016/j.csr.2003.06.013.

Theiler, R., Cook, J. C., and Hager, L. P. (1978): Halohydrocarbon synthesis by bromoperoxidase, *Science*, 202, 1094-1096, doi: 10.1126/science.202.4372.1094.

Thompson, A. E., Anderson, R. S., Rudolph, J., and Huang, L. (2002): Stable carbon isotope signatures of background tropospheric chloromethane and CFC113, *Biogeochemistry*, 60, 191-211, doi: 10.1023/a:1019820208377.

Tokarczyk, R. and Moore, R. M. (1994): Production of volatile organohalogens by phytoplankton cultures, *Geophysical Research Letters*, 21, 285-288, doi: 10.1029/94gl00009.

Tokarczyk, R. and Saltzman, E. S. (2001): Methyl bromide loss rates in surface waters of the North Atlantic Ocean, Caribbean Sea, and eastern Pacific Ocean (8 degrees-45 degrees N), *Journal of Geophysical Research-Atmospheres*, 106, 9843-9851, doi: 10.1029/2000jd900742.

Tokarczyk, R., Saltzman, E. S., Moore, R. M., and Yvon-Lewis, S. A. (2003): Biological degradation of methyl chloride in coastal seawater, *Global Biogeochemical Cycles*, 17, 1057, doi: 10.1029/2002gb001949.

Tsunogai, U., Yoshida, N., and Gamo, T. (1999): Carbon isotopic compositions of C2-C5 hydrocarbons and methyl chloride in urban, coastal, and maritime atmospheres over the western North Pacific, *Journal of Geophysical Research*, 104, 16033-16039, doi: 10.1029/1999jd900217.

Turner, S. M., Malin, G., and Liss, P. S. (1989): Dimethyl Sulfide and (Dimethylsulfonio)propionate in European Coastal and Shelf Waters, in: *Biogenic Sulfur in the Environment*, ACS Symposium Series, 393, American Chemical Society, 183-200.

UNEP (1987): The Montreal Protocol on Substances that Deplete the Ozone Layer, United Nations Envrionmental Program, Vienna, Austria.

Urhahn, T. (2003): Leichtflüchtige ECD-aktive Verbindungen in der marinen Grundschicht (MBL) des Atlantischen Ozeans: Vorkommen, Quellen und Verteilung, PhD thesis, University of Ulm, Ulm, Germany

Valentine, J. and Duffy, J. E. (2006): The central role of grazing in seagrass ecology, in: *Seagrasses: Biology, Ecology, and Conservation*, edited by: Larkum, A. W., Orth, R. J., and Duarte, C. M., Springer Netherlands, 463-501.

Valtanen, A., Solloch, S., Hartikainen, H., and Michaelis, W. (2009): Emissions of volatile halogenated compounds from a meadow in a coastal area of the Baltic Sea, *Boreal Environment Research*, 6095, 1-17.

Van der Nat, F. J. and Middelburg, J. J. (2000): Methane emission from tidal freshwater marshes, *Biogeochemistry*, 49, 103-121, doi: 10.1023/a:1006333225100.

Varner, R. K., Crill, P. M., and Talbot, R. W. (1999): Wetlands: a potentially significant source of atmospheric methyl bromide and methyl chloride, *Geophysical Research Letters*, 26, 2433-2435, doi: 10.1029/1999gl900587.

Varns, J. (1982): The release of methyl chloride from potato tubers, *American Potato Journal*, 59, 593-604, doi: 10.1007/bf02867599.

von Glasow, R. and Crutzen, P. J. (2003): Tropospheric halogen chemistry, in: *Treatise on Geochemistry*, edited by: Heinrich, D. H. and Karl, K. T., Pergamon, Oxford, 1-67.

von Glasow, R. (2008): Atmospheric chemistry - Sun, sea and ozone destruction, *Nature*, 453, 1195-1196, doi: 10.1038/4531195a.

Wahman, D. G., Katz, L. E., and Speitel, G. E. (2005): Cometabolism of trihalomethanes by Nitrosomonas europaea, *Applied and Environmental Microbiology*, 71, 7980-7986, doi: 10.1128/aem.71.12.7980-7986.2005.

Wahman, D. G., Henry, A. E., Katz, L. E., and Speitel, G. E., Jr. (2006): Cometabolism of trihalomethanes by mixed culture nitrifiers, *Water Research*, 40, 3349-3358, doi: 10.1016/j.watres.2006.07.033.

Wanninkhof, R. (1992): Relationship between wind speed and gas exchange over the ocean, *Journal of Geophysical Research-Oceans*, 97, 7373-7382, doi: 10.1029/92jc00188.

Watling, R. and Harper, D. B. (1998): Chloromethane production by wood-rotting fungi and an estimate of the global flux to the atmosphere, *Mycological Research*, 102, 769-787, doi: 10.1017/S0953756298006157.

Waycott, M., Duarte, C. M., Carruthers, T. J. B., Orth, R. J., Dennison, W. C., Olyarnik, S., Calladine, A., Fourqurean, J. W., Heck, K. L., Jr., Hughes, A. R., Kendrick, G. A., Kenworthy, W. J., Short, F. T., and Williams, S. L. (2009): Accelerating loss of seagrasses across the globe threatens coastal ecosystems, *Proceedings of the National Academy of Sciences of the United States of America*, 106, 12377-12381, doi: 10.1073/pnas.0905620106.

Weinberg, I., Bahlmann, E., Michaelis, W., and Seifert, R. (2013): Determination of fluxes and isotopic composition of halocarbons from seagrass meadows using a dynamic flux chamber, *Atmospheric Environment*, 73, 34-40, doi: 10.1016/j.atmosenv.2013.03.006.

Weinberg, I., Bahlmann, E., Eckhardt, T., Michaelis, W., and Seifert, R.: A halocarbon survey from a seagrass dominated subtropical lagoon, Ria Formosa (Portugal): Flux pattern and isotopic composition, *in prep.*

Werner, U., Billerbeck, M., Polerecky, L., Franke, U., Huettel, M., van Beusekom, J. E. E., and de Beer, D. (2006): Spatial and temporal patterns of mineralization rates and oxygen distribution in a permeable intertidal sand flat (Sylt, Germany), *Limnology and Oceanography*, 51, 2549-2563.

WMO (2003): Scientific Assessment of Ozone Depletion: 2002, World Meteorological Organization, Geneva, Switzerland.

WMO (2007): Scientific Assessment of Ozone Depletion: 2006, World Meteorological Organization, Geneva, Switzerland.

WMO (2011): Scientific Assessment of Ozone Depletion: 2010, World Meteorological Organization, Geneva, Switzerland.

Wofsy, S. C., McElroy, M. B., and Yung, Y. L. (1975): The chemistry of atmospheric bromine, *Geophysical Research Letters*, 2, 215-218, doi: 10.1029/GL002i006p00215.

Wuosmaa, A. and Hager, L. (1990): Methyl chloride transferase: a carbocation route for biosynthesis of halometabolites, *Science*, 249, 160-162, doi: 10.1126/science.2371563.

Xiao, X., Prinn, R. G., Fraser, P. J., Simmonds, P. G., Weiss, R. F., O'Doherty, S., Miller, B. R., Salameh, P. K., Harth, C. M., Krummel, P. B., Porter, L. W., Muehle, J., Greally, B. R., Cunnold, D., Wang, R., Montzka, S. A., Elkins, J. W., Dutton, G. S., Thompson, T. M., Butler, J. H., Hall, B. D., Reimann, S., Vollmer, M. K., Stordal, F., Lunder, C., Maione, M., Arduini, J., and Yokouchi, Y. (2010): Optimal estimation of the surface fluxes of methyl chloride using a 3-D global chemical transport model, *Atmospheric Chemistry and Physics*, 10, 5515-5533, doi: 10.5194/acp-10-5515-2010.

Yamamoto, A., Hirota, M., Suzuki, S., Oe, Y., Zhang, P., and Mariko, S. (2009): Effects of tidal fluctuations on CO2 and CH4 fluxes in the littoral zone of a brackish-water lake, *Limnology*, 10, 228-237, doi: 10.1007/s10201-009-0284-6.

Yokouchi, Y., Ikeda, M., Inuzuka, Y., and Yukawa, T. (2002): Strong emission of methyl chloride from tropical plants, *Nature*, 416, 163-165, doi: 10.1038/416163a.

REFERENCES

Yokouchi, Y., Nagashima, Y., Saito, T., and Mukai, H. (2010): Identification of coastal emissions of methyl chloride and methyl bromide based on high-frequency measurements on Hateruma Island, Geochemical Journal, 44, 173-179.

Yvon, S. A. and Butler, J. H. (1996): An improved estimate of the oceanic lifetime of atmospheric CH3Br, *Geophysical Research Letters*, 23, 53-56, doi: 10.1029/95GL03022.

Yvon-Lewis, S. A. and Butler, J. H. (2002): Effect of oceanic uptake on atmospheric lifetimes of selected trace gases, *Journal of Geophysical Research*, 107, 4414, doi: 10.1029/2001jd001267.

Yvon-Lewis, S. A., Saltzman, E. S., and Montzka, S. A. (2009): Recent trends in atmospheric methyl bromide: analysis of post-Montreal Protocol variability, *Atmospheric Chemistry and Physics*, 9, 5963-5974, doi: 10.5194/acp-9-5963-2009.

Zafiriou, O. C. (1974): Photochemistry of halogens in marine atmosphere, *Journal of Geophysical Research*, 79, 2730-2732, doi: 10.1029/JC079i018p02730.

Zafiriou, O. C. (1975): Reaction of methyl halides with seawater and marine aerosols, *Journal of Marine Research*, 33, 75-81.

Zhang, H., Lindberg, S. E., Barnett, M. O., Vette, A. F., and Gustin, M. S. (2002): Dynamic flux chamber measurement of gaseous mercury emission fluxes over soils. Part 1: simulation of gaseous mercury emissions from soils using a two-resistance exchange interface model, *Atmospheric Environment*, 36, 835-846, doi: 10.1016/s1352-2310(01)00501-5.

Zhou, Y., Varner, R. K., Russo, R. S., Wingenter, O. W., Haase, K. B., Talbot, R., and Sive, B. C. (2005): Coastal water source of short-lived halocarbons in New England, *Journal of Geophysical Research-Atmospheres*, 110, D2130210, doi: 1029/2004jd005603.

Zuiderweg, A., Holzinger, R., and Rockmann, T. (2011): Analytical system for stable carbon isotope measurements of low molecular weight (C-2-C-6) hydrocarbons, *Atmospheric Measurement Techniques*, 4, 1161-1175, doi: 10.5194/amt-4-1161-2011.

11. Appendix

Appendix to Chapter 3: A high volume sampling system for isotope determination of volatile halocarbons and hydrocarbons

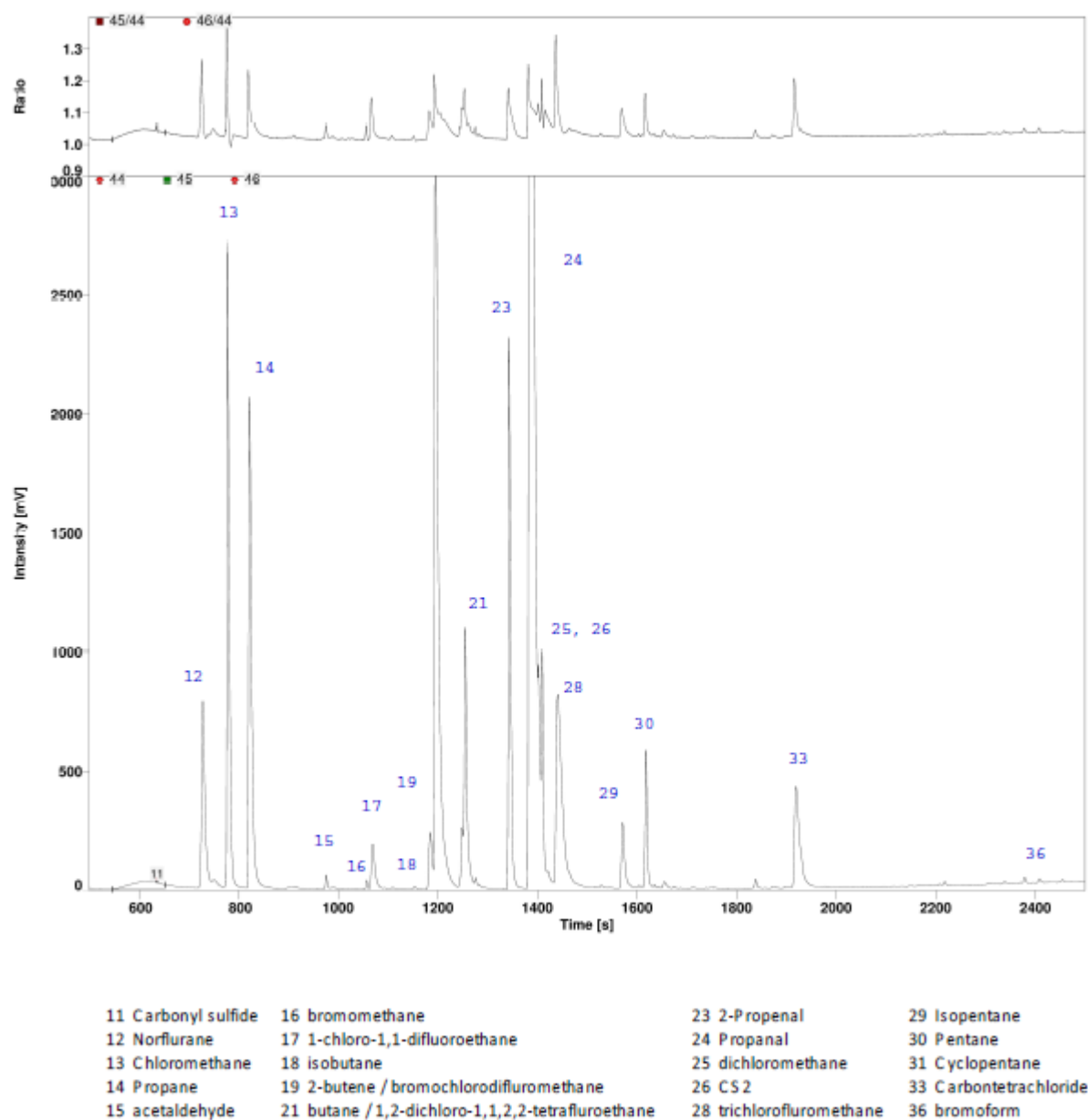|			
11 Carbonyl sulfide	16 bromomethane	23 2-Propenal	29 Isopentane
12 Norflurane	17 1-chloro-1,1-difluoroethane	24 Propanal	30 Pentane
13 Chloromethane	18 isobutane	25 dichloromethane	31 Cyclopentane
14 Propane	19 2-butene / bromochlorodifluromethane	26 CS 2	33 Carbontetrachloride
15 acetaldehyde	21 butane / 1,2-dichloro-1,1,2,2-tetrafluroethane	28 trichlorofluromethane	36 bromoform

Figure A1: Mass 45 trace and mz 46/45 ratio of fraction A of a representative air sample from the coastal site
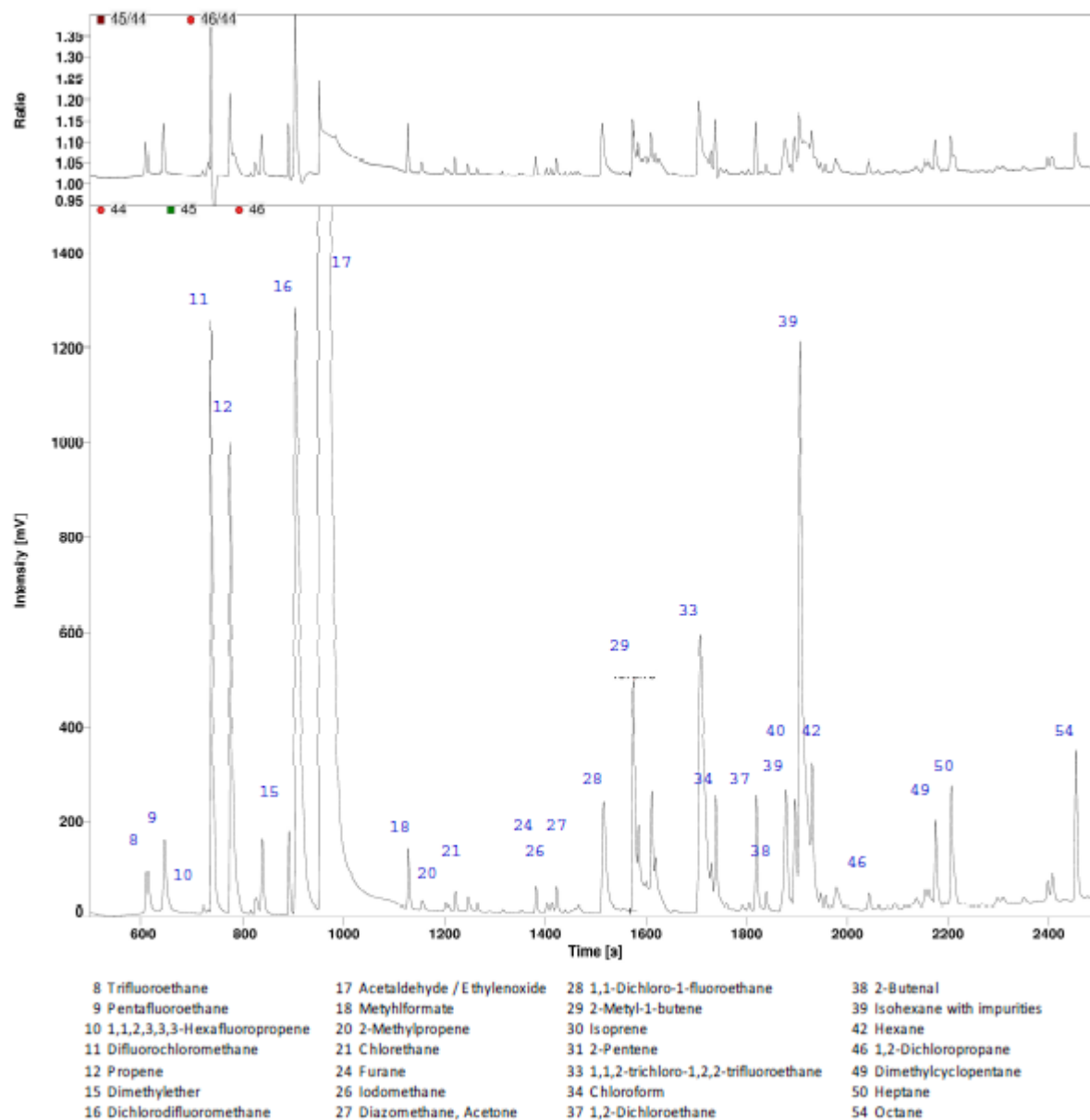
Figure A2: Mass 45 trace and mz 46/45 ratio of fraction B of a representative air sample from the coastal site

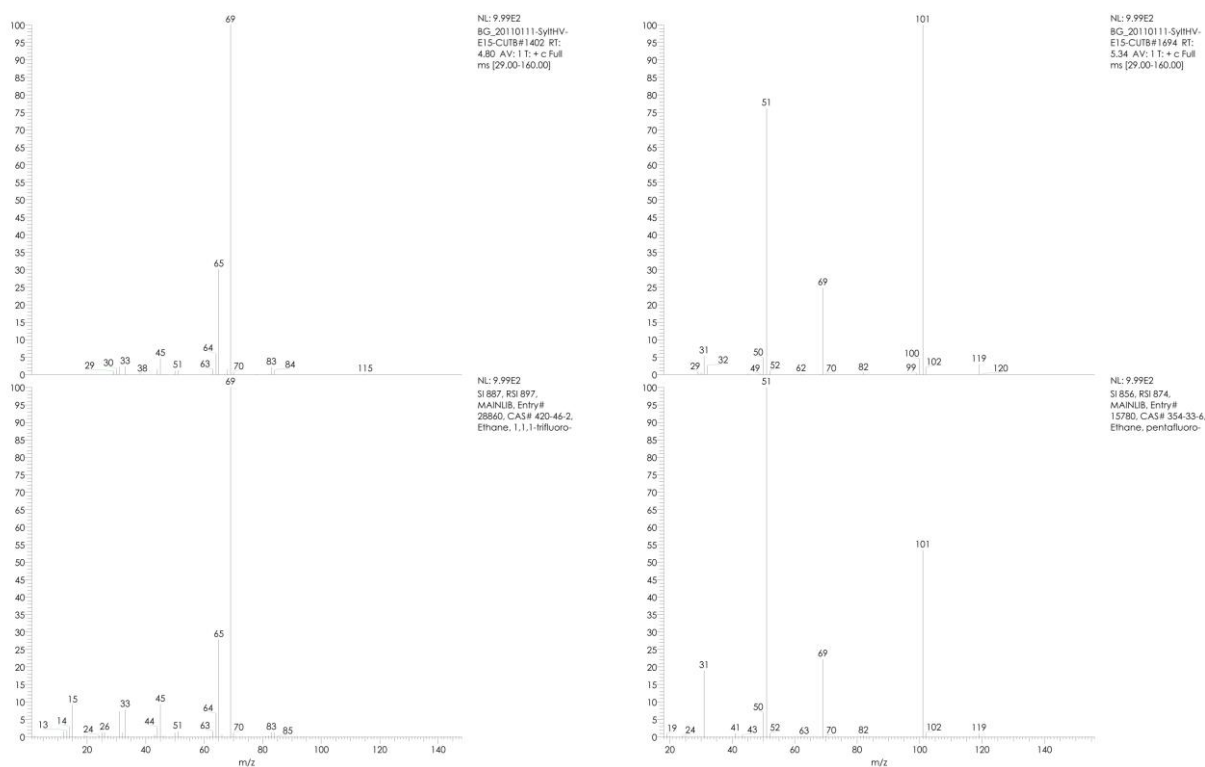|			
8 Trifluoroethane	17 Acetaldehyde / Ethylenoxide	28 1,1-Dichloro-1-fluoroethane	38 2-Butenal
9 Pentafluoroethane	18 Metyhlformate	29 2-Metyl-1-butene	39 Isohexane with impurities
10 1,1,2,3,3,3-Hexafluoropropene	20 2-Methylpropene	30 Isoprene	42 Hexane
11 Difluorochloromethane	21 Chlorethane	31 2-Pentene	46 1,2-Dichloropropane
12 Propene	24 Furane	33 1,1,2-trichloro-1,2,2-trifluoroethane	49 Dimethylcyclopentane
15 Dimethylether	26 Iodomethane	34 Chloroform	50 Heptane
16 Dichlorodifluoromethane	27 Diazomethane, Acetone	37 1,2-Dichloroethane	54 Octane

Figure A3: Spectra of trifluoroethane (left) and pentafluoroethane (right), respectively, from the concurrent quadropole-MS run in order to assess the peak purity. Upper mass traces are mass fragments of the respective compound in the air samples (fraction B) in comparison to those from the NIST library (lower mass traces).

Figure A4: Spectra of Chlorodifluoromethane (left) and dichlorodifluoromethane (right), respectively, from the concurrent quadropole-MS run in order to assess the peak purity. Upper mass traces are mass fragments of the respective compound in the air samples (fraction B) in comparison to those from the NIST library (lower mass traces).
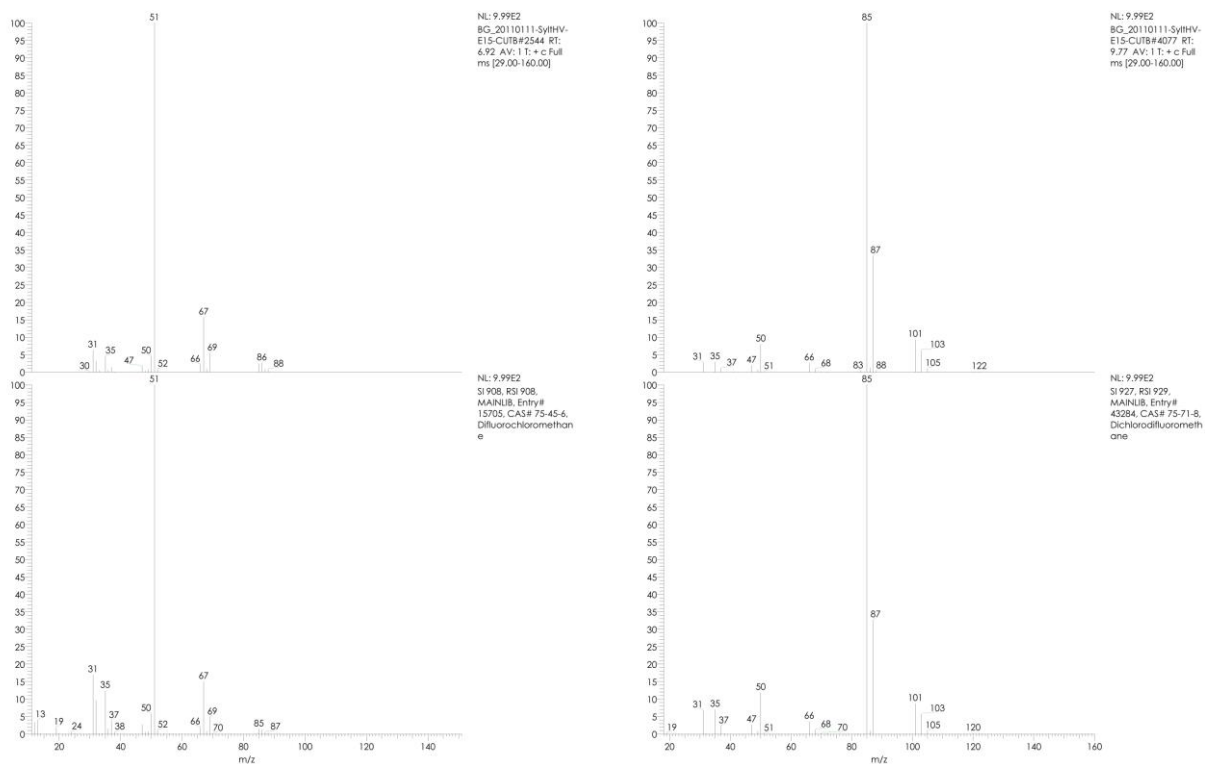
Figure A5: Spectra of iodomethane (left) and 1.1.2 Trichloro-1.2.2-trifluoroethane (right), respectively, from the concurrent quadropole-MS run in order to assess the peak purity. Upper mass traces are mass fragments of the respective compound in the air samples (fraction B) in comparison to those from the NIST library (lower mass traces).
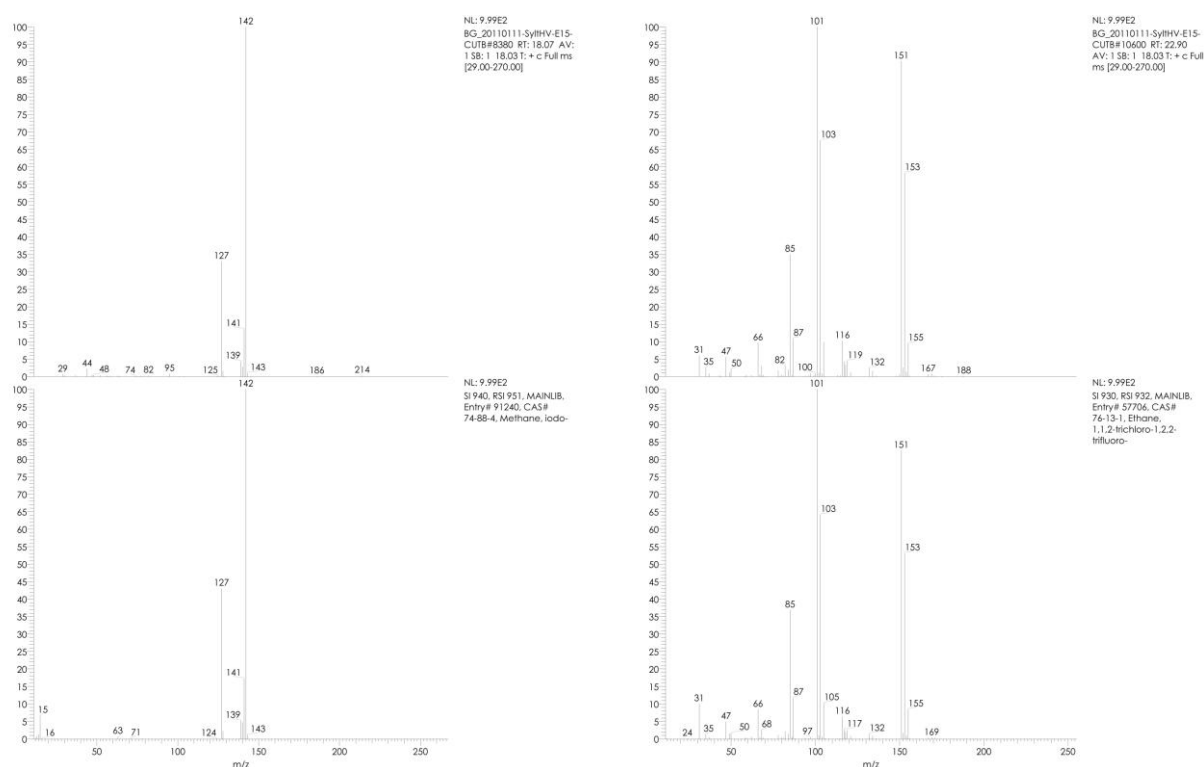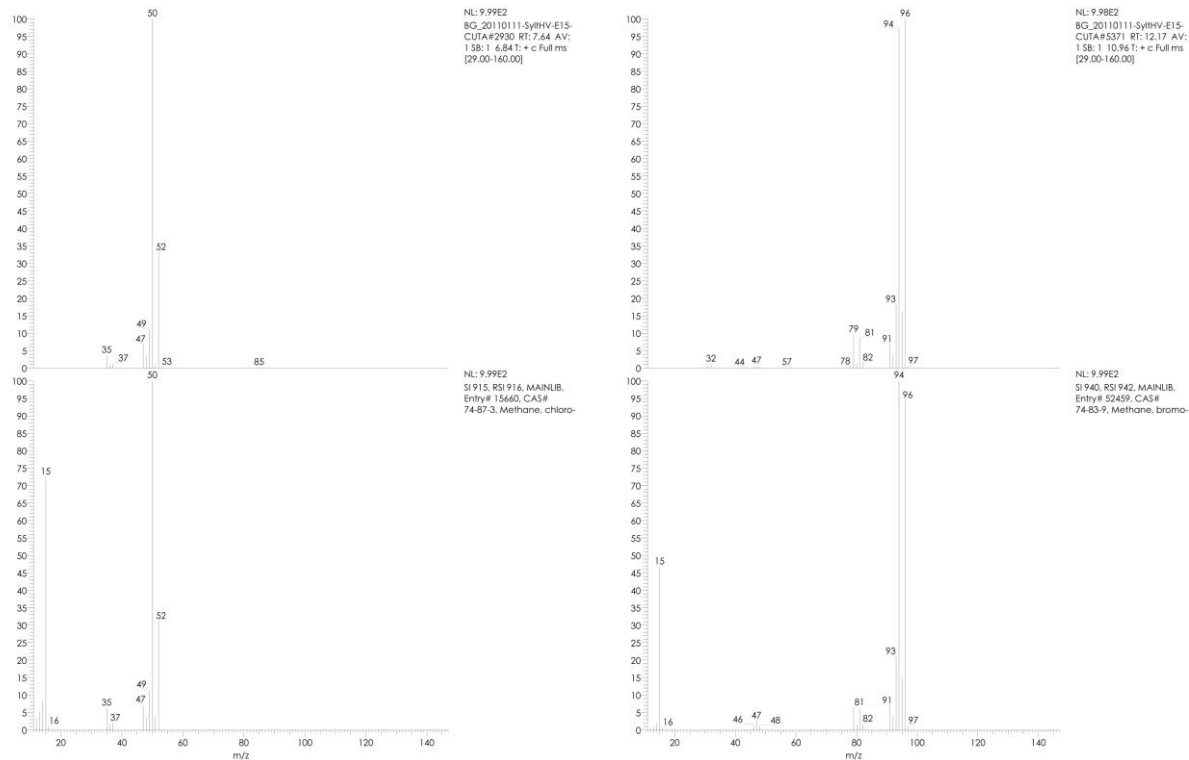

Figure A6: Spectra of chloromethane (left) and bromomethane (right), respectively, from the concurrent quadropole-MS run in order to assess the peak purity. Upper mass traces are mass fragments of the respective compound in the air samples (fraction A) in comparison to those from the NIST library (lower mass traces).
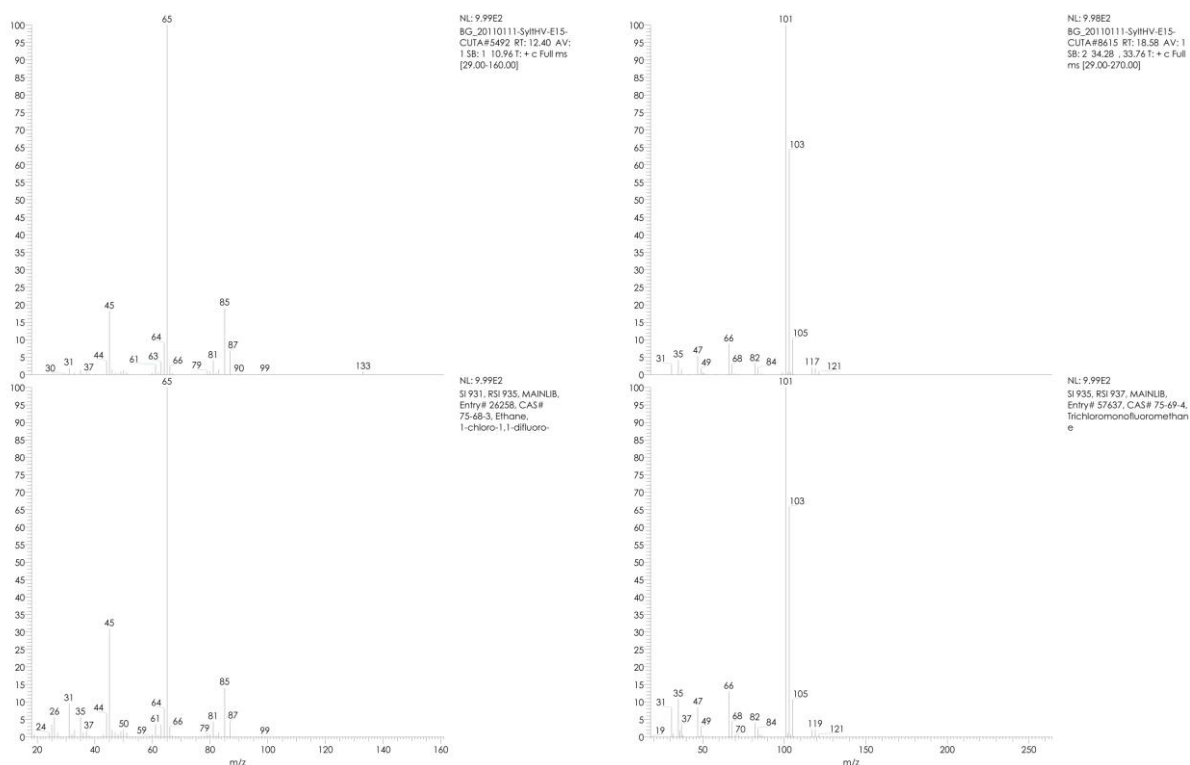
Figure A7: Spectra of 1-Chloro-1.1-difluoromethane (left) and trichlorofluoromethane (right), respectively, from the concurrent quadropole-MS run in order to assess the peak purity. Upper mass traces are mass fragments of the respective compound in the air samples (fraction A) in comparison to those from the NIST library (lower mass traces).

Figure A8: Spectra of tetrachloromethane (left) and bromoform (right), respectively, from the concurrent quadropole-MS run in order to assess the peak purity. Upper mass traces are mass fragments of the respective compound in the air samples (fraction A) in comparison to those from the NIST library (lower mass traces).
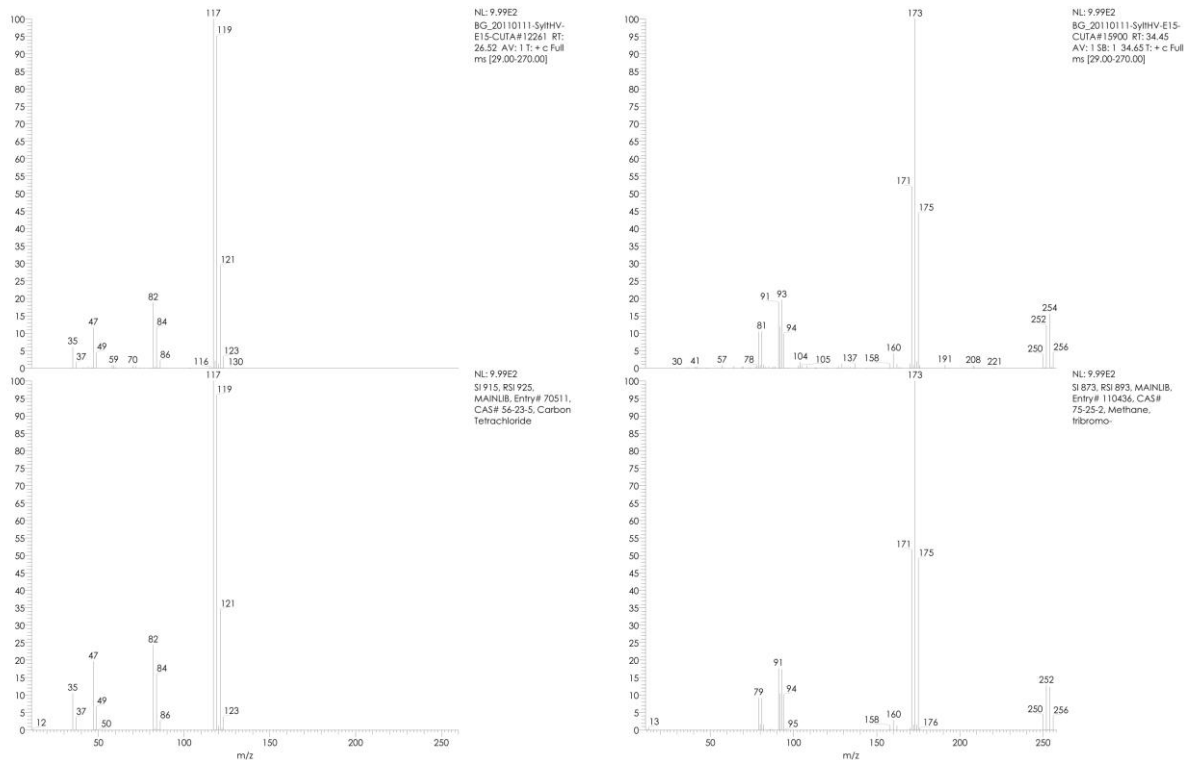
Appendix to Chapter 4: Determination of fluxes and isotopic composition of halocarbons from seagrass meadows using a dynamic flux chamber

Table A1: Net fluxes (nmol m^{-2} h^{-1}) of halocarbons from the two seagrass species *Z. marina* and *Z. noltii* as well as the sampling conditions, n.d. detected.

Sample type	Date	Local time	CH$_3$Cl	CH$_3$Br	CH$_3$I	CHBr$_3$	T$_{Air}$ (°C)	Solar Radiation (W m^{-2})
Z. Marina1	26.08.2010	10:00	2.27	0.03	0.37	0.76	16.9	516
Z. Marina2	27.08.2010	09:30	1.23	-0.01	0.13	0.04	14.8	273
Z. Marina3	27.08.2010	12:00	9.26	0.13	1.12	0.40	15.8	362
Z. Marina4	04.09.2010	15:30	9.70	0.21	2.29	0.02	16.4	275
Z. Marina5	04.09.2010	17:30	1.25	-0.03	0.27	0.27	16.2	181
Z. Noltii1	31.08.2010	12:00	9.40	0.16	0.76	0.08	16.0	617
Z. Noltii2	31.08.2010	13:00	9.49	0.25	0.52	0.44	15.6	368
Z. Noltii3	03.09.2010	15:00	10.11	0.36	1.37	0.46	16.3	434
Z. Noltii4	03.09.2010	17:00	2.29	0.29	0.93	0.50	15.8	224
Sediment1	30.08.2010	12:00	-2.16	-0.08	0.17	n.d.	16.9	595
Sediment2	30.08.2010	13:00	-3.66	-0.04	0.02	n.d.	17.1	461

Table A2: Calculated $\delta^{13}C$ values (‰) CH$_3$Cl and CH$_3$Br without sink correction and with sink correction. Respective KIEs and degradation rates (mol h^{-1}x 0.001) in the scenarios are derived from two incubation experiments above bare sediment. Values in parenthesis depict outliers (Grubbs test, $p<0.05$).

	CH$_3$Cl (‰)		
	without sink correction	with sink correction	
		Scenario A KIE= 5.81 deg. rate= -0.00025	Scenario B KIE= 8.94 deg. rate= -0.00063
Z. Marina1	-60.4	-53.5	-52.1
Z. Marina2	-18.9	-31.7	-38.8
Z. Marina3	-45.9	-46.6	-48.4
Z. Marina4	-56.1	-54.1	-53.8
Z. Marina5	-83	-62.2	-57
Z. Noltii1	-49.8	-48.8	-49.4
Z. Noltii2	-43.9	-44.1	-45.4
Z. Noltii3	-53.7	-52.8	-53.2
Z. Noltii4	-71.3	-55.4	-53.6
mean	-53.7	-49.9	-50.2
SD	18	8.6	5.5
n	9	9	9
Mean Scenario A and B	-	-50	
SD	-	7	
n	-	18	

	CH$_3$Br (‰)		
	without sink correction	with sink correction	
		Scenario A KIE= 22.47 deg. rate= -0.00199	Scenario B KIE= 59.24 deg. rate=-0.00085
Z. Marina1	(-5.8)	-42.7	-61.6
Z. Marina2	(-225.8)	-31.9	-59.4
Z. Marina3	-35.1	-49.6	-60.6
Z. Marina4	-32	-47.2	-57.6
Z. Marina5	-26	-63	(-175.4)
Z. Noltii1	-29.4	-45.1	-54.5
Z. Noltii2	-30.2	-42.7	-49.6
Z. Noltii3	-41.9	-53.4	-59.7
Z. Noltii4	-36	-48.7	-53.8
mean	-32.9	-47.2	-57.1
SD	5.2	8.5	4.2
n	7	9	8
Mean Scenario A and B	-	-51.8	
SD	-	8.3	
n	-	17	

Appendix to Chapter 5: A halocarbon survey from a seagrass dominated subtropical lagoon, Ria Formosa (Portugal): Flux pattern and isotopic composition

Design of cryotraps used for air and seawater samples (Purge and trap)

The analytic procedure is based on those of Bahlmann et al. (2011) for the isotopic determination of trace gases with some adjustments. We changed the design of the cryotraps in order to establish a better temporal resolution by reducing the sample preparation/analysis time. The self-made cryotraps were ¼" siltek capillary (40 cm) connected to a stainless steel capillary (60 cm) and were bowed forming a U-shape. This allows the cryotrap being easily submersed in the dry shipper (Voyageur 12, Air Liquide, Germany) as cooling source during sampling. The cryotraps were filled with Tenax TA (20-35 mesh, 5 cm, Grace, Deerfield, USA) at the lower end of ¼" capillary and fixed with silanized glass wool at the top and bottom of the packing material. The inlet and outlet were capped with Swagelok fittings and endcaps allowing rapid connection and closure before/after sampling and measurements.

Measurement of air and seawater samples

The measurement procedure for air and water samples was as follows (Figure A9):
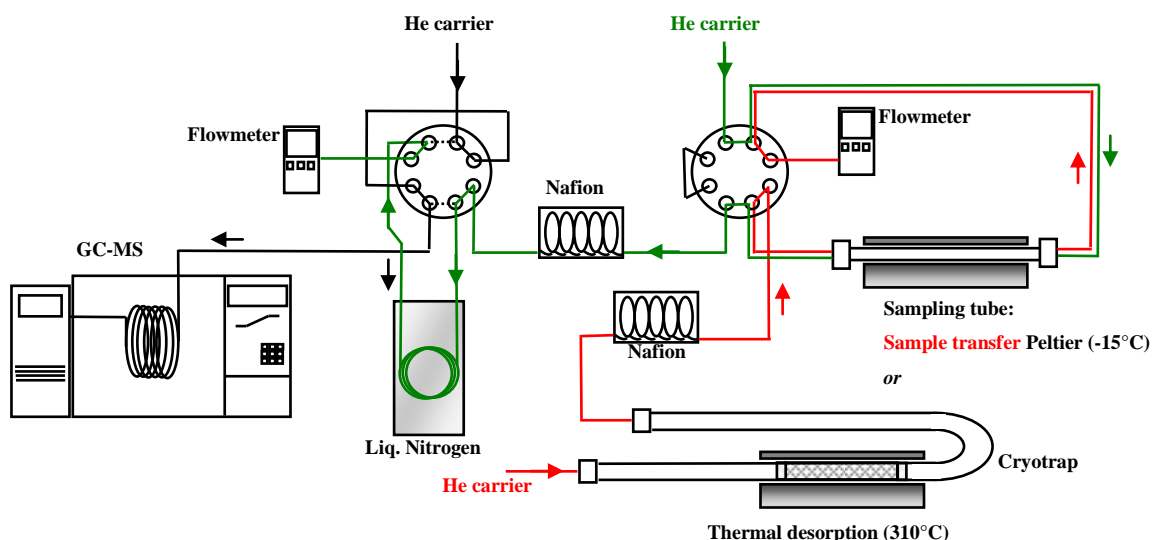

Figure A9: Scheme of the analytical system for the determination of halocarbons from air and water samples.

After sampling (air sampling or purge&trap of water samples), the samples were thermally desorbed from the cryotrap (310°C) under a flow of high-purity helium (50 mL min^{-1}, 99.999%, Linde, Germany) for 15 min (red lines/arrows). The analytes were re-trapped on peltier-cooled sampling tubes (Bahlmann et al., 2011) at -15°C using a Valco eight port valve (VICI, Valco instruments, Houston, USA). After sample transfer, the valco valve was switched and analytes were thermally desorbed (330°C) from the adsorbent tubes in counter-flow direction (He, 30 mL min^{-1}), here indicated

as green lines/arrows. During the desorption (20 min), the analytes were then refocused on a cryotrap (quartz capillary, 60 cm, 0.32 i.d.) submerged in liquid nitrogen. The refocusing of analytes and injection into the GC-MS system proceeds using a second eight port valco valve. After retrapping, the valve is switched and compounds are sent to the GC-MS system in counterflow direction (black (dotted) lines/arrows) under ambient temperature. Due to high water amounts in air and water samples, the water was removed by two Nafion dryers (in silica gel), each after thermal desorption from the cryotraps and the adsorbent tubes.

The GC-MS (6890N/5975B, Agilent, Waldbronn, Germany) was equipped with a CP-PorabondQ column (25 m, 0.25 μm i.d., Varian). The flowrate was set to 3°mL. The oven temperature program was as follows: 40 °C, hold 4 min; 12° C min^{-1} to 200°C, hold 2 min, 8° C min^{-1} to 240°C; 30° C min^{-1} to 280°C, hold 5 min. The MS was operated in the electron impact mode at 70 eV. Temperatures of quadrupole, source, and transfer line were 150°C, 230°C, and 250°C. Acquisition was executed in full scan mode (33-300 u).

Target analytes were identified by their retention times and respective mass spectra and quantified using their major mass fragments. Quantification of air and water samples was done by using aliquots of Scott EPA TO 15/17 gas standard (1 ppm in nitrogen, Sigma Aldrich, Germany) and CH$_3$I gas standard (100 ppm in nitrogen, Air Liquide, Germany) injected to the GC-MS. The trapping and desorption efficiency (recovery rates) of the cryotraps was tested (n=4). 2 mL of Scott EPA TO 15/17 gas standard (1 ppm in nitrogen) and 20 μL CH$_3$I (100 ppm nitrogen) was injected to the cryotraps

Figure A10: Mean recovery rates and their absolute standard deviations of halocarbons from recovery experiments (n=4).

submerged in the dry shipper using a stream of helium. Simulating "real" air sampling, helium was stream was set to 1L min^{-1} for 30 min (resulting in 30 L). The whole sample treatment procedure was applied as described above. The mean recovery rates of a suite of halocarbons were 96% ranging from 93± 4% (CH$_3$Br) and 93± 10% (CCl$_4$) to 100± 4% for CHBr$_3$. Individual recovery rates are displayed in Figure A10.
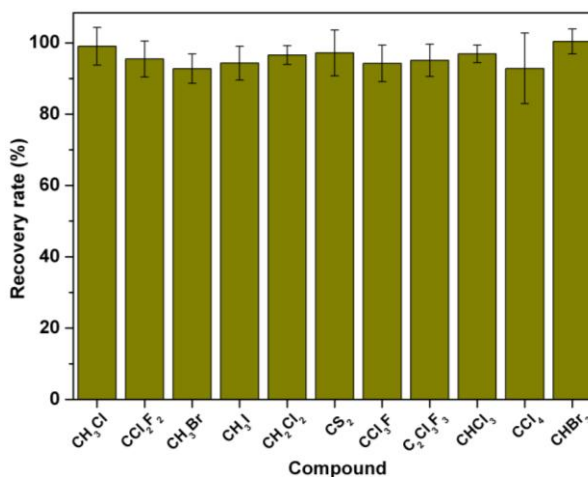
Appendix to Chapter 6: Tidal controls on trace gas dynamics in a subtropical seagrass meadow of Ria Formosa lagoon (southern Portugal)

Table A3: Mean trace gas fluxes (bold) obtained from seagrass meadows along the tidal cycle. Fluxes are given in nmol m^{-2} h^{-1}. Numbers in parenthesis are the range of fluxes. Fluxes during high tide are given as single values.

Compound	low tide (n=17)	methane peak (n=5)	feeder current (n=6)	high tide (n=2)	ebb flow (n=5)
Halocarbons					
CH$_3$Cl	**1.0** (-29.6- 69.0)	**40.1** (-14.2- 99.7)	**11.4** (-14.7- 36.6)	**-18.1, -58.3**	**21.3** (-13.5- 46.2)
CH$_3$Br	**0.4** (-0.8- 3.9)	**2.7** (0.1- 8.3)	**1.8** (0.2- 3.3)	**-0.5, -1.6**	**2.1** (0.1- 4.4)
CH$_3$I	**0.6** (-0.6- 2.6)	**3.3** (0.1- 8.0)	**1.6** (0.1- 2.9)	**0.1, 0.1**	**1.5** (0.2- 3.0)
CHCl$_3$	**0.3** (-0.8- 2.8)	**2.4** (0.1- 6.6)	**2.0** (0.5- 3.0)	**-0.1, -2.0**	**2.0** (-0.6- 3.7)
CHBr$_3$	**0.4** (-0.5- 1.3)	**2.9** (0.2- 10.6)	**2.8** (0.2- 5.1)	**0.5, -0.1**	**4.5** (-0.4- 8.6)
S-Compounds					
CS$_2$	**52** (-34- 192)	**216** (22- 544)	**135** (-5.5- 200.0)	**420, 398**	**129** (-13.4- 230)
COS [1]	-	**3.8** (0.1- 7.1)	**2.1** (0.3- 5.1)	**22, 21**	**4.5** (1.0- 10.5)
DMS [1]	-	**2** (0.1- 3.0)	**1.5** (0.7- 1.9)	**0.2, 0.2**	**1.3** (0.1- 3.2)
Hydrocarbons					
propene	**56** (-26- 377)	**167** (91- 331)	**91** (-5.1- 170)	**33, 27**	**182** (3.4- 407)
propane [1]	-	**6.0** (-0.2- 14)	**3.6** (-2.7- 7.8)	**48, 44**	**16.6** (5.7- 37)
butane [1]	-	**0.9** (-0.5- 3.4)	**1.5** (-0.2- 2.8)	**3.5, 2.3**	**5.7** (2.6- 12)

[1] Fluxes are expressed as relative enhancement to the average flux during low tide experiments.

Danksagung

Zunächst bedanke ich mich bei Dr. Richard Seifert für die Möglichkeit meine Dissertation in diesem herausfordernden Themenfeld anzufertigen. Richard, vielen Dank für die mir gewährten Freiheiten meine eigenen Ideen umzusetzen, für deine stete Diskussionsbereitschaft und für deine hilfreichen Hinweise den eigenen Blick auf das Wesentliche zu richten.

Bei Prof. Dr. Hartmann bedanke ich mich für die freundliche Übernahme des Zweitgutachtens.

Mein besonderer Dank gilt Dr. Enno Bahlmann für die Bereitschaft meine löchernden Fragen rund um die Themen halogenierte Verbindungen, Kohlenstoffisotope, und Flusskammern zu beantworten. Die resultierenden, teils kontroversen, Diskussionen mit dir und deine vielfältigen Ideen haben einen wesentlichen Teil zu meiner Arbeit beigetragen.

Prof. Dr. Michaelis danke ich für die ermutigenden Hinweise und Ratschläge, die sehr wertvoll für den Verlauf dieser Arbeit waren.

Ein besonderer Dank gilt Ralf Lendt und Sabine Beckmann, die mich in letzten Jahren immer mit helfender Hand begleiteten und immer da waren, wenn es mal eng wurde. Unvergessen ist immer noch die Zeit mit euch auf der Messkampagne in Portugal. Ralf, ich danke dir für die sehr angenehme Zeit im Büro und insbesondere für deine unglaubliche Gelassenheit, die auf mich sehr ansteckend wirkte.

Ich danke dir, Tim, für deine grandiose Hilfe auf der Portugalkampagne und im Labor. Berit, Lise, Uli, Peggy, Frauke, Philip, Imke, Markus, Nick, Tom, Wilma L. und F.Bernd, ich danke euch für die angenehme Arbeitsatmosphäre und dafür, dass ihr immer für einen Schnack zu haben wart. Danke Berit, für deine aufmunternden Gedanken während der Endphase und das Korrekturlesen.

Prof. Dr. Rui Santos möchte ich herzlich für die freundliche Aufnahme und Unterstützung während der Messkampagnen in der Ria Formosa danken. Seiner Arbeitsgruppe, insbesondere João Reis und Bruno Fragoso, gilt für ihre unverzichtbare Hilfe im Feld und in der Ramalhete Station mein großer Dank. Ich danke Dr. Justus van Beusekom und der unteren Naturschutzbehörde des Kreises Nordfriesland für den Zugang zu den Seegraswiesen und die Unterstützung im Feld.

Für die Finanzierung des Projekts danke ich dem Bundesministerium für Bildung und Forschung (Förderkennzeichen: 03F0611E) sowie dem Forschungsverbund ASSEMBLE für die Kofinanzierung des Faroaufenthalts.

Mein besonderer Dank gilt meinen Eltern und meiner Schwester Katja, die mich während meiner gesamten Studienzeit und insbesondere der letzten Jahre immer unterstützt und begleitet haben.

Mein abschließender Dank gilt meiner Britta. Ich danke dir für die tagtägliche Aufmunterung und die Geduld auch schwierige Phasen mit mir durchzustehen. Ohne dich hätte ich diese Arbeit nie fertig gestellt.

Eidesstattliche Erklärung

Hiermit erkläre ich an Eides statt, dass ich die vorliegende Dissertationsschrift selbst verfasst und keine anderen als die angegeben Quellen und Hilfsmittel benutzt habe.

Hamburg, den 12.03.2014

_____

Ingo Weinberg